NASA Contractor Report 158976

Evaluation of Laminar Flow Control System Concepts for Subsonic Commercial Transport Aircraft

BCAC Preliminary Design Department

BOEING COMMERCIAL AIRPLANE COMPANY
Seattle, Washington 98124

CONTRACT NAS1-14630
December 1978

National Aeronautics and
Space Administration

Langley Research Center
Hampton, Virginia 23665

FOREWORD

This document constitutes the final report covering engineering development and evaluation of laminar flow control system concepts under Contract NAS1-14630. This effort is titled: "Evaluation of Laminar Flow Control System Concepts for Subsonic Commercial Transport Aircraft." Work was conducted in three major tasks; namely, 1) Mission Definition and Baseline Configuration Development, 2) Concepts Evaluation, and 3) Configuration Selection and Design. The report covers the work conducted from September 1976 through September 1978. The NASA Technical Monitor for the entire period of the contract was Mr. J. W. Cheely of the Laminar Flow Control Project Office at Langley Research Center.

The studies and tests were accomplished within the Preliminary Design Department of the Vice President-Engineering Organization of the Boeing Commercial Airplane Company. The Engineering team assigned to this contract are listed below along with their primary areas of contribution:

L. B. Gratzer	Program Manager
R. W. Sudderth	Task Integrator
D. G. Andrews	Configurations
G. R. Swinford	Configurations
F. J. Davenport	Aerodynamics Task Leader
D. George-Falvy	Aerodynamics
L. J. Runyan	Aerodynamics
J. M. Hoy	Structures Task Leader
V. D. Bess	Structures
H. A. Dethman	Design Task Leader
J. Hunt	Design
L. C. Stevenson	Design
R. A. Mangiarotty	Acoustics
W. R. Lambert	Propulsion
F. J. Traeger	Systems
R. D. Anderson	Weights
K. H. Hartz	Weights
T. J. Kelly	Manufacturing
J. A. Davolt	Reliability/Maintainability
O. B. Brende	Safety

TABLE OF CONTENTS

TABLE OF CONTENTS (Concluded)

LIST OF ILLUSTRATIONS

LIST OF TABLES

1.0 SUMMARY

This report presents the results of a two-year study carried out under NASA Contract NAS1-14630 in Phase I to extend the development of laminar flow control (LFC) technology and evaluate LFC systems concepts. The overall objective of the LFC program is to provide a sound basis for industry decisions on the application of LFC to future commercial transports. The study was organized into major tasks to support the above objectives through application of LFC systems concepts to a baseline LFC transport initially generated for the study. Based on competitive evaluation of these concepts, a final selection was made for incorporation into the final design of an LFC transport which also included other advanced technology elements appropriate to the 1990 time period. In support of this activity, Boeing has expended company resources in basic LFC design studies and development of test facilities, including an LFC wing panel wind tunnel model, to carry out wind tunnel tests at near full-scale Reynolds numbers.

The initial task, titled Mission Definition and Baseline Configuration was directed toward the selection of mission requirements representative of an LFC transport application projected for the 1990 time period and generation of such a design suitable for tradeoff analysis in the subsequent concept evaluation tasks. The resulting configuration was a long-range tri-jet of conventional layout designed to carry 200 passengers plus baggage a distance of 10 190 km (5500 n mi) at 0.8 Mach number. It incorporated an LFC wing laminarized to 70% chord and the associated systems required for laminar flow. Laminarization of the empennage was not considered for the baseline airplane.

The major series of tasks was performed under the heading Concepts Evaluation. It involved the exploration of promising approaches to LFC design problems in three basic areas: (1) Aerodynamics, (2) Structures and Materials, and (3) Systems.

In the aerodynamics area, concepts were successfully developed for a basic high-speed wing design compatible with laminar flow requirements. A suitable suction surface and the associated ducting was integrated into the overall design to provide LFC throughout a practical flight envelope for representative environmental situations. Other configuration elements of the airplane, e.g., flaps, controls, engines, empennage, were studied in relation to their impact on LFC systems and the selection of the airplane arrangement was made to enhance the opportunities for successful LFC application to a long-range transport. A major wind tunnel program involving tests of an LFC wing panel, was successfully carried out to validate the suction surface design. It also provided design guidelines and data for evaluation of the susceptibility of laminar flow to various kinds of disturbances and the effects of off-design operation. Laboratory tests to evaluate the flow characteristics of suction surface openings and associated internal geometry were used to validate the selected opening concept.

At least twelve basic different structural arrangements for LFC wings and numerous options were studied and supported by limited structural tests to arrive at a selection which would satisfy structural requirements and provide a feasible design to approach minimum weight and cost. This work included the development of various concepts for suction surface openings (i.e., slots or perforated strips) in the form of inserts which would allow relatively convenient maintenance and repair of damaged areas. The concept finally selected incorporates a fiberglass cover or glove over a conventional wing structure using advanced aluminum

alloys. The fiberglass cover provides the suction surface and the associated chordwise ducting to distribute the suction airflow chordwise to trunk ducts in the wing leading and trailing edges. This design is considered applicable in the relatively near term. It is also adaptable to almost any advanced design, such as graphite/epoxy structure, which may appear practical in the future.

The complement of systems for an LFC airplane includes system elements additional to those of a turbulent airplane which must be provided specifically for LFC. The suction units and the associated ducting constitute the major additions which were selected following development and evaluation of a number of compressor and drive concepts. Each unit consists of a compressor section which provides two pressure levels, to match the pressure requirements on upper and lower wing surfaces, integrated with a turboshaft engine as the drive section. The wing units are located externally at the trailing edge of the wing-body intersection. For the final LFC airplane design (not the baseline) a tail suction unit, which doubles as the ground APU, is located at the base of the vertical tail near the trailing edge. This combination results in minimum weight and fuel consumption and provides satisfactory access for maintenance and repair while meeting safety and other operational requirements. The inclusion of devices to protect against the accumulation of insects at low altitudes is also unique to the LFC airplane. This subsystem is integrated with the anti-icing subsystem in the leading edge and both the wing and horizontal tail are provided with this combination. Since no resources were provided in the contract to develop these systems, several promising candidates were selected on the basis of feasibility studies for further development. These have been characterized as: 1) The liquid film, 2) Cryogenic frost device, and 3) High-pressure air shield. There are also requirements for controlling the laminar flow suction and monitoring LFC performance which will result in some additions to the usual complement of these type systems. All other airplane systems are representative of those generally included in a conventional turbulent transport.

With the completion of the concept development and evaluation studies, the results were assessed in relation to their adaptability to the final LFC airplane configuration. This activity was supported by parameteric trade studies to evolve a configuration judged to be most competitive with a turbulent airplane meeting the same mission and design requirements. The selected final configuration is similar to the baseline airplane but incorporating more extensive wing laminarization (i.e., to 80% chord on the upper surface and to 70% chord in the lower surface) and laminarization to 80% chord on both surfaces of the horizontal tail.

The final LFC airplane also incorporates advanced technology judged to be available in the 1990 time period. In addition to the LFC system itself, the use of an advanced high-speed airfoil constitutes an important advance in aerodynamics. The major benefits of active controls are secured by including a longitudinal stability augmentation system (SAS) which allows reduced longitudinal stability (SAS-off) thereby reducing weight and drag. Systems for gust and maneuver load alleviation are also included to provide significant weight savings in the wing box. A selection of advanced materials includes improved aluminum alloys in all load-carrying structure and bonded construction in the fuselage and empennage. Graphite/epoxy composites are used only for trailing edge surfaces. The main propulsion engines are an advanced turbofan type (bypass ratio (BPR) = 7.3) and incorporate technology advances in a number of areas to provide substantial gains in both fuel consumption (i.e., -14% relative to today's high bypass engines) and weight reduction (i.e., -13%).

The performance of the final LFC airplane design is based on the original mission and design requirements, modified to a somewhat lower cruise altitude of 12 190 m (40 000 ft), and to augment fuel reserves allowing completion of the mission even with total LFC failure at the halfway point. While no final economic analysis was made, the fuel utilization of the airplane is very attractive. A comparison with the 747 airplane shows a 70% improvement in fuel utilization due to LFC and the other technology advances incorporated in the final LFC airplane design. The effect of LFC alone, for a cycled design of the type presented here, is estimated to approach 45% increase in fuel utilization relative to an advanced turbulent design.

Phase I of the LFC program has produced substantial accomplishments which will serve as a good base for further progress. These can be summarized as follows:

1. A feasible structural concept has been defined which shows promise of evolving into a practical design that can be built and operated for reasonable cost. The fiberglass cover approach makes this concept adaptable to most structural arrangements including those using graphite/epoxy composites. However, extensive design development is still required to reduce weight and cost and to resolve operational and manufacturing concerns. Validation of the concept by analysis and tests is an essential step in advancing the design to a state of readiness for production.

2. The aerodynamic design of the LFC wing has been developed to the point where it could serve as a basis for further refinement in the wind tunnel. This development has been supported by wind tunnel tests on a representative LFC wing panel to provide design guidelines and evaluation of the effects of disturbances and off-design conditions. Advanced high-speed airfoils have been shown analytically to be compatible with LFC requirements and to provide a reasonable envelope to incorporate LFC systems and ducting. Although basic laminar boundary layer stability methods are becoming established, validation and streamlining of these methods for design purposes is necessary. While the current aerodynamic design appears viable, further optimization is necessary to minimize drag and reduce internal flow losses. Further objectives should include reducing sensitivity to off-design operation and various disturbances, minimizing the number of slots and reducing the criticality of the leading edge. Ultimately, validation in flight of the aerodynamic design is required throughout the operating envelope.

3. The additional systems required to implement application of LFC to a transport design are 1) the suction unit and associated ducting, 2) a device to protect the leading edge from insect accretion and 3) subsystems to control suction distribution and monitor LFC performance. Design options in the first category have been evaluated and a selection made for incorporation in the final airplane configuration. Several promising approaches have been identified for the leading edge protection system but further innovation and development is required to arrive at a practical solution. Identification of systems required in the third category is incomplete as would be expected for the current stage of LFC development.

4. Key operational problems have been identified and explored, the most important of which are: a) Protection against wing leading edge damage, b) Avoiding insect contamination, c) Establishing operational reliability, particularly in the presence of ice

clouds and d) Evolving procedures and techniques that will provide low-cost maintenance and repair characteristics. Solutions to these problems must be developed and validated either in the laboratory or in flight before serious consideration of LFC application to a production airplane can be expected.

5. A LFC transport configuration has been generated incorporating the most promising structural arrangement and systems concepts developed during this study. Combining other elements of advanced technology with LFC provides attractive fuel utilization benefits which will have a very favorable impact on airplane economics. Nevertheless, further trade studies are needed to define the combination of features that will lead to a design most competitive with a turbulent airplane. In particular, more work is necessary to establish better design criteria and operational requirements (such as turbulent climb capability and cruise altitude) since these have been shown to have a substantial influence on airplane performance and economics.

2.0 INTRODUCTION

The implementation of new initiatives by the NASA to develop Laminar Flow Control (LFC) technology is due largely to the urgency of the energy problem and the realization that successful application to long-range transport aircraft can produce substantial improvement in fuel economy and airline economics.

The USAF/Northrop X-21 airplane program in the early 1960's (Ref. 1) was a major effort to demonstrate the feasibility of LFC on large subsonic aircraft. While substantial success in maintaining laminar flow was achieved, significant design compromises and the lack of overall reliability in a variety of flight conditions left many technical and operational questions unresolved and provided serious concern about the eventual adaptability of LFC to practical operation. In this light, the need for further research and development became obvious and provided the justification for the NASA Laminar Flow Control program which has been planned in three phases to culminate in the design, development and flight testing of a demonstrator aircraft. The demonstrator will be flown under representative conditions to establish the economic and operational feasibility of this type of aircraft in airline service.

The subject of this report is the work accomplished by Boeing during Phase I of the LFC program under contract to NASA. The study activity is directed toward the further development of LFC technology and solutions to critical problems which must be solved before practical application of LFC can be successful. The overall objective of the LFC program is to provide a sound basis for industry decisions on the application of LFC to future commercial transports.

The study was organized into a series of major tasks and subtasks to develop and evaluate the most promising LFC concepts applicable to commercial air transports. The study approach is illustrated in Figure 2.0-1 which shows the major elements involved, their sequencing and the interaction between these activities. The result of the first task was the definition of a baseline aircraft to serve as the basis for LFC systems concepts evaluation and trade studies. Concurrent with development and evaluation of candidate concepts, a series of parametric studies was conducted to establish tradeoff relationships between airplane geometry and design requirements. This interactive effort led to a selection of system concepts for incorporation in the final LFC airplane configuration. The final configuration design was accomplished in the last step which included the calculation of the airplane performance and comparison of its fuel efficiency with that of a representative turbulent transport aircraft.

Many of the technical problems associated with an LFC airplane are considered routine engineering developments similar to those expected in any new aircraft of more conventional design. Therefore, the tasks undertaken were limited to address problems uniquely related to LFC systems. This has resulted in the selection of concepts and systems for incorporation into a final LFC airplane design judged to have the highest probability of success consistent with safety and airline operational suitability. It has also yielded a strong technical and design base for the further development and testing required in later phases of the program.

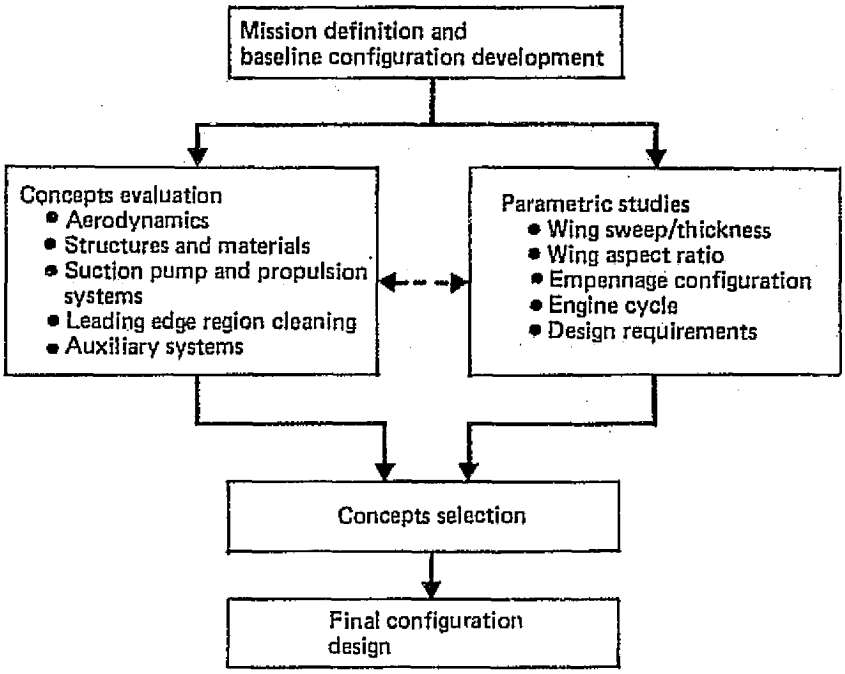

Figure 2.0-1. Study Approach

In support of the study, Boeing devoted company resources to initiating and expanding certain study elements and to providing improved test facilities. Toward this end, the Boeing Low Speed Research Wind Tunnel was modified to provide valid laminar flow data at high Reynolds numbers. In addition, the design and construction of a large swept wing LFC model was accomplished. This combination was used successfully to carry out selected investigations under a variety of conditions representing critical flight situations. Major objectives included: 1) Verification of airfoil leading edge design, 2) Validation of suction flow requirements at high Reynolds numbers, 3) Definition of allowable disturbances, including noise and 4) Exploring sensitivity to off-design conditions.

Major emphasis was also placed on the development of structural concepts for LFC wings. The definition of attractive design options and the generation of sufficient data to permit credible evaluation of these options together with evaluation of structural integrity and manufacturing producibility was a primary goal of these studies. This activity, which led to a structural concept selection, was supported by limited hardware and environmental tests as appropriate to this stage of the development process. Sample hardware to indicate manufacturing feasibility is also provided to support the conclusions of these studies.

The technical team assigned to the program has continued to draw on government and industry experiences with LFC. Consulting agreements with United Airlines and the Northrop Corporation were arranged to support the contract work during the entire period. Working agreements with Pratt and Whitney Aircraft and AiResearch Manufacturing Company were made to provide for exchange of data on a mutual interest basis.

The following sections of this document provide a detailed reporting of the technical activity according to the major tasks defined in the original work statement of the contract, NAS1-14630, as modified by supplemental agreement (Amendment/Modification No. 6) dated October 1, 1977. The reporting also reflects changes effected through rescheduling via the C-63 forms during the contract period. The report is organized into chapters which, starting with Chapter 4.0 and continuing through Chapter 6.0, have titles corresponding to the major study tasks. These are: 4.0 – Mission Definition and Baseline Configuration Development, 5.0 – Concepts Evaluation and 6.0 – Configuration Selection and Design. The sections in Chapter 5.0 also are titled to correspond to the subtasks which are included in the Concepts Evaluation Task.

3.0 SYMBOLS AND ABBREVIATIONS

A	disturbance amplitude
AR	aspect ratio
A_{π}	frontal area
a	speed of sound
b	wing span
b_F	spanwise extent of trailing edge flap
BPR	bypass ratio
c	airfoil chord length
c'	airfoil chord length with flap extended
c_F	flap chord
C_D	drag coefficient
C_{D_P}	profile drag coefficient
$\Delta C_{D_{SU}}$	incremental drag coefficient for suction engine
ΔC_{D_M}	incremental drag due to compressibility
c_d	local section drag coefficient
c_{d_w}	local wake drag coefficient
c_{d_s}	local equivalent suction drag coefficient
C.G.	center of gravity
C_L	lift coefficient
C_n	normal force coefficient
C_{n_β}	directional stability derivative
c_ℓ	airfoil section lift coefficient
C_p	pressure coefficient

ΔC_{p_s}	suction pressure coefficient
C_Q	integrated suction flow coefficient
C_q	local suction flow coefficient
D	drag
d	diameter of disk-type surface protuberances
DOC	direct operating cost
ECS	environmental control system
EPNL	effective perceived noise level
EPNdB	effective perceived noise decibel (unit of EPNL)
f	frequency
F_n	net thrust
FAR	Federal Aviation Regulations
g	gravitational acceleration
H	boundary layer shape parameter
h	altitude
KEAS	equivalent airspeed in knots
k	height of surface protuberance or wave amplitude
L/D	lift to drag ratio
ℓ	width of surface depression or gap
M	Mach number
M_D	drag divergence Mach number
P	pressure
ΔP_s	pressure differential across a slot
P_M	acoustic pressure
P&WA	Pratt and Whitney Aircraft

Q	suction flow rate
q	dynamic pressure
r	radius of curvature
Re	Reynolds number
Re_1	Unit Reynolds number
Re_c	Reynolds number based on streamwise chord
Re_n	Reynolds number based on the chord measured normal to leading edge
Re_s	slot Reynolds number
$Re_{\theta_{a.l.}}$	momentum thickness Reynolds number at the leading edge attachment line
S_{ref}	reference wing area
s	distance along airfoil surface measured from leading edge
Δs	slot spacing
SAS	stability augmentation system
SFC	specific fuel consumption
SPF/DB	super plastic formed/diffusion bonded
SPL	sound pressure level
SL	sea level
SLST	sea level static thrust
t	wing thickness
U	velocity component normal to the wing leading edge
U_e	local velocity at edge of boundary layer
u	tangential mean velocity within the boundary layer
u_h	velocity fluctuation derived from hot-wire measurement
u_m	velocity fluctuation derived from microphone data
V_∞	freestream velocity

V_A	approach speed
V_R	takeoff rotation speed
V_S	stall speed
V_s	slot inflow velocity
V'	velocity fluctuations in a stream
$V_{H,(V)}$	horizontal (or vertical) tail volume coefficient
v_w	distributed suction inflow velocity
W	weight
w	crossflow velocity component within the boundary layer
w_s	slot width
x	distance from leading edge measured along airfoil chord
y	distance from longitudinal axis measured along the span
z	distance from wing surface; also airfoil ordinate perpendicular to the chord

Greek Symbols

α	angle of attack
α_i^*	spatial amplification rate (dimensional)
δ	boundary layer limit thickness, also atmospheric pressure ratio
δ_F	flap deflection angle
η	spanwise position on wing in fraction of semi-span
Θ	wing twist angle
θ	boundary layer momentum thickness
κ	ratio of local lift coefficient to airplane lift coefficient
λ	wing taper ratio; also wave length
Λ	wing sweep angle, refers to 1/4 chord line unless otherwise noted
μ	viscosity coefficient
ν	kinematic viscosity

ρ	density
σ	atmospheric density ratio
ψ	angle between disturbance phase velocity and local velocity at the edge of the boundary layer
ω^*	dimensional disturbance frequency
ω_r	nondimensional disturbance frequency

Subscripts

a.l.	airflow attachment line on wing leading edge
A	approach
c	value based on streamwise chord
e	outer edge of boundary layer
E	empty
F	fuel
L	laminar boundary layer extent
LE	leading edge
M	manifold chamber
n	value based on normal chord
o	reference or initial condition, also pertinent to leading edge
PL	plenum chamber
R	takeoff rotation
s	slot or suction
S	stall
SU	suction unit
∞	freestream condition

4.0 MISSION DEFINITION AND BASELINE CONFIGURATION DEVELOPMENT

The initial task of this contract was the definition of a representative mission and a baseline airplane configuration to serve as a basis for the aerodynamic, structural, and systems studies of the concepts evaluation tasks. This work was conducted as a follow-on of previous Boeing IR&D LFC studies.

4.1 MISSION SELECTION

Selection of the mission was based on airline traffic trends projected into the 1990's, cost sensitivity studies, Boeing marketing studies on payload size, compatibility with normal airline operation and other airline traffic, and passenger acceptance standards for the long range missions. Long range missions were considered the most likely first application since LFC is functionally more reliable at high altitude and the performance and economic benefits greatest for long-range cruise.

4.1.1 AIRLINE TRAFFIC TRENDS

Traffic projections for long-range missions for the 1990's are presented in Table 4.1-1. As seen in this projection a substantial requirement exists to serve routes with 7410 to 11 110 km (4000 to 6000 n mi) range. Only two of the routes shown have ranges significantly less than this, and as will be seen later, these could well be served by an airplane designed for the longer range. From this information it was decided the range should be between 7410 and 11 100 km (4000 and 6000 n mi). Further definitive information was needed to make a design range selection. This additional information was provided by a cost sensitivity study discussed in a later paragraph.

4.1.2 PAYLOAD SIZE

Boeing marketing studies indicated a need for an airplane in the 200 passenger category for a 10190 km (5500 n mi) range mission. Passenger density on long-range missions is not sufficient to justify the greater payloads of 300 to 400 passengers except for specialized missions. A 200 passenger payload was therefore selected as the payload size for the baseline airplane.

4.1.3 PASSENGER ACCEPTANCE AND ROUTE COMPATIBILITY

For long range missions a higher comfort level provided by dual aisles was believed desirable. Therefore, a seven abreast seating arrangement with dual aisles utilizing a 15/85% mix between first class and tourist was developed. This arrangement is presented in Figure 4.1-1 and results in a final passenger count of 201 which remained the baseline payload size throughout the study.

An airplane of this type must also be compatible with airline operation requirements and other airline traffic. Therefore, unusual arrangements such as a high aspect ratio strut-braced wing configuration with lower Mach number cruise capability were not considered. Such a configuration would present ground handling problems due to restricted gate spacing and

Table 4.1-1. 1990's Long-Range Yearly Passenger Traffic

Rank	General route	Yearly long-range traffic (%)		General range, km (nmi)
1.	North Atlantic	24	50% of total	5550 to 6480 (3000 to 3500)
2.	U.S. transcontinental	13		3330 to 3700 (1800 to 2000)
3.	U.S. Midwest to Europe	13		6480 to 7410 (3500 to 4000)
4.	U.S. to Southern Europe	10	25% of total	5550 to 7410 (3000 to 4000)
5.	U.S. west coast to Europe	6		8300 to 9200 (4500 to 5000)
6.	U.S. west coast to Honolulu	5		3700 to 4600 (2000 to 2500)
7.	Europe to Southeast Asia	4		10 200 to 11 100 (5500 to 6000)
8.	Europe to Miami	3.5	9.6% of total	6480 to 8300 (3500 to 4500)
9.	U.S. west coast to Orient	3.4		7410 to 9200 (4000 to 5000)
10.	Europe to Orient	2.7		9200 to 11 100 (5000 to 6000)
		84.6% of total		

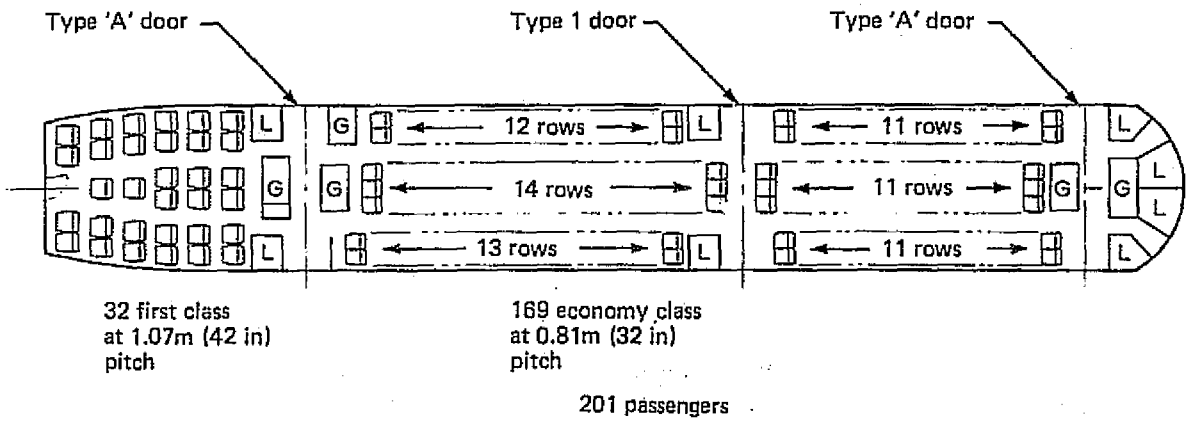

Figure 4.1-1. Baseline Interior Arrangement

taxiway clearances. Also, a lower Mach number cruise, such as 0.75, would present traffic clearance problems on routes such as the North Atlantic which presently have altitude corridors allocated according to speed. For these reasons, a conventional wing configuration limited to moderate wing span was initially selected. Also, a cruise Mach number of 0.8 was selected to avoid traffic corridor problems in the 1990 time period and to maintain satisfactory trip times for long-range flights.

4.1.4 COST SENSITIVITY TO DESIGN RANGE

Examination of economic trends was necessary to provide a final basis for defining the design range. These trends were developed by comparing relative direct operating cost (DOC) data for two airplanes having design ranges of 7410 km (4000 n mi) and 10 190 km (5500 n mi). Results of this comparison are presented in Figure 4.1-2 and show the cost relationships for these two airplanes operating at ranges from 1852 km (1000 n mi) to 14 810 km (8000 n mi). It is apparent that the 10 190 km (5500 n mi) range airplane provides much more favorable economics beyond 7410 km (4000 n mi) miles with a relatively small penalty in DOC at shorter ranges. It also has good economics at 11 110 km (6000 n mi) and beyond. Therefore, based on these analyses the design range was selected as 10 190 km (5500 n mi).

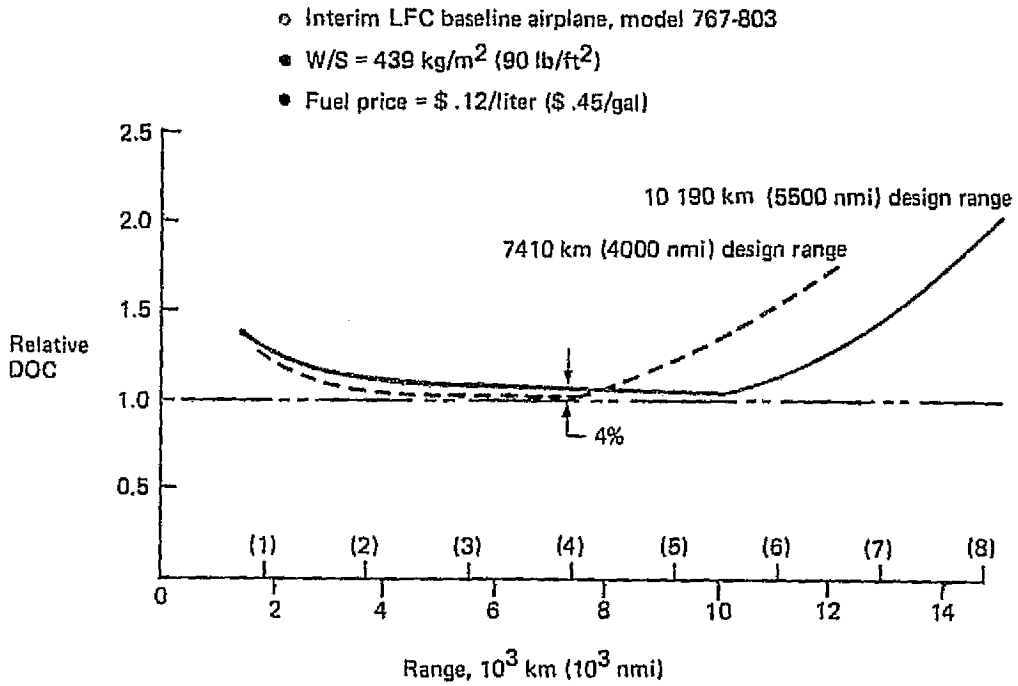

Figure 4.1-2. Effect of Design Range on DOC

4.2 DESIGN REQUIREMENTS

The final selection of the baseline airplane design requirements was based on the considerations previously discussed and those normally considered appropriate for a long-range airplane. For example, the wide body maintains passenger acceptance and Mach 0.8 cruise assures air traffic compatibility while recognizing the need for fuel economy. Also, the body width is sufficient to accommodate two LD-3 containers side-by-side in the lower cargo compartment.

Other design requirements were established based on maintaining compatibility with the operational demands of laminar flow control. These requirements (i.e., cruise altitude, turbulent climb capability and fuel reserves) tend to result in some performance or economic penalty since they impose operational constr .nts relative to a normal turbulent airplane. However, meeting these requirements enhances the dependability of LFC operation and therefore results in a significant improvement in real performance. While an initial selection of these requirements has been made for the baseline airplane, it was recognized that any requirement that penalizes the airplane performance due to LFC considerations must be scrutinized for opportunities to redefine requirements for application to the final configuration. The baseline airplane design requirements are listed in Table 4.2-1.

Table 4.2-1. Baseline Airplane Design Requirements

Item	Value
Design range	10 190 km(5500 nmi)
Payload	201 passengers
Cruise mach number	0.8
Cruise altitude	12 810m (initial) (42 000 ft)
Turbulent climb capability	1.52 m/s at 10 670m (300 ft/min at 35 000 ft)
Takeoff field length	3566m (11 700 ft), or less
Approach speed	250 km/h (135 kn)
Fuel reserves	1967 ATA international rules (turbulent flow)

4.3 AIRPLANE OPERATING ENVELOPE

The operating envelope for the baseline airplane is defined in Figure 4.3-1. As seen in this figure, an off-design envelope is defined as well as a principal LFC operating envelope and a design point. The LFC principal operating envelope defines the flight conditions over which the airplane should maintain full laminar flow over all laminar flow design surfaces. The more extensive envelope is the anticipated extreme operating envelope where only partial laminar flow performance is expected. Only the principal LFC operating envelope and design point were used as a basis for program studies. Initially they were treated as design objectives subject to later validation rather than firm requirements.

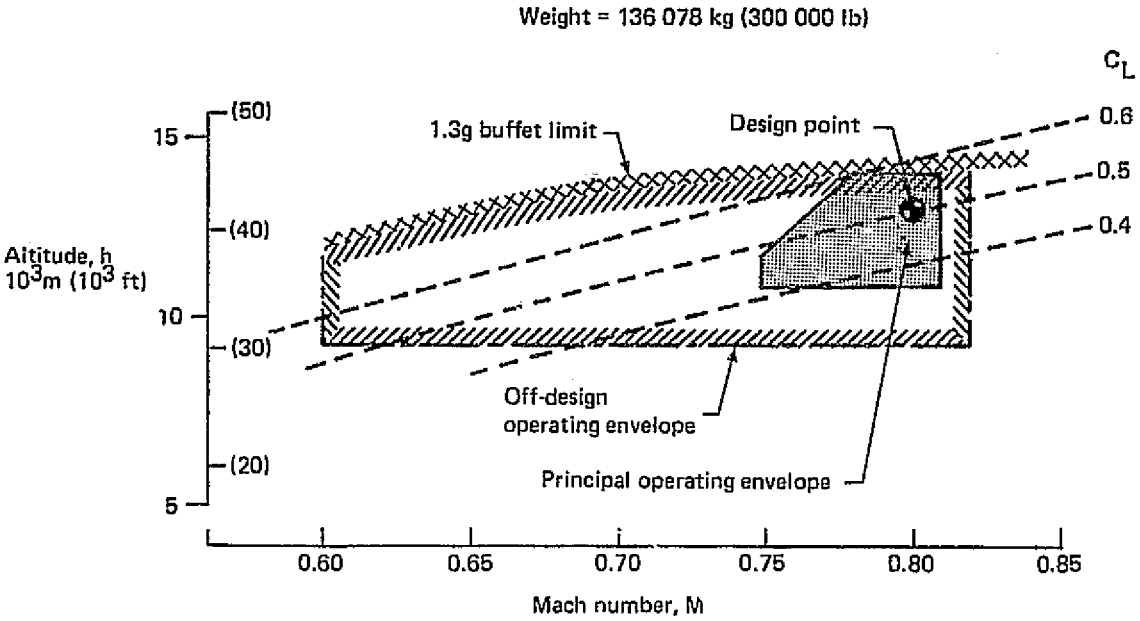

Figure 4.3-1. LFC Baseline Airplane Operating Envelope

4.4 DESIGN APPROACH

The design approach for the baseline airplane was aimed at establishing a workable configuration on which to conduct LFC concept trade studies as quickly as possible. The configuration was also selected to allow concentration on primary LFC design problems rather than problems resulting from configuration decisions such as the engine location, empennage arrangement and extent of laminar flow.

Initially, the three-engine aft configuration was selected to eliminate the design problems and uncertainty associated with wing-mounted engines on an LFC airplane. The uncertainty regarding engine noise interaction and pressure distribution effects on the wing laminar flow were determined to require extensive investigation. However, wing-mounted engines appeared to offer some weight and balance advantages so such investigation was delayed to later in the program.

The extent of laminarization was selected to cover the most important area (i.e., where LFC provides the greatest benefit), the first 70% of the wing. Laminarization of the empennage was not considered at this time since no additional technical challenge would be encountered and the results of the wing studies were considered to be directly applicable. Laminarization aft of the rear spar was initially considered to involve special ducting problems across the spar and physical interference of the laminar surface with the flight controls. Once an adequate basic wing design concept was achieved, extension of the laminarized area behind the rear spar and also onto the empennage surfaces was considered.

4.5 BASELINE AIRPLANE TECHNOLOGY

The advanced technology items selected for the baseline airplane were those considered appropriate for an LFC airplane entry into service in the 1990 time period. These technology items are summarized in Table 4.5-1. The gains in each technology area are shown relative to an airplane designed with existing levels of technology. As can be seen, no consideration has been given to such items as laminarized empennage, composite structures and gust load alleviation. Advancement in the technology base by including these items was reserved for definition during the final LFC airplane design process.

4.6 CONFIGURATION DEFINITION

The final version of the baseline airplane is a long-range, wide-body trijet designated Model 767-807. A three-view drawing of this configuration is presented in Figure 4.6-1

Table 4.5-1. Baseline Airplane Technology (1990 Certification)

	Δ Component weight	Δ (L/D)	ΔSFC
Aerodynamics Laminar-flow control Advanced airfoil section	To be determined	26% 3%	2.3%
Advanced structures Improved aluminum alloys Bonded construction Carbon brakes	-7% wing box -4% fuselage -4% empennage -5% fuselage -5% empennage -10% landing gear	—	—
Active controls Reduced longitudinal stability	-20% horizontal tail	4%	—
Propulsion STF482 engine (BPR = 7.5)	-13%	—	-14%
Reference: Existing levels			

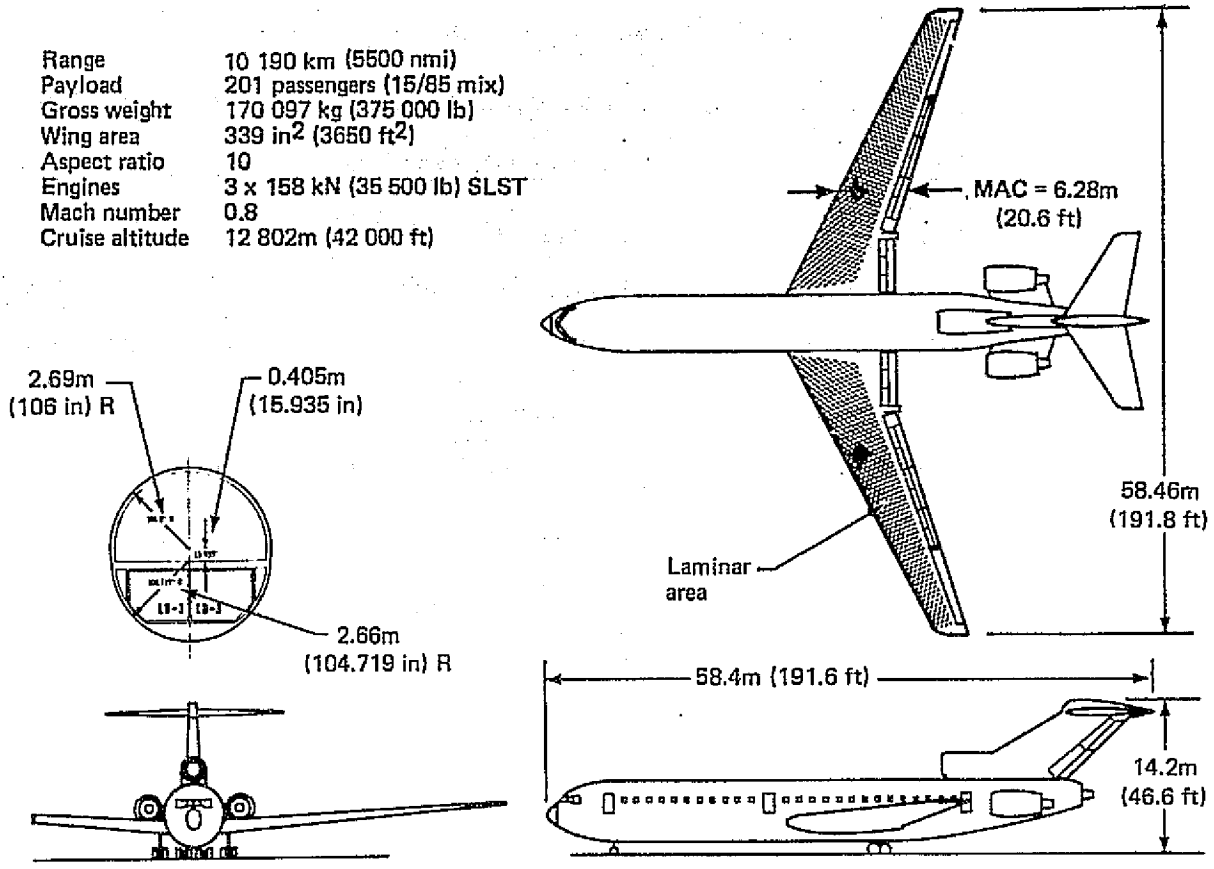

Figure 4.6-1. LFC Baseline Airplane—Model 767-807

and details of the airplane characteristics are presented in Table 4.6-1. The mission and physical characteristics are based on studies discussed in the preceding paragraphs of this section of the report.

The wing is laminarized to 70% chord permitting the use of an outboard aileron for low-speed operation only, with the remainder of the span occupied by single slotted Fowler flaps and 10% chord spoilers to provide high speed lateral control and the normal speed brake functions. The two LFC suction units are located at the planform break with suction airflow converging at this point from both wing root and wing tip. The engines are located on the aft body to provide a clean wing and minimize the influence of noise on the stability of the laminar boundary layer. The T-tail empennage is selected to be compatible with the aft-engine location and to provide greater potential trim drag reduction. Other characteristics of the airplane are quite representative of those found on a conventional turbulent long-range transport.

Table 4.6-1. Baseline Airplane Characteristics—Model 767-807

Item	Value
Gross weight	170 097 kg (375 000 lb)
OEW	97 849 kg (215 720 lb)
Block fuel	46 103 kg (101 640 lb)
Reserves	7 040 kg (15 520 lb)
Landing weight	124 216 kg (273 850 lb)
Wing area	339 m^2 (3650 ft^2)
Aspect ratio	10
Thickness ratio	0.14/0.11
Sweep	25 deg
Horizontal tail area	61.2 m^2 (659 ft^2)
Vertical tail area	64.4 m^2 (693 ft^2)
Body length/diameter	50.29m/5.38m (165 ft/212 in)
Engines (3-STF482)	158 kN (35 500 lb, SLST)
OEW/TOGW	0.576
Payload/TOGW	0.114
T/W	0.284
W/S	502 kg/m^2 (103 lb/ft^2)
TOFL at SL, 29°C (84°F)	2 347m (7700 ft)
V_{APP}	250 km/h (135 kn)

5.0 CONCEPTS EVALUATION

The objectives of this task were to evaluate the options available for aerodynamic design, structural concepts and subsystems selection for a viable LFC commercial transport. The evaluation included an assessment of the benefits versus complexity and cost for development, production and operation. This task was the predominant effort in the program. It was divided into the following five subtasks: 1) Aerodynamics, 2) Structures and materials, 3) Suction pump and propulsion system, 4) Leading edge region cleaning and 5) Auxiliary systems.

5.1 AERODYNAMICS

The purpose of the task reported in this section was to develop solutions to the basic problems of LFC wing design and the aerodynamic systems required to assure reliable operation of the LFC airplane throughout the flight envelope and in a realistic operating environment. Thus, major attention is given to the determination of the appropriate parameters for an LFC wing consistent with advanced high-speed airfoil concepts and the airplane design requirements and objectives. Also, a major effort to obtain critical data in the wind tunnel to support successful wing design was carried on during the contract and is reported in the subsection on Aerodynamics Test Programs.

5.1.1 DESIGN REQUIREMENTS AND OBJECTIVES

The central problem in the successful application of laminar flow control is the development of a wing design which permits the maintenance of laminar flow while making efficient accommodation for the structural arrangements and systems necessary to provide LFC. This must be accomplished for a range of flight and environmental conditions corresponding to practical operation in airline systems. Thus, it is important to develop a complete understanding of the behavior of the laminar boundary layer and the methods for its analysis under a variety of conditions encompassing those to be expected in actual operation. This is also essential for the intelligent pursuit of practical design solutions.

In describing the aerodynamic design of the present LFC study airplane it is appropriate to review first the major operational requirements that must be considered. These can be classified into four basic groups: 1) Environmental considerations, 2) Manufacturing tolerances, 3) Maintenance requirements and 4) LFC systems requirements.

5.1.1.1 Environmental Considerations

There are four major environmental considerations that impact the aerodynamic design:

1. Ice crystals (Cruise altitude)
2. Noise (Engine placement)
3. Insect contamination (Wing leading edge design)
4. Erosion (Suction surface design)

The presence of ice crystals is widespread throughout the upper atmosphere and can substantially influence the choice of cruise altitude even on a daily basis. This is illustrated by the data of Figure 5.1-1, taken from Reference 2 which show the effects of ice particles on LFC degradation at 12 190 m (40 000 ft) altitude and Mach .8. The threshold for significant loss of LFC depends on both particle diameter and concentration as shown and becomes higher as altitude increases. Based on data measured over Kwajalein Atol through the late summer months (Ref. 3), it is apparent that, near the equator, the ice particle distribution is such that some loss of LFC could be expected a substantial fraction of time. Fortunately, at higher latitudes, available evidence indicates that the critical particle distributions occur at lower altitudes and tend to diminish rapidly above the tropopause. Thus, an LFC airplane capable of cruise above 12 190 m (40 000 ft) could operate reliably over most of the major airline routes. However, long-range routes involving penetration of the lower latitudes would apparently need additional aids such as weather monitoring, particle sensors, etc., to permit economic operation. Additional data are needed to provide a clear understanding of the operational requirements associated with ice particles and the design requirements for cruise altitude capability.

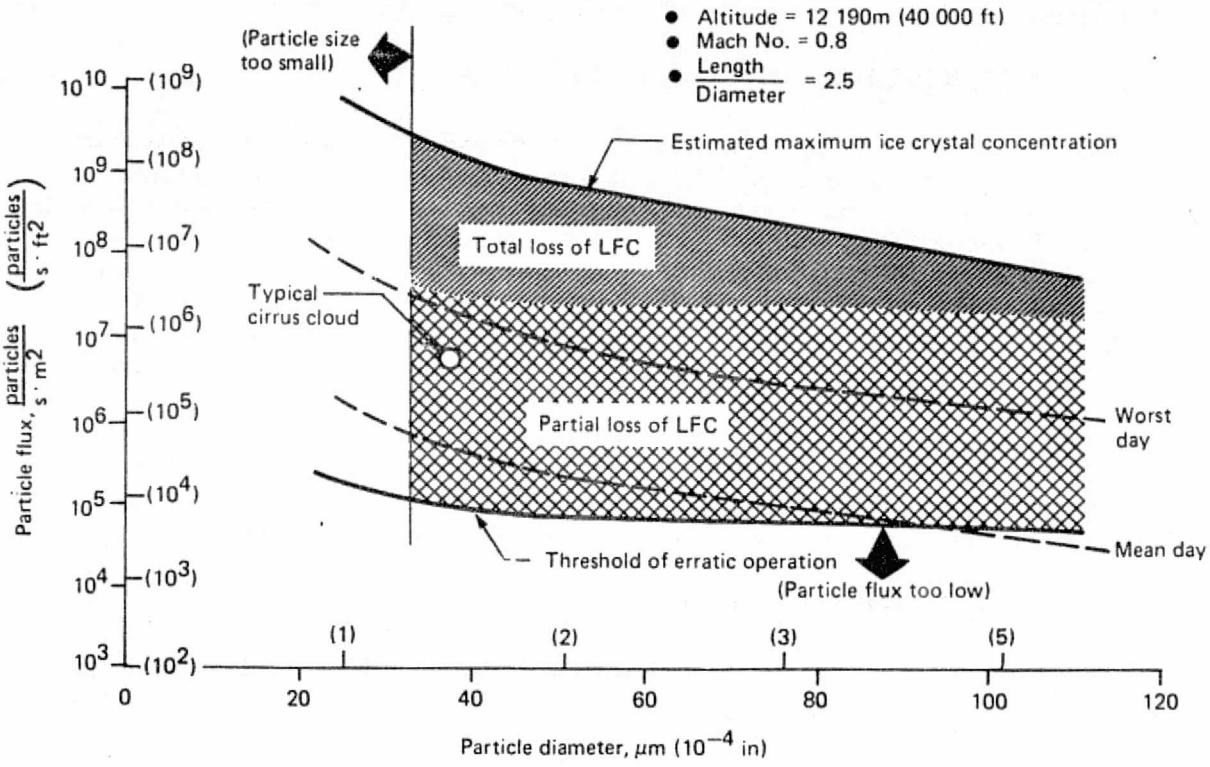

Figure 5.1-1. Estimated Effects of Atmospheric Ice Particles on LFC

It is well known that noise emanating from the propulsion or suction engines could upset the proper functioning of LFC and lead to early transition of the laminar boundary layer to turbulent conditions. This, of course, must be considered in the aerodynamic design regarding engine placement. Previous studies, (Refs. 1, and 4) have established criteria for allowable noise disturbance levels and those served as guidelines for the present work.

Insect contamination, or more precisely, its prevention must be considered in the aerodynamic design at least to the extent that the airfoil section and the leading edge region of the wing must be suitable to accommodate some type of an insect deposit prevention device.

Erosion due to rain (or snow, hail, sand, etc.) also has an impact in the aerodynamic design of the leading edge. This is reflected in restrictions on location of the first slot and the selection of wing sweep. Also, the definition of leading edge material is an important consideration in minimizing the impact of erosion on airplane operations.

5.1.1.2 Manufacturing Tolerances

The sensitivity of laminar flow to surface irregularities, especially at high Reynolds numbers, is well known. Hence the establishment of appropriate manufacturing tolerances for an LFC airplane are of critical importance. This problem has been studied in the past and some guidelines have been established, but the understanding is not yet complete and more work needs to be done. The main types of surface irregularities to be considered are: 1) Waviness, 2) Surface discontinuities such as steps, gaps, grooves, etc., 3) Isolated protuberances such as rivets, fasteners, etc., 4) Surface roughness such as graininess and scratches, and 5) Slot discrepancies such as burrs, mismatches, width inconsistencies, etc.

Criteria specifying surface wavines requirements for avoiding boundary layer transition have been determined primarily from flat plate wind tunnel tests without boundary layer suction effects (Ref. 5). Later studies that have investigated the effects of suction on surface waviness requirements, however, indicated that considerably less stringent tolerances would be applicable to an LFC wing (Ref. 6). Typical criteria for allowable surface waviness on an LFC wing are shown in Figure 5.1-2 as calculated on the basis of Reference 6. The wave amplitude limits quoted are applicable to multiple surface waves, forming along the span. For chordwise waves, according to Reference 6, the permissible wave amplitude would be twice as high as for spanwise waves. Also, for a single wave (in either direction) the tolerance limits would be three times higher than indicated in Figure 5.1-2.

It must be kept in mind, however, that the preceding criteria were derived from experiments done at low Mach numbers. Surface waves induce local pressure peaks that are amplified at higher Mach numbers. These waviness-induced pressure peaks introduce two problems:

- At the wave crest the difference between the surface pressure and the suction chamber pressure could be reduced to a point where outflow through the slots might occur.

- At a sufficiently high local Mach number, shocks may form due to the waves.

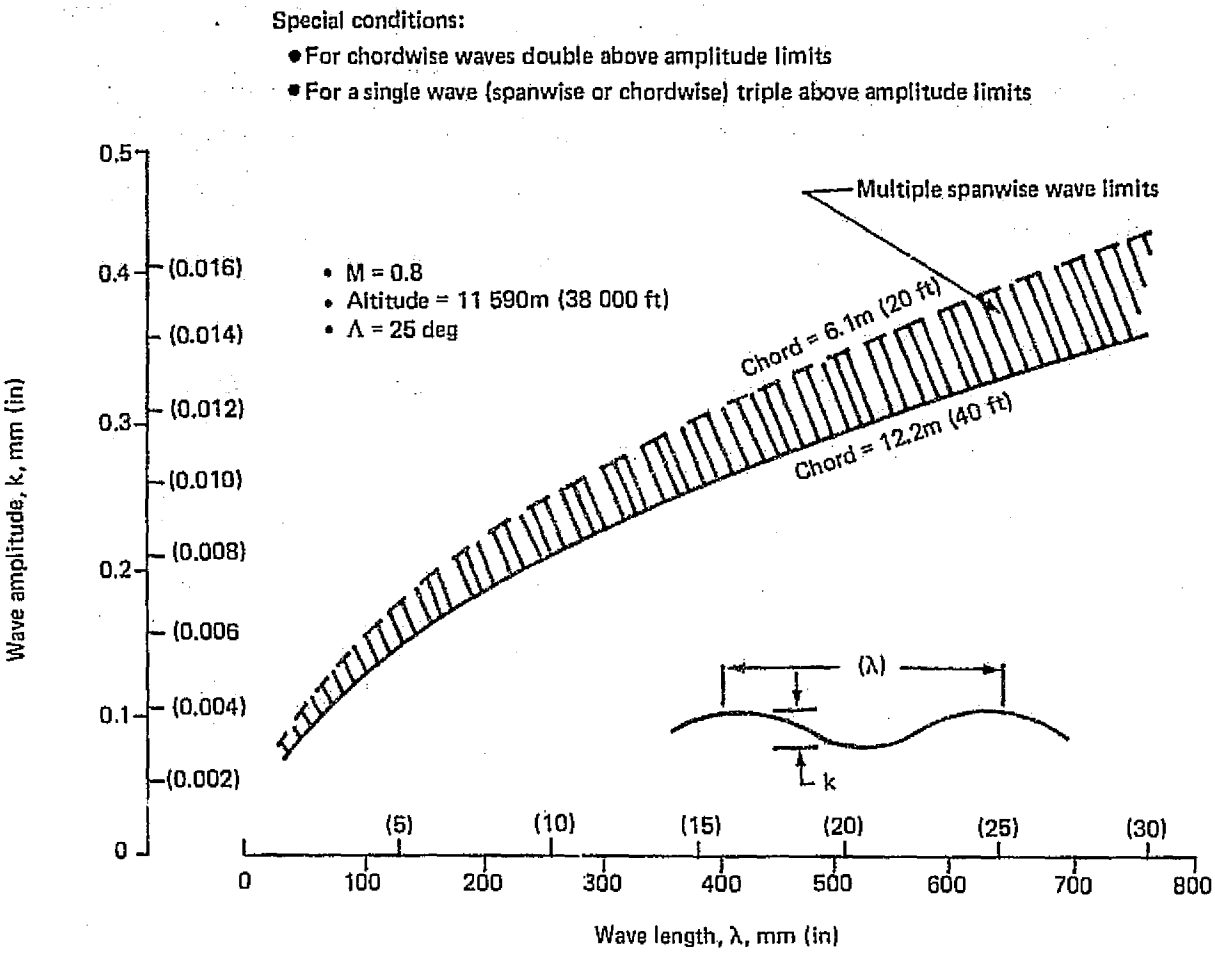

Figure 5.1-2. Typical Surface Waviness Criteria for an LFC Wing

Either of these conditions could reduce the effectiveness of LFC.

Tolerance criteria for discontinuities, protuberances and surface smoothness have been derived on the basis of References 7, 8 and 9. Some typical results are presented in Figure 5.1-3. More recent experiments (Ref. 10) however, indicated that the allowable height of a downstep can be doubled with appropriate boundary layer suction. This means that the aerodynamic design may compensate for an unavoidable surface discontinuity by properly administered suction. This generally would require that suction surface design should provide for special treatment in areas where structural or assembly joints are known to occur.

One of the principal goals of the wind tunnel test program conducted under this contract was to verify, and expand if necessary, the existing surface tolerance criteria. As it will be pointed out in the forthcoming discussion of the wind tunnel test results, the present study has found no contradictory information with the previous findings in regions where the

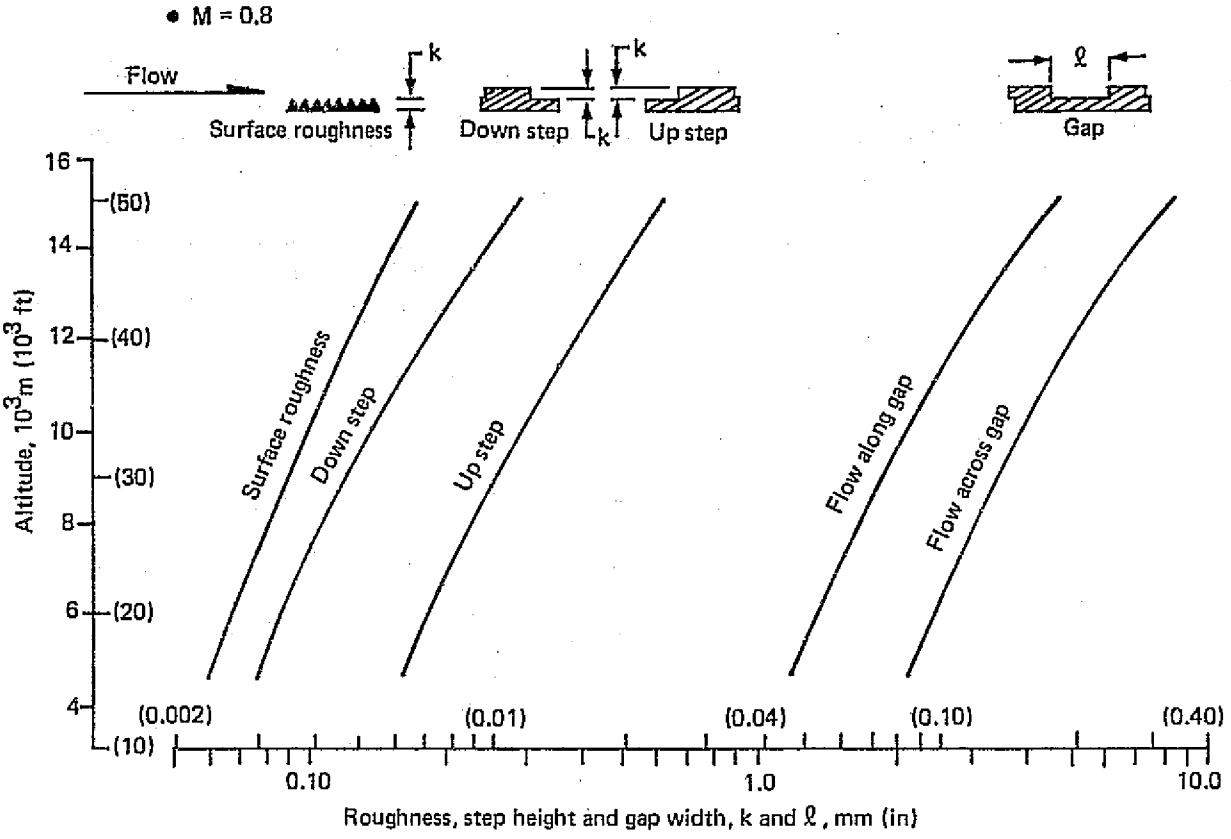

Figure 5.1-3. Typical Surface Roughness, Step Height and Gap Width Criteria for an LFC Wing

crossflow (i.e., sweep effect) was not strong. However, it seems apparent that in those regions of the test wing where significant crossflow prevailed, the sensitivity to disturbances was increased and consequently the applicable tolerance limits would tend to be lower. A precise definition and update of surface tolerance requirements will necessitate the accumulation of much more data supported by analysis and organization to provide a cohesive, validated set of design guidelines.

5.1.1.3 Maintenance Requirements

The aerodynamic design must also consider certain requirements related to maintenance. One of these is the need to provide access holes into the wing so that structure may be inspected from inside. But laminarization of the access hole cover plates appears to be quite difficult, and thus, a portion of the wing area (on the lower surface) may not be available for LFC. The slots and ducts must also be inspectable and cleanable periodically.

Accessibility to the collector ducts beneath the slots appears to be particularly important as this area would be most susceptible to clogging. The impact of these requirements on the aerodynamic design is such that specifications for slot spacing and sizes must be compatible not only with manufacturability but also with maintainability.

Another maintenance oriented requirement is that the design should allow the installation of sensing devices that would continuously monitor for proper functioning of the LFC system. Early detection of defective regions would be highly desirable from the standpoint of reliability and efficiency.

Restrictions imposed by practical repairability must also be kept in mind in connection with the aerodynamic design requirements. Thus for example, sufficient allowances should be provided in the suction system design both in terms of slot geometry and pumping capacity, for maintaining LFC even under slightly deteriorated surface conditions due to field repairs.

5.1.1.4 LFC Systems Requirements

An LFC airplane will have two unique systems not found in conventional aircraft: a) The suction system and b) The leading edge protection and/or cleaning system. The basic requirements regarding the suction system is to provide the necessary pumping power to remove the proper amount of boundary layer air from the wing and to do this in a highly efficient manner so that the losses in the ducting system would be minimal. The problem is complicated by the fact that the LFC system has to operate not only at a fixed design condition, but within a range of flight conditions involving variations in lift coefficient and Mach number. Since the pressure distributions over the wing surfaces may vary considerably with C_L and M variations, the suction system must be as adaptive as possible to the changing flight and associated flow conditions.

Distribution of the suction airflow is done by appropriate throttling but this again must operate within a range of conditions and with the minimum amount of energy loss. As a guideline for reducing duct losses the maximum allowable Mach number should be limited to $M < 0.3$. Propagation of compressor-generated noise through the duct system up to the slots has been noted as a potential problem. This arises because fluctuations in the suction air inflow can be produced, thereby creating disturbances in the external flow. The duct system, therefore, should not be conducive to sound transmission in the critical frequency range and specific noise treatment may be required to avoid this type of adverse interaction.

5.1.2 WING DESIGN

The fundamental concern of the designer of a laminar flow airplane is the aerodynamic design of the wing and the special provisions and systems required to assure essentially full, reliable achievement of laminar flow most of the time under a variety of operating conditions. This subsection deals with the study of the impact of the basic wing geometry and certain design features on meeting the above requirement. It concludes with a definition of the wing for the final LFC transport configuration which is a major result of the concept development activity.

5.1.2.1 Principal Wing Geometry Selection

One of the most critical aspects of the aerodynamic design of an LFC airplane is the selection of wing sweep angle. Experience with conventional turbulent airplanes has shown that

the most efficient designs for high subsonic cruise speeds can be achieved at sweep angles between $\Lambda = 25°$ and 35°. In the case of an LFC airplane, however, sweep has a very powerful adverse effect, inasmuch as increasing sweep will enhance crossflow instability and laminarization of a wing under such conditions will be increasingly more difficult. Figure 5.1-4 illustrates how the sweep affects crossflow instability in the leading edge region of a typical transport type wing such as considered in this study. For combinations of sweep angles and Reynolds numbers below the dotted threshold line, transition would occur principally due to Tollmien-Schlichting type instability somewhere aft of the x/c = 5% chord location. In this region there would not be an express requirement for providing closely spaced suction slots near the leading edge which is a practical difficulty. Above the threshold line, however, crossflow instability in the forward region of the wing becomes sufficiently strong to produce transition unless adequate suction is provided. At sufficiently high sweep angles and Reynolds number this could mean that suction would have to commence right at or very close to the leading edge, which is considered impractical due to the high exposure of the leading edge region to erosion by rain, snow or dust, and incidental ground damage. These considerations alone would tend to limit the applicable sweep angles to about $\Lambda = 20°$ or less if one intends to avoid coping with crossflow instability entirely. But a sweep angle of $\Lambda = 25°$ still seems to be acceptable with the first slot in the root region placed somewhat ahead of s/c = 2%.

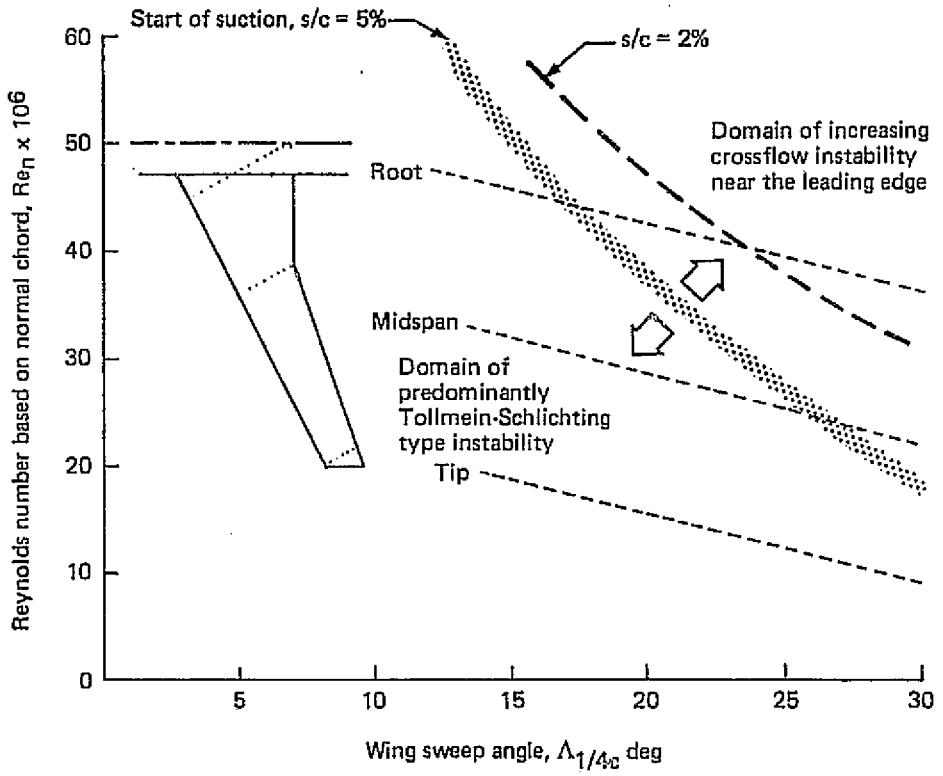

Figure 5.1-4. Effects of Wing Sweep and Reynolds Number on Leading Edge Cross-Flow Instability

The selection of wing sweep angle, however, is also influenced by other considerations, the structural weight of the wing in particular. Figure 5.1-5 illustrates the trade relations between sweep, thickness and relative wing weight. The upper part of the figure indicates the sweep and outboard wing thickness ratio required to achieve a given cruise Mach number, using advanced technology airfoil sections applicable to an LFC airplane in the 1990 time period. Accordingly, a cruise Mach number of M = 0.80 can be achieved at a number of sweep and thickness combinations such as $\Lambda = 10°$ and t/c = 8%, $\Lambda = 15°$ and t/c = 9%, $\Lambda = 20°$ and t/c = 10% or $\Lambda = 25°$ and t/c = 11%, respectively. The lower sweep angles would be desirable for the sake of easier laminarization (reduced crossflow instability), and the associated thinner wings would give lower profile drag and more cruise lifting capability for a given value of critical Mach number. However, the higher sweep angles will allow the wing to be thicker and therefore lighter. This is illustrated in the lower part of Figure 5.1-5, which shows the effect of sweep and thickness on the relative weight of the basic wing structure. It can be seen that for the case of $M_{LRC} = 0.80$ the minimum wing weight would be achieved at sweep angles between $\Lambda = 25°$ and $\Lambda = 30°$, and reducing the sweep below 25° would lead to progressively larger weight penalties. Based on these considerations, a wing sweep angle of 25° was selected for the initial baseline LFC airplane study with the recognition that further studies would be required to validate the selection for the final configuration, particularly with regard to the impact on leading edge viability.

Selection of the other principal geometric features of the wing were less controversial. An aspect ratio of AR = 10 was initially chosen for the baseline airplane on the basis of previous wing optimization studies and the desire to limit the wing span. Subsequent parametric studies, discussed in Section 6.3 verified that selection. A taper ratio of $\lambda = .35$ was chosen on the basis of past experience with long range transport airplanes. The thickness ratio of the outboard wing was again selected on the basis of past design experience to correspond to the sweep selection. As it follows from Figure 5.1-5, the allowable thickness ratio of the main wing panel for a long range cruise Mach number of $M_{LRC} = 0.80$ at a sweep angle of 25° is t/c = 11%. This is predicated on the availability of advanced technology airfoil sections specially tailored for LFC application which, to this date, have been partially validated by experiment. Selecting the appropriate airfoil family however, involved some special considerations which will be discussed in the next section.

5.1.2.2 Airfoil Selection

The principal design characteristics desired of the representative airfoil section are determined by the cruise speed and altitude requirements. In order to obtain a long range cruise Mach number of $M_{LRC} = 0.80$, the drag divergence Mach number of the wing must be at least $M_D = 0.81$. For a sweep angle of 25°, the corresponding section drag divergence Mach number is approximately:

$$M_{D_n} = 0.765$$

To convert from M_D to M_{D_n}, the following empirical formula was used:

$$M_{D_n} = M_D \cos^{.86} \Lambda_{eff}$$

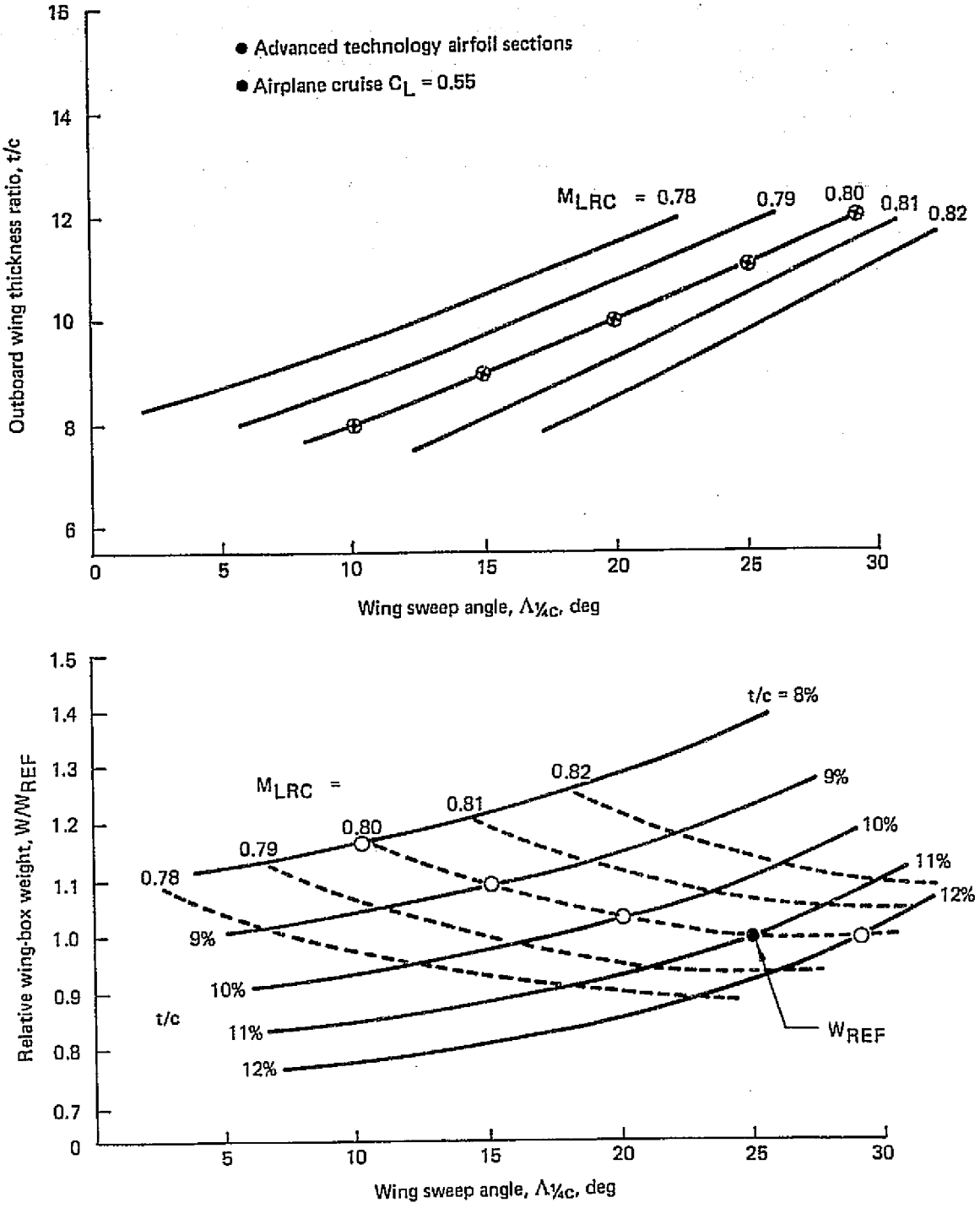

Figure 5.1-5 . Wing Sweep, Thickness, and Weight Trades

where Λ_{eff} is the effective sweep angle which can be closely approximated by the sweep angle of the wing element line at the start of the aft pressure recovery or the location of the shock. For the type of airfoils considered, the shock location at M_D is at about x/c = 70%, thus Λ_{eff} is approximately 20.5° for a 1/4 chord sweep of Λ =25°.

The applicable airplane cruise lift coefficient was selected early in the baseline development cycle based on an initial cruise altitude requirement of 12 190 m (40 000 ft) at M = 0.80, which takes appropriate account of climb fuel usage. This, with a tentative wing loading of W/S = 478 km/m^2 (98 lb/ft^2), requires an airplane lift coefficient of C_L = 0.55, which corresponds to a section lift coefficient of:

$$c_n = 0.70$$

In the conversion of airplane C_L to normal section C_n the following empirical formula was used:

$$C_n = C_L \frac{\kappa}{\cos \Lambda_{½c}}$$

where $\kappa = \frac{c_\ell}{C_L}$, the ratio of the outboard wing local lift coefficient to the airplane lift coefficient.

Figure 5.1-6 illustrates that the above cruise Mach number and lift coefficient requirements are within the capabilities of advanced technology airfoil sections that have been developed in recent years for turbulent airplanes.

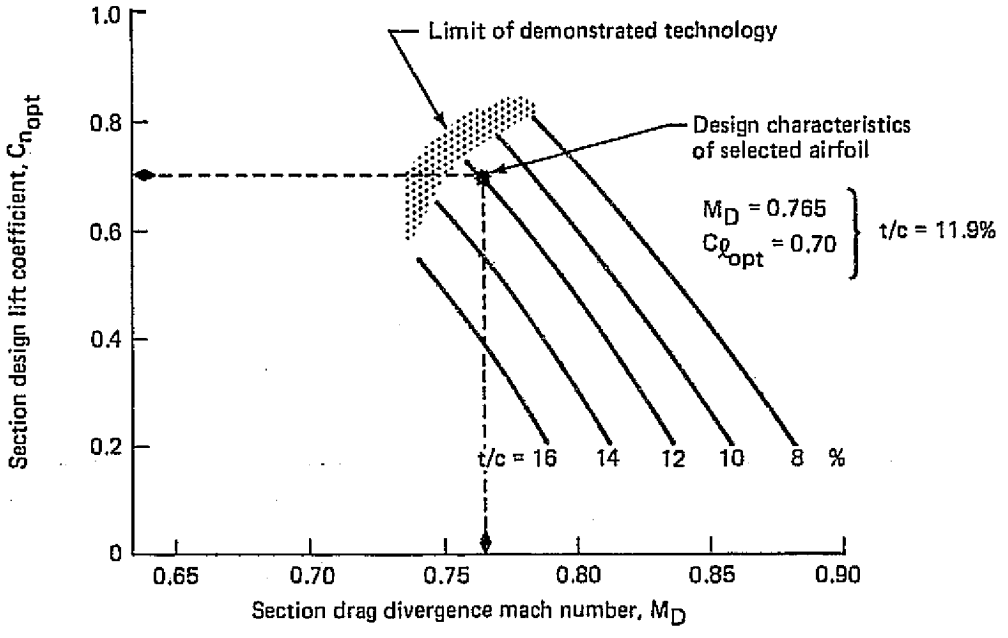

Figure 5.1-6. State-of-the-Art Airfoil Technology

For a number of reasons, the impact of advanced airfoils is even more favorable for LFC airplanes. The following are of principal importance:

1. The increased volume available with greater thickness provides critical accessibility and the space to accommodate internal ducting for suction airflow collecton and removal.

2. With laminar flow surfaces, no significant drag penalty due to thickness occurs as in the turbulent wing case.

3. Tailoring the wing pressure distribution to achieve straight isobars with relatively flat chordwise distributions is more easily achieved. This is highly important for LFC wings since proper suction inflow distributions must be achieved with minimum flow losses.

There are, however certain special requirements that must be considered in the design of an LFC airfoil. The principal ones are as follows:

1. Late pressure recovery to provide as large a fraction of the chord, amenable to laminarization, as possible.

2. Shock-free flow extending throughout the area of laminarization.

3. Narrow regions of rising or falling pressure to minimize crossflow instability.

4. Small leading edge radius, i.e., rapid flow acceleration near the leading edge, to limit the spanwise growth of the attachment line boundary layer that can trigger premature transition.

During the early phase of the work done under this contract an airfoil section was developed that meets the special requirements of the LFC application. The starting point for this airfoil development activity was a contemporary advanced airfoil section designed for turbulent airplane applications. This basic section was, in fact, tested and validated in the two-dimensional airfoil test rig of the Boeing Transonic Wind Tunnel.

The development work for the current application included transforming the section to a different thickness ratio, refining the upper surface contours and modifying the shape of the lower surface pressure distributions.

The resulting airfoil is illustrated in Figure 5.1-7. The geometric features of the leading edge region, as well as the computed initial velocity gradient are presented in Figure 5.1-8. The section pressure distributions, computed by the Korn-Garabedian transonic flow program, are shown in Figure 5.1-9, for several principal points of the design envelope. Based on these data, the attachment line flow characteristics were estimated, indicating that the attachment line boundary layer Reynolds number would not exceed the critical threshold of $R\theta_{a.1.} = 100$ throughout the outer 75% of the span. For the inner 25%, where the wing is considerably thicker than the basic airfoil section, $R\theta_{a.1.}$ would exceed the threshold value

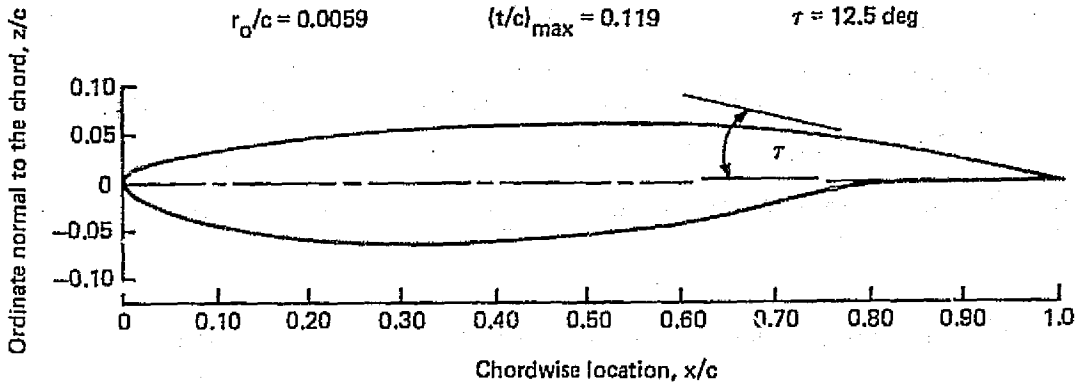

Figure 5.1-7. Representative Airfoil Section for the Outboard Wing (Normal Cut)

if no special treatment were applied. It is contemplated, however, that the leading edge near the wing root will have a special tailoring, which can be expected to eliminate the problem. This will be discussed later in connection with the wing geometric description.

One significant feature of the airfoil section of the LFC wing is an articulated trailing edge flap which appears to be highly desirable in order to provide the capability of maintaining a near-constant angle of attack, which corresponds to near-optimum flow conditions over the wing during cruise. This allows the airplane to cruise with fully effective LFC over a larger range of lift coefficients and Mach numbers and thus provides a reasonable operating envelope. Still another advantage of such a device is the capability to compensate for the change in pressure distribution that would occur in the case of loss of LFC. The trailing edge articulating system of course, must be integrated with the basic high-lift device in such a way that the initial movement of the flap would constitue the camber adjustment for cruise. The required flap deflection angles are, however, quite small and would cover a range of not more than about 5 degrees.

5.1.2.3 High Lift Systems

The principal difference between the high-lift system chosen for the present design and the one that would be used on a contemporary turbulent airplane is the lack of a leading edge device. The compelling reason for this choice was, of course, the practical difficulty associated with maintaining laminar flow across a surface discontinuity that would be unavoidable with any movable leading edge device. However, because of the high cruise altitude requirement for an LFC airplane, the resulting lower values of wing loading and thrust loading provide more than adequate takeoff and landing performance. Thus, a leading edge high lift device is not essential and, in fact, even the trailing edge flap system may be a relatively simple, single-slotted design.

Figure 5.1-10 illustrates the principal features of the high lift system chosen for the final airplane configuration developed in this study. The flap chord was kept to a minimum, c_F/c = 0.20, in order to make as large a fraction of the wing chord available for laminarization as possible. Application of LFC to the flap surface, however, is considered impractical. As mentioned in a preceding paragraph, the trailing edge flap system must also perform an

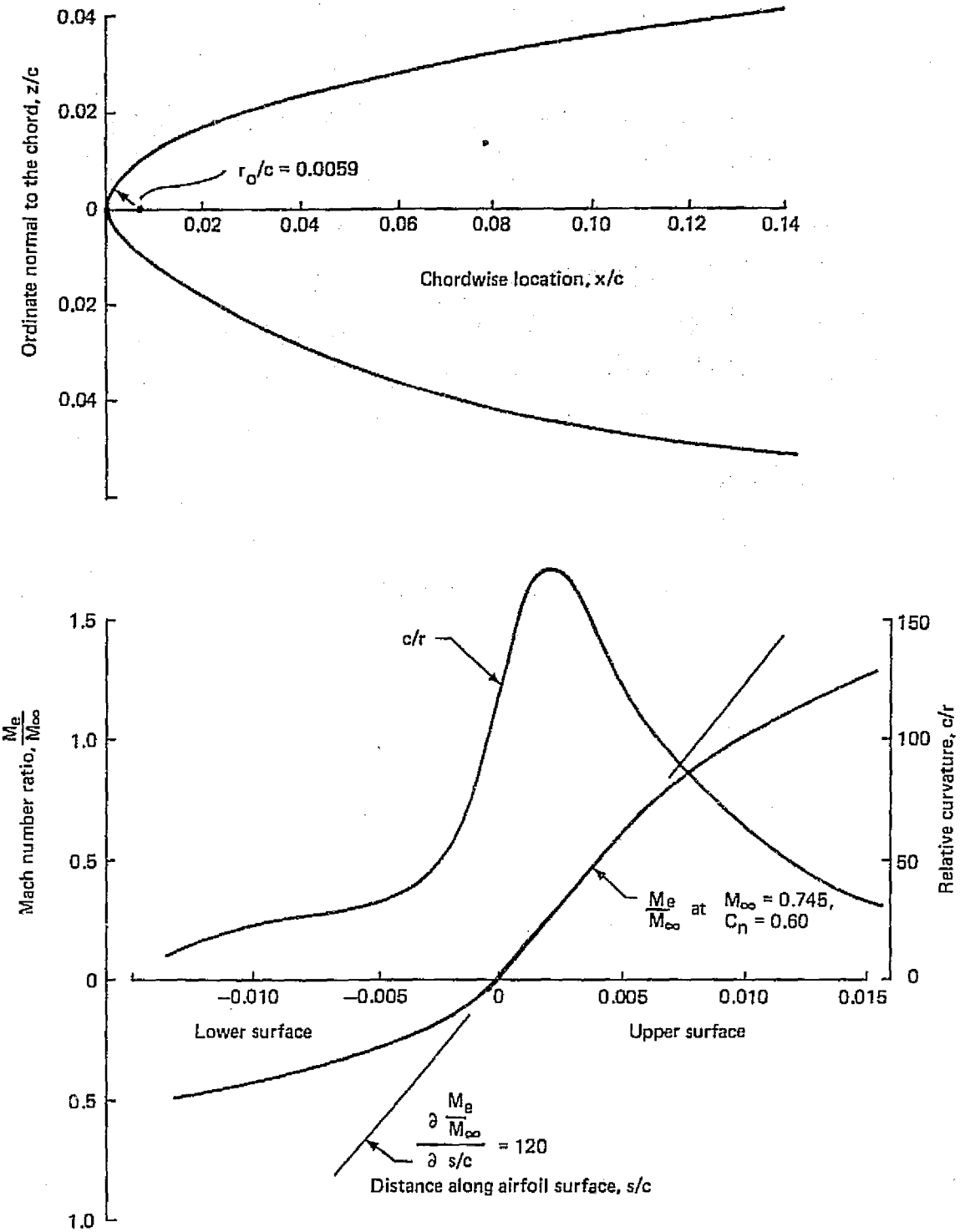

Figure 5.1-8. Nose Geometry of Basic Airfoil Section

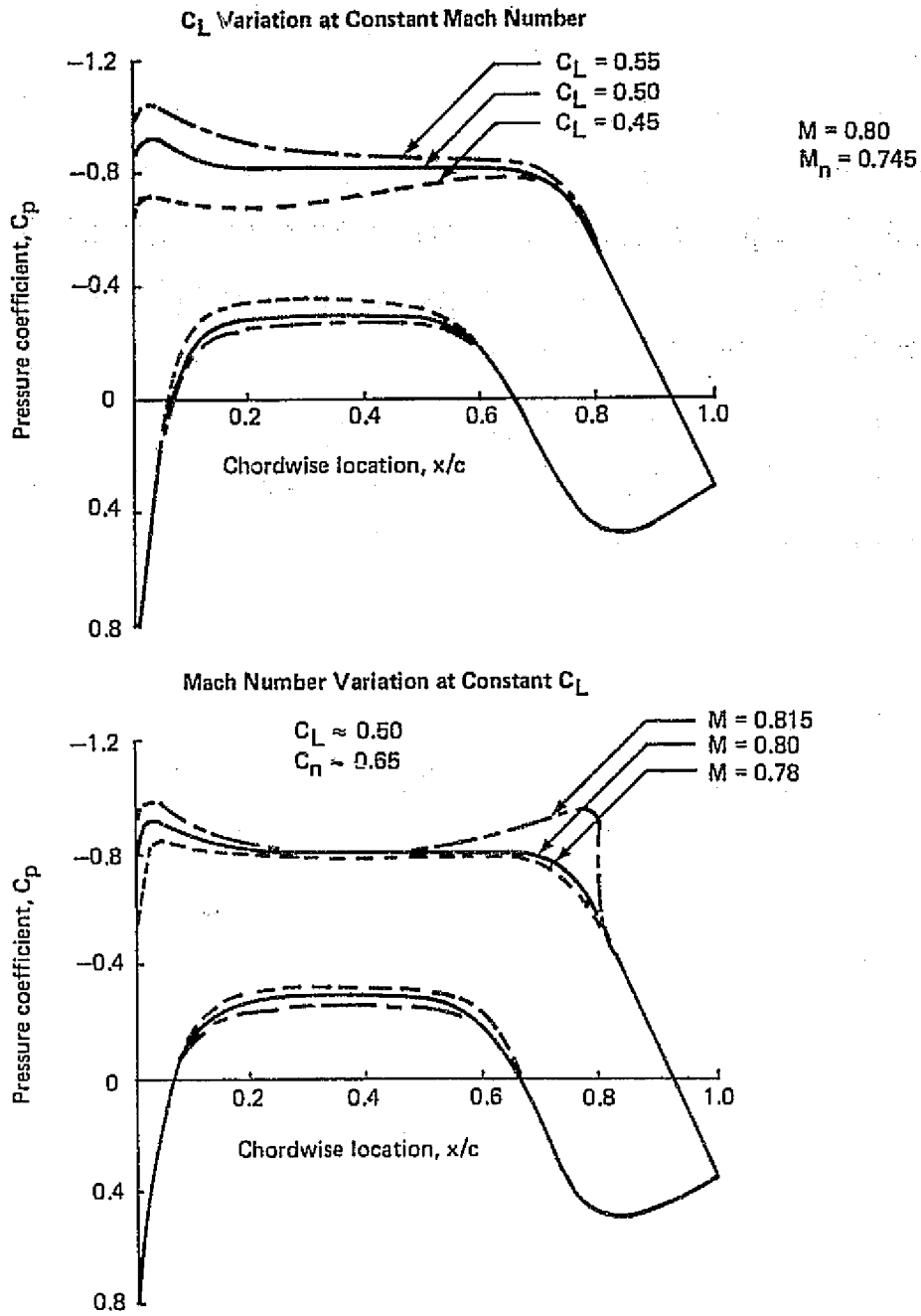

Figure 5.1-9. Theoretical Pressure Distributions for the Basic Airfoil Section (Inviscid Flow)

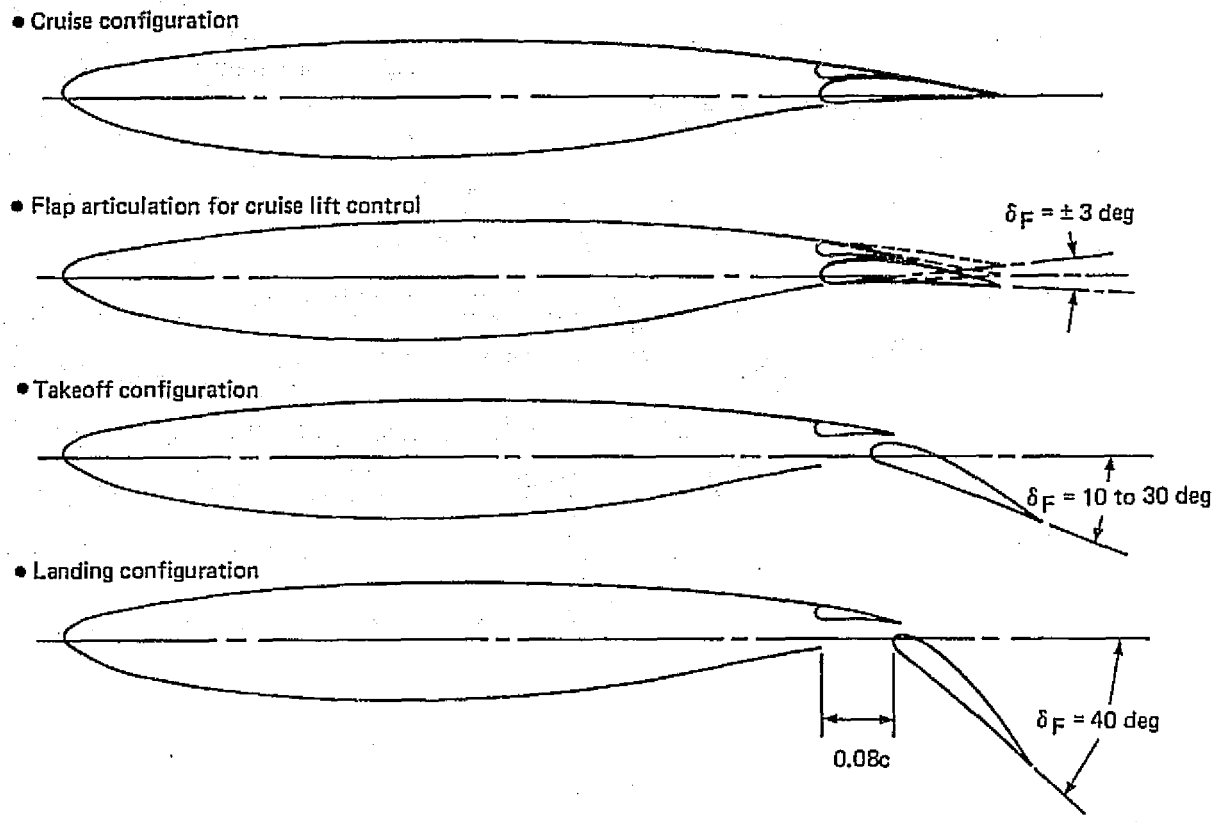

Figure 5.1-10. Principal Features of the High-Lift System

auxiliary function during cruise, that is to keep the pressure distribution near optimum through camber adjustment. In this mode of operation, the flap is still fully retracted and the spoiler remains in contact with the flap without any gap. In the takeoff configuration, the flap may deflect over a range of flap angles, between $\delta_F = 10°$ and 30°, with corresponding partial Fowler motion. For landing, the flap can be deflected up to $\delta_F = 40°$, with a maximum Fowler movement of $\Delta x_F = 0.08$ c.

The inboard ailerons are drooped with flap deflection up to a maximum angle of 20° in order to improve flap lift carry over and improve L/D. Also, the inboard flap is extended all the way to the fuselage underneath the suction engine, for the same reason. Figure 5.1-11 shows the arrangement of the high lift devices in relation to the wing planform.

5.1.2.4 Flight Controls

The lateral control system provided for this airplane is conventional, featuring both ailerons and spoilers. The inboard ailerons are intended for high speed application to augment the spoilers and provide control redundancy. The outboard aileron is used for low speed operation only. Both ailerons incorporate the camber adjusting feature for high speed flight and the inboard aileron is also drooped with the flaps (up to 20°) at low speeds. The spoilers occupy the same spanwise extent as the flaps. The spoilers also provide flight path control

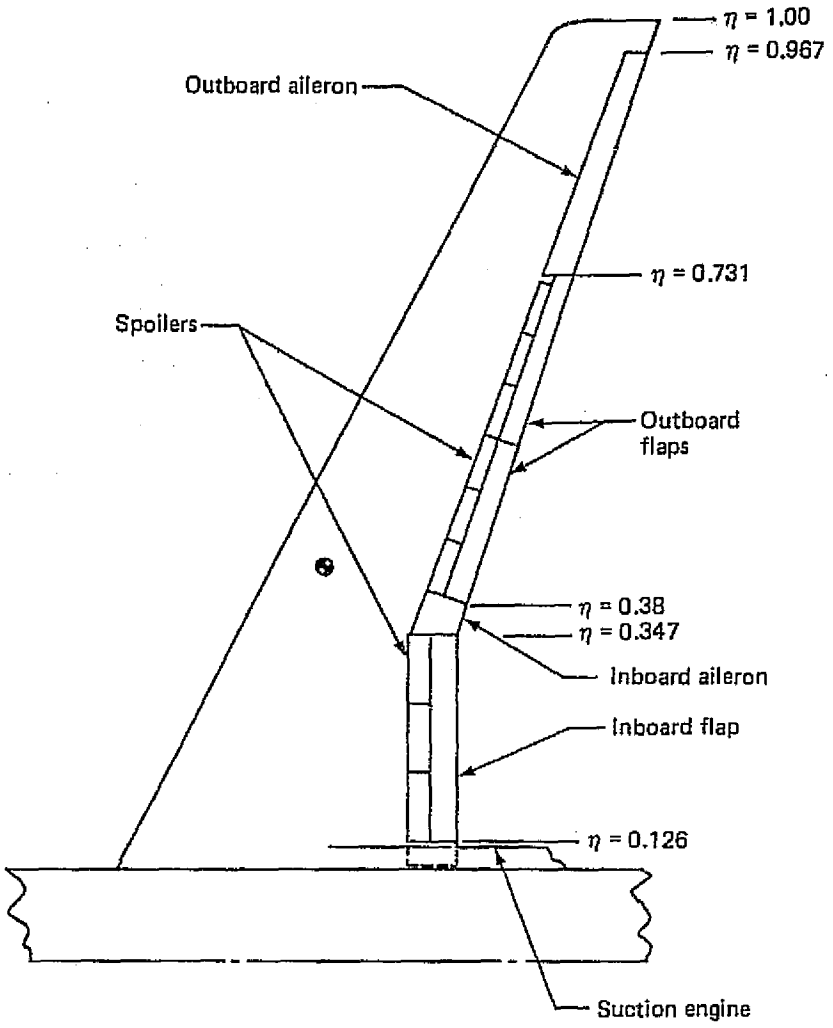

Figure 5.1-11. General Arrangement of High-Lift and Lateral Control Systems

for meeting emergency descent requirements in the case of loss of pressurization and are useful as lift reducing devices during landing roll. The application of spoilers, however, was adopted with some reluctance since they occupy a sizable portion of the wing area that could potentially be laminarized. Nevertheless, more detailed studies of the optimum extent of laminarization indicated that the area occupied by the spoilers would be quite difficult and uneconomical to laminarize anyway. Therefore, the incorporation of spoilers does not significantly reduce the airplane performance potential.

5.1.2.5 Extent of Laminarization

A much debated question regarding the practical application of LFC is the optimum extent of laminarization. Obviously, full chord laminar flow would yield the lowest drag, but it becomes more and more difficult, and hence costly, to maintain laminar flow throughout

the aft pressure recovery region of the wing. It is quite likely, therefore, that the optimum extent of laminarization would be less than full chord when all ramifications are considered.

To support the aerodynamic side of the argument, studies were carried out to determine the effect of progressive extension of LFC on wing section profile drag and on airplane cruise efficiency.

The initial phase of the study was concerned with wing section profile drag. The two principal drag components, the "wake drag" and equivalent suction drag were determined theoretically for the representative mid-span section of the wing as a function of the extent of laminarization. The wake drag was estimated on the basis of boundary layer calculations performed by computer code TEM 139, a Boeing quasi-three-dimensional computer program that can handle mixed boundary layers (partly laminar, partly turbulent) with or without suction. The suction rates applied to the laminar portion of the boundary layer were determined on the basis of stability calculations in the manner discussed in Section 5.1.3. The section profile drag coefficient itself was derived from the calculated momentum thickness and shape factor using the Squire and Young formula. Since it reflects the remaining momentum loss at the trailing edge, it may be also called the "wake" drag coefficient. The results are shown in Figure 5.1-12, separately for the upper and lower surface. The equivalent suction drag was calculated, using the approximate equation below, on the basis of the suction flow coefficient required for the maintenance of laminar flow, and the estimated plenum chamber pressure coefficient, C_{p_s} at the compressor face, which was assumed to be 20% lower than the minimum pressure coefficient on the wing surface. Although a more precise calculation of C_{p_s} may finally be desired, the error involved in overall drag is very small and seems permissible at this stage.

$$C_{d_s} = \int_0^1 C_q \left(1 - C_{p_s}\right) d\frac{s}{c}$$

Figure 5.1-13 illustrates the results showing the external and suction inflow distributions as well as the cumulative values of equivalent suction drag as a function of the extent of laminarization.

The final results of this study are summarized in Figure 5.1-14, which shows the individual wake drag components for the upper and lower surfaces, plus the sum of these, as well as the equivalent suction drag. It can be seen that the wake drag component decreases quite significantly as full chord laminarization is approached. The equivalent suction drag, however, is rapidly building up aft of about 70% chord laminarization so that the net gain in total profile drag reduction is not so significant for laminarization beyond 80% chord.

In a later phase of the study, the effect of the extent of laminarization on the cruise efficiency of the complete airplane was also estimated. These results are summarized in Figure 5.1-15. From the standpoint of pure aerodynamic efficiency, there appears to be a definite merit in carrying suction all the way to the trailing edge, even with equivalent suction drag being included. But the increased complexity and the associated weight and cost penalties tend to override the aerodynamic benefits. Thus, after all factors were considered, it was concluded that full chord laminarization, at the present state of the art, would not be prac-

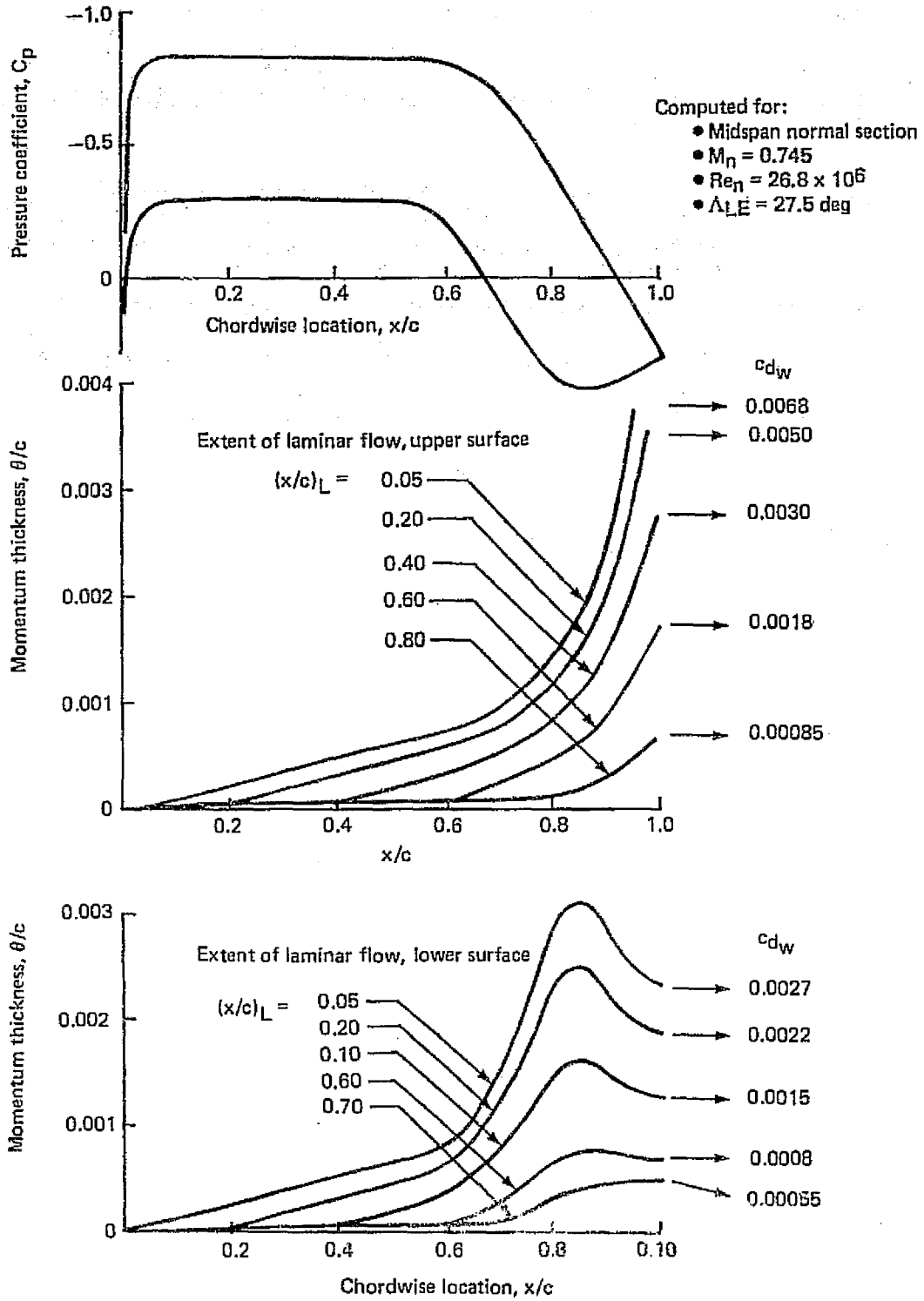

Figure 5.1-12. Momentum Thickness Growth as a Function of Laminarization

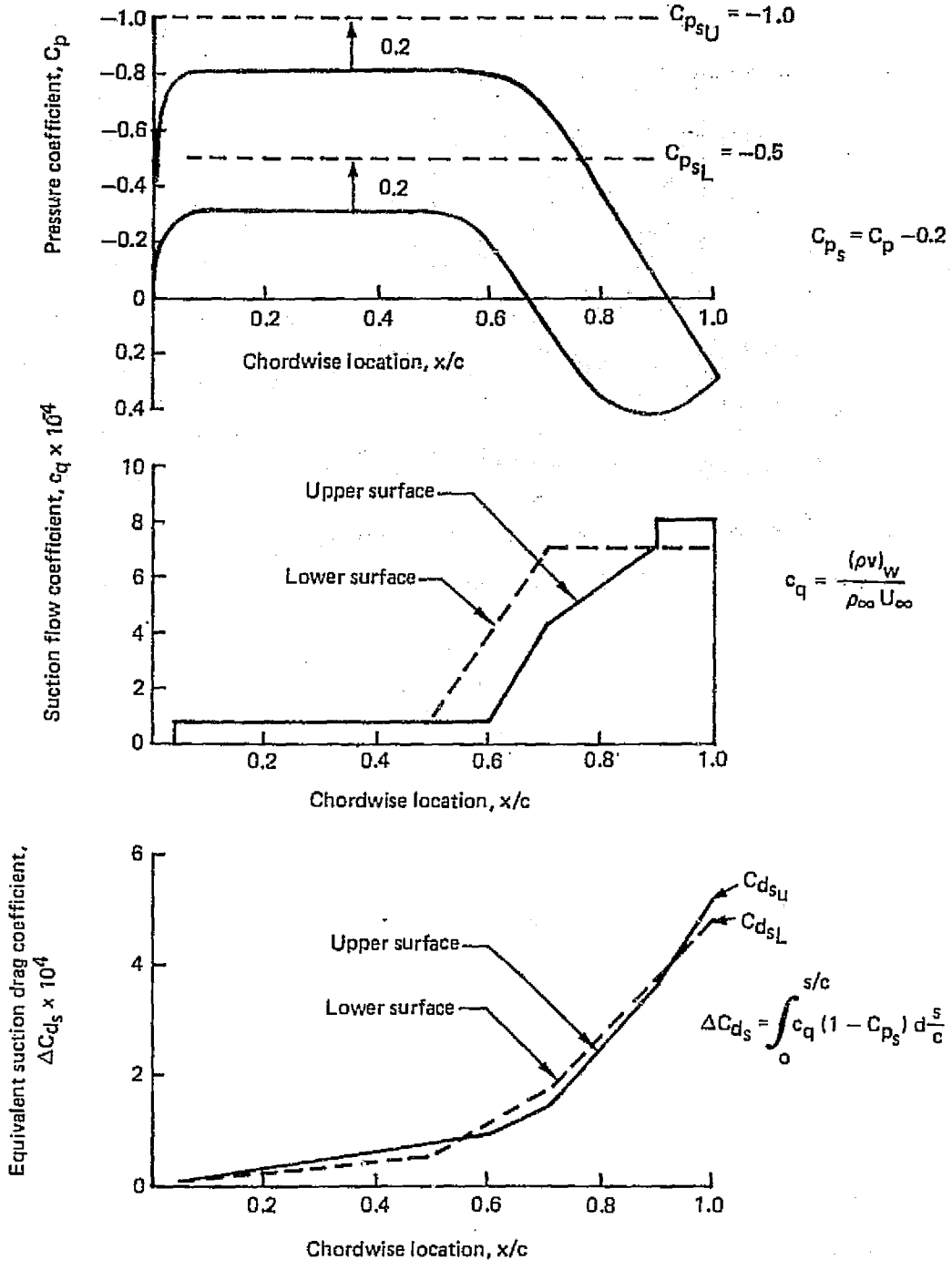

Figure 5.1-13. Flow Coefficient and Equivalent Suction Drag Coefficient as a Function of Laminarization

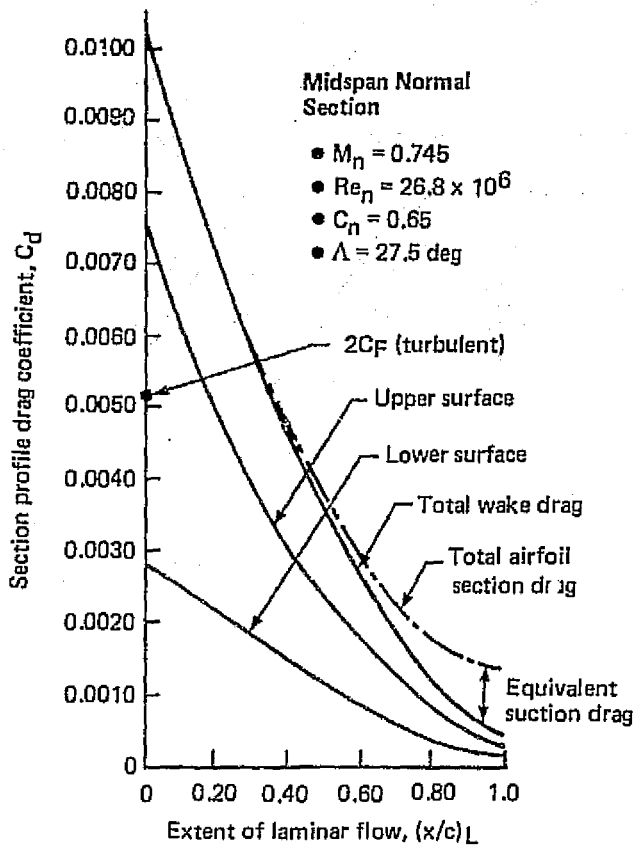

Figure 5.1-14. Wing Section Profile Drag as a Function of Laminarization

tical. The optimum extent of laminarization, appeared to be about 70% to 80% chord, that is the area forward of the flaps and control surfaces. Consequently, the limits of laminarization for the present design study were set as 80% of the upper surface and 70% of the lower surface. In the parametric trade studies, such as presented in Figure 5.1-15, a mean value of $(x/c)_L$ = 75% was used.

5.1.2.6 Wing Geometry Definition

Having selected the basic wing design parameters such as sweep, aspect ratio, thickness ratio and airfoil type, the principal tasks for the detail aerodynamic design of the wing remain the following:

- Provide a suitable wing root design which constitutes a transition from the representative outboard wing airfoil section to a considerably thicker and appropriately shaped root section. The main objectives are to avoid undue interference drag and preserve the characteristic shape of the outboard wing pressure distributions as far inboard as possible.

- Develop a twist distribution that provides a prescribed form of span-loading.

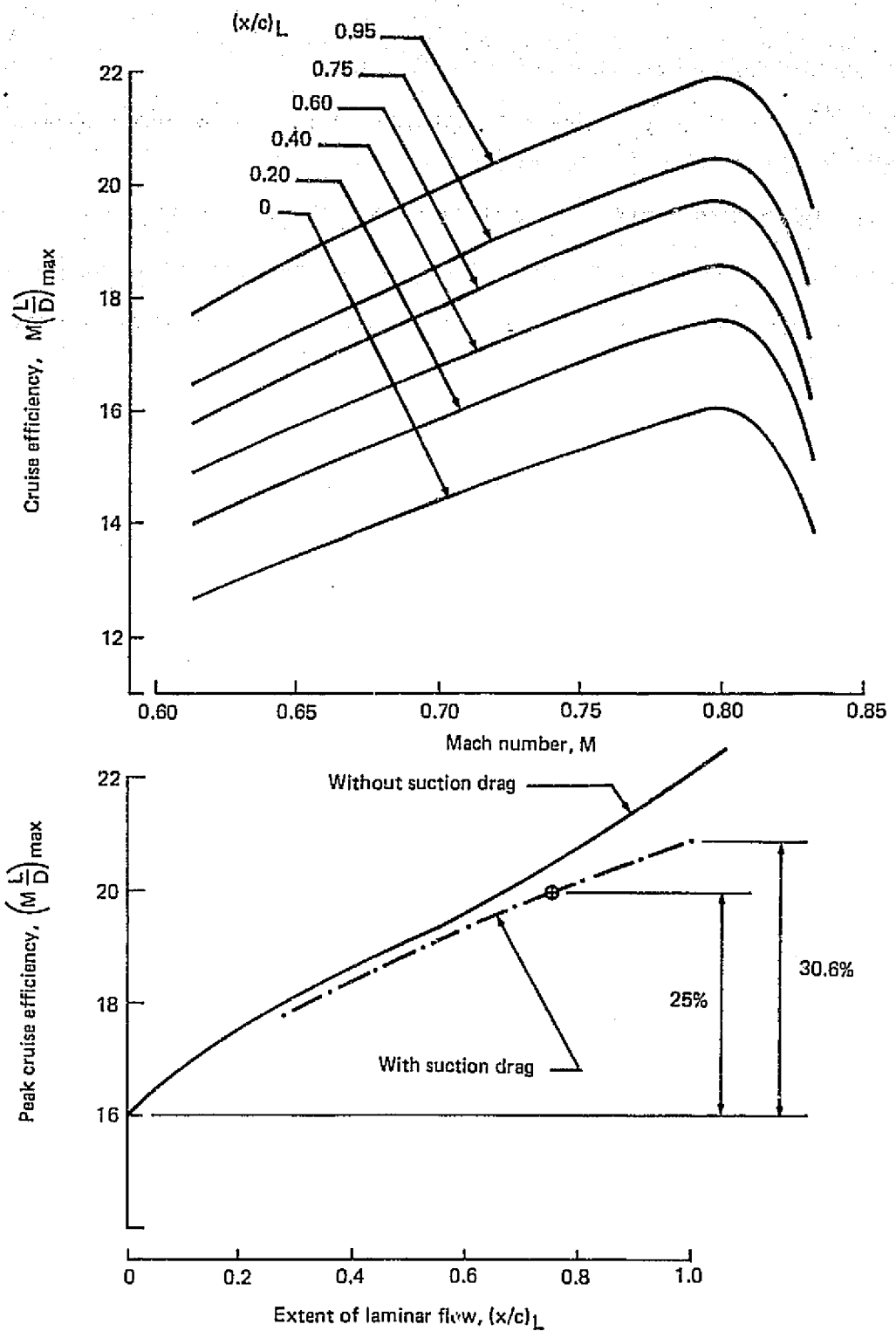

Figure 5.1-15. Cruise Efficiency as a Function of Laminarization

- Maintain an isobar pattern that is composed of essentially straight lines following the constant chord fraction element lines of the wing.

The requirements for an LFC airplane are more stringent in this respect than in the case of a turbulent airplane since excessive spanwise pressure gradients along slots are not tolerable.

The approach followed in the geometric definition of the wing was the same as currently practiced within the Boeing Company in the design of subsonic transport airplanes. This approach is based upon the combination of subsonic three-dimensional potential flow theory and developmental testing in the wind tunnel. Past experience has established the correlation between experimental data obtained in both subcritical and supercritical flows, and the correlation between theory and test in subcritical flows. Thus, the guidelines for designing for the supercritical case using computational methods valid only for the subcritical case have been well established.

During the present exercise, computer code A-236, a Boeing three-dimensional subsonic potential flow program, was used to analyze the total wing flow characteristics and provide a basis for the design of the root region. This approach, however, is adequate only for a tentative definition of the wing. Fine tailoring can be done only through wind tunnel testing. The use of recently introduced three-dimensional transonic flow programs was considered for this study as a substitute for testing. This option, however, has not been exercised for LFC wing design, due to the very costly and time consuming nature of these computations. Also, the limited experience with such methods to date has indicated that they are not developed to the point where they can supercede the established methodology.

The principal geometric features of the wing such as the planform, the spanwise variation of maximum thickness ratio and twist as well as a few representative airfoil sections are presented in Figures 5.1-16 and 5.1-17. The relatively blunt airfoil sections in the root region reflect the trends dictated by desirable transonic flow characteristics but, in fact, tend to be incompatible with the requirements of LFC. The adverse effects of the blunt leading edge in the root region, however, are fully realized and this problem will be a subject for further discussion. Previous experience with the Northrop X-21 LFC research aircraft emphasized the significance of spanwise contamination that is directly related to the wing leading edge radius and sweep. Subsequent research has developed some possible solutions such as, spanwise flow arresting fences, a leading edge bump to increase local curvature, and suction through chordwise slots at the immediate vicinity of the leading edge. The latter approach was found to be the most effective cure according to the Northrop experiments, but unfortunately, there has been a serious doubt as to the practicality of this solution. It would be much more plausible to solve the spanwise contamination problem with localized tailoring of the wing nose geometry. The most recent work of Dr. W. Pfenninger appears to be a promising approach toward this end.

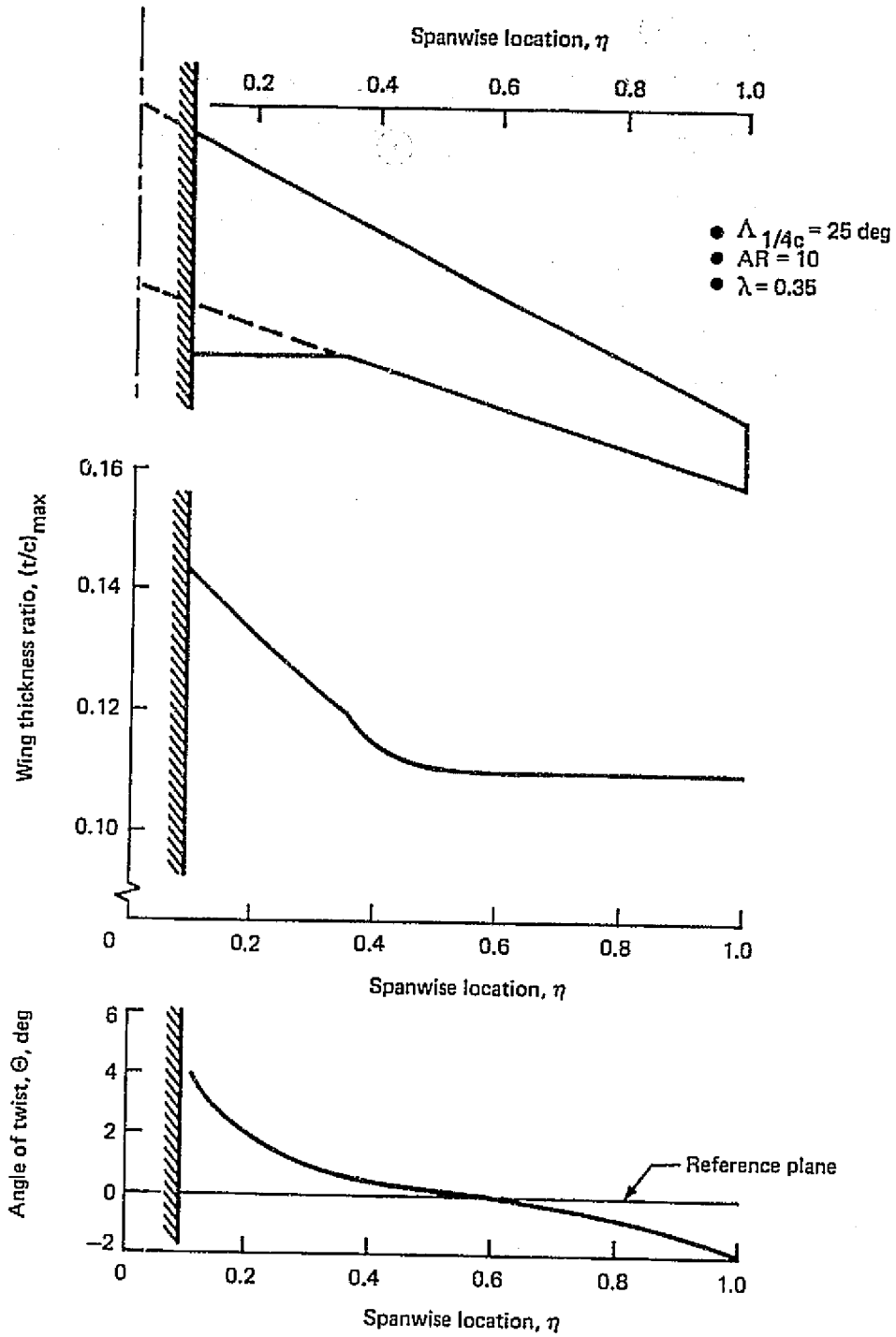

Figure 5.1-16. Principal Wing Geometry Definition—Planform, Thickness, and Twist

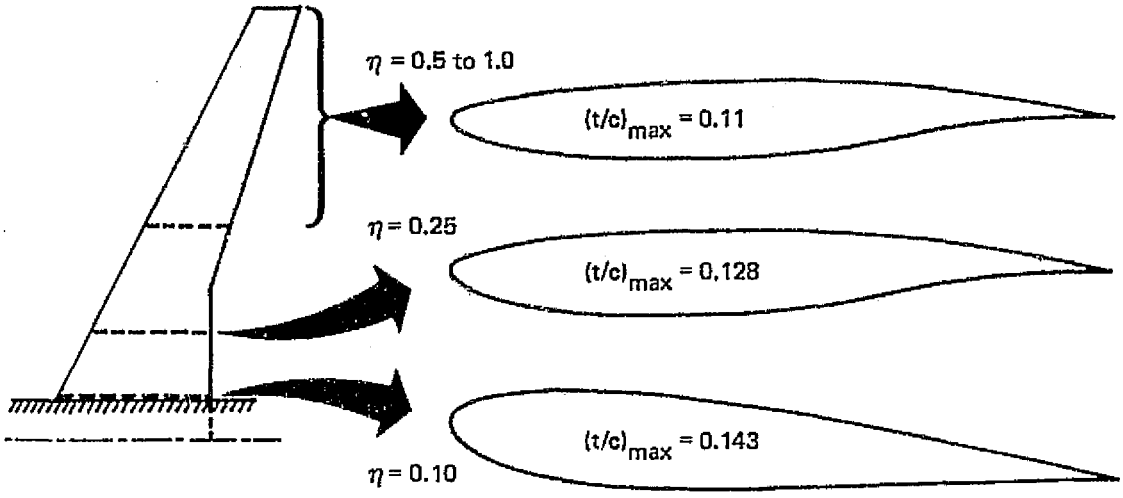

Figure 5.1-17. Representative Airfoil Sections

The variation of the estimated attachment line boundary layer Reynolds number, $Re\theta_{a.l.}$, along the span is shown in Figure 5.1-18 for the nominal cruise Mach number of M = 0.80 and two different altitudes. $Re\theta_{a.l.}$ was calculated by the following relation, given in Reference 2.

$$Re\theta_{a.l.} = \frac{\theta^*_{a.l.}\, V_\infty \sin \Lambda_{LE}}{\sqrt{\nu\, (\partial U/\partial s)_{a.l.}}}$$

where

$$\theta^*_{a.l.} = 0.405$$

The initial velocity gradient normal to the leading edge, $(\partial U/\partial s)_{a.l.}$ was determined on the basis of 2-D transonic flow computations. It is evident from Figure 5.1-18 that throughout the outer two-thirds of the span, $Re\theta_{a.l.}$ is below the critical threshold value of 100, but in the root region, due to the increased leading edge radius, the critical value of $Re\theta_{a.l.}$ would be exceeded if no special tailoring of the leading edge was made. The manner, in which the leading edge in the root region might be tailored, is illustrated in Figure 5.1-19. In carrying out such a tailoring of the root region, one must know the magnitude of the permissible leading edge radius. This can be estimated on the basis of the above relation by making $Re\theta_{a.l.} = 100$ and approximating the initial velocity gradient by

$$\left(\frac{\partial U}{\partial s}\right)_{a.l.} = \frac{U_\infty\, (1 + \tau_0)}{r_0}$$

where r_0 is the radius of curvature at the leading edge and τ_0 is the thickness ratio of the inscribed ellipse applicable to the wing section normal to the leading edge.

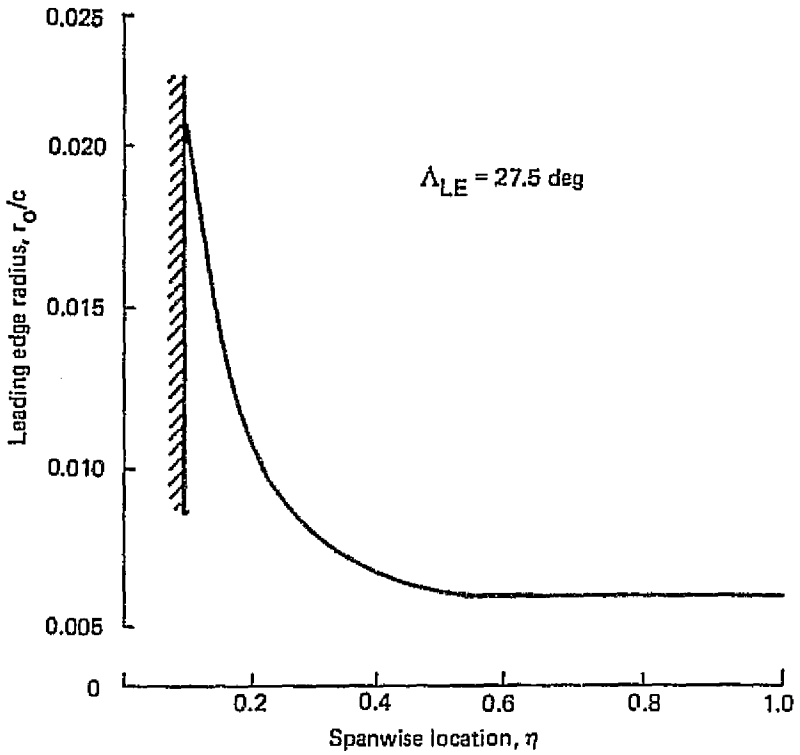

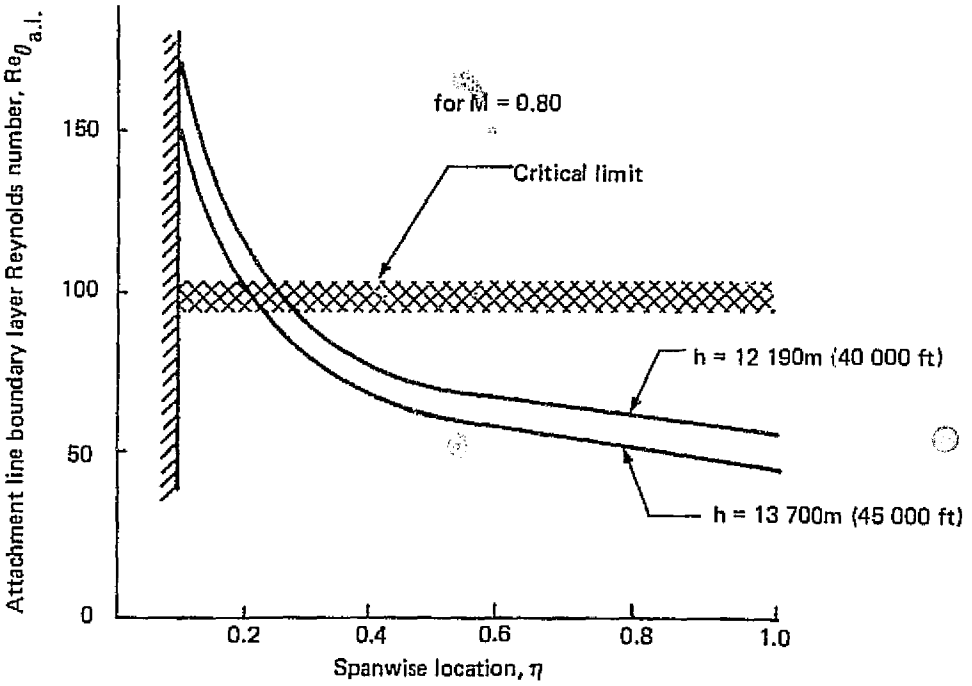

Figure 5.1-18. Variation of Attachment Line Boundary Layer Reynolds Number Along the Span

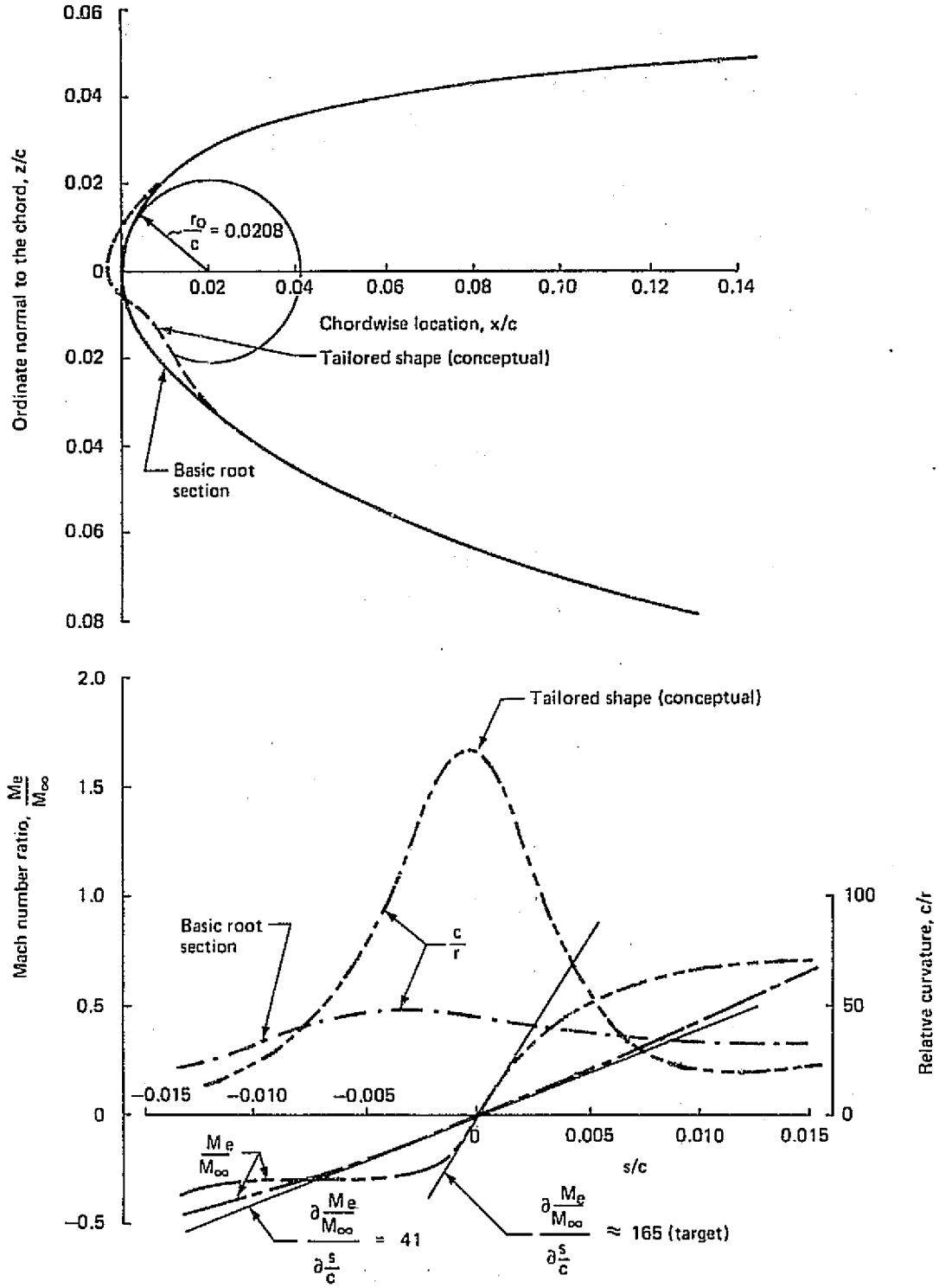

Figure 5.1-19. Nose Geometry of Root Airfoil Section

The results of such calculations for the present wing are shown in Figure 5.1-20. Accordingly, the maximum allowable radius in the root would be $(r_o/c)_{max} = 0.007$ at the nominal cruise condition of M = 0.8 and h = 12 190 m (40 000 ft) and $(r_o/c)_{max} = 0.009$ at h = 13 700 m (45 000 ft). If the allowable attachment line boundary layer Reynolds number could be raised to 125, the corresponding leading edge radius limit for the root would increase to $r_o/c = 0.011$. This type of tailoring appears to be feasible and would not alter the flow characteristics over the root airfoil section significantly as a whole.

It is also apparent from Figure 5.1-20 that the $Re_{\theta_{a.l.}} = 100$ criterion would allow substantially larger leading edge radii over the outboard portion of the wing than contemplated by the current wing definition. A more generous leading edge radius, however, may be desirable from the standpoint of favorable stall characteristics and could provide a leading edge less susceptible to erosion.

As a conclusion to the description of the basic wing design studies, the theoretical isobar patterns, calculated for subcritical flow at M = 0.70, are presented in Figure 5.1-21. It is apparent that the wing defined above would provide a reasonably straight isobar pattern under subcritical flow conditions which, according to the current experience, is a prerequisite of a

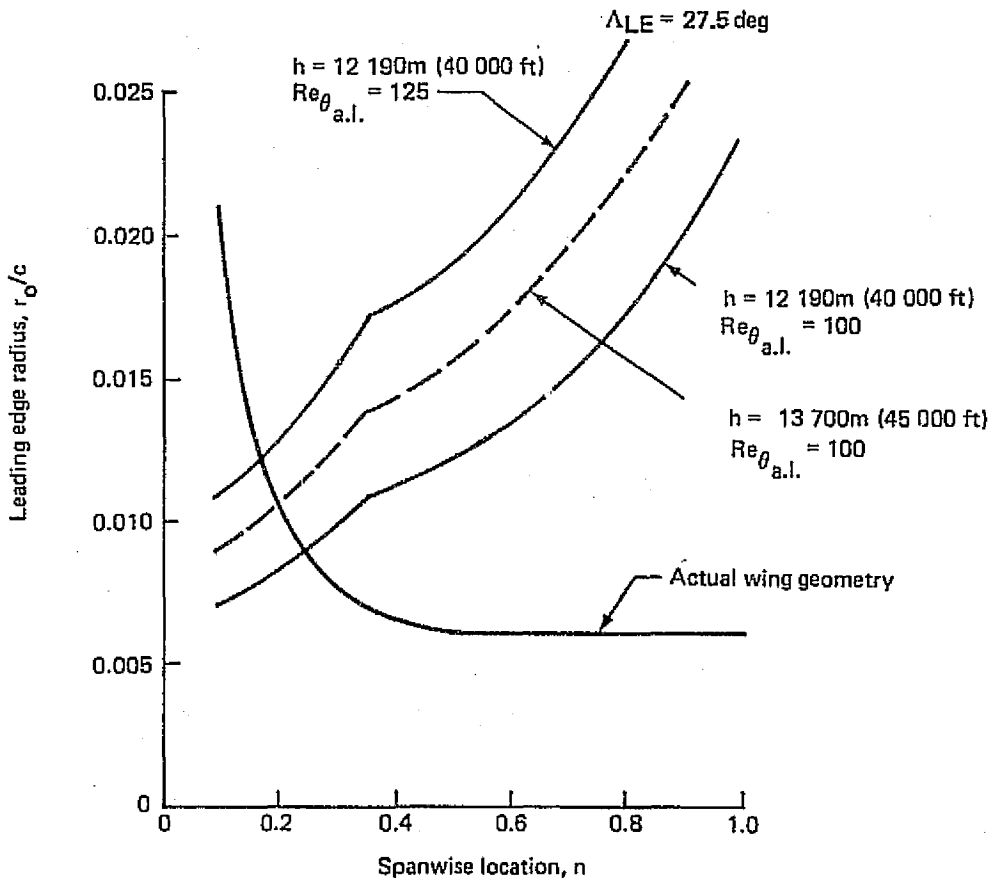

Figure 5.1-20. Desirable Leading Edge Radius To Keep $Re_{\theta_{a.l.}}$ Below the Critical Limit

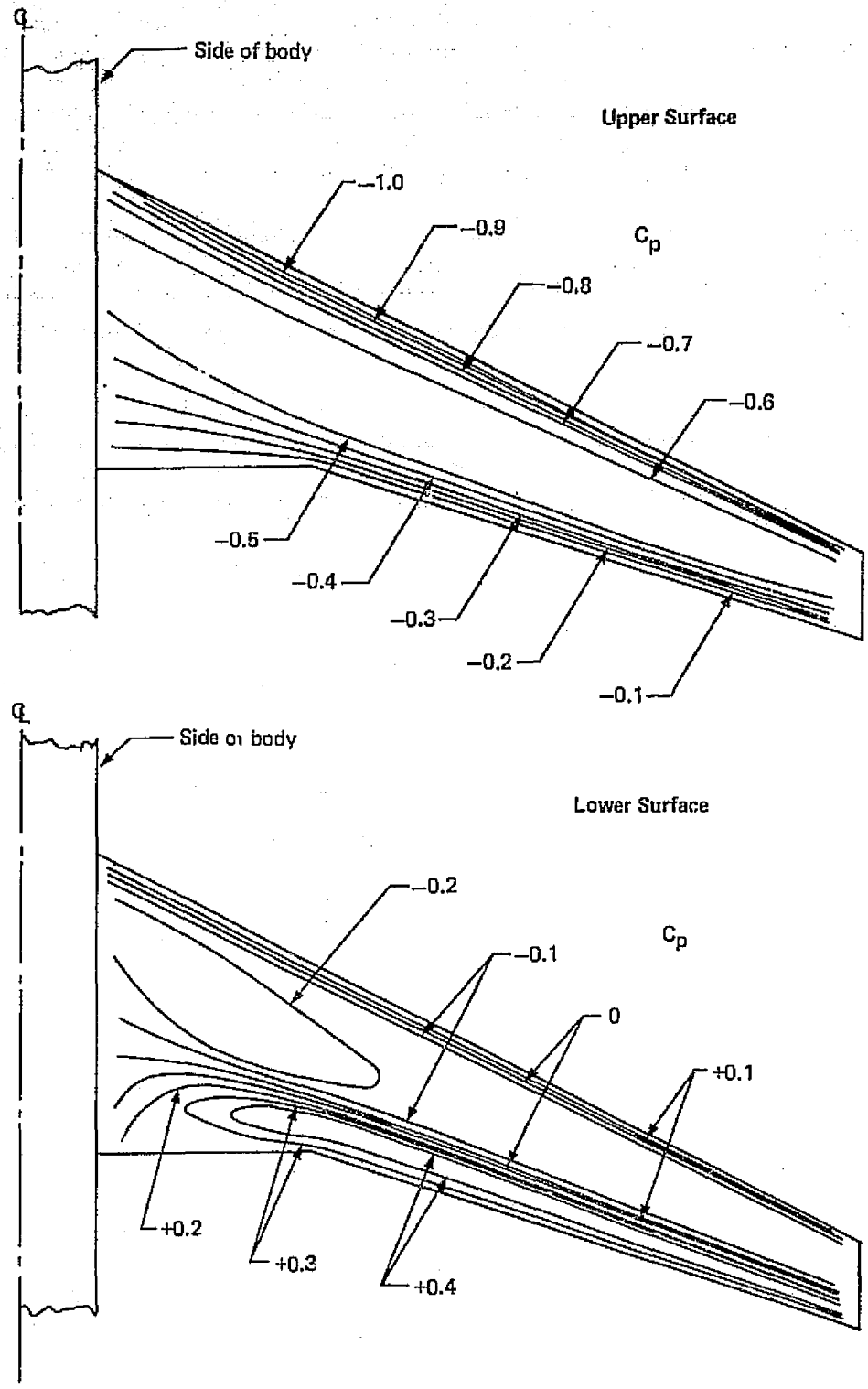

Figure 5.1-21. Theoretical Isobars for Subcritical Flow at M = 0.70, $C_L \approx 0.5$

successful design. The only area where the criteria for straight isobars would not generally be met is the inboard aft region of the lower surface. It is, however, not critical at all, since this particular region of the wing would not be available for laminarization anyway because of the presence of the landing gear doors.

As far as the transonic flow characteristics of this wing are concerned, it is judged that past experience with similar designs plus correlations between tests and transonic theory involving two-dimensional airfoils provide an adequate basis for estimating the performance of the wing under cruise conditions. Consequently, a three-dimensional transonic flow analysis, using the latest computer methods, was not carried out for the wing chiefly because of cost and time considerations. In addition, however, current Boeing experience indicates that the existing three-dimensional transonic wing design methods will not adequately predict the transonic flow characteristics at this stage of their development. Thus, the design approach taken here still serves as the best basis for defining a wing geometry which is the starting point for the detailed tailoring process normally carried out in the wind tunnel. The present level of analysis, in any case, has provided an adequate basis for the subsequent studies involving the design of the suction slot system, the internal ducting system, the suction pumps and the wing structure.

5.1.3 SUCTION SURFACE DESIGN

The essential feature of the wing with LFC is the provision for ingesting a portion of the boundary layer flow through suitable openings in the wing surface and into the internal flow passages. These direct the suction air to the trunk ducts leading directly to the suction units, which exhaust the flow overboard. The inflow distribution must be tightly controlled and the removal accomplished in a way that will minimize the effects of external disturbances and avoid the creation of additional disturbances during the ingestion process.

The design and analysis of the wing suction surface will be discussed in this section. This includes the methods used, the design studies conducted, and the suction and slot requirements of the selected configuration.

5.1.3.1 Boundary Layer Stability Analysis Methods

In order for laminar flow control to make a substantial contribution to overall airplane efficiency, it is important to minimize the amount of suction required to control the growth of disturbances in the boundary layer. Increased suction requirements will result in increased suction drag, increased duct volume requirements, an increased number of slots, and increased airplane weight. Too much suction beyond that required to limit disturbances in the boundary layer can even result in transition due to an excessive thinning of the boundary layer, which makes it more sensitive to surface disturbances.

The most accurate method available at the present time for analyzing the stability of laminar boundary layers is based on linear stability theory. According to this theory, transition is caused by the selective amplification of initially infinitesimal disturbances present in the boundary layer as they propagate downstream. Transition occurs when the amplitude of any disturbance exceeds a certain level. The method is used to compute the amplification of disturbances having a range of frequencies and propagation angles relative to the local freestream. Thus,

given an initial disturbance amplitude, the method can be used to compute the location at which the disturbance has grown to an amplitude which will cause transition. However, in most cases, the initial disturbance amplitude in the boundary layer is not known because of the difficulties involved in either measuring or predicting such small disturbances, especially under flight conditions. To circumvent this problem, the method relies upon the assumption that, for a given disturbance environment, such as flight conditions, the initial disturbance amplitudes in the boundary layer (at the neutral stability point) are fairly constant from case to case. Since the amplitude of the disturbance at transition will also be about the same from case to case, the ratio of the disturbance amplitude at transition to the disturbance amplitude at the neutral stability point will also be fairly constant from case to case. The natural logarithm of the ratio of the disturbance amplitude at any point to its amplitude at the neutral stability point is called the amplification factor. The amplification ratio (or the corresponding amplification factor) of the most amplified disturbance at transition is called the "amplification limit." Thus a given disturbance environment is characterized by a particular amplification limit. Dealing with amplification limits rather than amplitudes makes it possible to calibrate the method against flight test and wind tunnel test data, since a measurement of the transition location is sufficient, and nothing needs to be known about the actual disturbance amplitudes. When using the method to predict transition, the value chosen for the amplification limit is the key to the prediction of the transition location. The value chosen for the present study will be discussed in more detail later.

There are two basic types of boundary layer disturbance modes subject to instability on a swept wing. The first type has its direction of propagation close to the local flow direction at the edge of the boundary layer and, under certain conditions, exhibits viscous instability. A disturbance of this type is sensitive to the Reynolds number based on boundary layer thickness and to the shape of the mean velocity profile. It tends to become progressively more unstable as the profile develops inflection points under the influence of an adverse pressure gradient. This type of disturbance, traditionally referred to as a Tollmien-Schlichting wave, tends to occur in the mid-chord region of an LFC wing where the pressure distribution is fairly flat. Amplification of Tollmien-Schlichting waves is small in regions of favorable pressure gradient and large in regions of adverse pressure gradient.

The second type of disturbance mode has its direction of propagation nearly perpendicular to the local velocity at the edge of the boundary layer, U_e, and exhibits inviscid instability. A disturbance of this type is sensitive to the shape of the crossflow velocity profile. Any associated instability is characterized as inviscid because the instability results mainly from the presence of an inflection point in the crossflow profile and does not depend upon the effects of viscosity. These are generally referred to as crossflow disturbances or instabilities and are most troublesome near the leading and trailing edges of swept wings where the crossflow velocities in the boundary layer are the largest. In analyzing the boundary layer stability on a swept wing, both Tollmien-Schlichting and crossflow disturbances must be considered. The suction level must be such that no disturbance of either type is amplified beyond the amplification limit for each type of disturbance.

The overall stability analysis procedure is illustrated in Figure 5.1-22. The boundary layer characteristics of the wing are first computed using a Boeing program called TEM 139 which is comparable to and used in the same context as NASA's MAIN laminar boundary layer code. (Ref. 11). TEM 139, however, is adapted to analyzing the compressible flow over in-

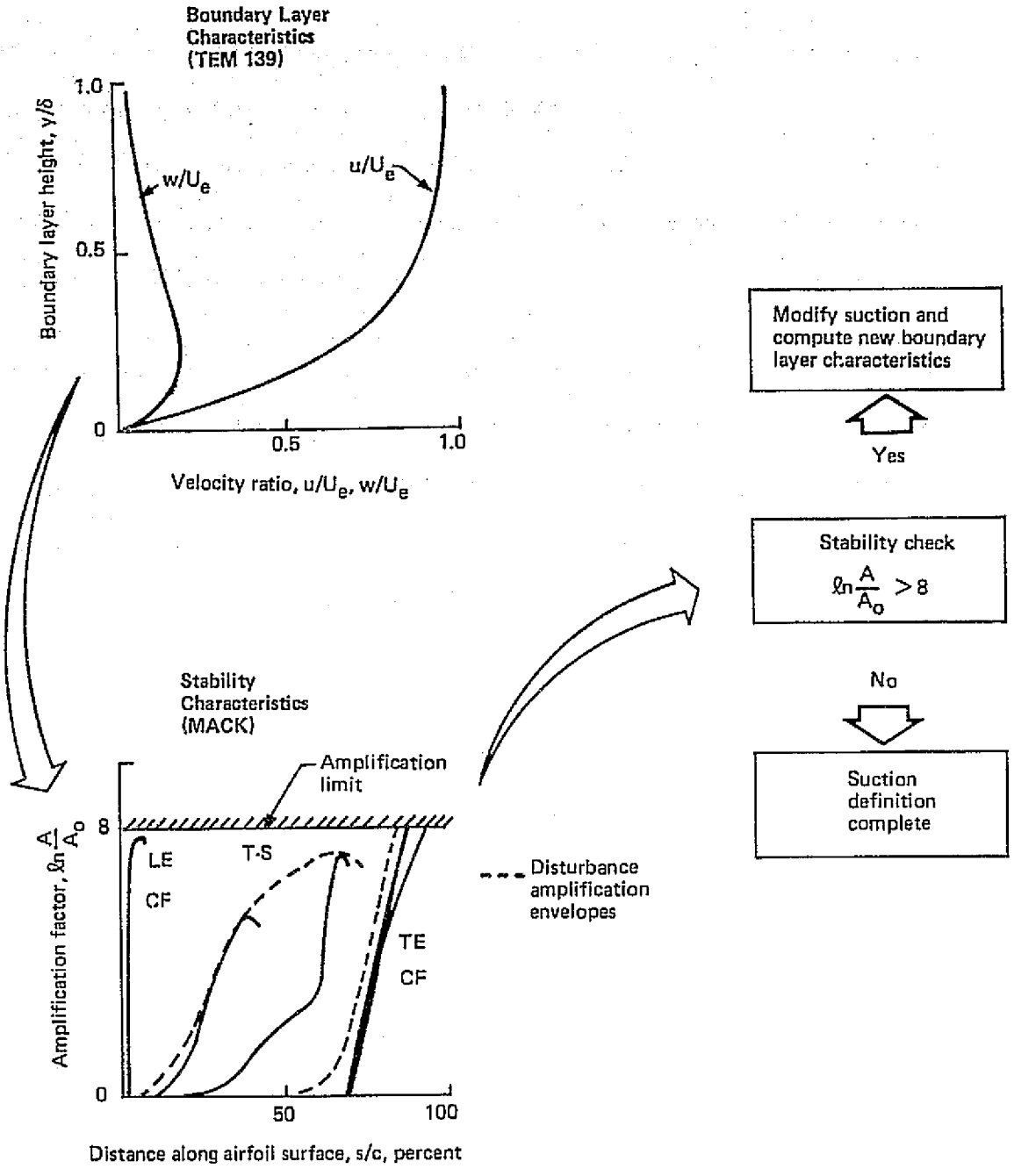

Figure 5.1-22. Stability Analysis Procedure

finite yawed wings. When the program is used to analyze a tapered wing, separate analyses are performed for the leading edge and the trailing edge regions to better approximate the sweep angle in each region. On a well-designed LFC airplane, the isobars will be nearly straight in all regions except near the root and tip. The yawed wing approximation implies straight isobars. Therefore, it is considered to be an adequate approximation except near the root and the tip, where full three-dimensional considerations may be important. Primary inputs to the program are the wing pressure distribution, suction distribution, Reynolds number, and Mach number. The primary outputs are the boundary layer velocity profiles parallel and perpendicular to the local flow direction at the boundary layer edge. These boundary layer velocity profiles then serve as the primary input to the stability analysis program, which is a Boeing modification of a computer program known as the MACK code. (Ref. 12.). This program computes the amplication of disturbances having various propagation directions in the boundary layer and various frequencies. In Figure 5.1-22, the quantity, $\ln A/A_0$ is the amplification factor. An allowable amplification factor or amplification limit of 8 was generally used for this study, for reasons which will be discussed later. If the amplification factor exceeds 8 at any point along the chord, the suction must be increased in the appropriate areas and the boundary layer and stability characteristics re-computed. If the amplification limit is not exceeded anywhere, and if the maximum amplification factors in any region are not extremely low (less than 3), which might indicate local oversuction, then the suction definition is assumed to be complete. This entire procedure must be repeated at several locations along the wing span in order to account for the varying chord Reynolds number caused by the wing taper.

As stated earlier, the selection of the disturbance amplification limit is the key to an accurate estimate of suction requirements. Jaffe, Okamura and Smith (Ref. 13) analyzed a large number of cases (primarily wind tunnel data) in which the pressure distribution and transition locations were known and found good correlation between the observed location of transition and a maximum amplification factor ($\ln A/A_0$) of 10 (corresponding to a maximum amplification ratio of e^{10}). This result is applicable only to Tollmien-Schlichting disturbances because all of the cases analyzed were for unswept wings. Since the cases studied consisted primarily of wind tunnel data, this result is likely to be conservative, since wind tunnel turbulence levels are higher than free flight turbulence levels, and since the turbulence level has a significant influence on the transition location.

As part of the present study, an analysis was made of transition data on a sailplane in flight (Ref. 14). The turbulence environment in free flight is significantly lower than that in any wind tunnel. Since the turbulence level has a significant influence on the transition location, it was felt that this case might give a better indication of the amplification limit, appropriate to the flight environment in which an LFC airplane must operate, than do the results of Jaffe, et al. The results of this analysis are shown in Figure 5.1-23. Disturbance amplification factors were calculated at lift coefficients of 0.52, 0.76, 1.14, and 1.42. The figure shows lines of constant amplification factor based upon the growth of the most amplified disturbance at each lift coefficient. The hatched line shows the measured transition location as a function of lift coefficient. The line corresponding to an amplification factor of 13 most closely matches the measured transition line. This results indicates that, in a flight environment, the amplification factor at transition may be somewhat higher than the value of 10 suggested by Jaffe, et al. Since the Phoenix sailplane wing is unswept, these results again only apply to the amplification of Tollmien-Schlichting disturbances.

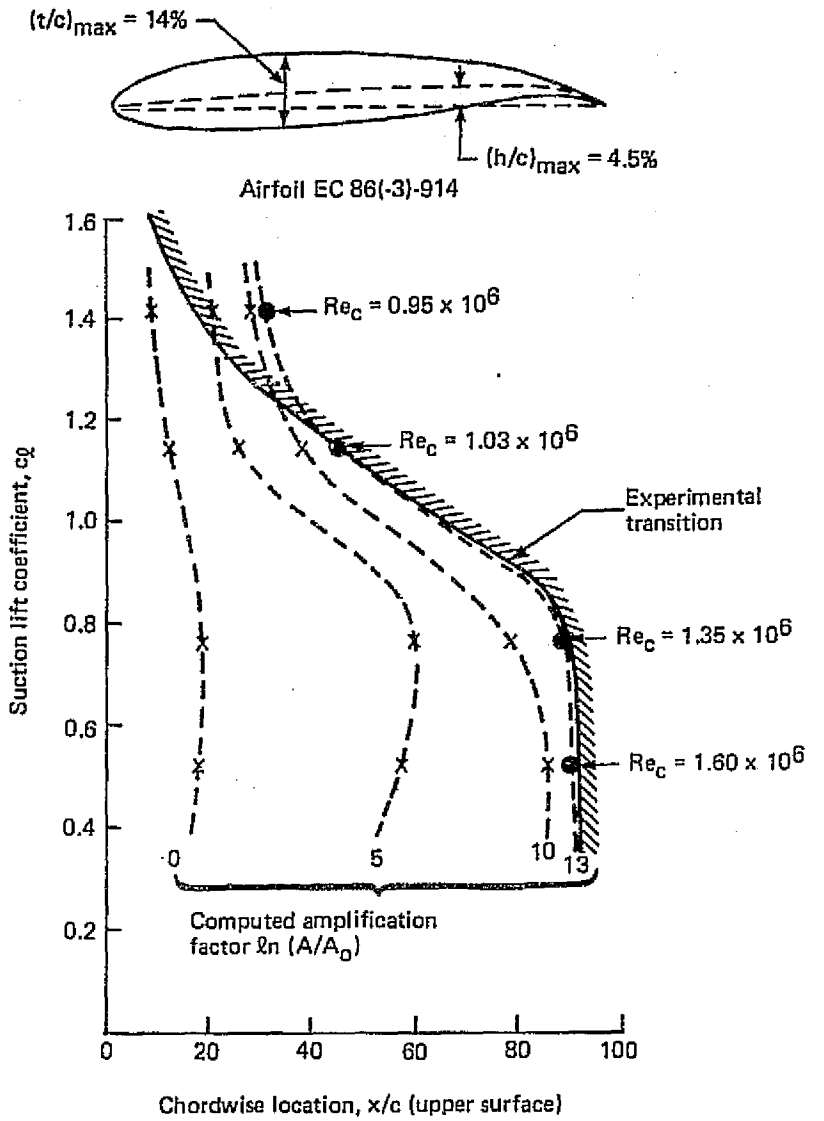

Figure 5.1-23 . Comparison of Theoretical and Experimental Transition Locations on the Phoenix Sailplane

In order to determine the amplification factors corresponding to transition for a case in which cross flow instabilities were the cause of transition, TEM139 and the MACK code were used to analyze the swept wing wind tunnel data of Boltz, et al (Ref. 15). In this case, wind tunnel data were used because of the scarcity of high quality flight test transition data on swept wings. The upper part of Figure 5.1-24 shows the pressure distribution corresponding to the four cases analyzed. For two cases the sweep angle was 30° and for the other two cases the sweep angle was 40°. The Reynolds number and Mach numbers varied from case to case. The lower part of the figure shows the growth of the most critical disturbance for each case. The calculation was stopped at the location where transition was measured. The amplification factors at transition ranged from 11.3 to 12.9.

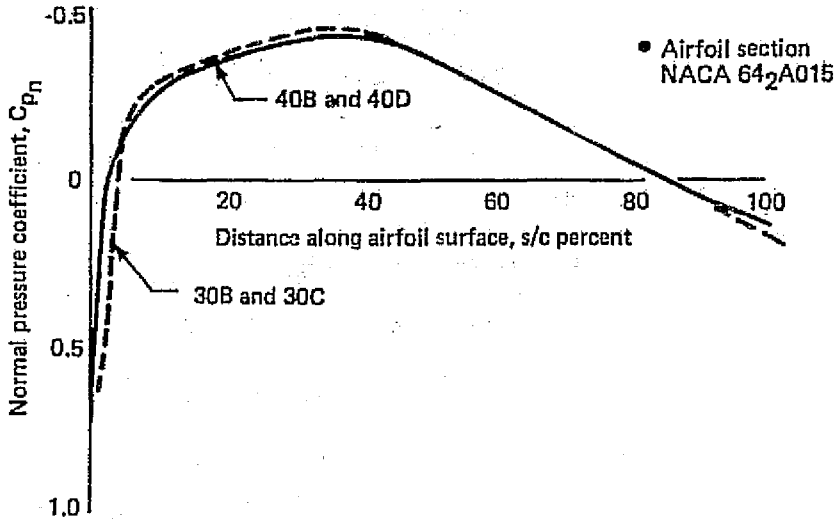

Case	Sweep	Re_n	M	Transition amplification factor
30B	30	9.26×10^6	0.30	11.3
30C	30	12.08×10^6	0.42	12.1
40B	40	7.81×10^6	0.27	12.3
40D	40	6.20×10^6	0.22	12.9

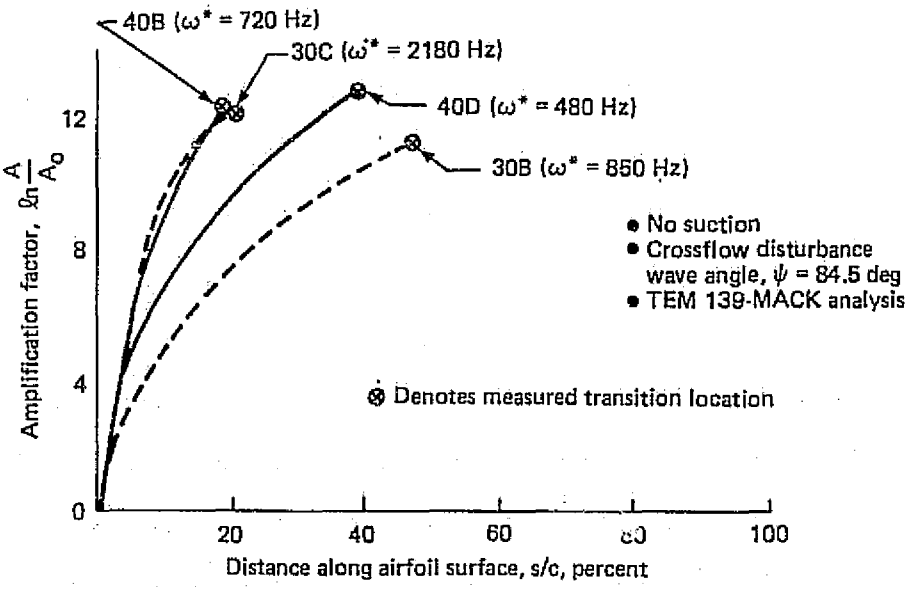

Figure 5.1-24 . Measured Boundary Layer Transition and Calculated Amplification Factors for Swept-Wing Wind Tunnel Data

Based upon the value of 10 recommended by Jaffe, et al, the value of 13 calculated for the Phoenix sailplane and the values of 11 to 13 calculated for the swept wing data, an amplification limit of 8 was chosen for the present study for both crossflow and Tollmien-Schlichting disturbances. It was judged that this value would be appropriately conservative, but not so conservative that excessive suction requirements would result.

All of these cases discussed previously involved low Mach numbers, where the effects of compressibility can be neglected. However, since the LFC airplane will be cruising at Mach 0.8, with local Mach numbers on the upper wing surface approaching $M_n = 1.2$, compressibility effects will be present. In order to determine the magnitude of these effects, the upper mid-span of the LFC airplane was analyzed using the MACK code in both the compressible and incompressible modes. The boundary layer velocity profiles input to the MACK code were the same in both cases and were from TEM139, which includes the effects of compressibility on the profile shapes.

Figure 5.1-25 shows the stability diagram corresponding to the leading edge crossflow region of the upper mid-span at a lift coefficient of 0.5. This diagram is for a disturbance propagation wave angle of 84.5° which was found to be the direction of largest amplification of crossflow disturbances. The solid lines are lines of constant non-dimensional spatial amplification rates computed using the MACK code in the incompressible mode and the dashed lines are lines of constant non-dimensional spatial amplification rates computed using the MACK code in the compressible mode. Amplification rates are highest for the largest values of $-\alpha^*_i\delta$. The only significant difference between the incompressible and compressible curves is that the compressible curves are shifted to a slightly higher non-dimensional frequency, ω_r. There is no significant difference in the maximum amplfiication rates. This results indicates that in regions where crossflow instabilities are dominant, the effects of compressibility on stability are likely to be small.

Figure 5.1-26 shows the stability diagram for amplification of Tollmien-Schlichting disturburances at the upper mid-span location at a lift coefficient of 0.55. Again, in this case, the largest amplification rates correspond to the largest number. For given values of position and frequency, the rates calculated using the MACK code in the incompressible mode are nearly twice as large as those calculated using the compressible mode. It should be noted that for the compressible stability case, the stability diagram is for a disturbance wave angle of 33°, which was found to be the angle for which the amplification rate is highest. For the incompressible case, the stability diagram corresponds to a wave angle of 0°, which is the angle for which amplification was found to be the highest. Figure 5.1-27 shows the effect of the larger incompressible amplification rates on the growth of the most critical disturbance. The maximum amplification factor for the incompressible MACK code case is about 28, while for the compressible MACK code case it is about 15. For the compressible case, both the 0° and 33° wave angle disturbance amplification factors are shown. It can be seen that the amplification factor is only slightly higher for the 33° compressible disturbance than for the 0° compressible disturbance. These results indicate that compressibility exerts a strong stabilizing effect on Tollmien-Schlichting disturbances.

In the development of the suction requirements, all of the calculations were performed using the MACK code in the incompressible mode because of certain economies in calculation effort and because compressibility effects were initially considered to be unimportant. Only

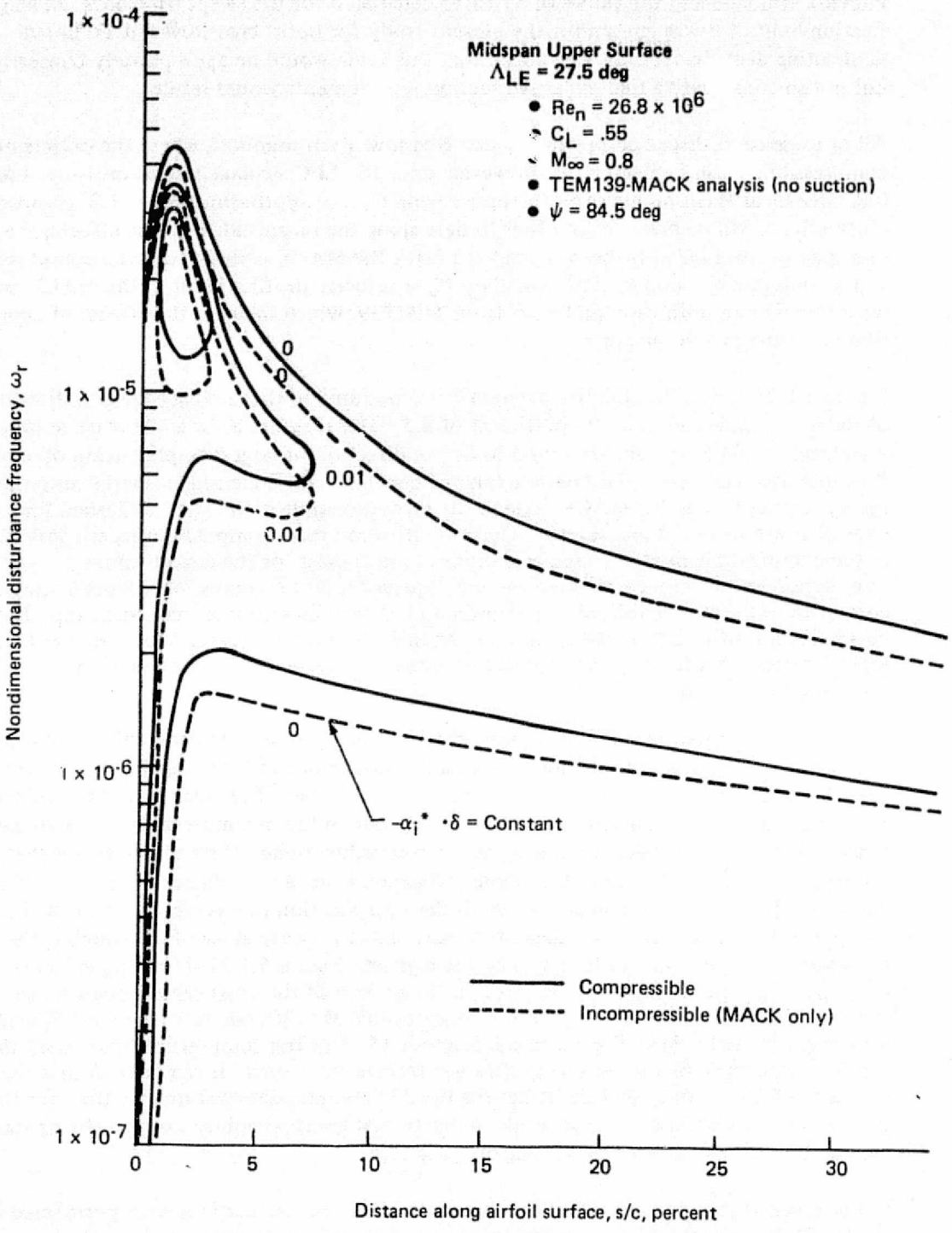

Figure 5.1-25. Effect of Compressibility on Calculated Crossflow Stability

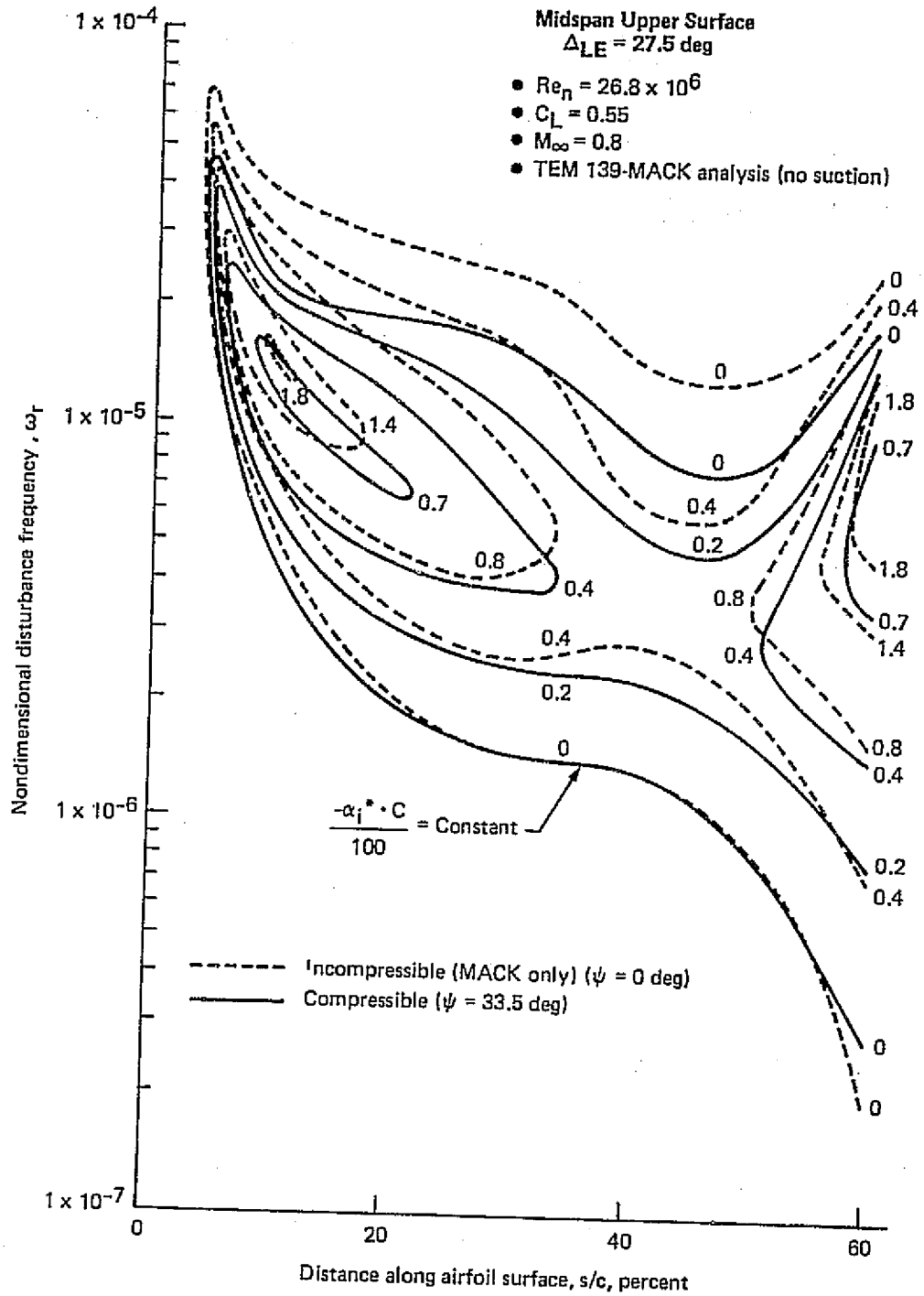

Figure 5.1-26. Effect of Compressibility on Calculated Tollmein-Schlichting Stability

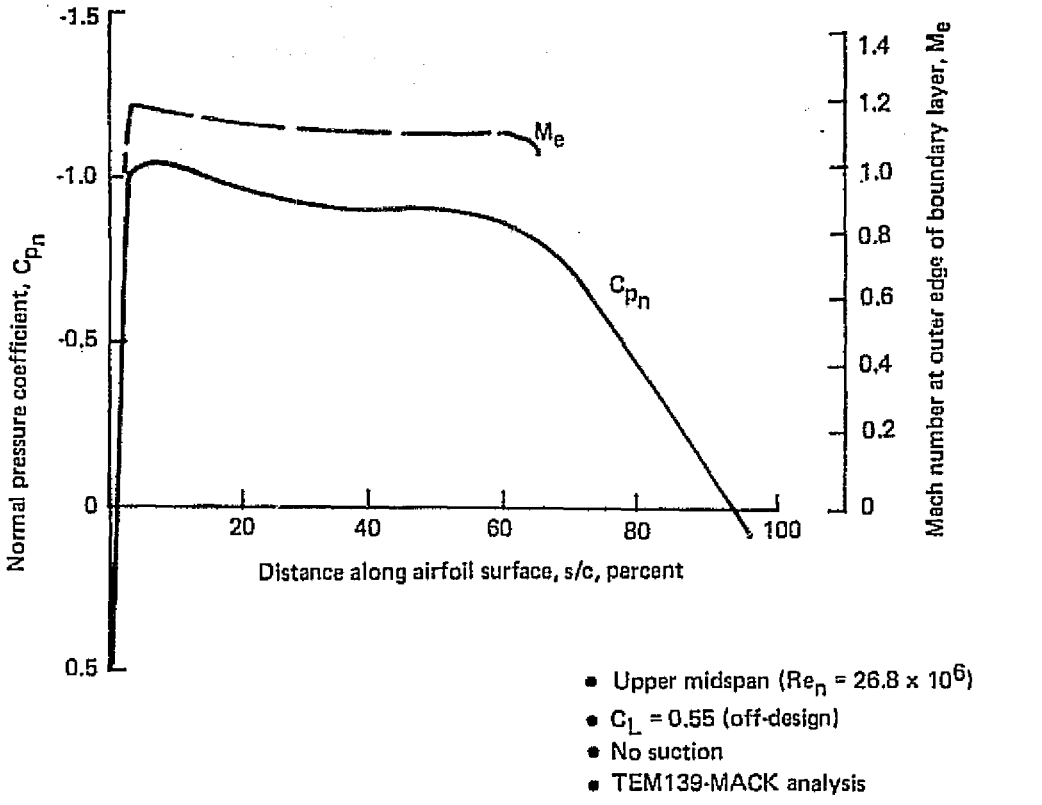

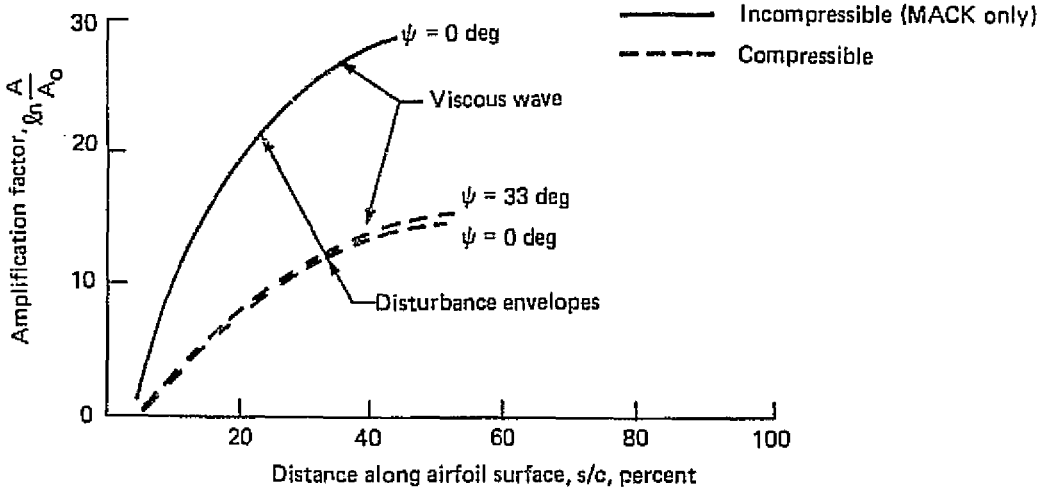

Figure 5.1-27 . Effect of Compressibility on Disturbance Amplification

later analyses have shown the influence of compressibility in sufficient detail However, since the results discussed above showed compressibility effects to be significant only in regions where Tollmien-Schlichting instabilities were dominant, and since suction levels in such regions are quite low compared to those in crossflow-dominated regions, the effect on total suction requirements of using only incompressible stability calculations will generally be quite small. Furthermore, since compressibility effects provide an additional, though not excessive, stability margin, suction requirements have not been re-calculated using compressible stability theory.

5.1.3.2 Design Studies

In an effort to minimize wing suction requirements, studies were conducted to determine the effect of sweep, Reynolds number, and pressure distribution on boundary layer stability and suction requirements.

On the upper wing surface, two different pressure distributions were analyzed, based upon a leading edge sweep angle of 27.5°. The two were identical except that one had a peak in the leading edge region, and the other did not. The two pressure distributions are shown in Figure 5.1-28, along with the amplification factors of the most critical crossflow disturbances

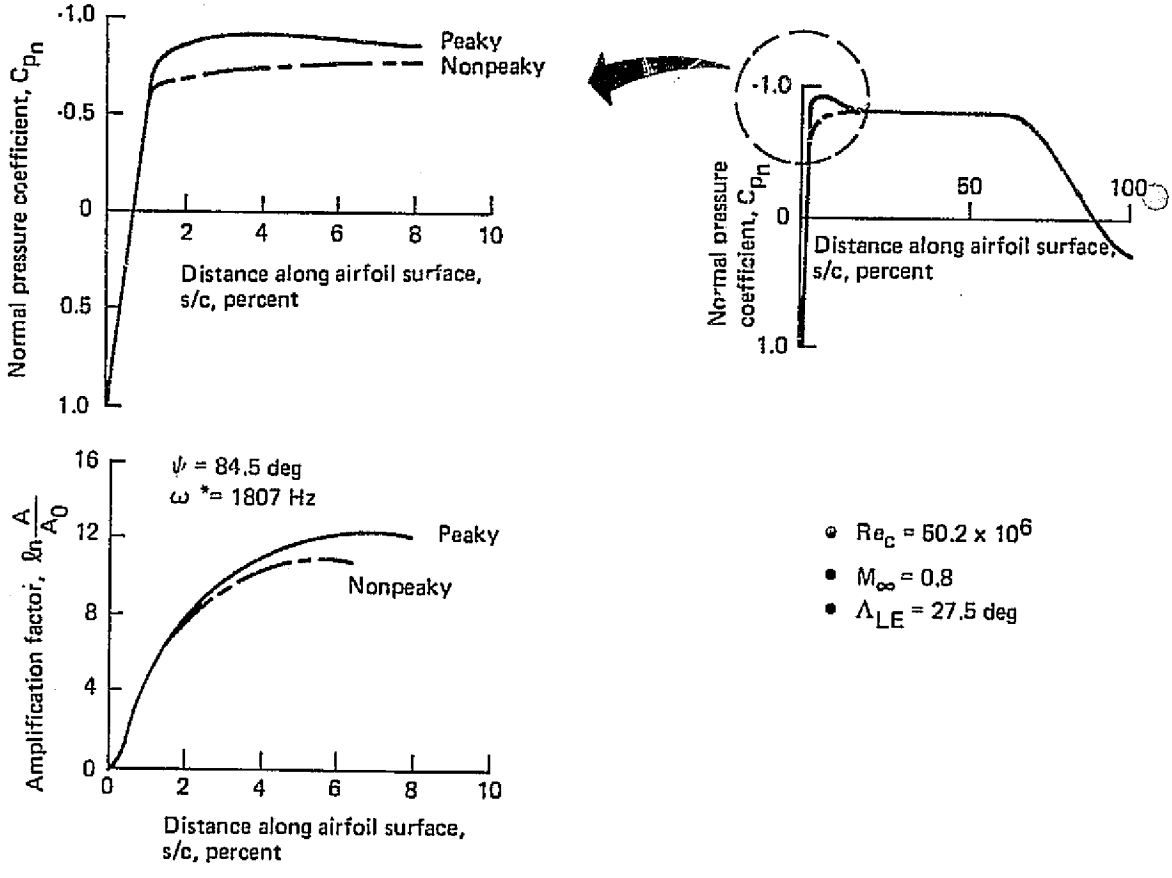

Figure 5.1-28. Effect of Pressure Distribution on Amplification—Upper Wing Root

for each case. For the peaky case, the maximum amplification factor is about 12, whereas for the non-peaky case it is only about 10.5. Thus, less suction would be required to stabilize the leading edge cross flow for the non-peaky pressure distribution. Furthermore, although the stability of the Tollmien-Schlichting disturbances was not computed, it is known that amplification of Tollmien-Schlichting disturbances is always higher in regions of adverse pressure gradients than in regions of favorable pressure gradients. Therefore, both from the standpoint of crossflow stability and Tollmien-Schlichting stability, the non-peaky pressure distribution is the better of the two. For this reason, it is the non-peaky pressure distribution that was chosen for the upper wing surface.

The upper part of Figure 5.1-29 shows the two pressure distributions that were considered for the lower wing surface. The lower part of the figure shows the amplification factors without suction for the most critical crossflow disturbances for each case. For the original pressure distributions, the maximum amplification factor is about 55. For the modified pressure distribution, the maximum amplification factor is only about 9. The reason for this large difference

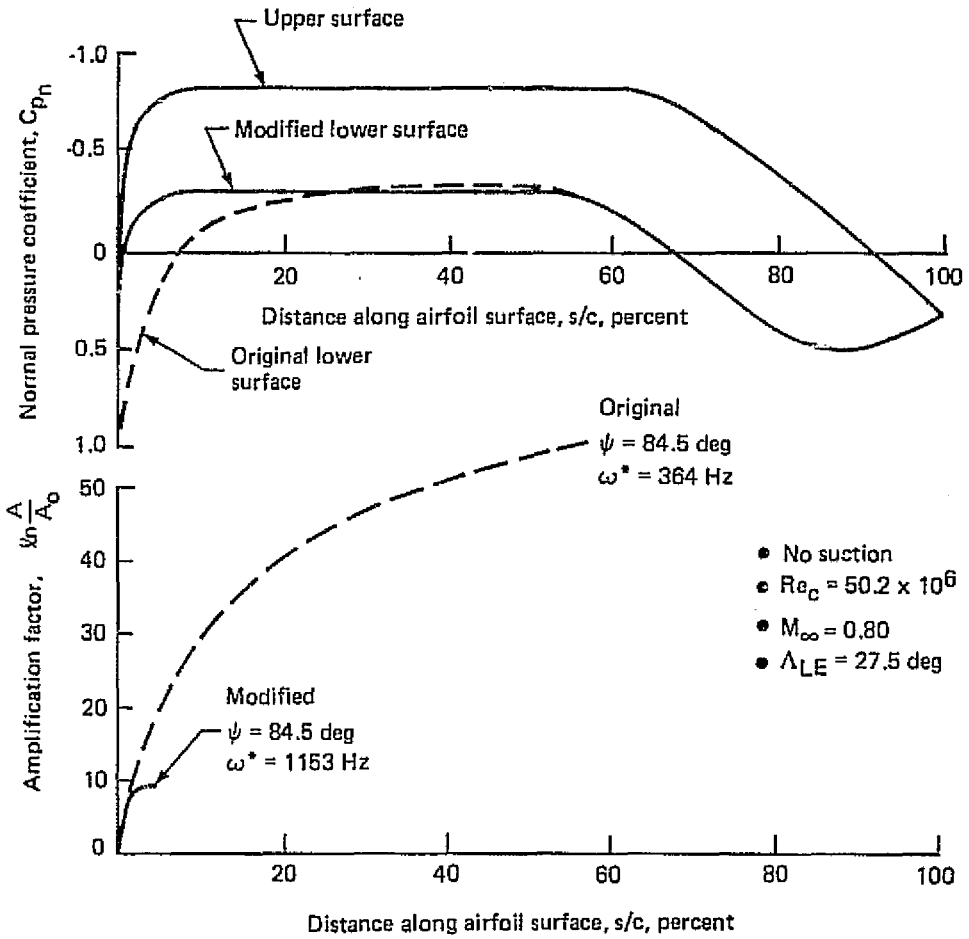

Figure 5.1-29. Effect of Pressure Distribution on Amplification—Lower Wing Root

is that the original pressure distribution has large pressure gradients over a much greater percentage of the chord than the modified pressure distribution. This produces a much larger crossflow velocity in the boundary layer, since crossflow results from the combination of sweep and pressure gradient. Studies of this type show that it is best to make the pressure gradient as large as possible near the leading edge where the boundary layer is thinner and more stable, and then flatten out the pressure distribution as soon as possible to stop any further increase in the crossflow velocity. The much lower maximum amplification factor for the modified pressure distribution would result in much lower suction requirements than for the original pressure distribution. Therefore, the modified pressure distribution was chosen for the lower surface of the wing.

After the pressure distributions had been determined, a study was conducted to determine the effect of wing sweep on boundary layer stability and suction requirements. Figure 5.1-30

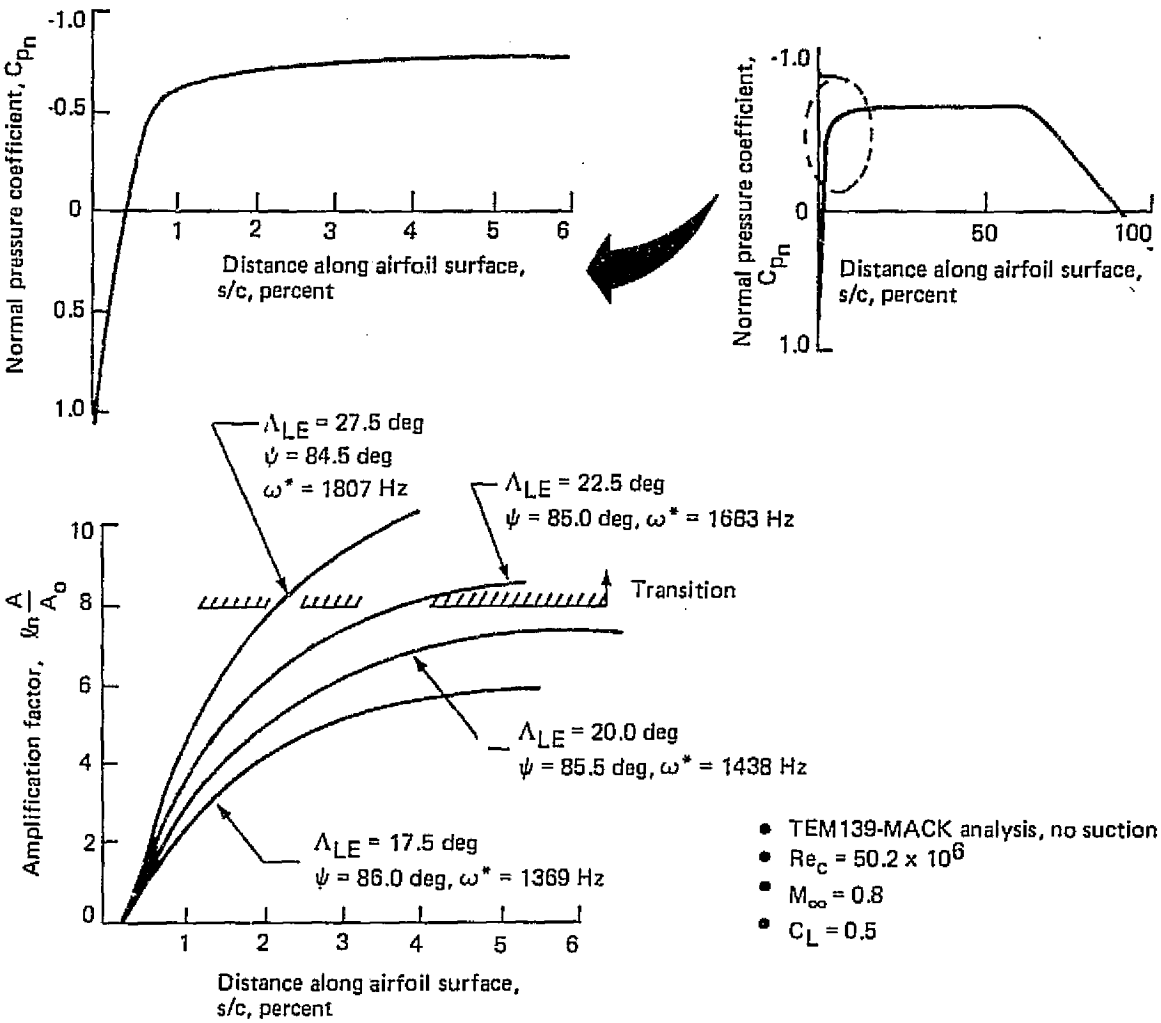

Figure 5.1-30. Effect of Sweep Angle on Disturbance Amplification—Upper Wing Root

shows the calculated effect of sweep on disturbance amplification at the upper root location in the leading edge crossflow region. The amplification factors for only the most critical disturbances for each case are shown. For a leading edge sweep angle of 27.5°, the maximum amplification factor is about 10.5; for 22.5° it is 8.5; for 20° it is 7.5; and for 17.5° it is about 6. No suction would be required to stabilize cases for which the amplification limit of 8 is not exceeded. Thus, for sweep angles of 20° or less, these results indicate that no suction would be required to stabilize the leading edge crossflow.

Figure 5.1-31 shows the most aft first slot location allowable as a function of leading edge sweep. For this study the first slot was located at the point where the amplification factor of the most critical disturbance was 7.5, since this would still allow the flow to be stabilized before the amplification limit was exceeded. At the upper root location the first slot can be no further back than x/c = 0.013 for a sweep angle of 27.5°; for a sweep angle of 20° the

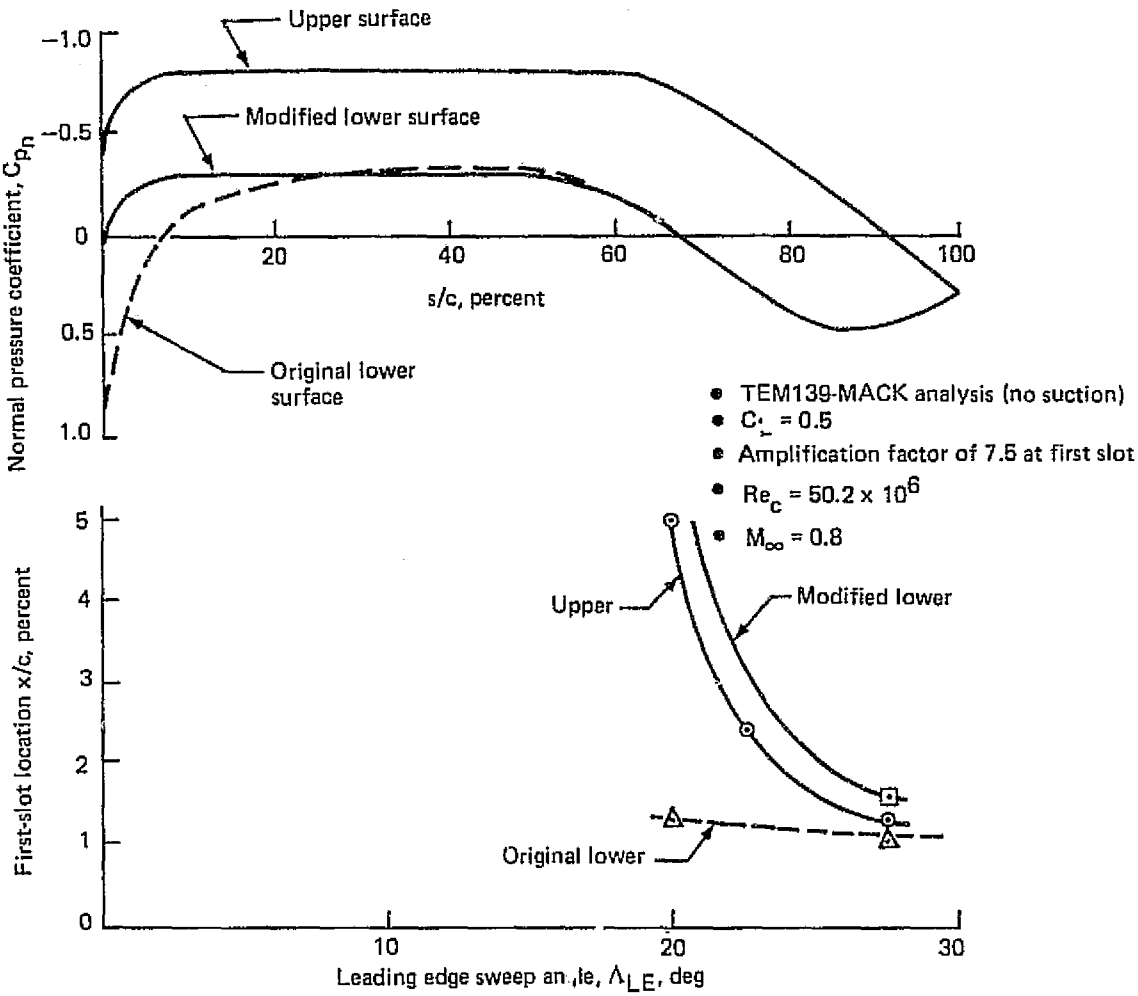

Figure 5.1-31. Effect of Sweep on First-Slot Location—Wing Root

first slot can be as far back as x/c = 0.05. On the lower surface, for the modified pressure distribution, the first slot can be no further back than x/c = .016 for a sweep angle of 27.5°, for a sweep angle of 20° it can be moved back to about x/c = 0.06. For the original lower surface pressure distribution, reducing sweep from 27.5° to 20° allows the first slot to be moved back only slightly from x/c = 0.011 to x/c = 0.013. Thus, if it were required that the wing leading edge be free of slots back to a certain location, reducing sweep by the appropriate amount would allow this to be done if the pressure distribution is essentially flat-topped.

Figure 5.1-32 is a composite showing the effect of both sweep and Reynolds number on the most aft allowable first slot location. For a sweep angle of 27.5°, the first slot must be no further back than x/c = 0.013 for a normal chord Reynolds number of 39.6 x 10^6 (corresponding to the root location). When the Reynolds number is reduced to 13.0 x 10^6 (corresponding to the tip location) the first slot may be located as far back as x/c = 0.164. These results show the most aft allowable slot location to be quite far from the leading edge in some areas. However, it is best in most cases to start the suction as far forward as possible because it is more effective to apply a small amount of suction over the entire region of disturbance growth than it is to apply a large burst of suction just before the amplification limit is reached.

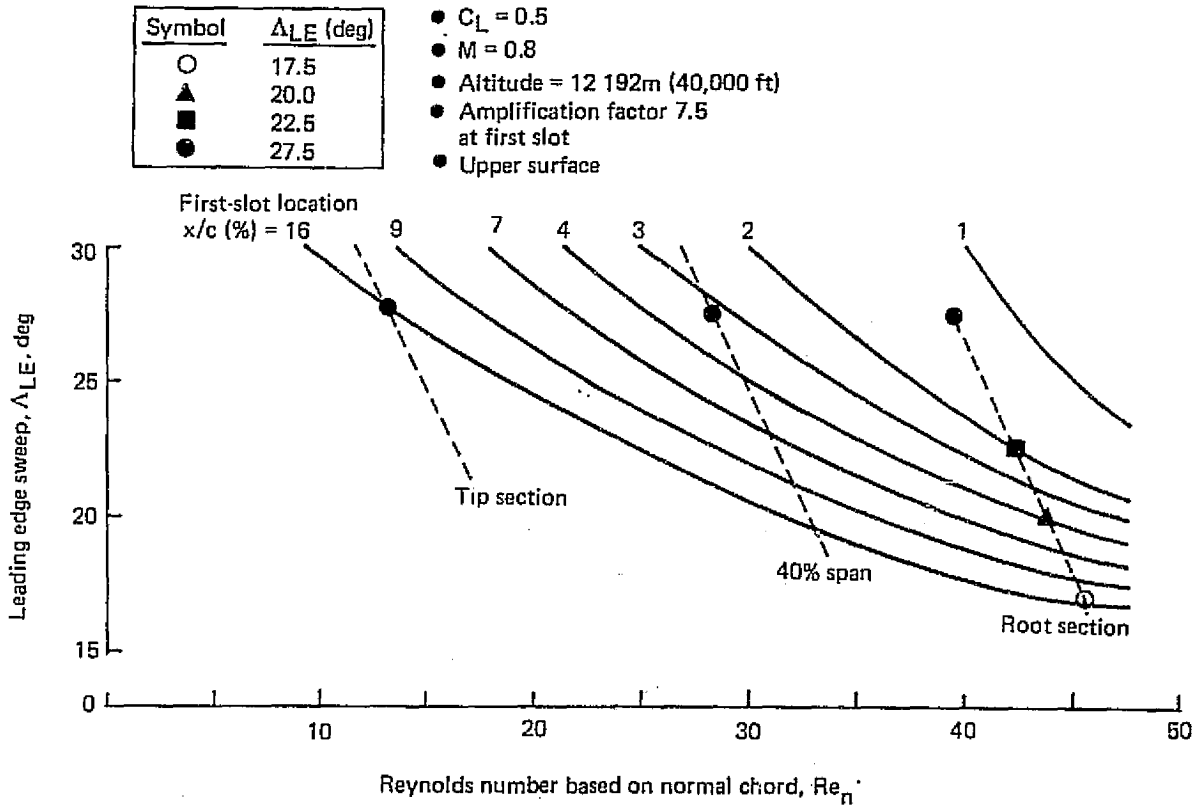

Figure 5.1-32. First-Slot Location as a Function of Sweep and Reynolds Number

The effect of sweep on suction requirements is shown in Figure 5.1-33. These results are for the upper surface pressure distribution corresponding to the design lift coefficient of 0.5. The Reynolds number corresponds to that at the root chord location. At a leading edge sweep angle of 27.5°, a large suction peak is required to stabilize the leading edge crossflow. When sweep is reduced to 22.5°, the size of this peak is cut in half. At 20° leading edge sweep, no suction is required to stabilize the leading edge crossflow. Sweep changes primarily affect the boundary layer crossflow velocities. In the mid-chord portion of the wing, Tollmien-Schlichting instabilities are dominant, and since they are not affected by the crossflow, sweep changes have little effect on the rate at which they are amplified.

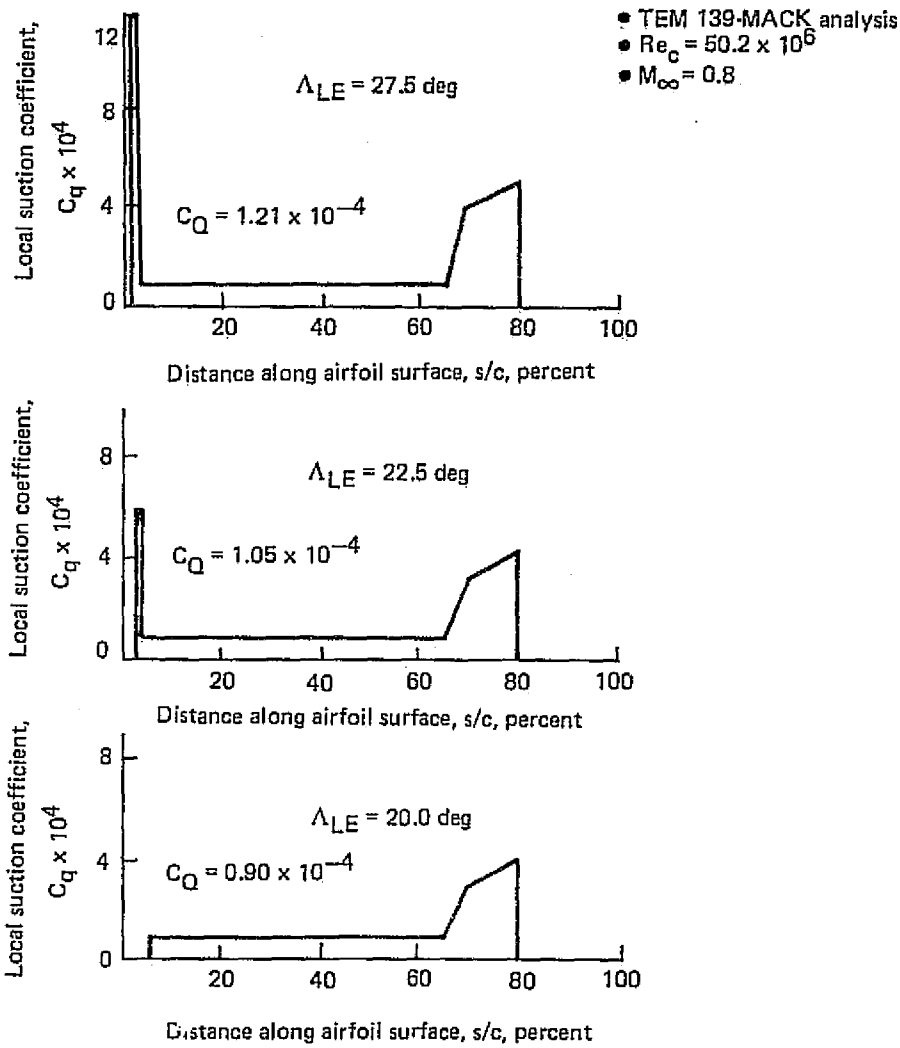

Figure 5.1-33. Effect of Sweep on Suction Requirements—Upper Wing Root

As a result, the amount of suction required in the mid-chord region is nearly independent of sweep. The amount of suction required to stabilize the rear crossflow (from 65% to 80% chord) decreases with decreasing sweep angle. Total suction, C_Q decreases by 30% as sweep is reduced from 27.5° to 20°. For off-design conditions, the effects of sweep may differ from those shown here.

Figures 5.1-34 through 5.1-37 show suction requirements and corresponding stability analysis results for the upper wing root, upper mid-span, upper tip, and lower mid-span, respectively. All of these results are for the pressure distribution corresponding to $C_L = 0.5$

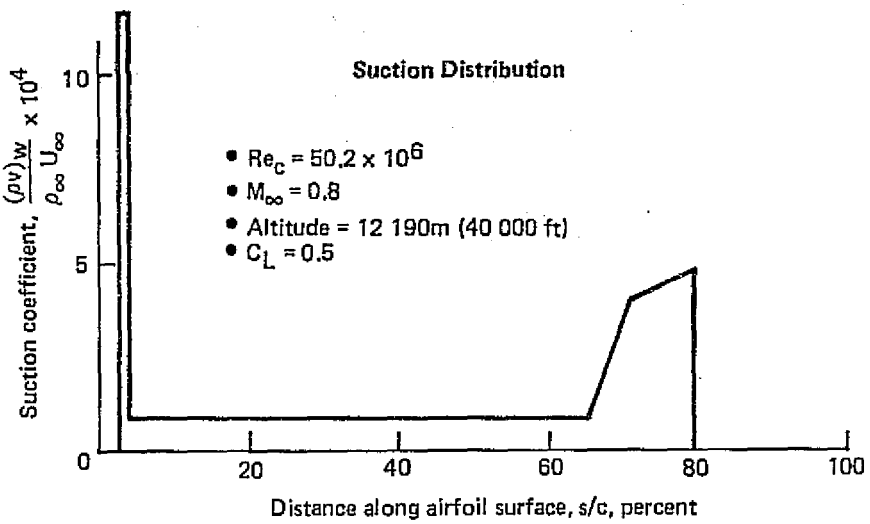

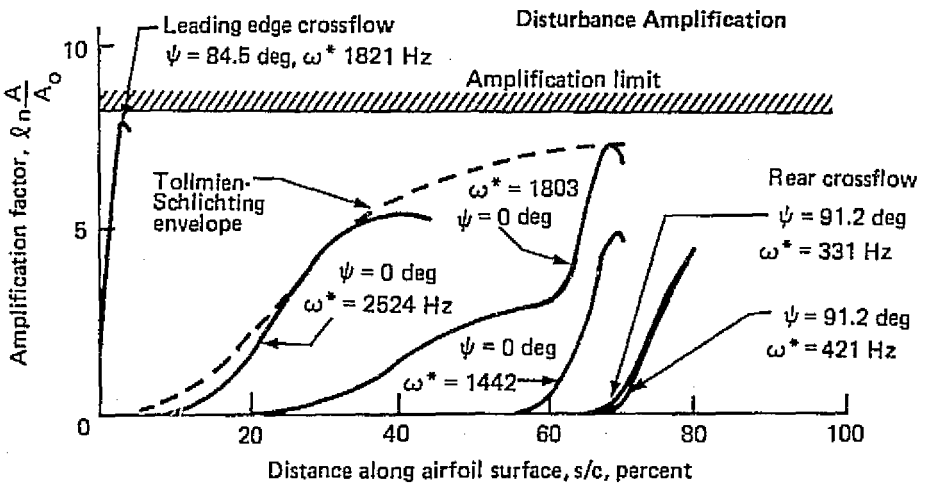

Figure 5.1-34. Disturbance Amplification Characteristics for Design Flight Condition—Upper Wing Root

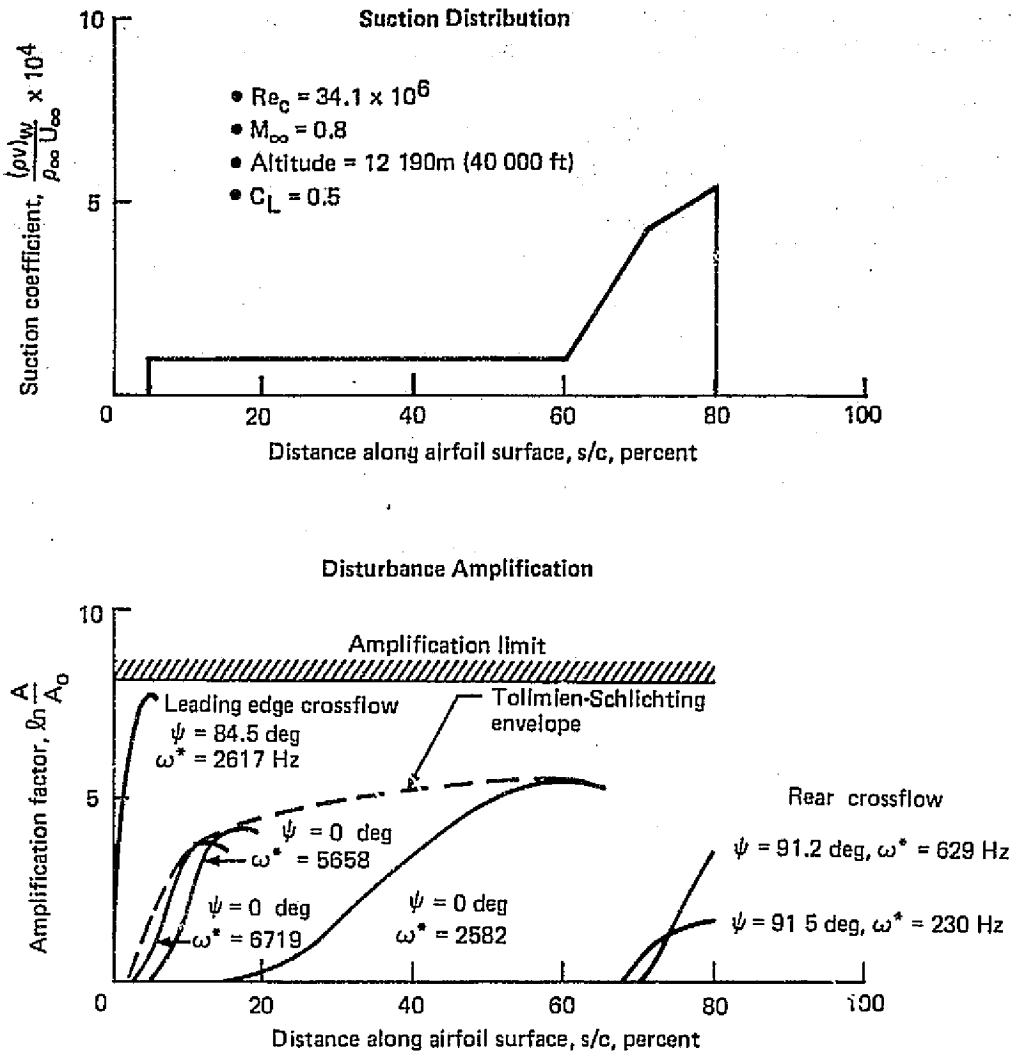

Figure 5.1-35. Disturbance Amplification Characteristics for Design Flight Condition—Upper Wing Midspan

and an altitude of 12 190 m (40 000 ft) as given in Figure 5.1-31. The same pressure distribution was used at each spanwise location. In each case the suction was adjusted to keep the maximum amplification factors below the amplification limit of 8. Also, in each case, there are three fairly distinct chordwise regions in which different types of disturbance growth takes place: the leading edge crossflow region, the mid-chord Tollmien-Schlichting region, and the rear crossflow region. The growth of the most amplified disturbances in each region is shown for each case.

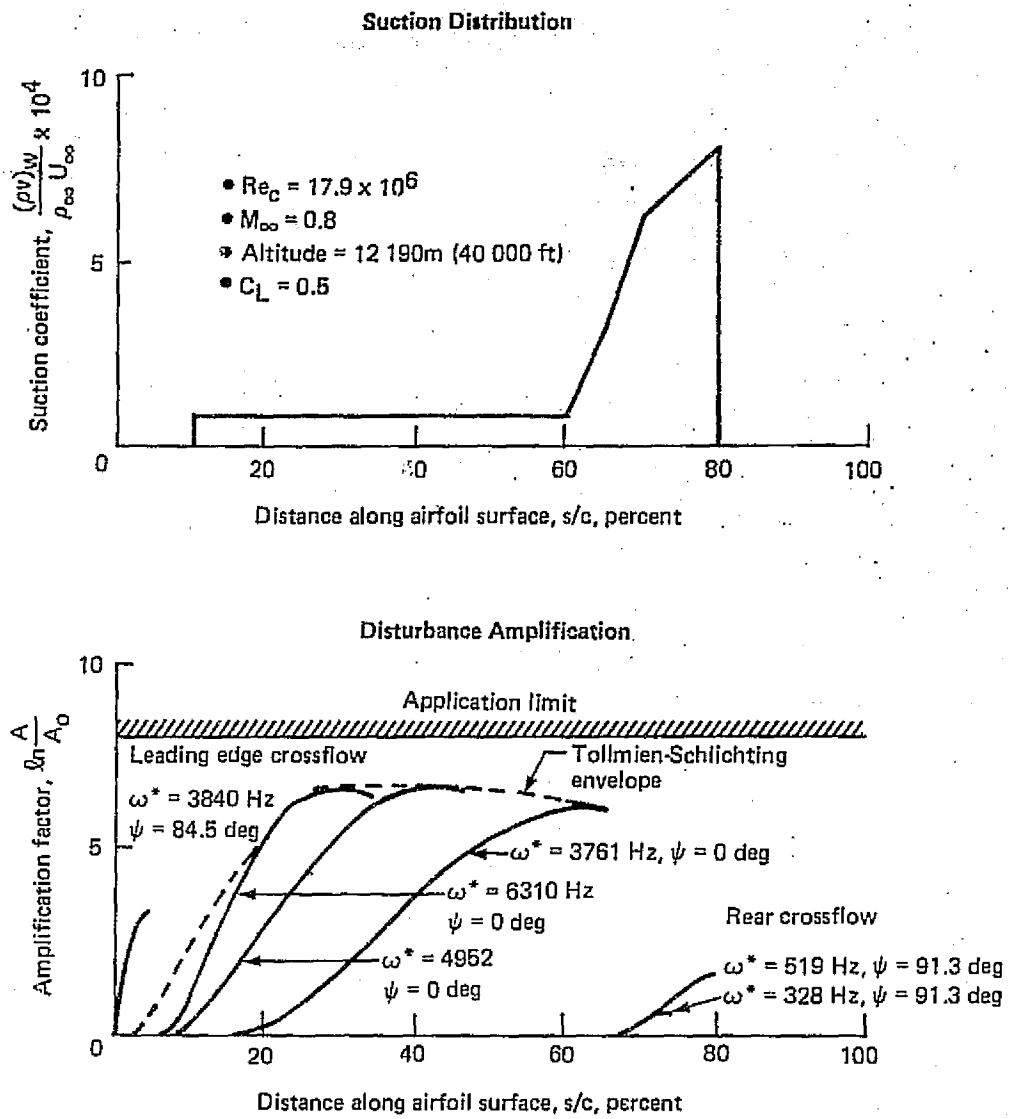

Figure 5.1-36. Disturbance Amplification Characteristics for Design Flight Condition—Upper Wing Tip

5.1.3.3 Suction and Slot Requirements

Required suction distributions at the design lift coefficient of 0.5 are shown in Figure 5.1-38. These distributions are based upon the results of the analyses shown in Figures 5.1-34 through 5.1-37. However, the initial suction slot locations have been moved forward relative to those shown in those figures so that both the design and the off-design suction requirements can be accommodated using a fixed slot configuration. As a result of moving the first slot location forward, the height of the suction peak required to stabilize the leading edge crossflow at the root location is reduced relative to that shown in Figure 5.1-34. Total suction is the same in both cases, however. A complete stability analysis was not performed

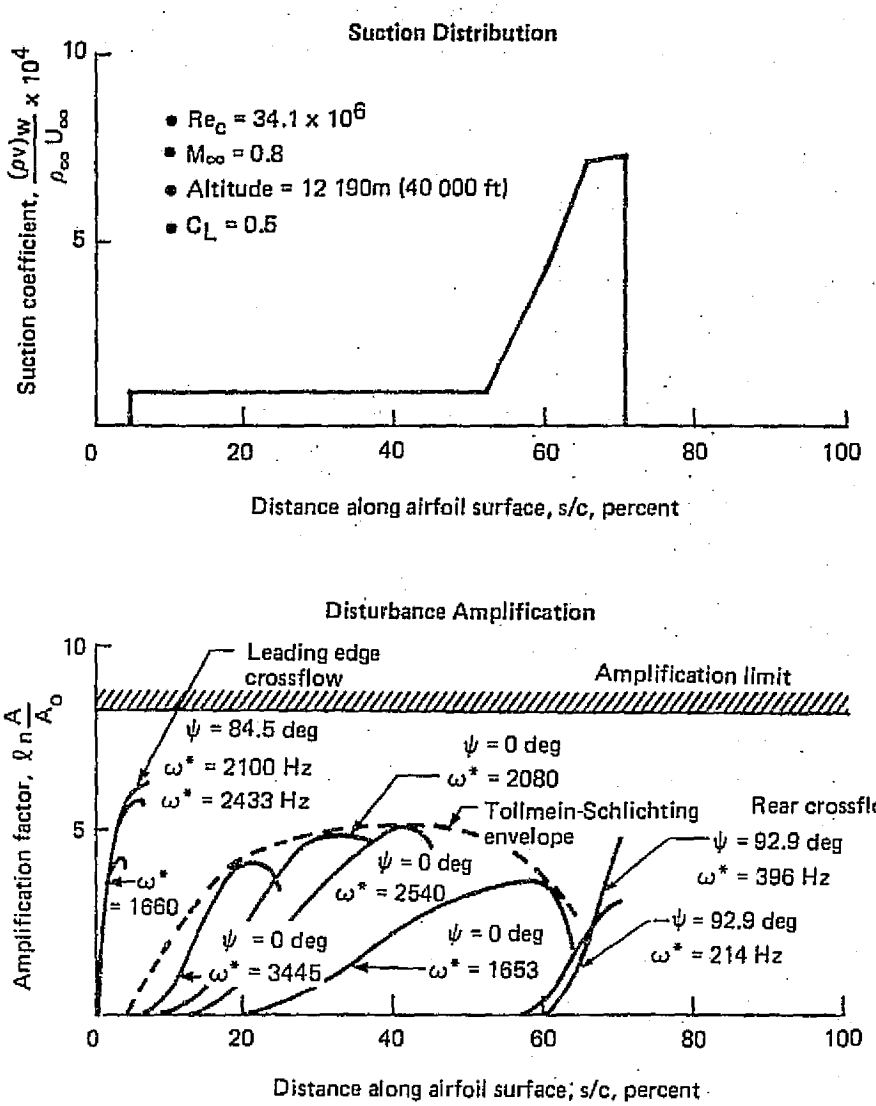

Figure 5.1-37. Disturbance Amplification Characteristics for Design Flight Condition—Lower Wing Midspan

at the lower root and lower tip locations. Suction requirements at these locations were estimated by scaling the computed mid-span lower surface suction distribution so that the variation of suction with spanwise location on the lower surface was similar to that on the upper surface. On the lower surface suction extends to 70% chord of the basic wing trapezoid. At the root location this amounts to 59% of the full chord. However, on the upper surface the suction extends to 80% of the full chord everywhere.

The powerful effect that changing from the design pressure distribution to an off-design pressure distribution can have on disturbance amplification is shown in Figure 5.1-39. The

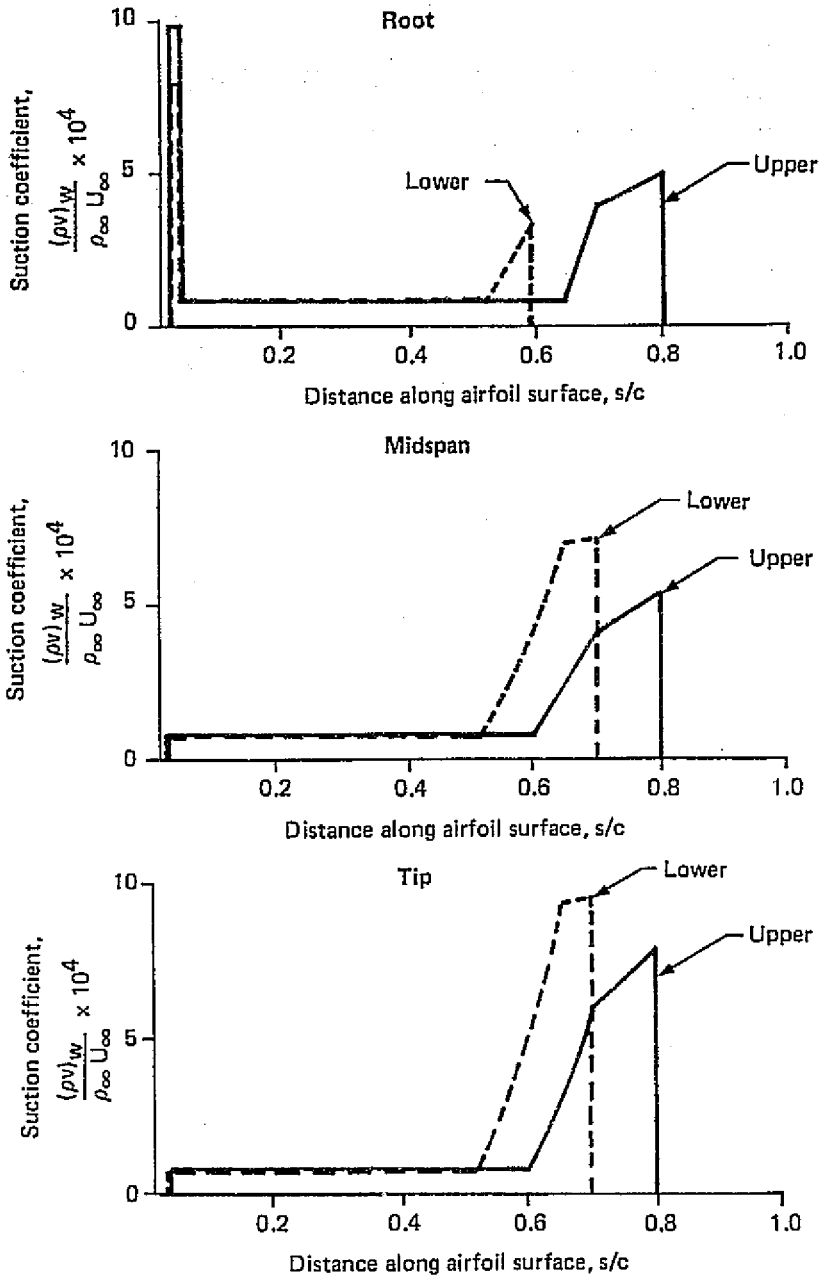

Figure 5.1-38. Suction Distributions—C_L = 0.5, h = 12 190m (40 000 ft), and M = 0.8

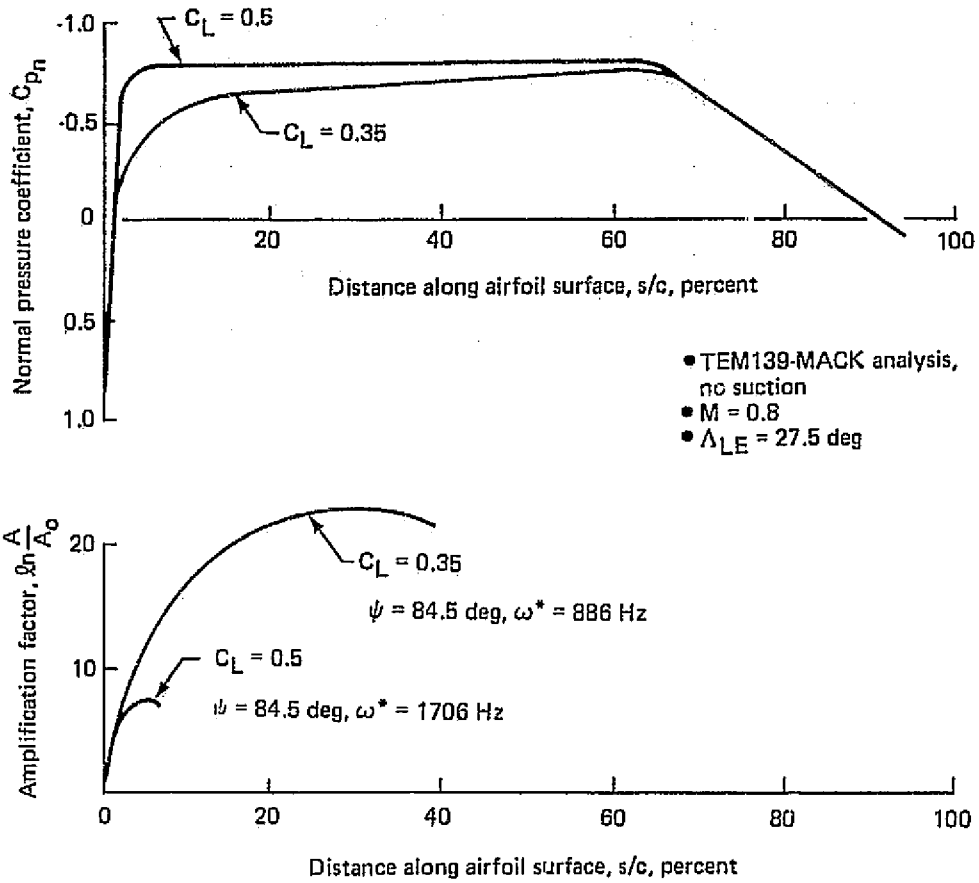

Figure 5.1-39. Effect of Off-Design Pressure Distribution on Disturbance Amplification—Upper Wing Midspan

growth of the most amplified leading edge crossflow disturbance is shown for the design lift coefficient of 0.5 and an off-design lift coefficient of 0.35. The maximum amplification factor without suction is about 22 for the off-design case compared to about 7.5 for the design case. The larger amplification for the off-design case results from the more gradual pressure rise, which results in large pressure gradients as far back as about 20% chord. Because of its larger amplification, suction must start further forward and be stronger for the off-design case than for the design case. This result is similar to that shown in Figure 5.1-29 where the effect of design pressure distribution on the wing lower surface is presented.

Figure 5.1-40 compares off-design suction requirements to the design suction requirement at the upper mid-span location. The large amplification factors shown in Figure 5.1-39 for C_L = 0.35 result in the large suction peak requirement shown in the leading edge crossflow region. A large suction peak in the leading edge area is also required for C_L = 0.55. This contrasts with the suction distribution for the design lift coefficient of 0.5 which has no peak at all in the leading edge area at the mid-span location. In the mid-chord portion

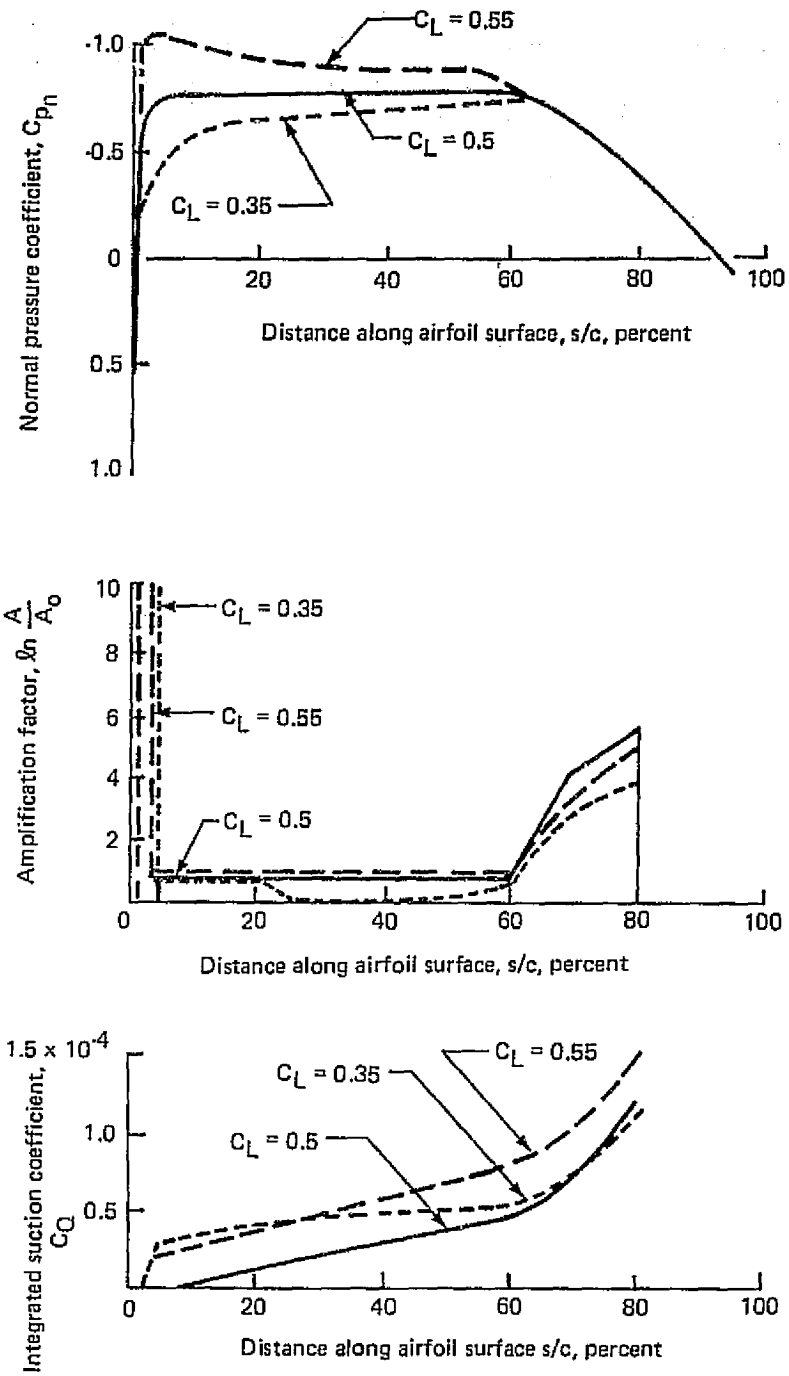

Figure 5.1-40. Off-Design Suction Requirements—Upper Wing Midspan

of the wing slightly more suction is required for $C_L = 0.55$ than for $C_L = 0.5$ because of the slightly adverse pressure gradients in this region for the high lift coefficient case. For $C_L = 0.35$, very little suction is required in the mid-chord region because of the slightly favorable pressure gradients, which have a stabilizing influence on Tollmien-Schlichting disturbances. In the rear crossflow region, suction requirements are slightly lower for both off-design lift coefficients than for the design lift coefficient. Total suction requirements to 80% chord in terms of C_Q are about 20% higher for $C_L = 0.55$ than for $C_L = 0.5$ and about 7% lower for $C_L = 0.35$ than for $C_L = 0.5$.

The slot arrangement must be able to accommodate the off-design suction requirements in addition to the design suction distribution. Because of this, the slots were extended further forward than would have been necessary if the design condition were the only consideration. Also, slot spacing in the leading edge area was decreased from that required at the design condition so that slot Reynolds numbers in this area would not exceed 150 at the off-design condition. A schematic of the resulting slot configuration is shown in Figures 5.1-41 and 5.1-42. The purpose of these figures is only to indicate the general slot arrangement, since not all of the slots can be shown at this scale. At the root location there are 48 slots on the upper surface and 43 on the lower surface. There are 37 slots on the upper surface and 40 on the lower surface at the mid-span location. At the tip there are 23 slots on the upper surface and 22 slots on the lower surface. The first slot is at $x/c = 0.007$ on both the upper and lower surface at both the root and mid-span locations. At the tip the first slot is at $x/c = 0.024$ on both the upper and lower surfaces.

A detailed slot definition is given in Table 5.1-1. This table shows the x/c location of each slot, the spanwise locations at which they begin and end, the slot widths, and the slot Reynolds numbers.

Given a continuous suction distribution which has been shown to be adequate for maintaining laminar flow over the required portion of the airfoil, the slot spacing depends only upon the chord Reynolds number and the maximum allowable slot Reynolds numbers. For this study a maximum allowable slot Reynolds number of 150 was used in regions of high suction. Keeping the slot Reynolds number at or below these levels minimizes disturbances from the slots due to non-uniform inflow conditions. The inboard slot ends lie along a 7° wedge line which starts at the 10% semispan location of the leading edge. Interference from the body boundary layer prevents laminarization inboard of this line. The outboard slot endings were determined by the requirements for a decreasing number of slots at larger semispan locations resulting from the decreasing chord Reynolds number. The number of slots at each spanwise location is such that the slot Reynolds numbers for the design condition will not exceed 150 and 75 in the regions of high and low suction, respectively, anywhere on the wing.

The slot widths were defined so as to be approximately equal to the sucked height at the high off-design suction levels. Boundary layer sucked height is that height at which the total mass flow in the boundary layer below that point is equal to the mass flow going through the slot. In other words, the sucked height is the height of the local stagnation streamline several slot widths ahead of the slot. Making the slot width approximately equal to the sucked height at each location prevents excessive acceleration of the flow entering the slots.

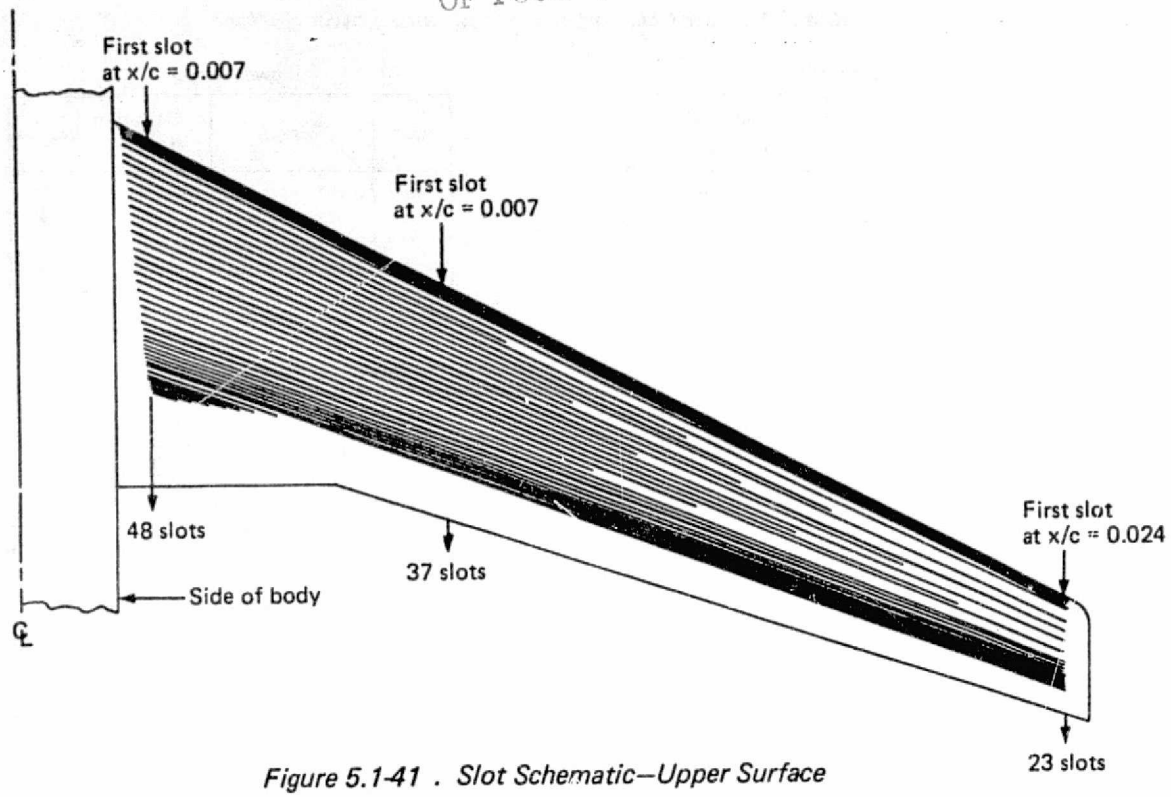

Figure 5.1-41 . Slot Schematic—Upper Surface

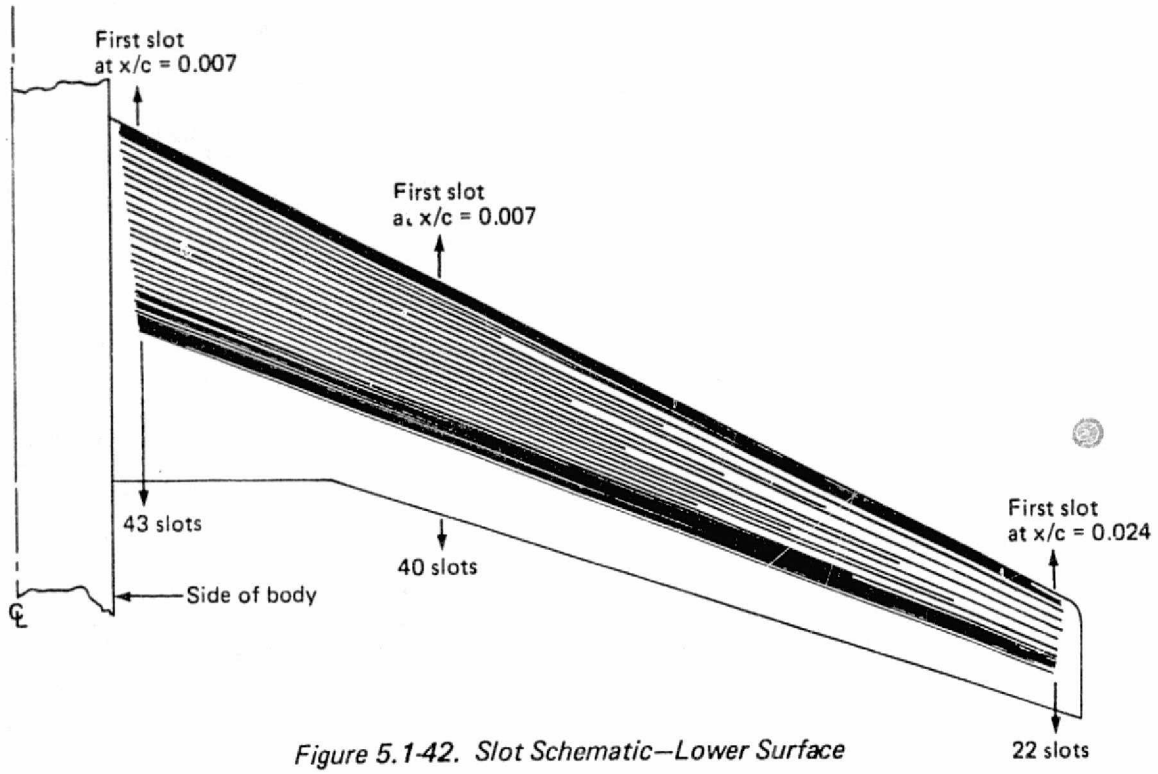

Figure 5.1-42. Slot Schematic—Lower Surface

Table 5.1-1. Slot Definition—Upper and Lower Surface

Upper surface

x/c*	η_{ENDS}	Slot width cm (in)	Re_s**
0.007	0.101 → 0.628	0.013 (0.005)	75
0.009	0.101 → 0.231	↑	↑
0.012	0.101 → 0.735	↕	↕
0.015	0.101 → 0.300	↕	↕
0.018	0.101 → 0.873	↕	↕
0.021	0.101 → 0.360	↕	↕
0.024	0.102 → 0.982	↓	↕
0.028	0.102 → 0.982	0.013 (0.005)	↕
0.036	0.102 → 0.982	0.015 (0.006)	↕
0.063	0.102 → 0.982	0.015 (0.006)	↕
0.090	0.103 → 0.982	0.015 (0.006)	↕
0.118	0.104 → 0.452	0.018 (0.007)	↕
0.146	0.105 → 0.981	0.018 (0.007)	↕
0.174	0.106 → 0.607	0.020 (0.008)	↕
0.202	0.106 → 0.760	↑	↕
0.230	0.106 → 0.980	↕	↕
0.258	0.107 → 0.520	↕	↕
0.286	0.108 → 0.661	↕	↕
0.314	0.109 → 0.979	↕	↕
0.342	0.110 → 0.827	↕	↕
0.370	0.110 → 0.570	↕	↕
0.398	0.111 → 0.978	↕	↕
0.426	0.111 → 0.725	↕	↕
0.454	0.112 → 0.877	↕	↕
0.482	0.113 → 0.977	↕	↕
0.510	0.114 → 0.635	↕	↕
0.538	0.115 → 0.776	↕	↕
0.566	0.115 → 0.976	↓	↕
0.594	0.116 → 0.976	0.020 (0.008)	↓
0.621	0.116 → 0.975	0.025 (0.010)	75
0.649	0.117 → 0.975	0.025 (0.010)	100
0.670	0.117 → 0.975	0.030 (0.012)	125
0.690	0.118 → 0.974	0.030 (0.012)	150
0.705	0.118 → 0.974	0.036 (0.014)	↑
0.720	0.119 → 0.974	0.036 (0.014)	↕
0.735	0.119 → 0.974	0.041 (0.016)	↕
0.749	0.120 → 0.974	0.041 (0.016)	↕
0.764	0.120 → 0.973	0.041 (0.016)	↕
0.779	0.120 → 0.973	0.041 (0.016)	↕
0.794	0.121 → 0.973	0.036 (0.014)	↕
0.811	0.122 → 0.259	0.036 (0.014)	↕
0.829	0.123 → 0.233	0.036 (0.014)	↕
0.839	0.123 → 0.218	0.030 (0.012)	↕
0.849	0.123 → 0.205	↑	↕
0.859	0.124 → 0.190	↕	↕
0.869	0.124 → 0.176	↕	↕
0.879	0.124 → 0.160	↓	↓
0.888	0.125 → 0.146	0.030 (0.012)	150

Lower surface

x/c*	η_{ENDS}	Slot width cm (in)	Re_s**
0.007	0.101 → 0.628	0.013 (0.005)	60
0.009	0.101 → 0.231	↑	↑
0.012	0.101 → 0.755	↕	↕
0.015	0.101 → 0.300	↕	↕
0.018	0.101 → 0.873	↕	↕
0.021	0.101 → 0.360	↕	↕
0.024	0.102 → 0.982	↓	↓
0.028	0.102 → 0.982	0.013 (0.005)	60
0.036	0.102 → 0.982	0.018 (0.007)	75
0.063	0.102 → 0.982	0.018 (0.007)	↕
0.090	0.103 → 0.982	0.018 (0.007)	↕
0.118	0.104 → 0.462	0.023 (0.009)	↕
0.146	0.105 → 0.981	↑	↕
0.174	0.106 → 0.607	↕	↕
0.202	0.106 → 0.760	↕	↕
0.230	0.106 → 0.980	↕	↕
0.258	0.107 → 0.520	↕	↕
0.286	0.108 → 0.661	↕	↕
0.314	0.109 → 0.979	↕	↕
0.342	0.110 → 0.827	↕	↕
0.370	0.110 → 0.570	↕	↕
0.398	0.111 → 0.978	↓	↕
0.426	0.111 → 0.725	0.023 (0.009)	↕
0.454	0.112 → 0.877	0.025 (0.010)	↕
0.482	0.113 → 0.977	0.025 (0.010)	↓
0.510	0.114 → 0.635	0.025 (0.010)	75
0.538	0.115 → 0.977	0.036 (0.014)	100
0.555	0.115 → 0.785	0.036 (0.014)	125
0.572	0.115 → 0.976	0.046 (0.018)	150
0.586	0.115 → 0.940	0.046 (0.018)	↑
0.601	0.115 → 0.976	0.051 (0.020)	↕
0.612	0.115 → 0.975	↑	↕
0.622	0.116 → 0.975	↕	↕
0.630	0.116 → 0.975	↕	↕
0.638	0.116 → 0.975	↕	↕
0.646	0.117 → 0.686	↕	↕
0.652	0.117 → 0.975	↕	↕
0.660	0.117 → 0.751	↕	↕
0.665	0.118 → 0.975	↕	↕
0.673	0.118 → 0.835	↕	↕
0.680	0.118 → 0.974	↕	↕
0.687	0.118 → 0.910	↓	↓
0.693	0.118 → 0.974	0.051 (0.020)	150

*Chord length is based upon trapezoidal planform.
**Nominal at $C_L = 0.5$, altitude = 12 190m (40 000 ft), $M_\infty = 0.8$

However, a slot somewhat wider than the height of the sucked layer also functions satisfactorily, since the flow behaves essentially as if bounded only by the rear wall of the slot, with a bound vortex being formed in the forward portion of the slot (Ref. 9). Thus, at the design condition, these slots will still function satisfactorily because the slot width will then be somewhat larger than the sucked height.

The slot Reynolds numbers shown in Table 5.1-1 are nominal values at the root location based on suction levels at the design lift coefficient ($C_L = 0.5$). At the off-design suction levels, the slot Reynolds numbers in the leading edge region will be about twice as large as those shown.

Adjustments for the different suction requirements for the design and off-design conditions will require adjustable valve settings on the suction trunk ducts. However, the entire leading edge area back to 10% chord is served by a single duct for the upper surface and a single duct for the lower surface. As a result, it may not be possible to change from the design suction distribution to exactly the required off-design suction distribution. The off-design case has a large peak which extends back to only about 4% chord, and at the design condition at the mid-span location there is no suction peak near the leading edge. Thus, at the off-design condition, the leading edge suction peak may be wider than is actually required. However, this can be compensated for by making the peak slightly lower, and by lowering the suction levels in the mid-chord region.

In conclusion, the suction slot arrangement will be compatible with operations over the required lift coefficient range. Sucked heights and slot Reynolds numbers will be highest, but still at or below maximum allowable levels for the high-suction off-design conditions and lower at the design condition. The system will be adjustable to allow the closest possible match with the design suction requirements and an acceptable approximation to the off-design requirements.

5.1.4 INTERNAL DUCT SYSTEM DESIGN

The internal duct system provides the means to collect the suction air from the slots and conduct this air to the suction pumps. This system is designed to minimize the potential for internal disturbances to propagate back through the slot and cause boundary layer transition. In addition, the duct system losses are held to a minimum to ensure that suction compressor weight and pumping penalties do not significantly degrade the drag reduction benefits achieved through laminar flow control. The duct system also incorporates the necessary elements required for balancing the suction manifold system to provide the appropriate flow distribution during normal and off-design operation.

The concept of the suction surface and internal ducting arrangement adopted for the final configuration is shown in Figure 5.1-43. The suction surface and associated collector duct system is superimposed on the basic wing structure in the form of a glove. This consists of a foam-filled fiberglass sandwich outer skin and a spanwise array of hard foam spacers. The slots are contained in prefabricated inserts, which are bonded into machined channels in the skin. The suction airflow, after passing through a slot, is first collected in a shallow groove called the slot plenum; from there, it passes into another plenum (i.e., subplenum) via a pattern of bleedholes in the lower part of the insert. This provides the throttling stage.

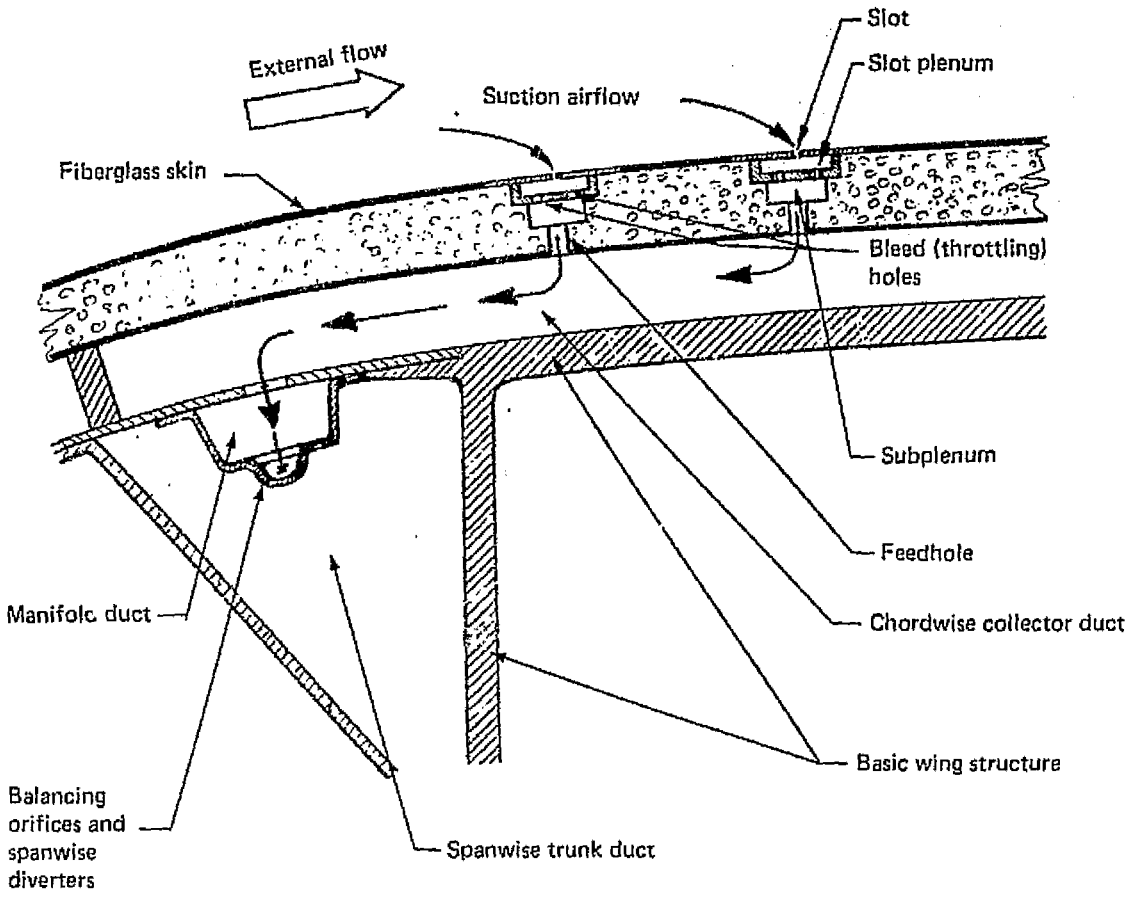

Figure 5.1-43. Suction Surface and Internal Duct System Concept

From the subplenum another row of holes (i.e., feed holes) transmits the suction air into the chordwise collector ducts. These chordwise ducts, then, feed into the main trunk ducts which run along the span ahead of and behind the structural wing box. An intermediate manifold duct, located inside each trunk duct, contains a row of louvers. These louvers direct the suction flow spanwise and provide just enough throttling to offset the pressure gradient in the trunk duct. Each trunk duct is provided with a control valve upstream of the suction pump. This allows adequate in-flight adjustment of the suction flow distribution to accommodate off-design operation. The discussion of the characteristics of the selected structural concept (Subsection 5.2.6) provides an overall-view of the suction system arrangement, the system components and the flow paths leading to the suction unit.

The criteria applied to the duct system design are given in Table 5.1-2. The suction slot Reynolds number was limited to 150 (based on total slot width). Suction slot and flow collection system flow velocities were limited to a level that would not cause separation and/or external slot disturbance. Duct airflow velocities were limited to 0.2 Mach maximum to minimize collection system losses. Additional requirements were: a) To provide for adequate overboard drain provisions throughout the duct system to eliminate water and/or

Table 5.1-2. Internal Duct Design Criteria

Item	Requirements	Remarks
Suction slot	Slot Reynolds number limited to 150	Minimizes potential for slot-generated disturbances to trip external boundary layer
	Slot width equal to collected boundary layer height	Minimizes boundary layer shear gradients
	Uniform slot inflow velocity (±1.5%)	Limits potential to generate large external boundary layer eddies that could result in transition
Collection plenum (under slot)	Shallow to minimize slot flow wake instability	Northrop experience indicates external flow disturbances are directly related to slot wake flow stability
	Low flow velocities, 15.2 m/s (50 ft/s)	Minimize potential to degrade uniform slot inflow velocity
Bleed holes:		
Nonflow restricting	Diameter equal to 3 times collection plenum height. Spacing equal to 15 times collection plenum height	Based on Northrop test experience
Flow restricting	Maximum spacing same as above; minimum spacing and diameter to be obtained by test	Test required to establish validity of design. Sufficient number of holes required to minimize potential flow spillage and excessive slot inflow gradients
Subplenum (if used)	Low flow velocities	Minimizes inflow disturbance and system pressure loss
Feed holes:		
Without bleed holes or subplenum	Same as bleed holes	Same as bleed holes
With bleed holes and subplenum	Low flow velocities (0.2 mach)	Minimize system pressure losses
	Spacing determined by test	Ensure that slot inflow velocity gradients are within limits
Tributary ducts (if used)	Low longitudinal flow velocities, 15.2 m/s (50 ft/s) and pressure loss less than 3% of upstream elements	Ensure that slot inflow velocity gradients are within limits
	Ducts aligned to augment flow	Minimize system pressure losses
Collector ducts:		
Chordwise in glove	Use constant maximum area duct (objective is constant static pressure)	Minimize flow balancing adjustment requirements Minimize flow variations for off-design operation
Chordwise in wing box	Size for 0.2 mach maximum flow velocity	Minimize pressure losses
Spanwise	Size for 0.2 mach maximum flow velocity (use maximum available area)	Minimize pressure losses
Trunk	Size for 0.2 mach maximum flow velocity (use maximum available flow area)	Minimize pressure losses and flow balancing requirements
	Utilize augmented mixing (ejector action) when joining flow streams	Reduce system mixing losses
Compressor inlet ducts	Reduce duct area to match compressor design requirements	Provide system/compressor optimum flow velocity match
	Avoid abrupt flow area or change of airflow direction immediately upstream of compressor	Minimize compressor inlet flow distortion
Compressor discharge ducts	Size for 0.25 mach airflow velocity maximum	Minimize system losses
Overboard discharge duct	Size for discharge pressure ratio sufficient to provide free stream flow velocity	Minimize system losses
	Locate discharge duct for minimum drag	

other potential liquid spillage from collecting in the ducts, and b) To ensure that potential fuel or fuel vapor entrapment in the duct system will not present a fire hazard for operation under normal and failure conditions. Fluid drain holes would incorporate check valves to prevent air inflow during operation of the suction system.

5.1.4.1 Internal Duct System Sizing

The internal duct system size is determined by the requirement to achieve optimum suction distribution for the design operating flight condition and provide acceptable suction distribution within the LFC operational flight envelope. This is illustrated by the following outline of the system sizing techniques used for the Model 767-810 updated baseline configuration. The suction distribution and suction slot locations were established using techniques previously described. These requirements were converted into individual slot airflow quantities for the design conditions shown on Figure 4.3-1. using the pressure distributions given on Figure 5.1-13.

Evaluation of the required suction surface pressures and airflows showed that operation at high gross weights at maximum altitude resulted in both the largest duct and largest suction compressor size. The duct volumes required exceed those normally available in conventional wing planforms. To provide the increased duct volumes required for LFC there is an associated increase in wing weight. To minimize the weight increase, it was decided that the duct system should be optimized for normal cruise conditions and the compressor unit power capability matched to operation at maximum altitude and high gross weight conditions. This resulted in reduced duct and wing system weight for a slight increase in suction power unit size and weight.

5.1.4.2 Suction Surface Coliection System

The X-21A suction airflow collection system consisted of the suction slot, a plenum, and bleed holes to vent the plenum to a tributary duct similar to the arrangements shown in Figures 5.1-44 and 5.2-3. The X-21A configuration utilized the tributary duct discharge vent to balance the pressure losses from the suction surface to the collection manifold. It is apparent that this vent would be inaccessible when the wing was assembled and could not be adjusted. A modified surface collection system geometry which utilizes an insert containing a second plenum (subplenum) between bleed holes and the chordwise collector duct (see Fig. 5.1-44) provides the required adjustment capability and ready access through removal of the surface insert strips. Tests described separately show that this configuration would provide the required throttling capability near the surface and maintain acceptable slot inflow gradients.

5.1.4.3 Collector Ducts

Collector ducts provide the means to collect and direct the suction airflow to the main trunk ducts. Pressure losses in the total collector/trunk duct system are minimized to ensure that the suction compressor engine size and power requirements are not excessive. This is done by utilizing augmentation or ejector action where possible when airflow is throttled for control purposes and by limiting the duct airflow velocity to .2 Mach maximum. With spanwise collector ducts, direct tributary duct discharge augmentation should be used if

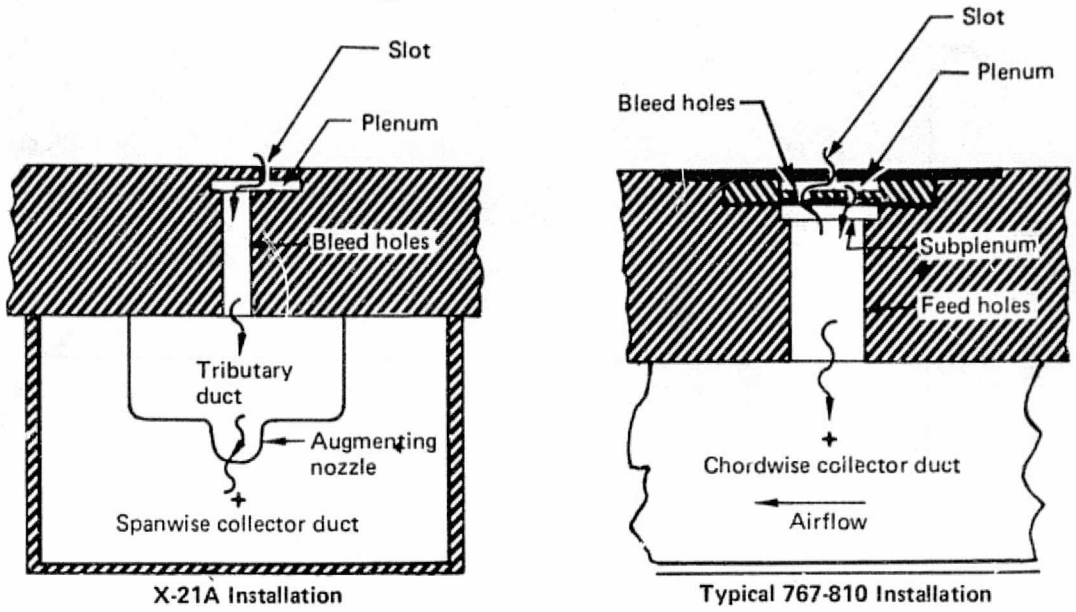

Figure 5.1-44. Surface Suction Collection Geometry Comparison

practicable means of access to the discharge nozzles can be attained. In chordwise collector ducts, as used on the Model 767-810, the ducts cross through a relatively large variation in pressure levels. The chordwise collector ducts are made as large as possible to minimize the chordwise pressure gradients. With the bleed holes sized to provide the proper chordwise throttling variation at the design condition, significant variations in airflow will occur for off-design operation. A typical suction airflow variation over 10% to 60% wing chord and from wing root to tip is shown in Figure 5.1-45 for a range of wing lift coefficients. While not ideal, these variations can be controlled within acceptable limits by adjustment of individual trunk duct valves to accommodate a particular flight condition.

5.1.4.4 Trunk Ducts

Trunk ducts collect the airflow from either spanwise or chordwise collector ducts and deliver the airflow to the suction compressor. The X-21A spanwise collector ducts grouped several slots together in a collection plenum. The pressure level in each collection plenum was throttled by electrically actuated gate valves that balanced the total suction system. This was a test installation and would not be acceptable on a production airplane without a considerable reduction in the number of valves. Spanwise collection duct configurations studied considered the use of adjustable flow augmenting valves that would be preset on the ground. However, these configurations were not studied in sufficient detail to establish if operation adjustment would normally be required in flight.

The Model 767-810 trunk duct system utilizes an intermediate tributary duct with nozzle openings adjusted to provide for pressure equalization between chordwise collection ducts by compensating for the normal pressure gradient due to flow in the trunk duct. This

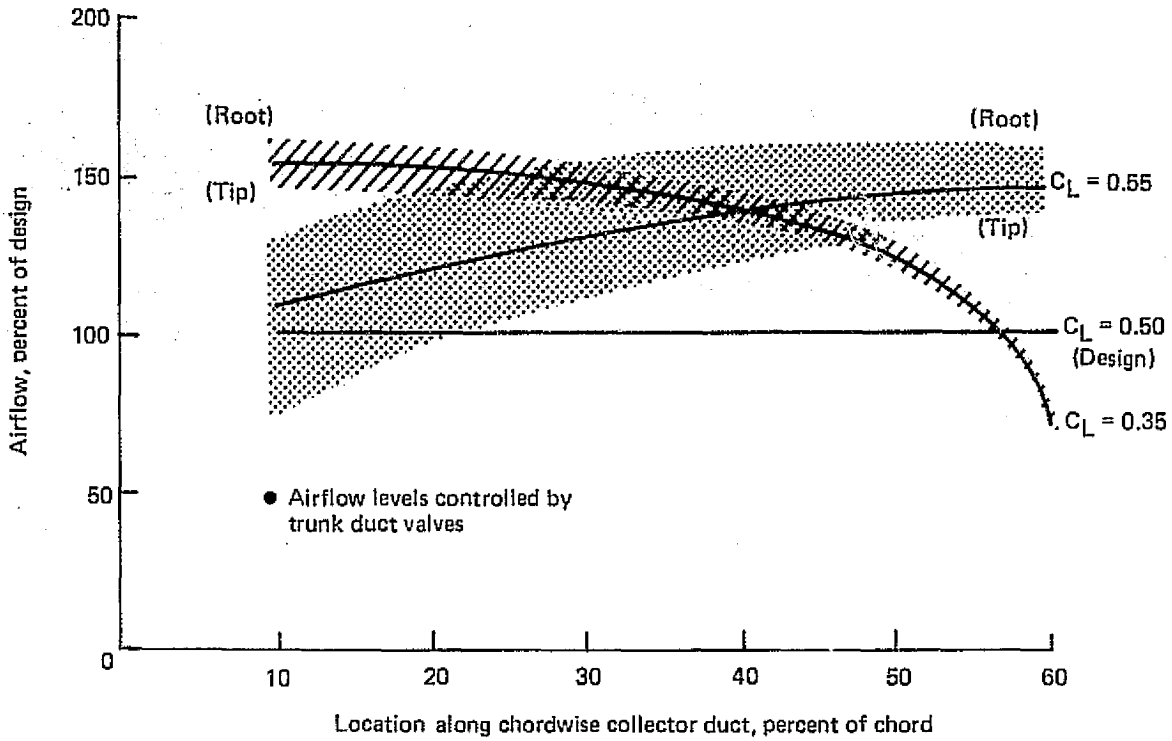

Figure 5.1-45. Effect of C_L Variation on Suction Distribution— With Variable Trunk-Duct Suction

would be expected to result in modest amounts of spanwise flow in the tributary ducts, particularly for off-design conditions. The combined flow interactions and duct pressure loss characteristics result in an estimated flow variation from wing tip to root of up to ±25% (see Fig. 5.1-45) for the extreme off-design case. The manifolds which collect the airflow from the wing trunk ducts and deliver the air to the suction compressors would include provisions for flow mixing to provide augmentation and minimize system losses. In addition, automatically operated valves would be used at the ends of the trunk ducts to balance the system for off-design operation.

The trunk duct system was sized on the basis of .2 Mach maximum duct airflow velocity and the two suction pressure levels provided by the suction compressor. These suction levels were selected to correspond to the wing upper surface for 0 to 80% of wing chord and the lower surface for 0 to 70% of chord. The duct velocity was increased to 0.25 Mach at the compressor inlet face.

5.1.4.5 Suction Compressor Discharge Duct

The suction compressor discharge duct was sized for .25 Mach airflow at the design operating condition. Pressure losses to the overboard discharge opening were assumed to be equal to 100% of the dynamic head based on duct flow velocity. Overboard pressure losses were based on providing discharge velocities equal to free stream velocity.

5.1.4.6 Empennage Internal Duct System

Auxiliary system trades were not conducted in sufficient detail to define the design of an integrated airplane secondary power/suction drive system. However, the empennage suction system power requirements were found to be compatible with the airplane APU based on a conservative selection of suction airflow requirements and duct flow loss characteristics.

The suction duct system arrangement is defined to be similar to the wing suction duct system except that only one suction pressure level was used since the design operating condition for the stabilizer is zero lift coefficient. The empennage (horizontal tail only) upper and lower surface suction distribution was assumed to be similar to the wing mid-span upper surface distribution. The surface pressures were based on the average value of the upper and lower surfaces. Surface suction was applied from 0 to 80% of chord for both upper and lower surfaces. The design altitude is 13 560 m (44 500 ft) and the operating altitude is 12 190 m (40 000 ft).

Based on the above considerations, the ducting and suction flow distribution system for the empennage was defined so that it would be compatible with a typical APU installation. The arrangement would allow the APU to function in the normal fashion for ground operation and be functionally convertible to provide LFC suction for the horizontal tail in cruise flight. Such an arrangement would probably not be practical if both the horizontal and vertical tail were laminarized since the power and airflow requirements would then substantially exceed the nominal APU capability.

5.1.5 INTERNAL DUCT SYSTEM PRESSURE LOSS CHARACTERISTICS

The duct system pressure loss characteristics described in this subsection apply only to the system selected for the final airplane configuration. Primary effort in this area was expended to support configuration feasibility studies based on preliminary estimates of duct loss factors. Detailed analyses were performed only where they were required to validate the selection of specific critical duct section geometry. Furthermore, the duct system has not been optimized in the sense that features which tend to minimize losses were traded against these which would produce other desirable characteristics such as improved flow stability, controllability or adaptability to off-design conditions.

5.1.5.1 Surface Suction Collection Geometry

The suction slot/plenum/bleed hole pressure loss calculation methods established by Northrop (Ref. 1) have been used to calculate suction surface element losses. These methods are well defined and should require no further discussion. A basic change in the surface suction element geometry over that of the X-21A is the use of a bleed hole strip for flow balancing and a subplenum with feed holes in place of the flow velocity augmenting tributary duct (Figure 5.1-44). In general, the loss across the suction slot/bleed hole/subplenum combination is from 4 to 6% of free stream dynamic pressure when no selective throttling is applied to control the suction inflow distribution throughout the wing surface area. During off-design operation, with throttling, the loss can locally approach 20% of freestream dynamic pressure. This loss is due to the throttling arrangement required to accommodate both duct

pressure levels and distribution as well as the wing surface pressure variations which are a function of both wing lift coefficient and Mach number.

5.1.5.2 Collector Ducts

The collector ducts gather air from the subplenums and route this air to the main trunk ducts. The flow losses in the collector duct contribute significantly to the pressure drop between the wing surface slots and the wing trunk ducts. Analysis has shown that spanwise collector duct losses in a well designed duct system utilizing flow augmentation should be less than 10% of free stream dynamic pressure. The chordwise collector duct system used in the glove concept represented a special problem in that flow from a series of spanwise slots had to be collected into an array of single ducts for a wide range of wing surface pressures including those corresponding to off-design conditions. The range of the wing pressure coefficients is shown as a function of chord for the values of lift coefficient appropriate to the principal flight envelope in Figure 5.1-46. Typical associated wing surface pressures are shown on Figure 5.1-47. Also, in the same figure, the dashed line gives the typical pressure variation in a duct of constant cross section in order to illustrate the loss associated with flow control at the design lift coefficient ($C_L = 0.5$). The duct pressure level would obviously be adjusted either up or down to accommodate the off-design case and this would lead to somewhat higher losses and changes in surface inflow. Analyses of flow characteristics were performed for both a tapered and a constant area chordwise duct. The pressure loss is about 2% of free stream dynamic pressure versus 10% for a uniformly tapered duct. Thus the constant section duct was selected for the flow distribution system. The corresponding chordwise duct slot airflow characteristics are shown in Figure 5.1-45.

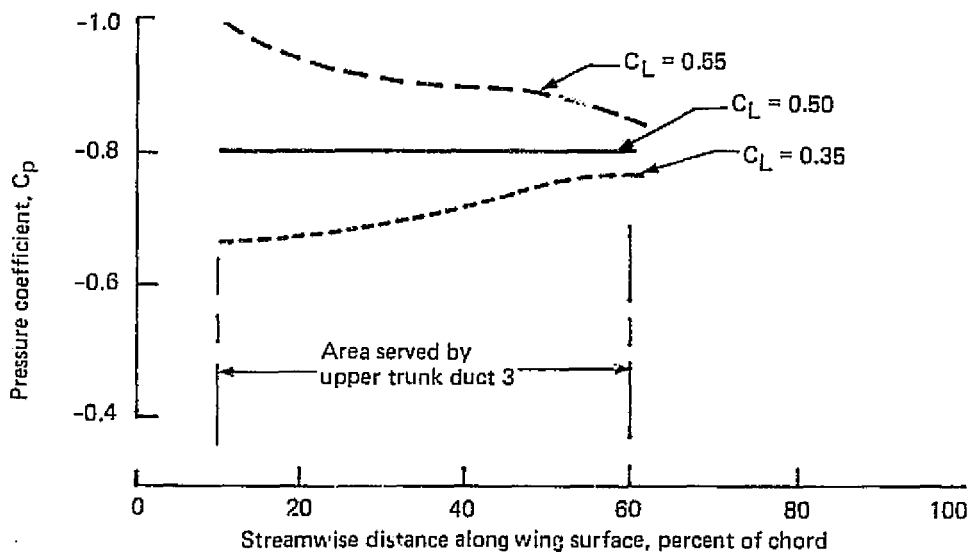

Figure 5.1-46. Upper Wing Surface Pressure Coefficient Variation

The chordwise collection ducts feed into a pressure equalizing tributary duct which in turn feeds into a large spanwise trunk duct. This duct would have loss characteristics similar to that of the augmented single slot spanwise collection duct or approximately 10% of free

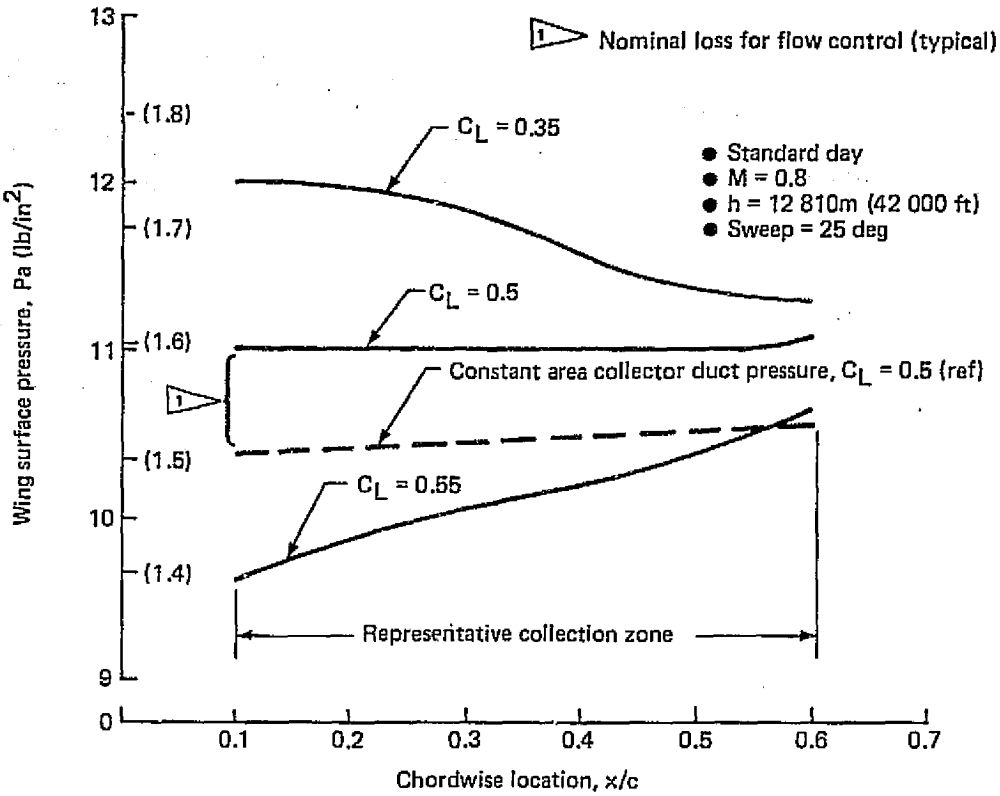

Figure 5.1-47. Wing Upper Surface Pressure Variations

stream dynamic pressure. Operation at higher off-design wing lift coefficients (e.g., C_L = .55) will require pressure levels about 10% higher than design at mid-span to provide adequate wing tip suction with corresponding higher airflows. Increased suction airflow levels result from the need to provide minimum acceptable airflow intensities in critical (i.e., low pressure) areas which produces excess suction airflow in other areas where surface pressures are higher. Under these conditions, the spanwise duct pressure losses will about double, thereby increasing the spanwise pressure gradient. This effect causes wing root suction to increase and wing tip suction to decrease relative to the average levels as shown on Figure 5.1-45. For lower wing lift coefficients with resultant higher wing and duct pressures, the effect on spanwise distribution is notably reduced as shown on the above figure.

The pressure losses due to combining the suction flows and to deliver the airflow to the suction compressor have not been studied in sufficient detail to determine the combined effects of duct losses and augmented flow mixing. A preliminary analysis indicated that augmentation should essentially compensate for friction losses. However, because of the limited analysis, a pressure loss equivalent to 5% free stream dynamic pressure was assumed. A similar loss was assumed for the duct to the overboard discharge port.

The losses in the suction airflow distribution system for the selected LFC wing concept are summarized in Table 5.1-3 for operation at the design lift coefficient (C_L = .5). The overall effect aggregates between 27% and 30% of free stream dynamic pressure assuming exhaust nozzle coefficients very close to unity. This range is small enough (±5%) so that consistent estimates of power requirements for performance calculations can be made.

5.1.6 EMPENNAGE DESIGN

The principal considerations for the empennage design were to achieve the required stability and control characteristics with near-minimum size of tail surfaces. Furthermore, the empennage should also be suitable to accommodate laminar flow control at least to a significant extent. The incorporation of active controls (SAS) extends the allowable C.G. range and contributes to reducing the size of the tail surfaces thereby reducing weight and drag. The aft-fuselage mounted powerplant installation selected for this airplane requires a T-tail empennage configuration which also provides the best opportunity to reduce trim drag. In recognition of the fact that this type of tail arrangement is susceptible to unfavorable deep-stall characteristics at high angles of attack, incorporation of an α-limiter is contemplated.

5.1.6.1 Airfoil Selection

Considerations for the selection of the horizontal tail airfoil section included, first of all, those that would be generally applicable to any jet transport airplane, that is, a high speed M_D capability exceeding that of the wing and a low speed lift capability adequate to provide trimmed flight in the landing approach configuration at the forward C.G. limit. But, since laminarization of the horizontal tail surface was also set as a design objective, this introduced certain additional requirements that would not normally be considered for a turbulent airplane.

Table 5.1-3. Internal Duct System Pressure Losses

Duct section	Loss* (%)
Slot/plenum/bleed holes/subplenum	5
Collector duct (chordwise)	2 to 5
Trunk duct (spanwise)	10
Manifold to compressor	5
Compressor to overboard discharge	5
Overboard discharge	As required for discharge velocity equal to free stream

*Percent of free-stream dynamic pressure

One of these special requirements was a limitation on the horizontal tail sweep angle, which, of course, had an impact on the airfoil selection. Normally, the horizontal tail of a turbulent airplane has more sweep than the wing and also a lower thickness ratio in order to assure flow conditions free of shock induced separation during recovery from a dive at the structural design speed limit. But, as pointed out in the preceding paragraphs, laminarization becomes more difficult at higher sweep angles and this tends to put a limitation on the allowable sweep.

Based on these considerations, the sweep of the horizontal tail for the present design was chosen so that the leading edge sweep angle would be the same as that of the wing, i.e., $\Lambda_{LE} = 27.5°$. Using a planform that corresponds to the customary design trends, that is an aspect ratio of 4 and taper ratio of 0.4, the effective sweep angle of the horizontal tail becomes approximately 22°. With the design limit Mach number of the airplane taken as $M_{Dive} = 0.90$, the required drag divergence Mach number for the representative airfoil section of the horizontal tail becomes $M_{D_H} = 0.845$. According to Figure 5.1-6 of Section 5.1.22, the available airfoil technology permits, at this Mach number, a thickness ratio of approximately 11% for the normal section at $C_n = 0.2$. Based on this consideration the streamwise thickness ratio of the horizontal tail was chosen to be 10%.

The next step was to select the airfoil shape. Traditionally, jet transports use inverse cambered airfoil sections for the horizontal tail to provide sufficient downward lift capability for trimmed flight in the landing approach configuration. For the present airplane with more aft C.G. location than normal, however, a symmetrical section was chosen since the operating tail lift coefficients are near zero. This also provides the conditions most compatible with LFC and avoids the unfavorable pressure distributions that would result if a cambered airfoil were operated near zero lift. The slightly larger tail size needed to meet the landing approach condition was accepted as an appropriate compromise in this case.

Figure 5.1-48 shows the shape of the equivalent two-dimensional airfoil section and the computed pressure distributions corresponding to the nominal design condition of the airplane. In cruise, the horizontal tail is expected to operate at near zero lift but in any case within the range of $C_n = \pm 0.2$.

5.1.6.2 Extent of Laminarization

Originally an "all flying" horizontal tail was considered for this airplane which, of course, would lend itself readily to full chord laminarization. In consideration of this, a brief study was made regarding the merits of complete laminarization versus partial. The approach for this evaluation was similar to the one done for the wing and discussed in connection with Figures 5.1-12, 5.1-13 and 5.1-14 of Section 5.1.2.5. The representative section profile drag and corresponding equivalent suction drag were estimated on the basis of boundary layer calculations and tentative definition of suction requirements. The results are presented in Figures 5.1-49 and 5.1-50. It is evident that the benefits of extending LFC much beyond 75% chord location are not very significant and probably would not justify the added weight and complexity. It was, therefore, decided to terminate LFC at 80% chord. This also allowed the incorporation of a geared elevator over the last 20% of the horizontal tail chord that was deemed desirable from the standpoint of handling characteristics. In addition, the elevator provides a means of adjusting the pressure distribution to favor LFC for a range of C.G. positions.

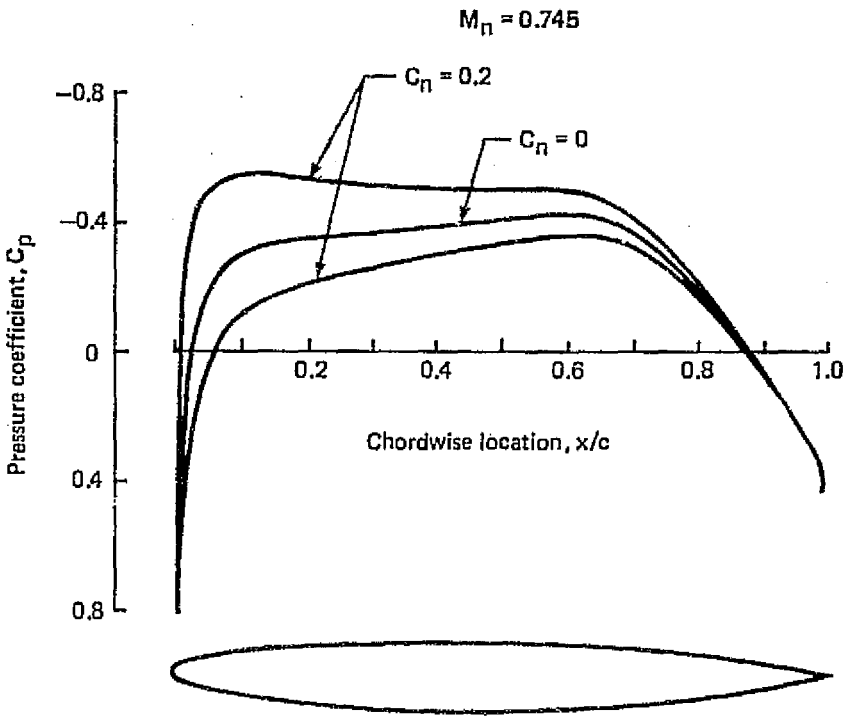

Figure 5.1-48. Horizontal Tail Airfoil Section and Theoretical Pressure Distributions at the Nominal Design Condition

Laminarization of the vertical tail was also considered. The problem, however, would be more difficult in this case because of the presence of the center-engine inlet and because of the higher sweep angle that the vertical tail would generally require. The selected configuration of the center engine inlet would allow at best the laminarization of the upper part of the vertical only. An alternate configuration, using four engines enclosed in twin side nacelles, that would permit full span laminarization of the vertical tail was also considered. The trades between various options regarding the extent of laminarization for the empennage were estimated and the results, expressed in terms of drag, weight and fuel savings, are presented in Figure 5.1-51. Based on this evaluation, it was concluded that laminarization of the vertical tail for the present airplane could not be justified since the added cost and complexity would more than offset the gain in fuel saving and gross weight reduction.

5.1.6.3 Empennage Geometry Definition

To approach minimum tail size with LFC application, the horizontal tail was chosen to be an "all flying" type with a 20% chord geared elevator. The horizontal tail was sized to provide an unaugmented time-to-double amplitude (t_2) of 6 seconds at M_{Dive}/V_{Dive} at the

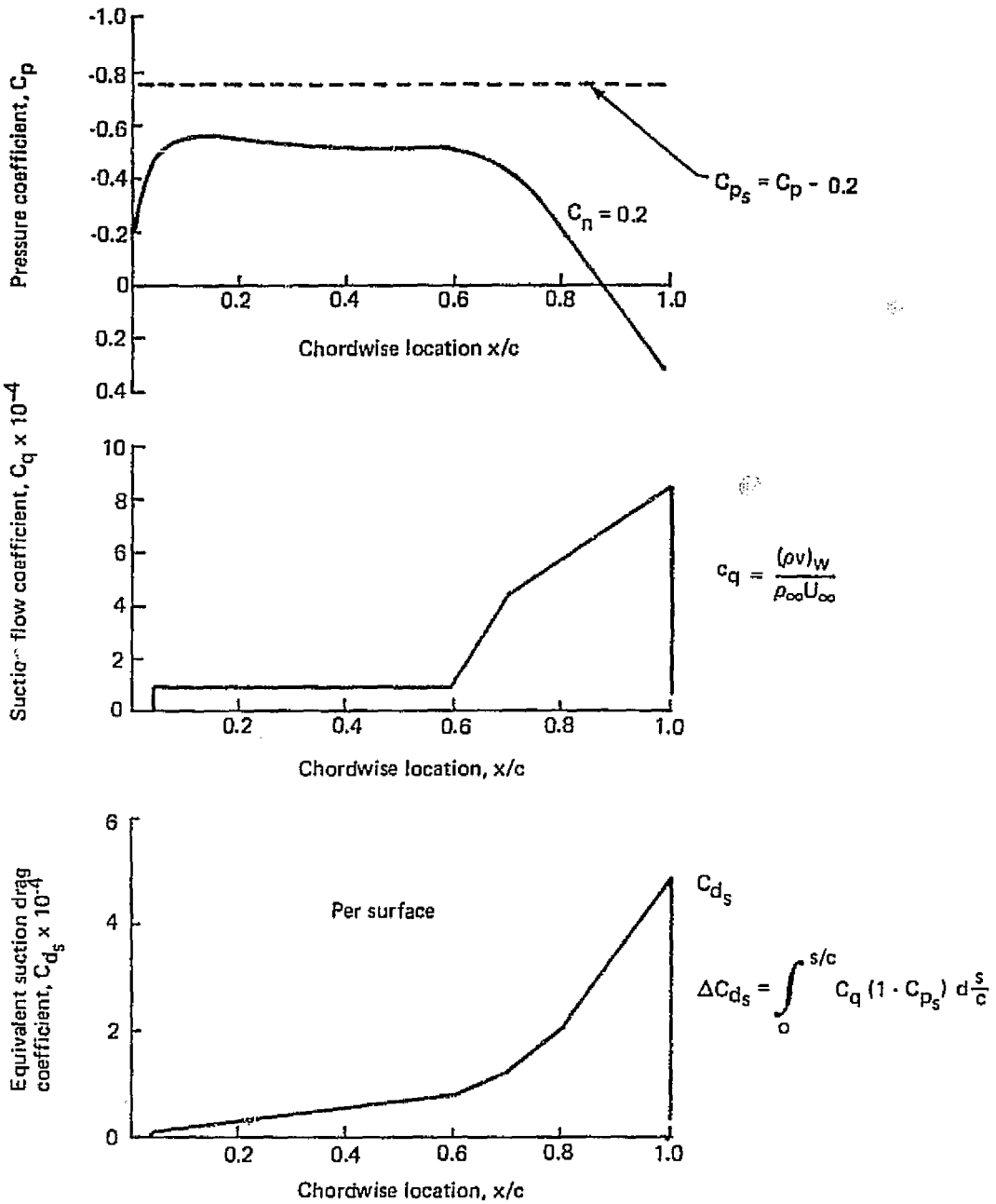

Figure 5.1-49. Flow Coefficient and Equivalent Suction Drag of the Horizontal Tail Section as a Function of Laminarization

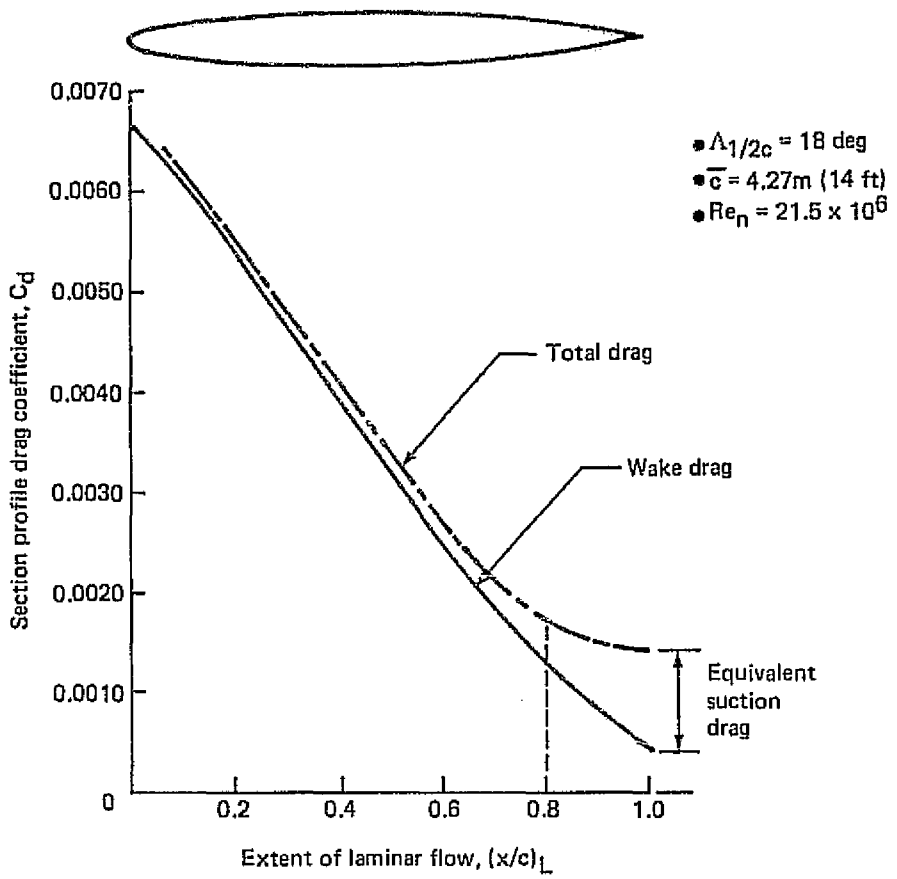

Figure 5.1-50. Horizontal Tail Section Profile Drag as a Function of the Extent of Laminarization

aft C.G. limit and also to provide control for takeoff rotation at the forward C.G. limit. A 1990 technology, non-flight critical stability augmentation system (SAS) is incorporated in the airplane to allow aft balance and to provide satisfactory handling qualities throughout the flight envelope. The tail sizing chart, Figure 5.1-52, shows that a horizontal tail volume coefficient of $V_H = 0.744$ could accommodate a C.G. range of 40% to 10% MAC at a minimum rotation speed of 254 km/h (137 kt). A 9.2 km/h (5 kt) increase in the minimum V_R would allow the forward C.G. limit to be extended to 5% MAC.

The vertical tail was sized by a minimum unaugmented directional stability requirement of $C_{n_\beta} \geq .0015$ per deg. The lateral-directional stability will also be augmented by a non-flight critical SAS to provide satisfactory handling qualities throughout the flight envelope.

The rudder control arrangement was selected according to the current design practice accepted for transport airplanes. For a trijet configuration this generally means sizing to meet appropriate crosswind landing criteria.

	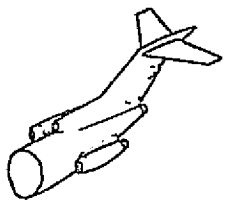 No laminarization (Baseline)	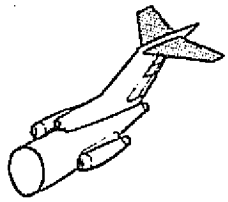 Horizontal laminar	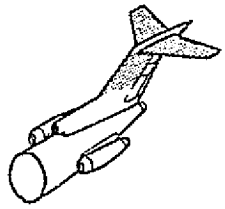 Horizontal and partial vertical laminar	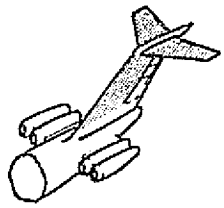 Horizontal and vertical laminar
$\frac{\Delta C_D}{C_D}$	0	−5.3%	−8.0%	−7.8%
$\frac{\Delta SFC}{SFC}$	0	0.42%	0.62%	0.47%
ΔW_E	0	898 kg (1980 lb)	1442 kg (3180 lb)	2436 kg (5370 lb)
$\frac{\Delta W_F}{W_F}$	0	−5.4%	−8.1%	−7.2%
$\frac{\Delta W}{W}$	0	−1.5%	−2.2%	−1.3%

Figure 5.1-51. Empennage Configuration Trades

5.1.7 AERODYNAMIC DESIGN INTEGRATION

This subsection provides a discussion of the considerations leading to the selection of the critical elements of the LFC airplane, and assembles the basic aerodynamic characteristics and drag polars used in sizing the final LFC transport configuration (see Section 6.0) and evaluating its performance characteristics.

5.1.7.1 General Objectives and Concerns

The principal objective of the aerodynamic design integration was to define a configuration that would take full advantage of the benefits of laminar flow control. This implies that keen attention must be paid to avoiding or at least minimizing all forms of aerodynamic interference drag. Two items, namely, interference drag due to the powerplant installation and interference drag due to the suction unit installation are of particular concern.

According to current design trends regarding turbulent airplanes, the wing-mounted engine installation is preferable to the aft-fuselage mounting. In the case of an LFC airplane, however, the wing-mounted installation would have a disadvantage inasmuch as a substantial portion of the wing lower surface, adjacent to the nacelles, might not be laminarized due to

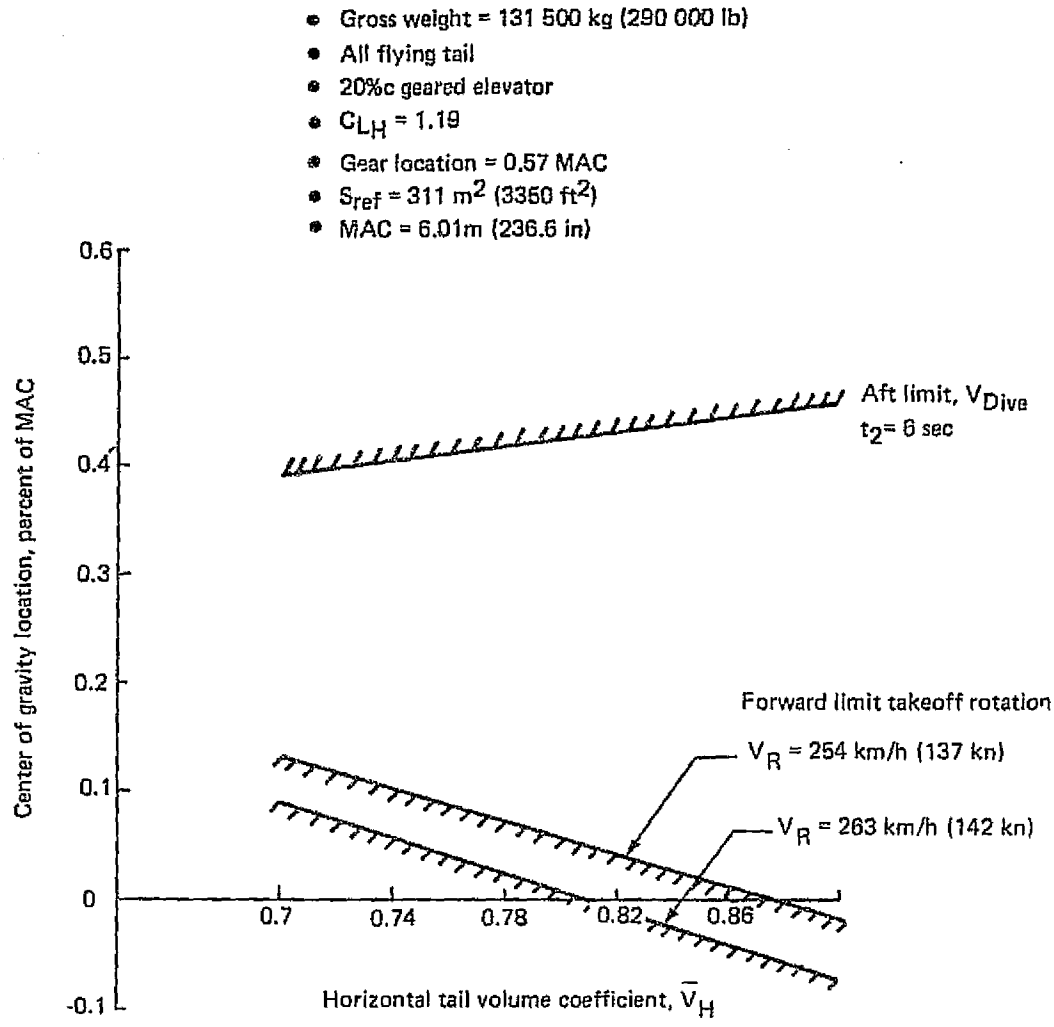

Figure 5.1-52. Horizontal Tail Sizing

interference of the nacelle with the flow field (distorted pressure gradients on the wing) and impingement of engine noise. Since the magnitude of the interference effects and the means of alleviating the associated problems are not sufficiently well understood at this time, it is appropriate to choose an aft fuselage nacelle installation for this preliminary stage of development of an LFC airplane.

But the aft-fuselage mounted nacelles are not free of problems either. Recent experience at Boeing has shown that, while the relatively small size low-bypass-ratio engine nacelles (such as used on the Boeing 727) can be installed without significant interference drag penalty, the current high bypass ratio engine nacelles would be likely to produce significant interference drag unless a rather sophisticated design is worked out involving special contour

tailoring and localized area ruling. Consequently, the configuration which has evolved during this study contemplates having such an elaborate aft-fuselage and nacelle design as a necessary measure to avoid excessive interference drag due to the engine installation.

The other area of concern is the suction engine installation. The options regarding this question have been investigated in detail by the Propulsion and Systems Groups (these studies are summarized in Section 5.3) which concluded that the most preferred location for the suction unit would be in the wing root region. From the aerodynamic standpoint, this poses a potential interference drag problem, inasmuch as the wing root area is known to be very sensitive to contour shape at high speeds. However, it is conceivable that the installation of the suction engines in the wing root would not present insurmountable difficulties and with a dedicated development effort an acceptable design could be achieved. This assumption has been made on the basis of a preliminary wind tunnel test of a wing-root-mounted suction engine nacelle on a swept wing model in the Boeing Transonic Wind Tunnel. This experiment will be discussed in the forthcoming Paragraph 5.1.7.4.

5.1.7.2 Cruise Drag Estimates

The estimates of high speed drag characteristics, presented in this paragraph, were made in support of the performance evaluation that will be discussed in Section 6.6.

According to the thrust-drag bookkeeping procedure adopted, the aerodynamic drag estimates do not include the equivalent suction drag, that is the equivalent of the power consumed by the suction pumps. This term, for the sake of convenience, is treated in the sizing exercise and subsequent performance calculations as an added fuel flow to the propulsion system. The advantage of this arrangement is that it permits sizing of the propulsion engines according to the actual airplane drag and the sizing of the suction units according to the pumping power requirements.

The drag estimates, in essence, were made on the basis of standard Boeing procedures used in preliminary design. But, since these procedures have been developed mainly for turbulent airplanes, the present application required certain deviations in order to account for the effects of partial laminarization of the wing and horizontal tail. Thus, estimates of the profile drag of the wing and horizontal tail were made on the basis of actual boundary layer calculations (such as discussed in connection with Figures 5.1-14 and 5.1-50 in Sections 5.1.2 and 5.1.6) instead of the standard approach which is based on the turbulent flat plate skin friction coefficient and appropriate form factors. The boundary layer calculations were carried out for the representative normal section of the wing with appropriate suction applied and thus, could be expected to give a better representation of the drag characteristics than the simplified approach using form drag factors.

The basic component profile drag breakdown, calculated for subcritical flow at design C_L, is shown in Figure 5.1-53. Laminarization of the wing to the selected limits (upper surface 80% c, lower surface 70% c) results in a 71% reduction of the wing profile drag. Similarly, the profile drag of the horizontal tail is reduced by 71.5%. In terms of the total profile drag, counting all components, the drag reduction is 33.9%.

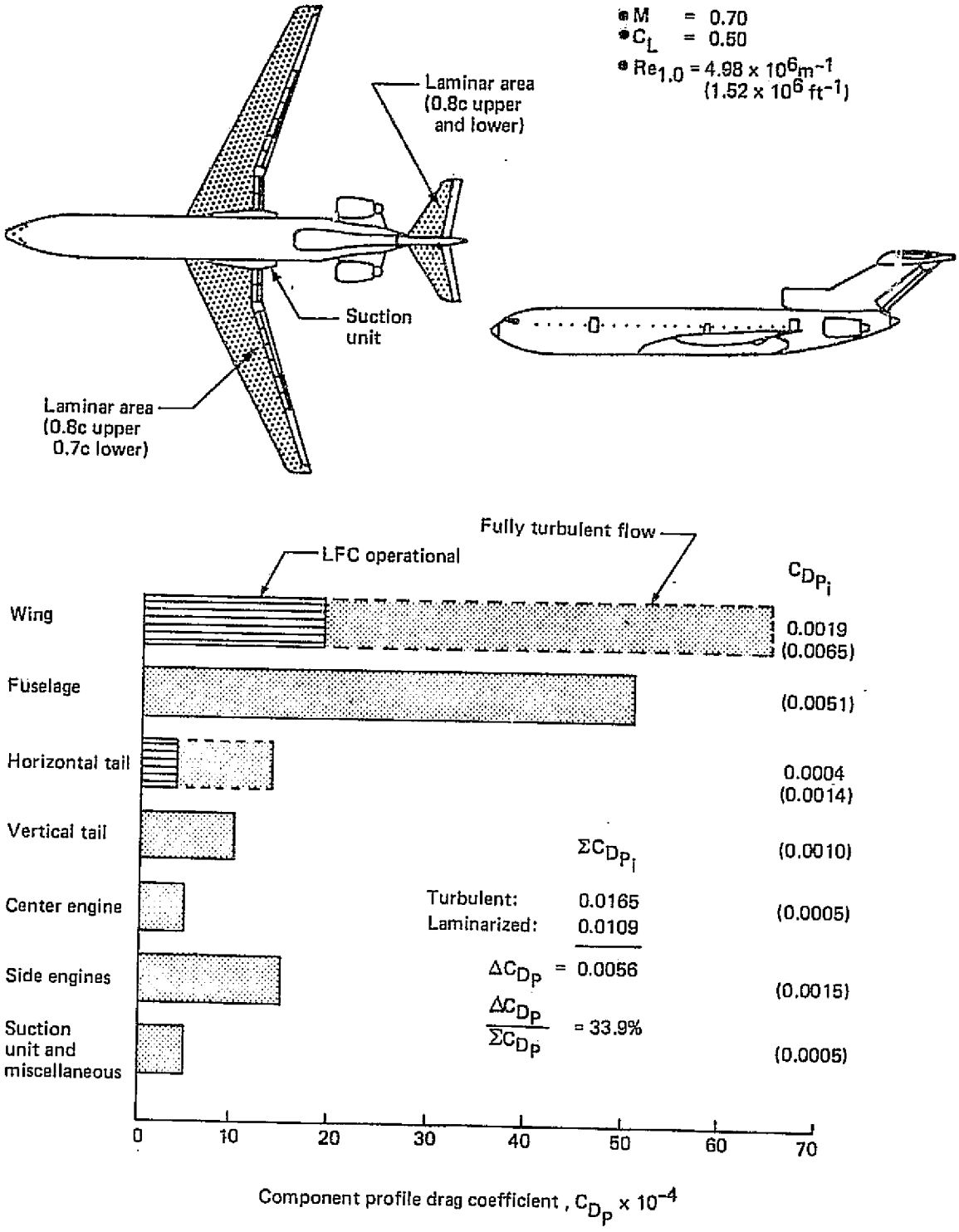

Figure 5.1-53. Component Profile Drag Breakdown

The component drag levels quoted include the basic viscous drag, a proportionate allowance for surface roughness and excrescences as well as interference drag. In the case of the side nacelle installation, for example, 67% of the quoted $C_{DP_{NAC}} = 0.0015$ is due to the nacelles alone, while 13% is allotted for the struts and 20% for interference. In the case of the suction unit installation only 25% of the quoted drag increment is due to skin friction, the rest is attributed to interference.

Furthermore, it is anticipated that the interference drag due to the nacelle installation and the suction unit installation would increase somewhat with Mach number even though a careful tailoring of both areas is made. For this reason a modest amount of compressibility drag rise due to interference was allotted. This is reflected on the combined body/empennage/nacelle drag estimate shown in the upper part of Figure 5.1-54.

The lower part of Figure 5.1-54 shows the estimated drag rise characteristics of the wing at the design lift coefficient ($C_L = 0.50$). The upper curve represents the case of fully turbulent flow whereas the lower one reflects a hypothetical situation that would occur if the wing could be laminarized to the intended limits throughout the entire Mach number range. This, of course, would hardly be possible with the type of airfoil section selected for this wing because of the pronounced pressure peak near the leading edge at lower than the design Mach number. Thus, fully effective LFC can be expected only within a rather narrow Mach number range, which, according to the present estimates, falls between M = 0.78 to M = 0.81. A transitional curve from the fully turbulent case to the fully effective LFC segment has been drawn intuitively to illustrate the expected variation of wing profile drag as a function of Mach number.

The estimated drag polar for the complete airplane at the nominal cruise Mach number of M = 0.80, is shown in Figure 5.1-55. The polar is constructed in a manner similar to that of the wing drag rise curve, shown in the previous figure. This indicates the expected C_L range for fully effective LFC (marked by a solid line, which extends from $C_L = 0.45$ to $C_L = 0.55$), and intuitively drawn transitional curves that blend into the fully turbulent polar at $C_L = 0.35$ and $C_L = 0.60$. The drag reduction, achieved by fully effective LFC, at $C_L = 0.5$ amounts to about 23% of the total turbulent drag.

Figure 5.1-56 illustrates the impact of LFC on the cruise efficiency expressed in terms of $(M\ L/D)_{max}$ vs. Mach number. The improvement in $(M\ L/D)_{max}$ is 27.5%.

It will be noted that the range of lift coefficient and Mach number for which LFC is fully effective is well within the principal operating envelope given in the design requirements of Section 4.2. It should be recognized that the data of Figure 4.3-1 represent apriori estimates which were intended to serve as design goals for the study rather than firm requirements. Nevertheless, the envelope corresponding to the above quoted values for list coefficient and Mach number are considered to be quite satisfactory for cruise operation.

Finally, the estimated lift and drag divergence boundaries are presented in Figure 5.1-57 together with the corresponding 1.3g buffet margin, the C_L's for L/D_{max}, and lines of constant $W/S\delta$. It can be seen that the nominal design point (M = 0.8 and $C_L = 0.5$) is well within the drag divergence boundary and the 1.3g buffet margin.

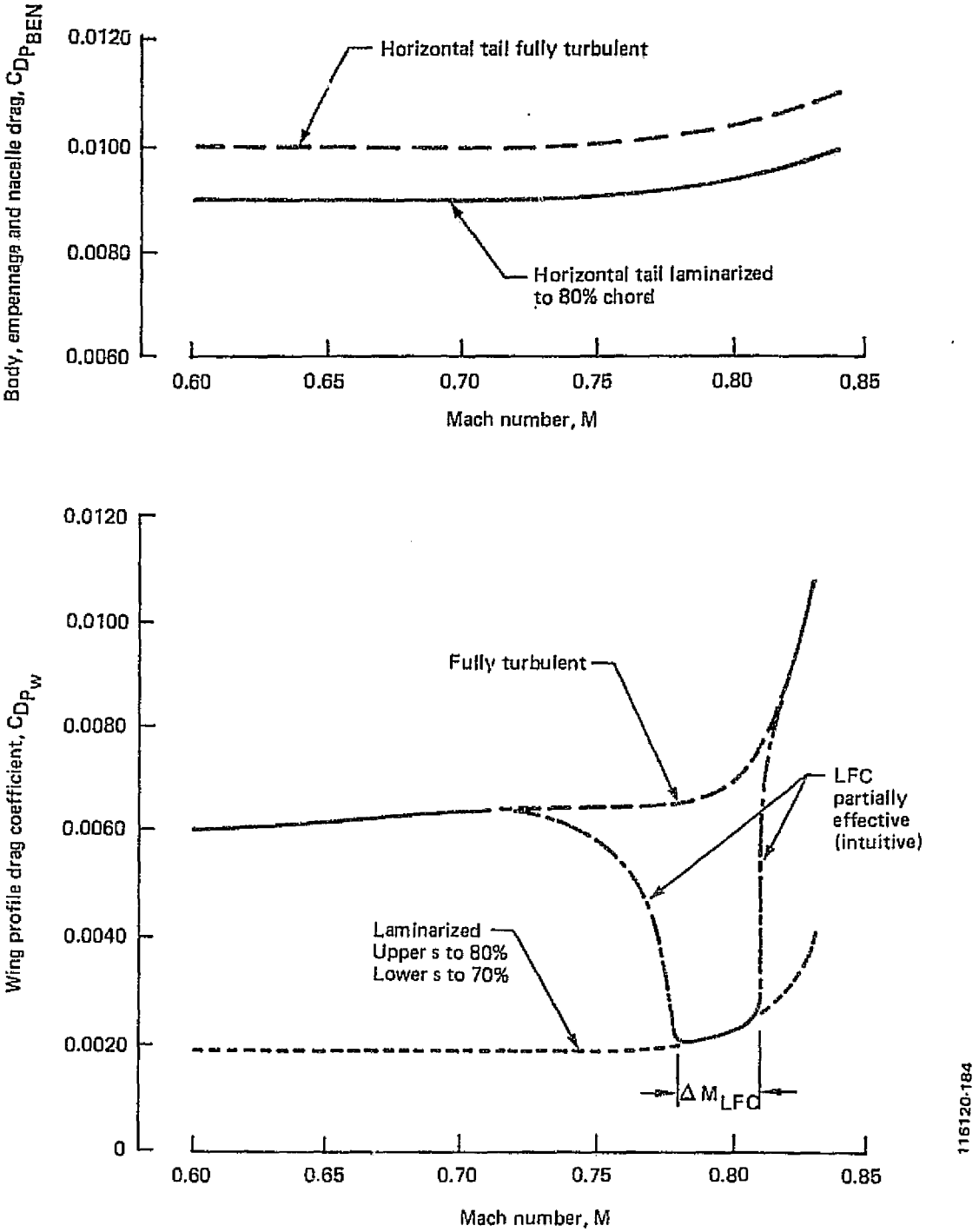

Figure 5.1-54. Estimated Drag Rise Characteristics at $C_L = 0.5$

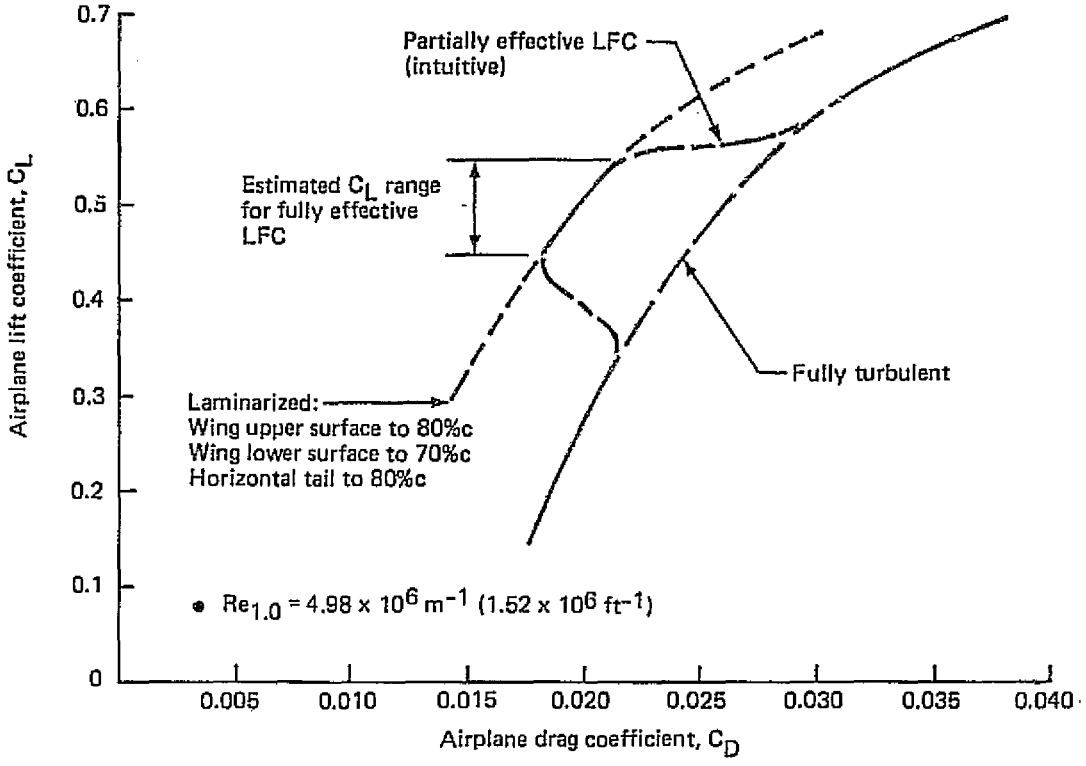

Figure 5.1-55. Estimated Drag Polar for M = 0.80

5.1.7.3 Low Speed Drag Estimates

The estimates of low speed drag characteristics were made using the standard Boeing computer program called LOWLAM. As described in paragraph 5.1.2.3, the high-lift system selected for this airplane consists of a single-slotted trailing edge flap (built in three segments) having a chord ratio of $c_F/c = 0.20$ and an extension ratio of $x_F/c = 0.08$, combined with a droopable inboard aileron. Leading edge devices are not used in order to avoid surface discontinuities that would prevent LFC.

Figure 5.1-58 presents the estimated lift curves for various flap configurations with and without ground effect. In the clean configuration, the maximum lift coefficient is 1.48 without ground effect and 1.36 with ground effect, respectively. At maximum flap deflection ($\delta_F = 40°$) $C_{L_{max}}$ is 2.04 in free flight and 1.80 with ground effect.

The estimated low speed L/D envelopes are shown in Figures 5.1-59 and 5.1-60 for the takeoff and landing configurations, respectively. The data presented correspond to trimmed flight with C.G. position at 0.10 MAC, based on a one-g stall limit which was selected in anticipation of the generally unfavorable pitch-up characteristics of swept wing configurations with deflected flaps which do not have leading edge devices or other stall control devices (e.g., fences, vortilons, etc.).

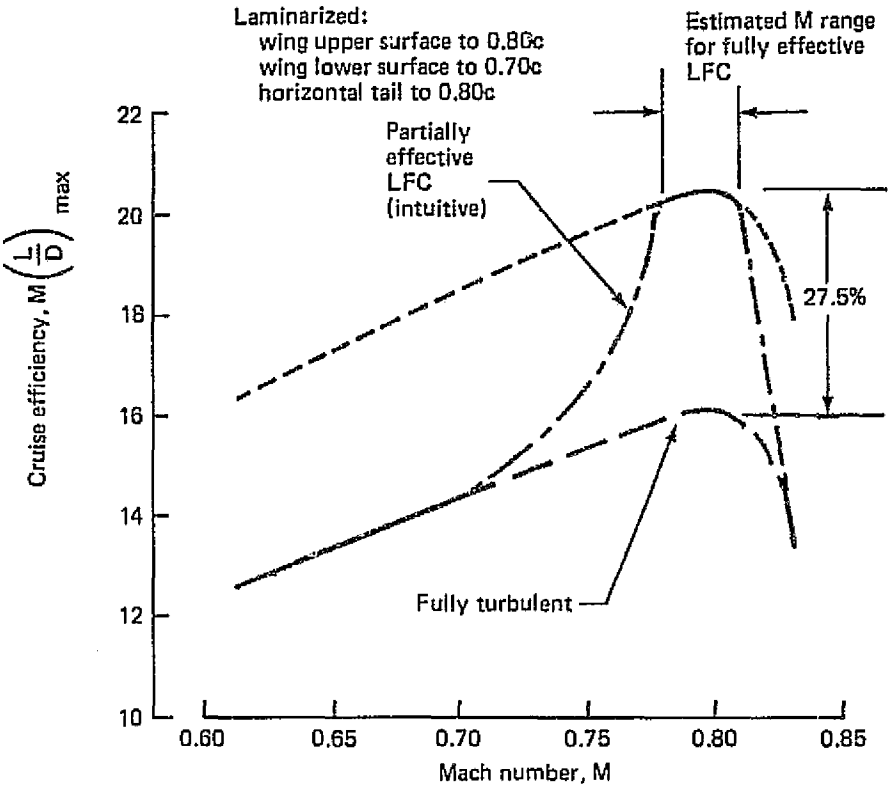

Figure 5.1-56. Estimated Cruise Efficiency With and Without Laminarization

5.1.7.4 Preliminary Test of a Wing-Root-Mounted Suction Engine Installation

As it was pointed out in the preceding paragraphs, the potential interference drag caused by a wing-root-mounted suction engine installation has been a concern for the configuration integration. In order to size up the magnitude of this problem and get a better understanding of the principal flow phenomena involved, a preliminary test was conducted in the Boeing Transonic Wind Tunnel, using a current developmental model. The wing-root-mounted suction engine nacelles installed on this model were representative of the design worked out initially for the baseline LFC airplane, as it was configured in the middle of 1977. The contours of the nacelle were developed merely to accommodate the suction engine and pump without any specific effort for aerodynamic tailoring. A photograph of the model, showing the wing root region with the suction engine nacelle installed, is presented in Figure 5.1-61.

The test data included six-component force balance measurements throughout the Mach number and C_L ranges of interest, as well as flow visualization photographs at a representative test condition. Figure 5.1-62 illustrates the flow pattern observed around the suction engine nacelle. It is apparent that the disturbed area extends beyond the normal turbulent wedge that forms at the wing/body intersection. Also, there is evidence of flow separation on the fuselage and at the closure of the nacelle which, apparently, was too abrupt.

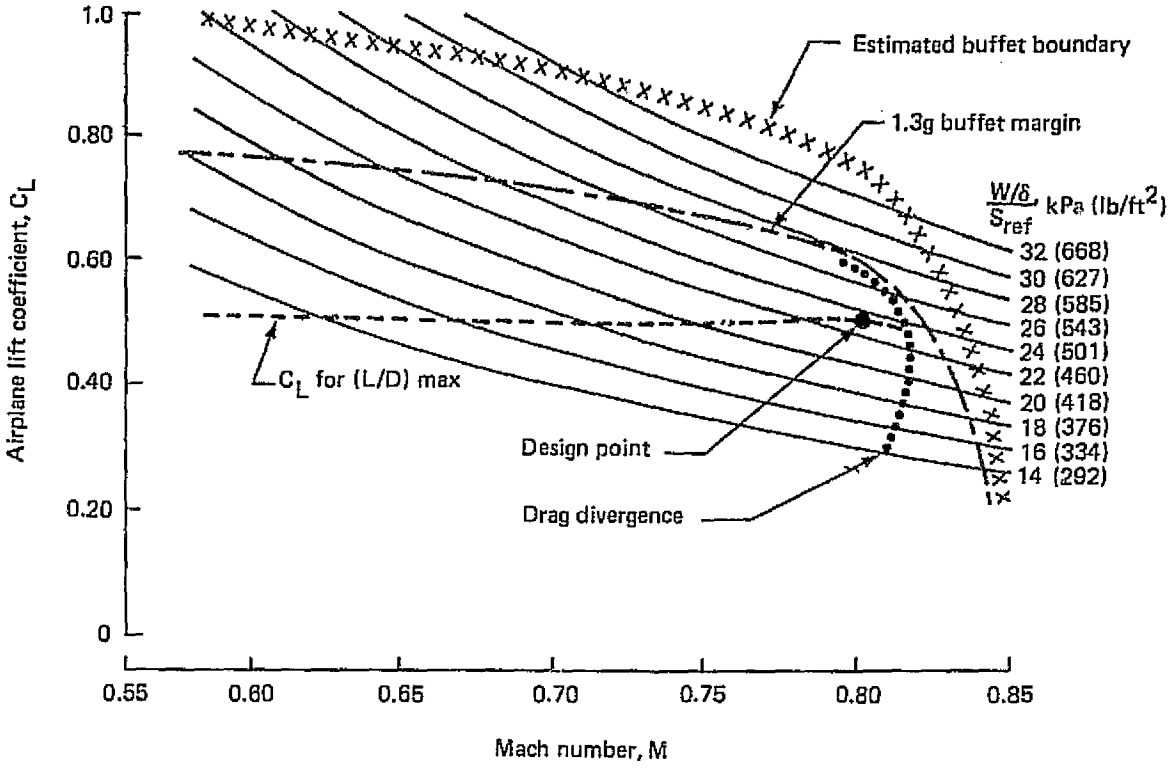

Figure 5.1-57. Estimated Lift and Drag Divergence Boundaries

The force balance measurements showed a quite significant drag increment due to the suction engine nacelle installation. Figure 5.1-63 illustrates the results. The drag increment, $\Delta C_{D_{SU}}$, varies, with both the Mach number and lift coefficient, which is understandable since the flow conditions in the wing root become more critical with increasing M and C_L. At the nominal cruise condition of this particular wing (i.e., at M = 0.80 and C_L = 0.4) the drag increment due to the suction engine nacelle installation was $\Delta C_{D_{SU}} = 0.0010$. The corresponding loss in the drag divergence Mach number is approximately $\Delta M_D = -0.008$, as shown by the lower part of Figure 5.1-63 (M_D being defined as the Mach number at which the drag due to compressibility effects reaches the value of $\Delta C_{D_M} = 0.0020$).

The lift and pitching moment characteristics of the configuration were also affected by the suction engine installation, but to a lesser extent than the drag.

Based on these results, it was concluded that a wing-root-mounted suction engine nacelle installation would require a careful aerodynamic tailoring to reduce the adverse interference effects to an acceptable level. It is felt that this task could be best accomplished by a series of wind tunnel tests.

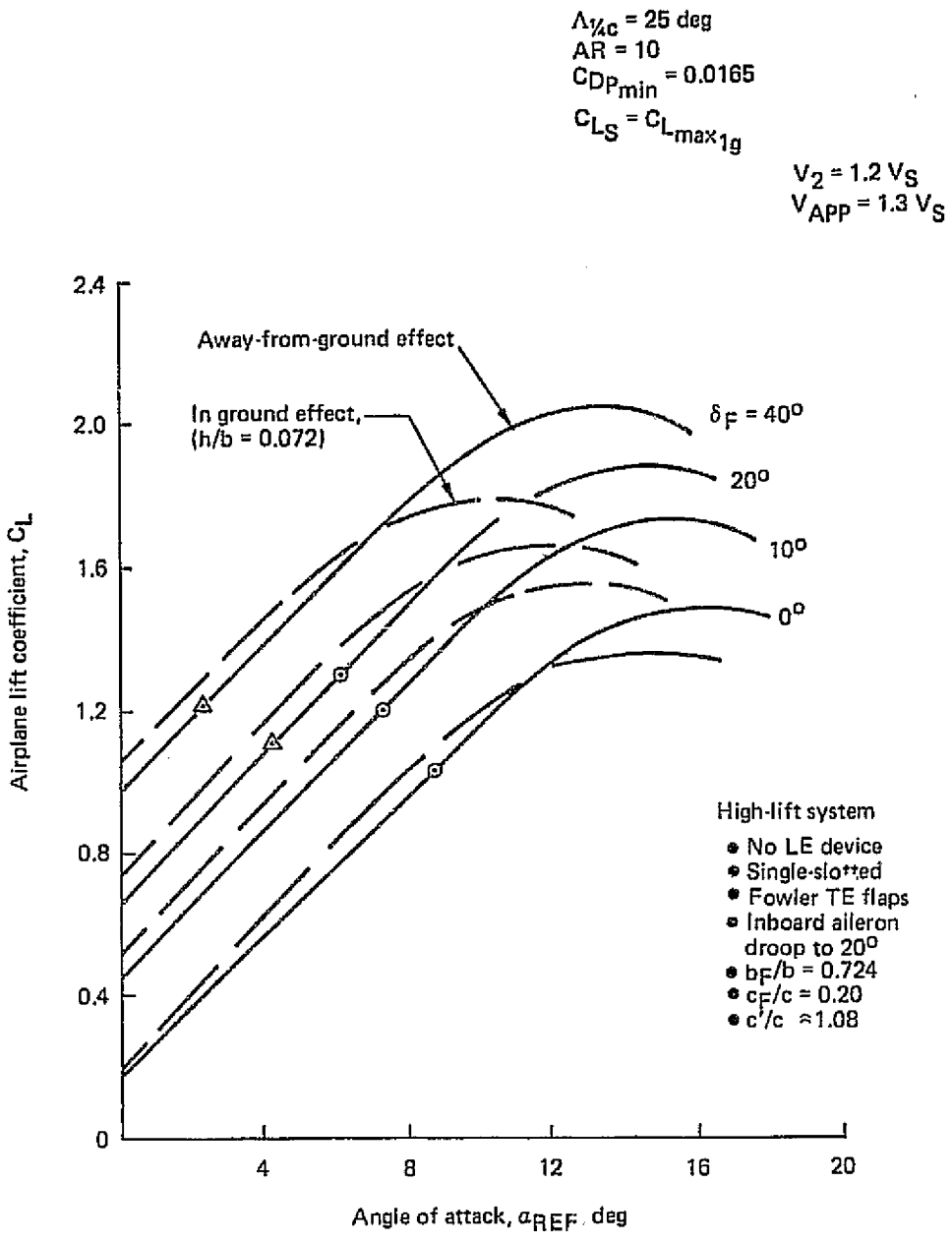

Figure 5.1-58. Low-Speed Lift Curves—Trimmed Flight With Center of Gravity at 0.10 MAC

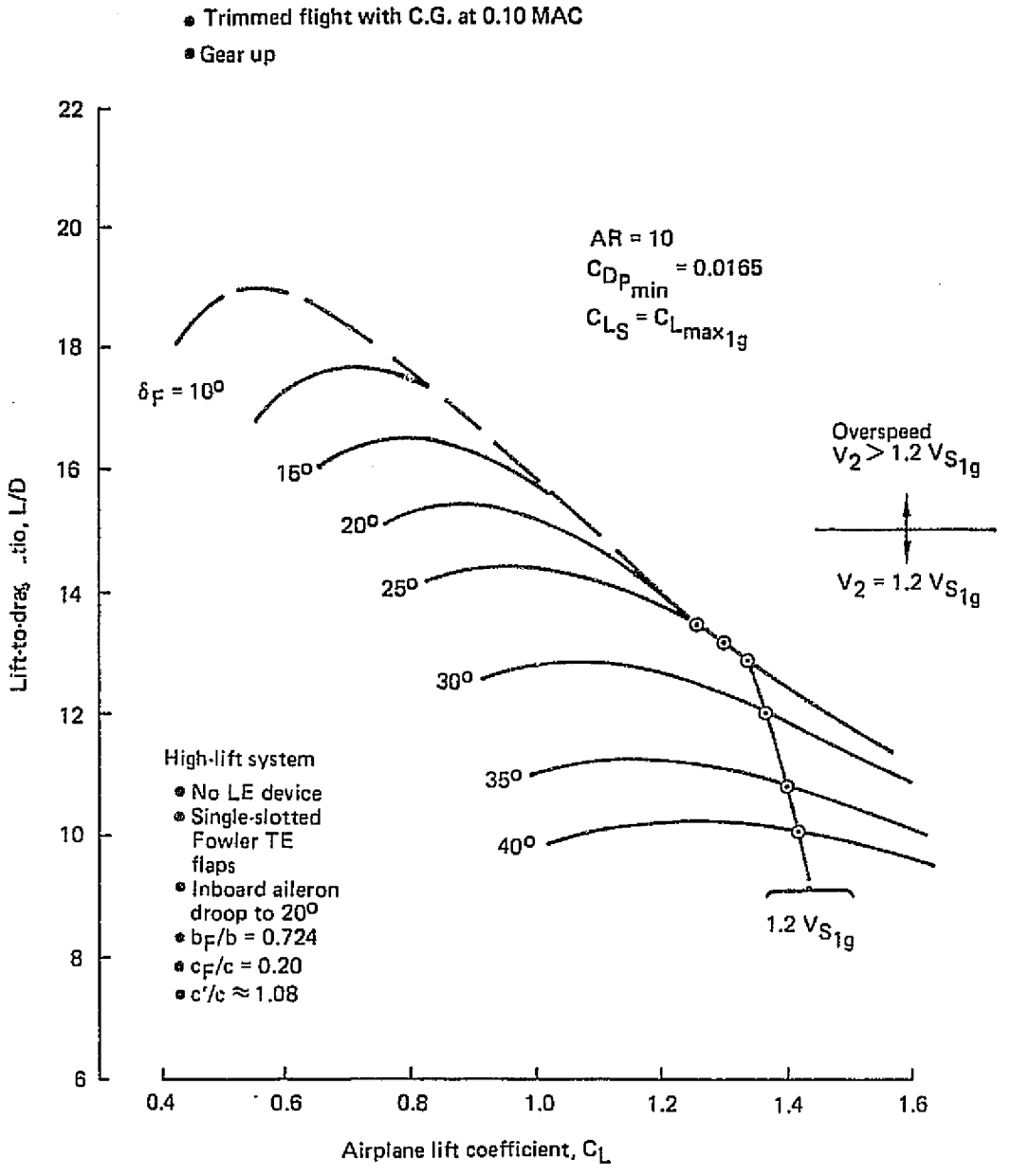

Figure 5.1-59. Low-Speed Performance Envelope—Takeoff Configuration

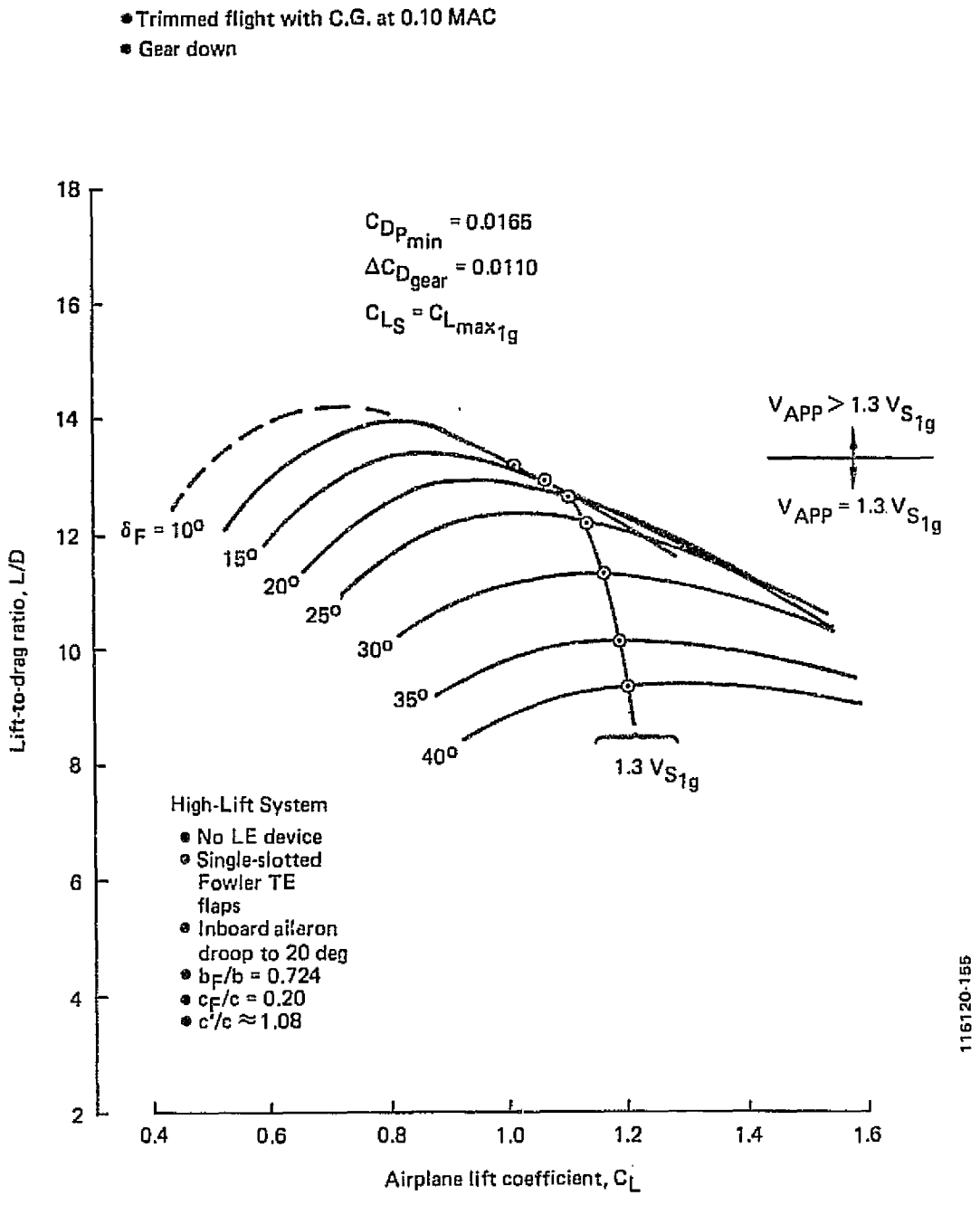

Figure 5.1-60. Low-Speed Performance Envelope—Landing Approach Configuration

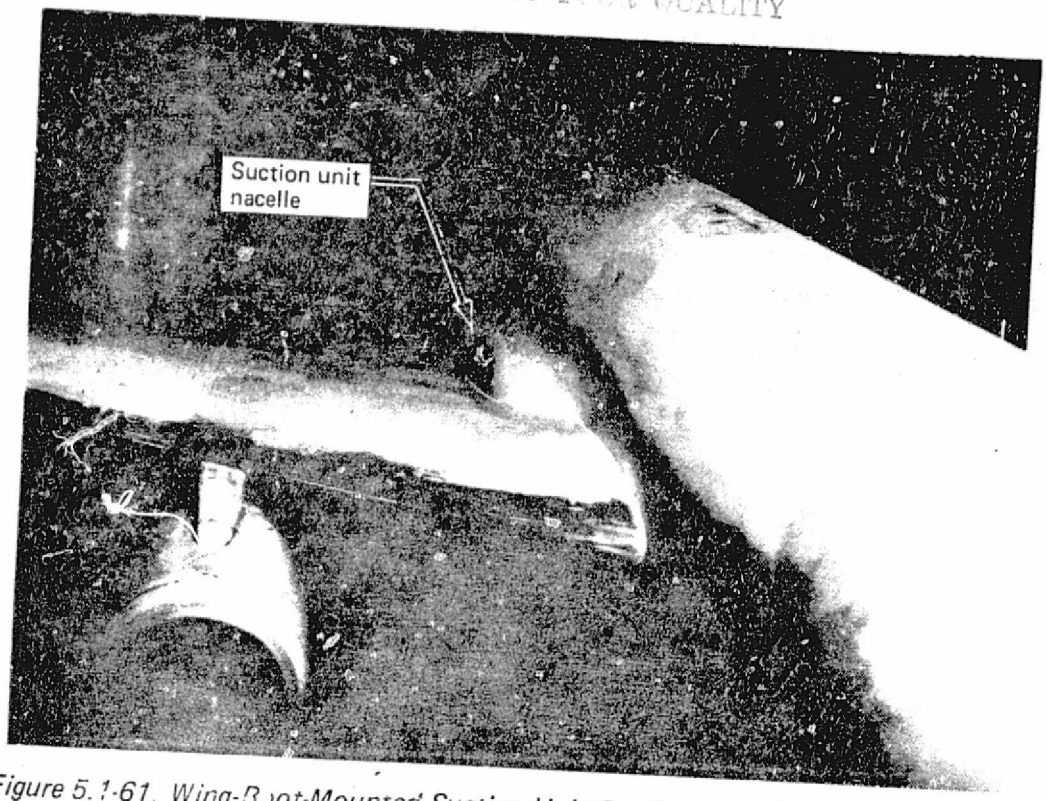

Figure 5.1-61. Wing-Root-Mounted Suction Unit Configuration in the Wind Tunnel

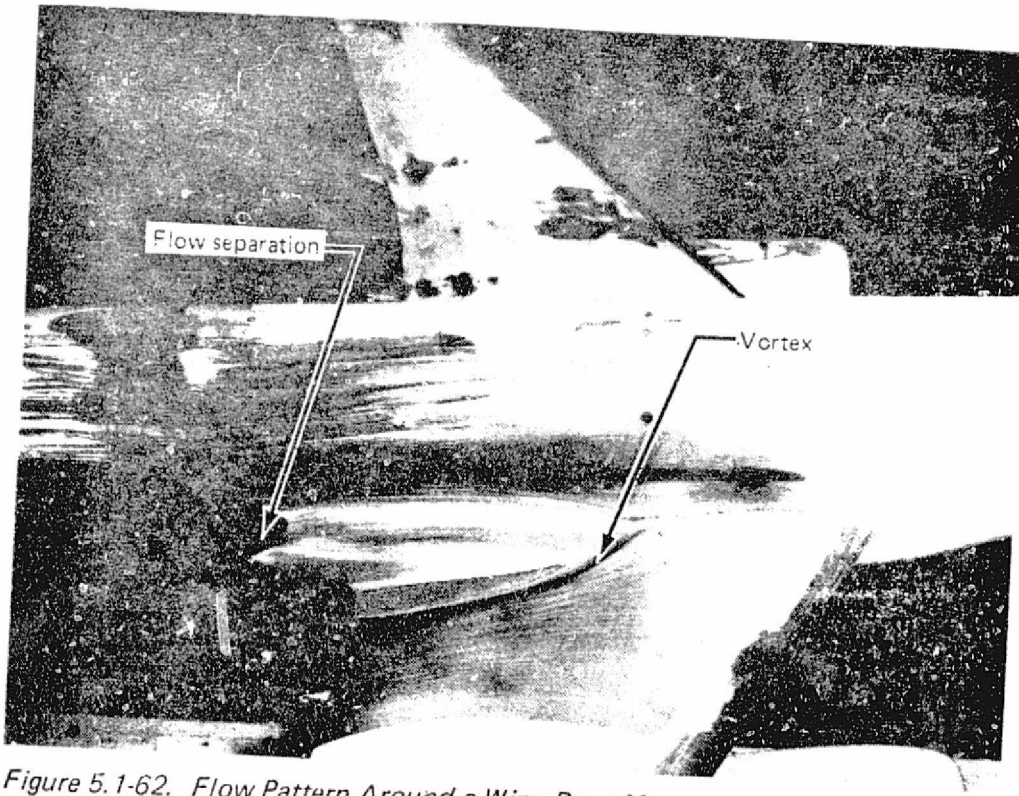

Figure 5.1-62. Flow Pattern Around a Wing-Root-Mounted Suction Unit Nacelle

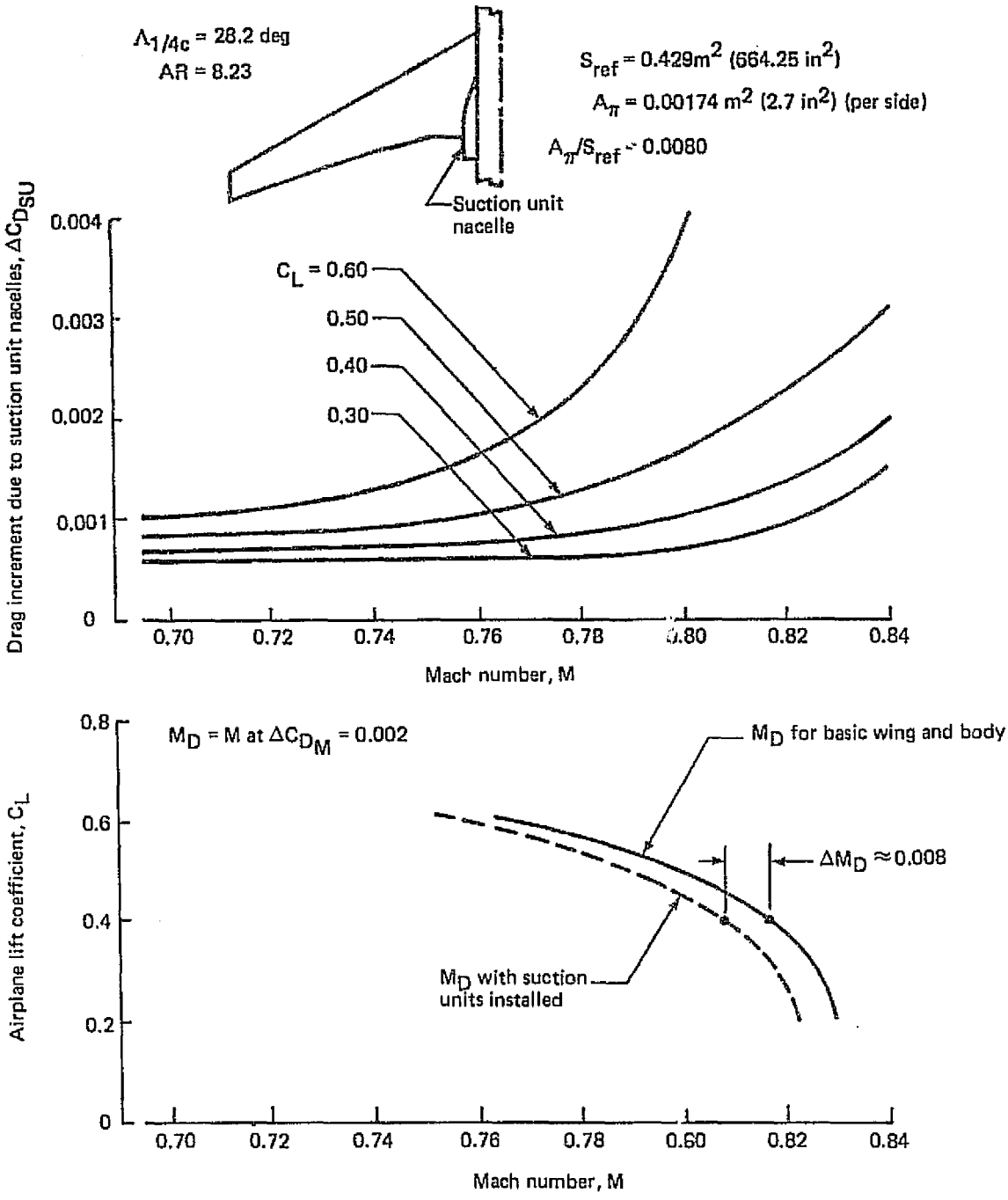

Figure 5.1-63. Drag Penalty Due to an Untailored Wing-Root-Mounted Suction Unit Nacelle

5.1.7.5 Wing-Mounted Engine Placement Study

In view of the inherent advantages of wing-mounted engines in terms of weight and balance, a study was conducted to assess the feasibility of locating main propulsion engines on the wings of an LFC aircraft as depicted in Figure 5.1-64.

An analytical procedure was developed for predicting the influence of an external acoustical disturbance on the stability of a laminar boundary layer with LFC. For the analysis, an engine noise data base was used which was derived from flight tests with a 1977 technology high bypass turbofan on a 747 airplane. The near-field engine noise measured on the wing lower surface was scaled to be representative of the noise forecast for a 1985-1990 technology engine.

It was concluded in the study that the near-field noise generated by a current technology engine would cause flow transition in the region of the engine. However, addition of a substantial amount of acoustical treatment to the engine would probably permit location of an engine on the wing. An analysis for a 1985-1990 technology engine, forecast to have lower engine noise generation and using improved acoustical treatment, showed that a wing engine installation would probably result in a minimal loss of laminar flow area.

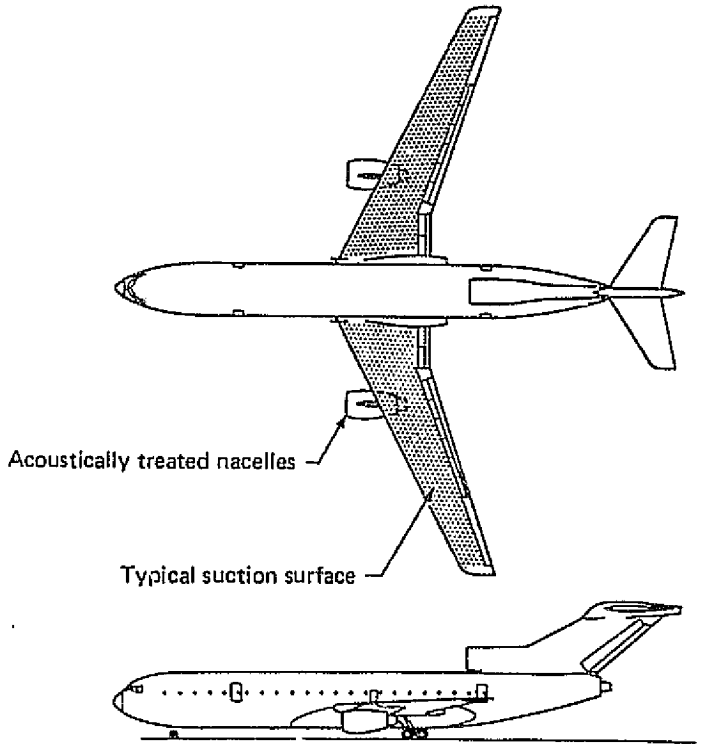

Figure 5.1-64. Engine Placement Study

A summary of the analytical results is given in Figure 5.1-65 which shows the areas of the wing affected by noise for both conservative (0.01) and optimistic (0.05) values of the transition criteria, $(\Delta u/U)_{TR}$. While the above results are encouraging, more extensive analysis based on better theory and definitive experimental results would be required to prove the feasibility of locating engines in the near proximity to laminar flow surfaces. In addition, the aerodynamic interference due to engine placement on wings would need careful evaluation to support a configuration choice with strut-mounted engines on wings.

5.1.8 AERODYNAMIC TEST PROGRAMS

The Aerodynamic Test Program accomplished during the contract was oriented to provide insight into some of the phenomena of controlled laminar boundary layers and to support the critical design decisions relative to basic aerodynamic design concepts considered in the Concepts Evaluation task. Thus major attention was focused on the validation of the basic aerodynamics of the suction surface design and the investigation of various types of disturbances including noise, as well as the sensitivity of LFC operation to off-design conditions. The test program was carried out in four phases over the contract period.

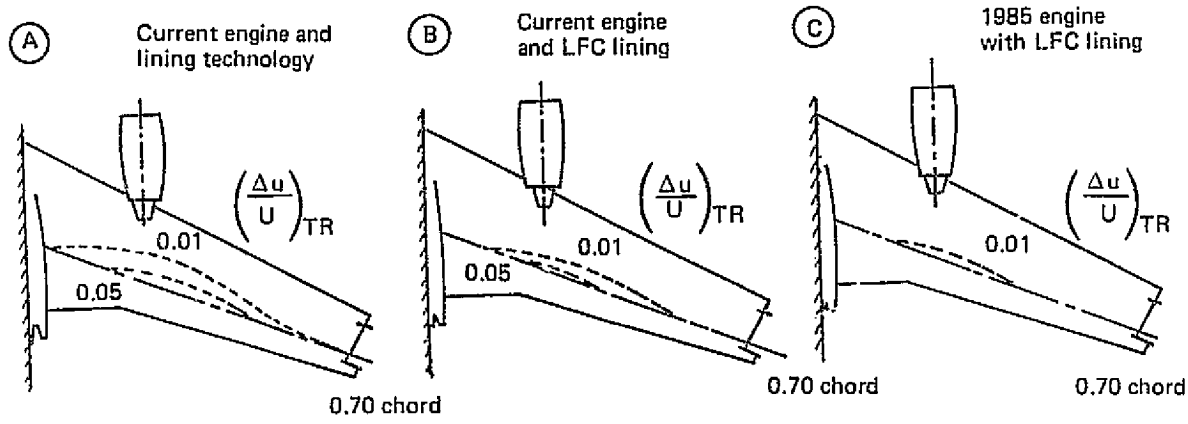

$\left(\frac{\Delta u}{U}\right)_{TR}$	Potential loss of lower surface laminar area at normal suction levels		
	(A)	(B)	(C)
0.01	20%	8%	2.5%
0.05	7%	1.5%	0%

Figure 5.1-65. Engine Noise Effects on Laminarization

5.1.8.1 Wind Tunnel Tests of an LFC Wing Panel

From the beginning of this program, it was apparent that wind tunnel tests would be vital to the successful development of LFC wings and the system elements which serve essentially aerodynamic functions. Furthermore, the need to conduct these tests under realistic conditions was also apparent, specifically including both unit Reynolds numbers and chord Reynolds numbers, primarily because of the overriding importance and sensitivity of these parameters in relation to boundary layer stability and the effects of disturbances. Because of the latter, the test environment should be one of low ambient disturbance levels—especially the stream turbulence and noise. The effects of Mach number, while significant, are generally not large and can readily be estimated for correlation between low-speed test results and expected flight performance. Some uncertainty currently exists as to the importance of local Mach number effects on slot inflow stability and possible induced downstream disturbances. Although the mechanism is not completely understood, it is not anticipated that the above effects will be of major importance.

On the basis of the above considerations, The Boeing Company decided to develop an experimental apparatus that would permit investigation of a variety of problems associated with laminar flow control by boundary layer suction applied to large subsonic transport aircraft. The 1.52 m by 2.44 m (5 ft by 8 ft) low-speed Boeing Research Wind Tunnel (BRWT) was chosen for the LFC related testing, since this tunnel has reasonably low turbulence and noise levels; i.e., $(V'/V_\infty) \leq 0.0015$, and SPL $\leq$ 113 db), respectively. Furthermore it is relatively inexpensive and readily available for long duration testing.

The unusually long test section of this wind tunnel permitted the installation of a very large model, with a chord length of up to 6.1 m (20 ft.) that could attain test Reynolds numbers of up to $Re_c = 25 \times 10^6$ at the maximum dynamic pressure of q = 2.87 kPa (60 lb ft^{-2}) at which the typical unit Reynolds number is $Re_1 = 4.1 \times 10^6$ per m (1.25×10^6 per ft). The model arrangement was chosen to represent a typical section of a swept LFC wing considered in this study.

The overall test program consisted of the following four phases:

(a) Model and test setup development.

(b) First test period—validation of the basic model without LFC.

(c) Second test period—validation of the model with LFC.

(d) Third test period—exploration of sensitivities to surface protuberances, off-design pressure distributions and imposed noise.

The forthcoming sections will provide a brief description and summary of the results regarding each of the above four phases.

(a) Model and Test Setup Development

The LFC wing model is shown in Figure 5.1-66, as installed in the BRWT between floor and ceiling. The 2.44 meter (8 ft) span, 6.1 meter (20 ft) chord model dimensions were chosen to represent a typical section of a 30° swept wing. The airfoil section was designed to provide, in the presence of the tunnel walls, and at a tunnel Mach number of M = 0.2, an upper surface pressure distribution typical of the mid-span portion of the full-scale LFC wing at cruise conditions, (M = 0.80, and $C_L = 0.5$). The leading edge was shaped to provide a value of $Re\theta_{a.l.}$ approaching 100 which is marginal for "spanwise contamination" based on X-21 criteria.

Figure 5.1-67 shows the layout of the complete test apparatus. The installation included fairings on the tunnel floor and ceiling to prevent significant spanwise

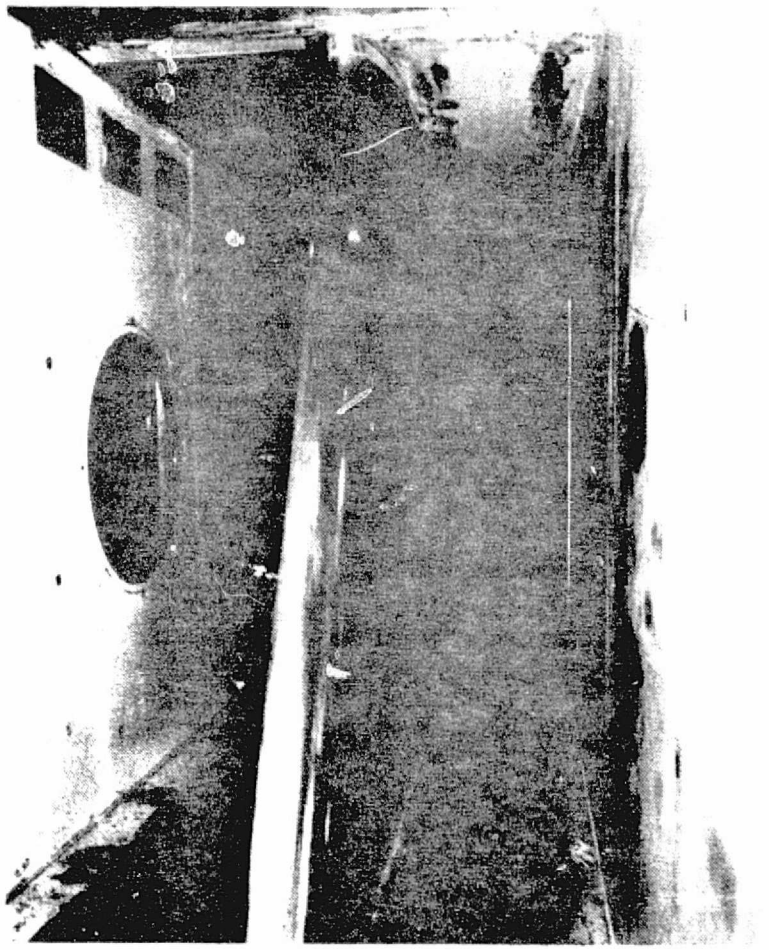

Figure 5.1-66. Front View of Model Installed in the Boeing Research Wind Tunnel

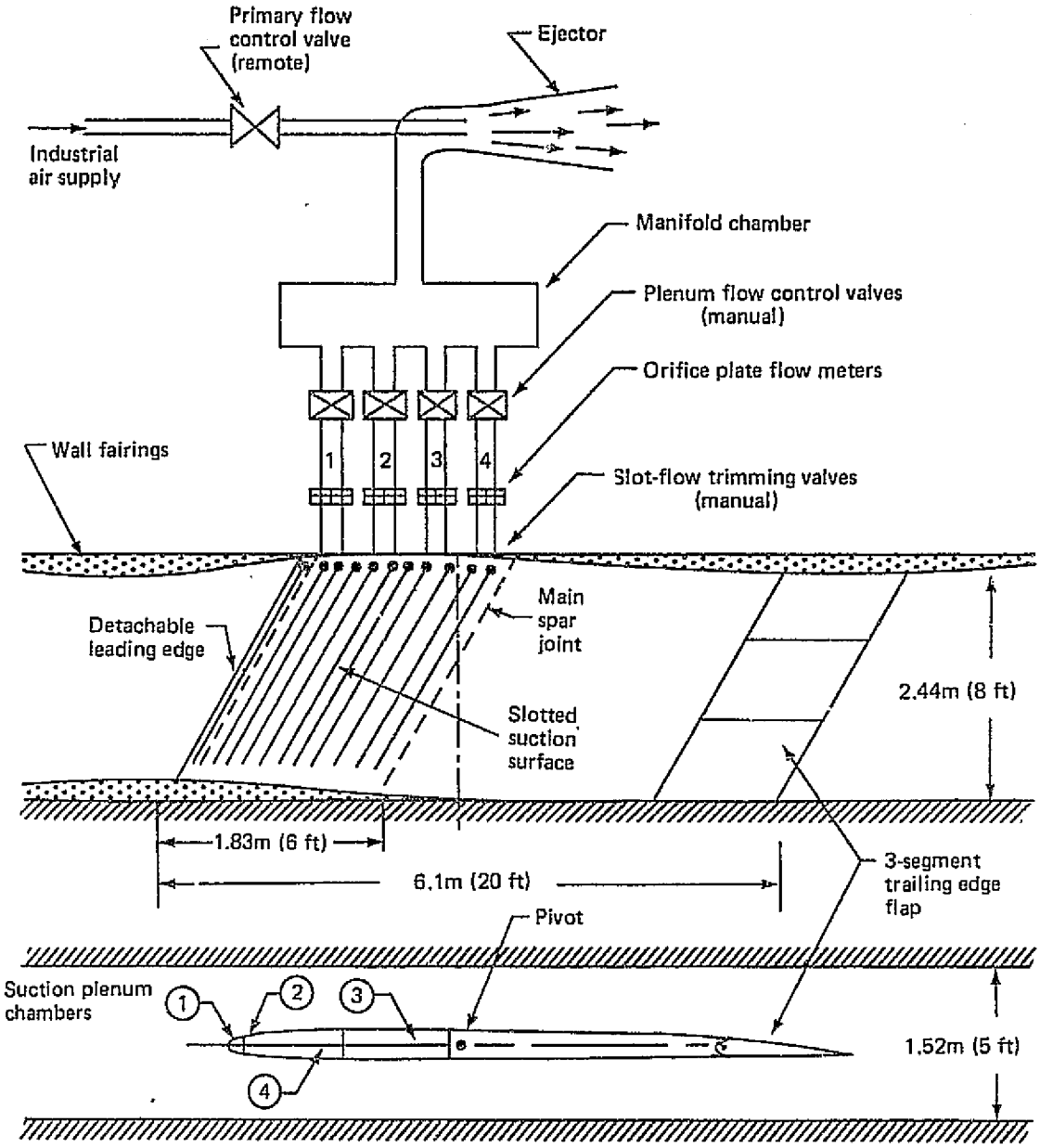

Figure 5.1-67. LFC Test Installation in Boeing Research Wind Tunnel

pressure gradients on the model. A three-segment trailing edge flap was also used to provide flexibility in pressure distribution adjustments. The model installation permits the changing of incidence angle as well as lateral position by manual adjustments.

For the initial series of tests planned under the Phase I contract, only the first 30% of the upper surface and the first 15% of the lower surface had provisions for LFC. These areas were considered the most critical because of the leading edge crossflow

instability; thus top priority was given to study this region first. The suction area, however, could ultimately be extended back to the flap hinge line (80% chord).

The suction surface of the model is divided into four regions, as indicated in Figure 5.1-67; each of these is served by a separate plenum chamber, and a separate flow metering valve and flow measuring device. The distribution of the suction flow between individual slots is controlled by slide-valves running the length of each slot. Pumping power is provided by an ejector driven by high pressure air.

Design of the model was begun in late 1976 and continued through February 1977. Fabrication of the model also started in late 1976 and an interim configuration, with an alternate forward section that did not have suction slots, was completed by May 1977. This configuration was used for the initial validation test. The suction module was completed in mid-June 1977 and the first test of the complete J FC model took place immediately thereafter.

Considerable development work was needed to master the techniques of how to keep surface waviness within acceptable limits and how to cut clean and uniform slots. A precision traversing saw was built to accomplish the latter task satisfactorily. A photograph showing the slot-cutting operation is presented in Figure 5.1-68.

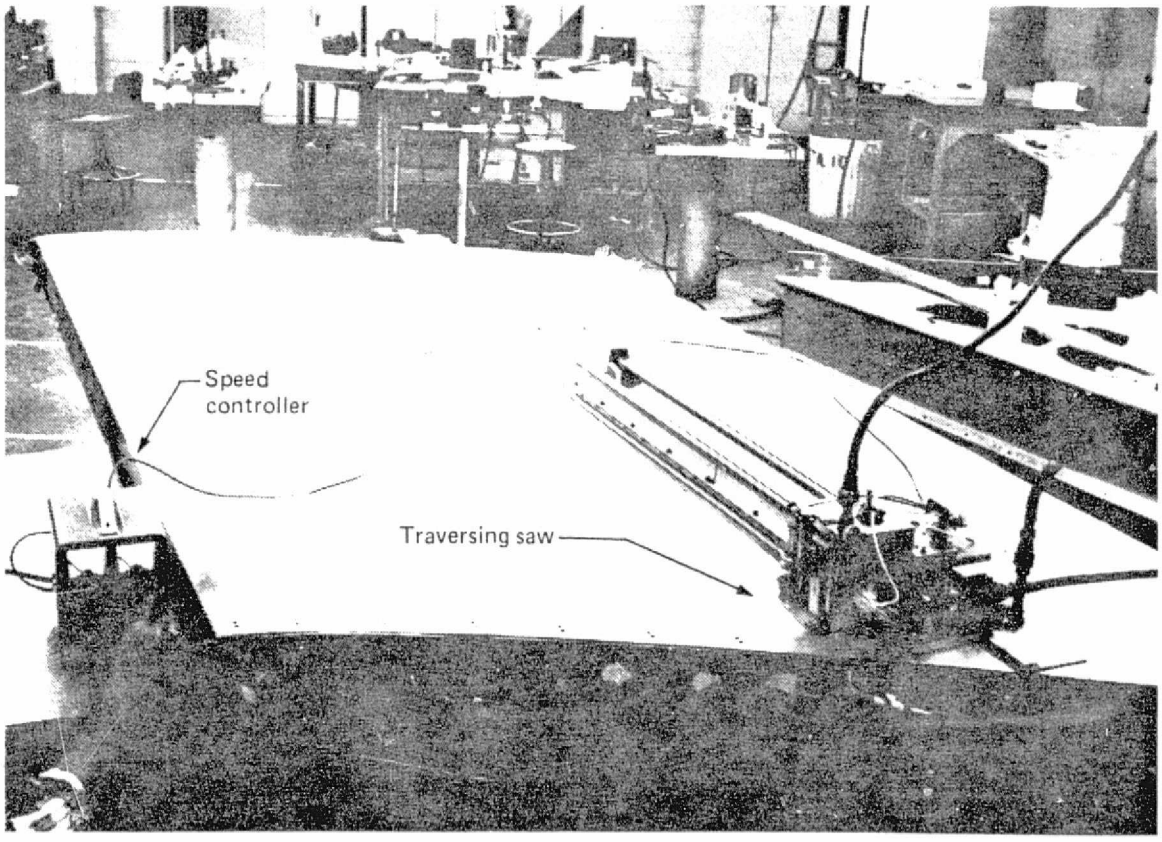

Figure 5.1-68. Slot-Cutting Operation on the LFC Wing Model

(b) First Test Period

Validation of the test apparatus has been accomplished in two steps. First, the model was tested with an alternate forward section which had no suction slots but incorporated an ample number of surface static pressure taps. The main objectives were: 1) to verify that the desired pressure distributions could be achieved by appropriate settings of the model incidence and flap deflection, and 2) to determine the extent of natural laminar flow and general boundary layer development on the test surfaces. This test, BRWT 103, took place in May 1977 and is reported in Reference 17.

The results showed that the target pressure distribution on the model upper surface could be achieved and, using various combinations of incidence and flap settings, a wide range of pressure distributions could be produced in order to simulate off-design operating conditions. Natural transition occurred approximately at 2% chord on the upper surface at maximum speed and the turbulent boundary layer development was consistent with theoretical estimates. (See Figure 5.1-69) Flow disturbances

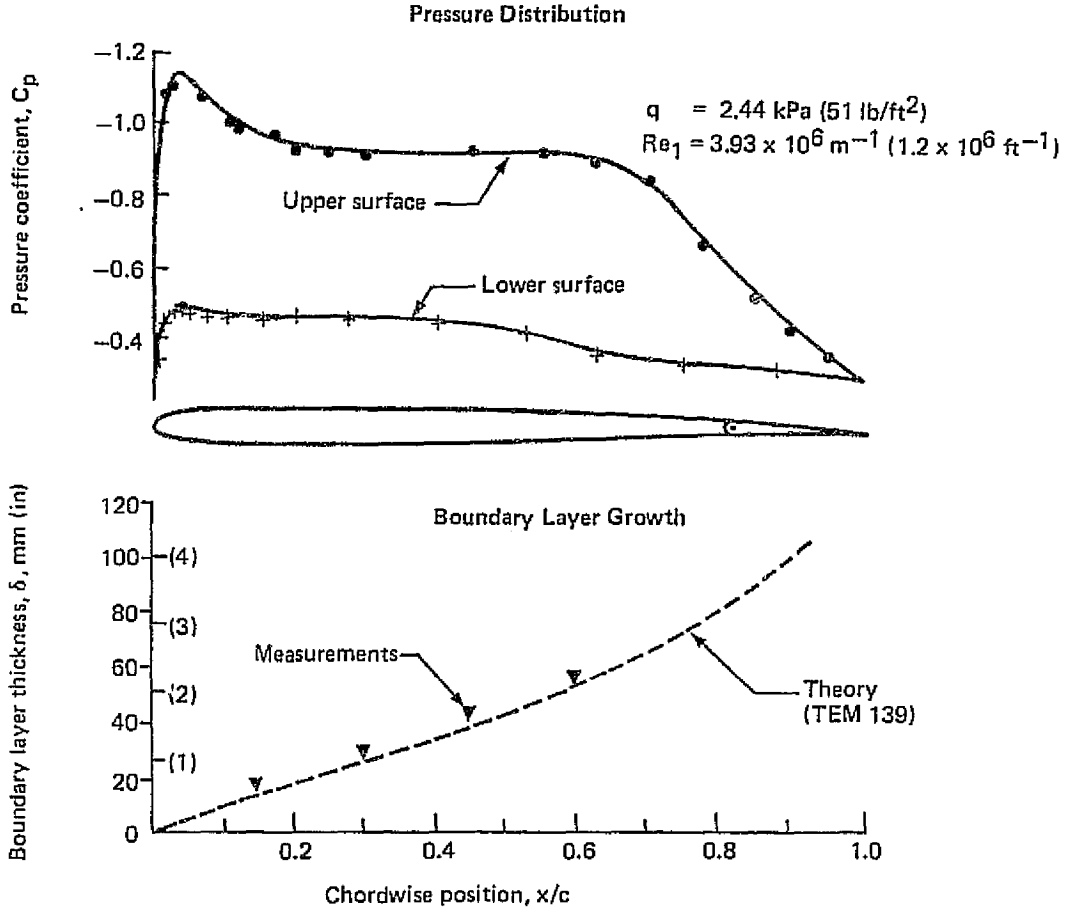

Figure 5.1-69. Flow Characteristics at Test Condition

Figure 5.1-70. Transition Pattern on the Leading Edge Without Suction

(i.e., vortex shedding) at the model/wall intersections were found to be minimal. However, the flow distortion that tends to produce non-uniform loading along the span, (characteristic to swept wing sections enclosed between tunnel walls), could not be completely eliminated with the simple, two-dimensional wall fairings and incremental deflection of the trailing edge flaps. It was apparent that this problem could be corrected by some revision of the wall fairings, but due to time limitations, implementation of this was deferred until the next test period.

A detailed investigation of the leading edge flow pattern by means of several flow visualization techniques clearly indicated the nature of the transition phenomena on the leading edge. Figure 5.1-70 is a photograph of the wing leading edge on which the flow pattern is made visible by painting the surface with a lampblack and kerosene mixture. After long exposure to the flow, the coating is thinly distributed downstream revealing the random wedge distribution pattern which tends to remain stable with time. Although it is apparent that disturbances originate at the apex of each wedge, later inspection generally showed no discernible surface imperfections or accumulation of particles at these locations. The progressive appearance of wedges as the flow velocity is increased indicates the sensitivity to unit Reynolds number and the onset

of unstable boundary layer flow conditions in the region of intense crossflow. Boundary layer measurements in the areas of wedge accumulations indicated early transition to turbulent flow, whereas in wedge-free areas the flow remained laminar. Based upon the infrequent appearance of disturbances forward of s/c = 0.01, it was concluded that the model would not be susceptible to premature transition due to attachment line flow instability, and hence there would be no need for additional chordwise suction slots in the immediate vicinity of the leading edge as contemplated earlier. Consequently, the location of the first slot was selected to be s/c = 0.013.

(c) Second Test Period

Having completed the initial validation experiments, testing of the suction model followed. This second test, BRWT 106, was conducted between June 20 and July 15, 1977. A complete description of the test apparatus and data analysis can be found in Reference 17.

The main objective was to demonstrate that the suction system would function properly and was capable of maintaining laminar flow reliably over the controlled areas. Specific objectives were: (1) to establish the suction distribution for maximum efficiency, (2) check the sensitivity to oversuction and (3) to observe the effects of shutting-off certain slots. A further goal was to evaluate several experimental techniques for detecting transition and monitoring LFC system effectiveness.

The test variables included different airspeeds between V_∞ = 40 m/s (130 ft/sec) and V_∞ = 70 m/s (230 ft/sec) and variations in suction airflow quantity and distribution. The unit Reynolds number at maximum speed was approximately $Re_1 = 4.1 \times 10^6$ per meter (1.25×10^6 per foot) which gave a representative chord Reynolds number of $Re_c = 25 \times 10^6$. The angle of attack and flap deflections were held constant throughout the test.

The principal result of the test was that laminar flow over the controlled areas of the model was consistently achieved with a suction flow rate and distribution reasonably close to the pre-test estimates. Figure 5.1-71 illustrates the extent of laminarized area on the model and the measured boundary layer velocity profiles at the 30% chord location just downstream of the last suction slot. Without suction, the characteristic turbulent boundary layer profile was recorded, as would be expected, with a velocity defect thickness of , δ = 22.8 mm (0.90 in) which agreed well with the theoretical prediction. With appropriate suction applied, the flow remained laminar along the test surface which was apparent from the reduced velocity defect thickness (δ = 2.8 mm) and the profile shape. It should be noted, however, that the profile shape was somewhat fuller than the characteristic Blasius profile, because of the suction and the thickness of the boundary layer with LFC is about 80% of the corresponding natural laminar boundary thickness.

The typical suction flow characteristics are illustrated in Figure 5.1-72, which shows the external pressure distribution over the airfoil upper surface and suction pressure differentials across the individual slots as well as the internal plenum chamber

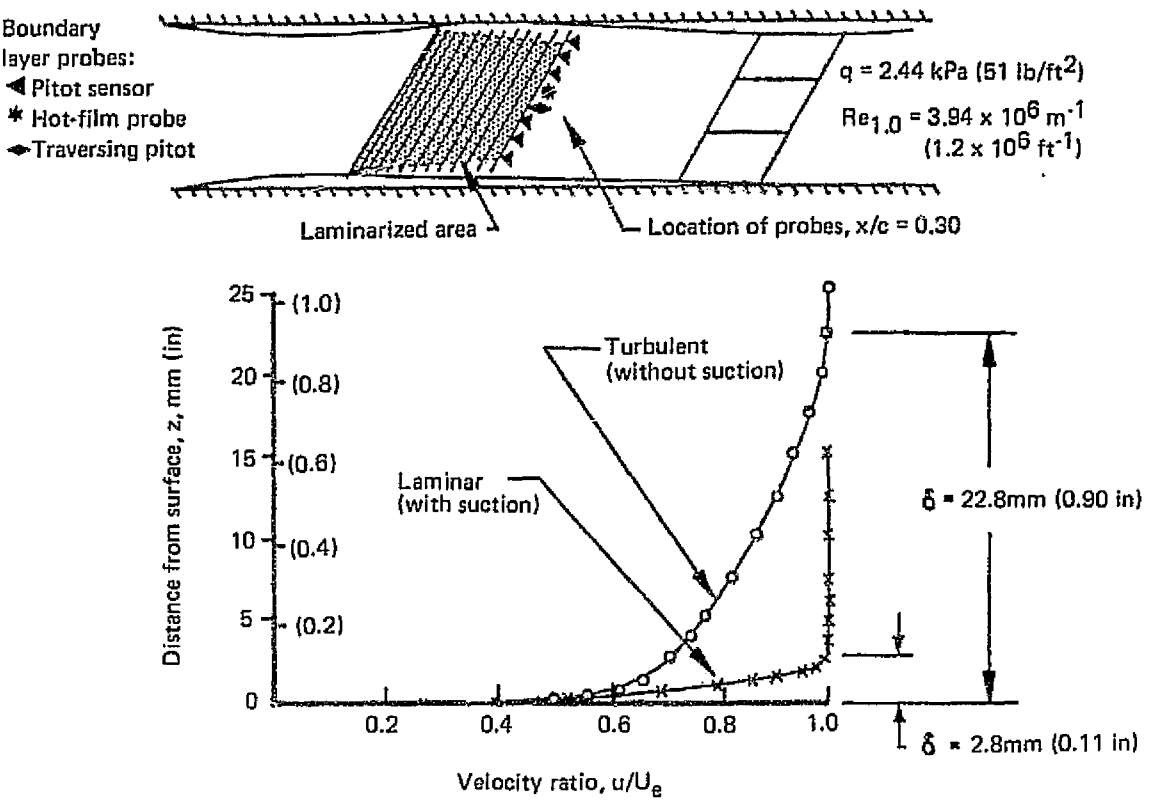

Figure 5.1-71. Extent of Laminarized Area and Typical Boundary Layer Profiles With and Without LFC

pressure levels. This case corresponds to an efficient suction level and distribution required to maintain laminar flow to 30% chord. The corresponding slot Reynolds numbers are shown on the lower plot indicating general adherence to the criteria, $Re_s = 100$. No difficulty was experienced with operation of the first slot beyond $Re_s = 150$ and, indeed, operation at suction levels 50% higher than normal, raising the average value of the slot Reynolds number to about $Re_s = 160$ and the initial value to $Re_s = 230$, exhibited no critical characteristics.

Figure 5.1-73 shows the variation of the two principal drag components, the "wake drag" and "equivalent suction drag", plus their sum, the total drag as a function of suction flow coefficient. Excessive suction, at least up to the tested limit, did not have any adverse effect except some increase in the level of equivalent suction drag.

One of the objectives of this test was the validation of suction estimation methods, hence, a comparison between the experimental results and theoretical estimates is of particular interest. Figure 5.1-74 shows such a comparison for a typical test case. It must be noted that the estimates of suction requirements and consequently, the slot arrangement specifications for the model, were made during the early phase of the program when only a simplified approximate method, based mainly on empirical

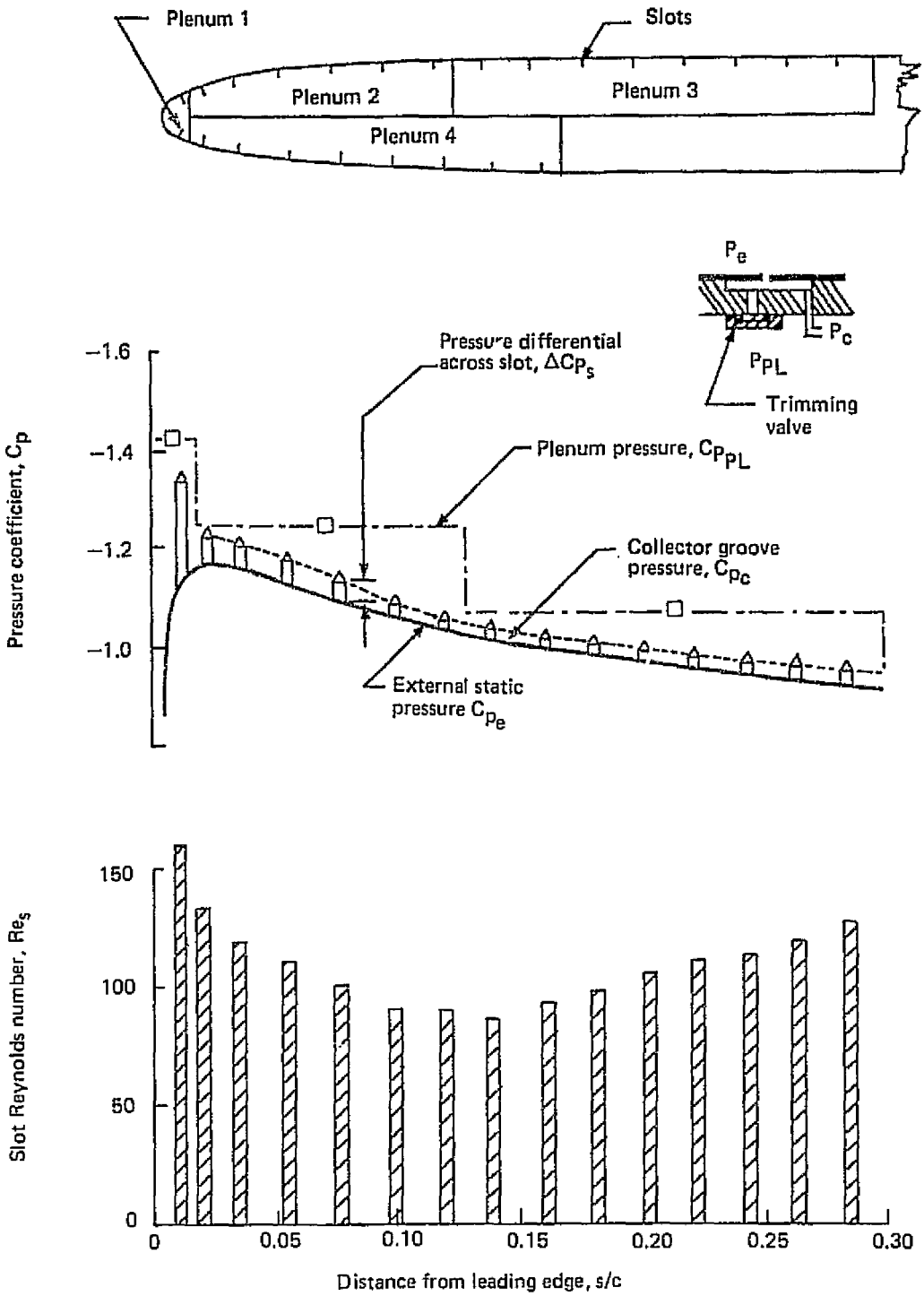

Figure 5.1-72. Suction Flow Characteristics

criteria from previous tests, was available. The estimated suction flow distribution exhibited a sharp peak just downstream of the leading edge, reaching to a maximum value of $c_q = 9.8 \times 10^{-4}$, and a flat region between s/c = 0.07 to 0.30 with $c_q = 1.6 \times 10^{-4}$. The slot spacing was chosen so that the slot Reynolds number would be approximately 75 throughout the entire suction surface and the slot widths would be equal to or slightly higher than the so-called "sucked height" of the boundary layer. Later studies, using the most recent computer techniques such as TEM 139 and MACK (see Section 5.1.2) however, indicated that there was no need for such strong suction near the leading edge, and the first slot, in fact could be as far back as s/c = 6 to 8%. The suction requirements over the main portion of the test surface, however, were in agreement with the initial estimates. By the time these new estimates become available, the model construction was well advanced and no revisions could be made except eliminating the first slot originally planned at s/c = 0.75% and the chordwise slots at the very leading edge. This, in fact, turned out to be quite fortunate since the test results indicated that suction within the region s/c = 1.25% to s/c = 8% was definitely required for laminarization of the test surface. Although this apparent contradiction with the theory needs to be further investigated, at this time one can conclude only that the earlier empirical estimates came closer to reality than the more sophisticated theoretical methods. To some extent this is explainable by the fact that the stability theory does not take into consideration such effects as the wind

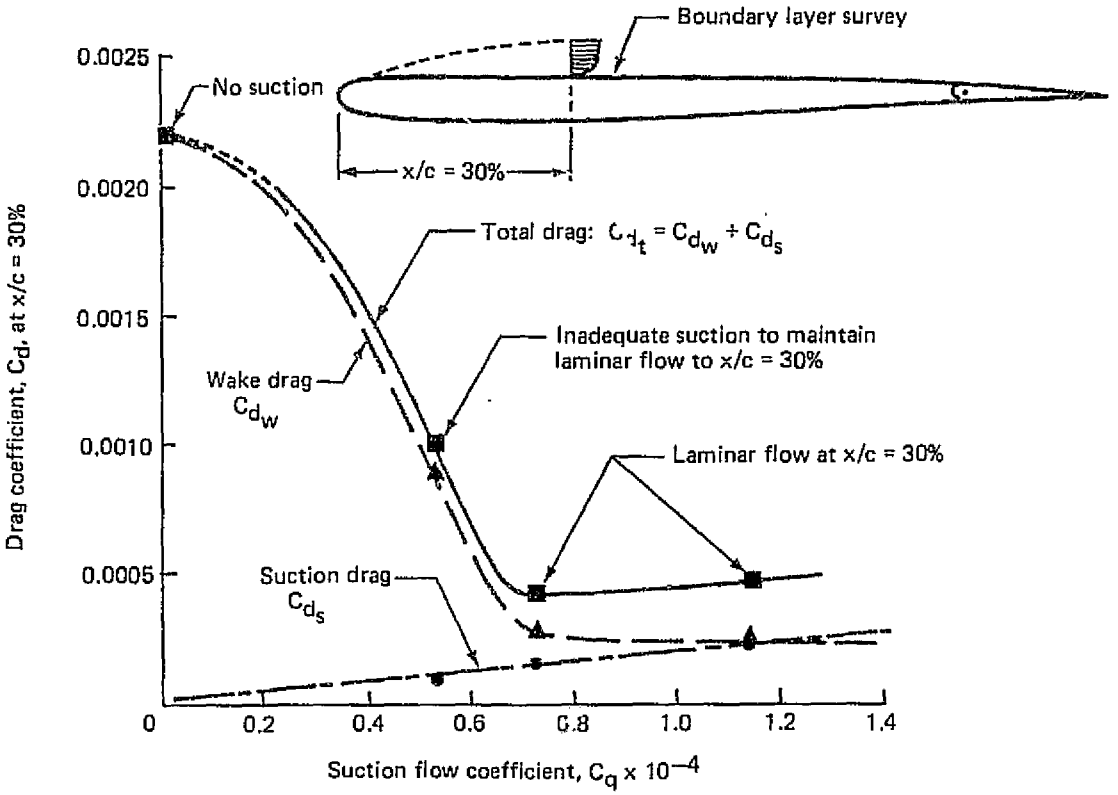

Figure 5.1-73. Variation of Drag With Suction Intensity

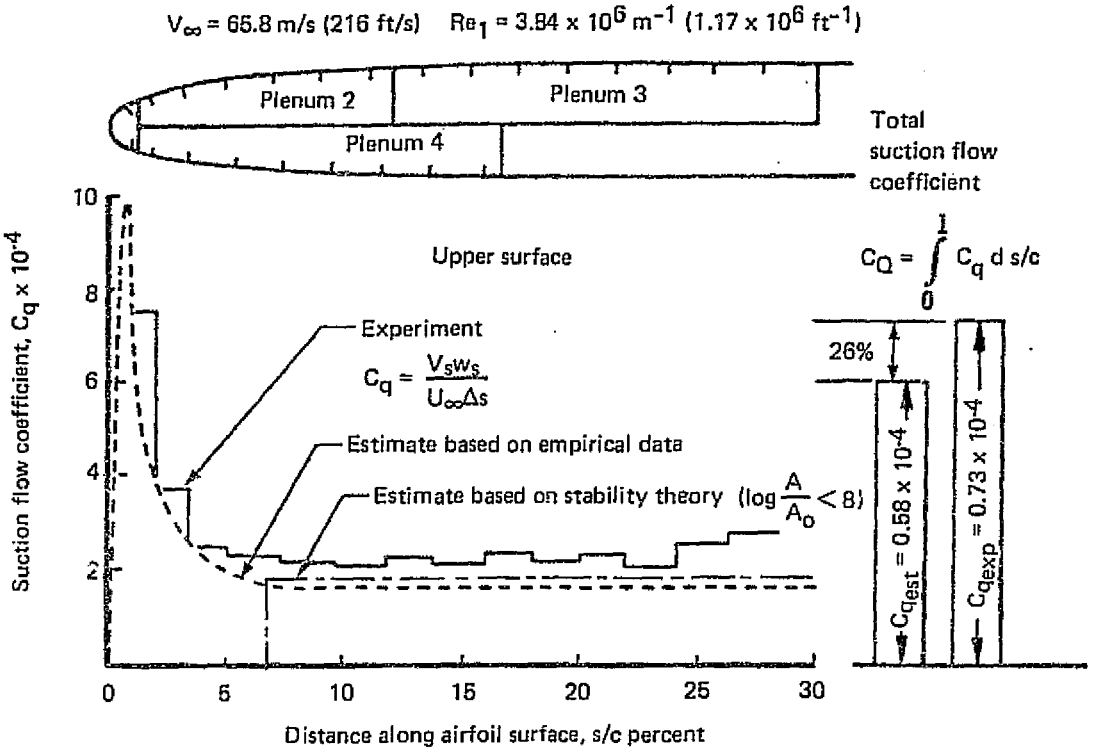

Figure 5.1-74. Estimated and Actual Suction Requirements

tunnel turbulence and noise or surface imperfections as well as a possible initial disturbance due to the attachment line flow whereas the empirical estimates can conceivably account for these.

It is apparent from Figure 5.1-74 that the peak in the experimental suction distribution is somewhat lower than the estimated value; nevertheless the experimental c_q level between x/c = 7% to 30% is definitely higher than estimated. Thus the cumulative value of the suction coefficient at the x/c = 30% chord location is about 26% greater than the estimate. A discrepancy of such magnitude, however, is not surprising, considering the approximate nature of the estimation method, the somewhat more pronounced pressure peak and subsequent adverse pressure gradient on the model than used in the estimates, and the undefined effects of the wind tunnel environment, such as turbulence, noise, etc.

Although an ultimate objective is to compare the suction requirements with theory, considerable analytical development will be required before valid comparisons can be made. This is because the presence of noise and turbulence in the wind tunnel, for example, introduces disturbances in the laminar boundary layer which can only be roughly accounted for. The best to be expected for the immediate future is to compare calculated disturbance amplification ratios corresponding to observed positions of transition in these wind tunnel tests for a variety of test conditions. These comparisons can also be assessed in relation to data from other sources. If a history of correspondence in amplification ratio can be shown to exist, a certain confidence in the validity of

this criteria may be established for known types and levels of the disturbance environment. Regardless, an assessment of the test results and the general experience to date leads to the conclusion that the objectives outlined above have been achieved.

The basic conclusion of this test period was that the experimental apparatus, including the model and the suction flow control system, as well as the tunnel flow environment were basically suitable for LFC investigations planned during later phases of the program.

(d) Third Test Period

The third series of tests, BRWT 117 and 118, were conducted between May 5 and June 17, 1978. The principal objectives of the test were to explore the sensitivity of suction controlled laminar flow to surface imperfections, contamination, off-design pressure distributions (increased crossflow) and imposed noise. The information obtained from the test results was intended to aid the development of design criteria for LFC airplanes regarding manufacturing tolerances and operational limitations.

This test series included the following four tasks:

1. Installation, checkout and acquisition of baseline data.
2. Testing the sensitivity of LFC to surface imperfections.
3. Testing the sensitivity of LFC to off-design flow conditions.
4. Surveying the acoustic environment of the model and testing the sensitivity of LFC to imposed noise.

In addition, a turbulence survey was also carried out in the BRWT test section with the LFC model installed as a part of the company-funded wind tunnel calibration and development program.

The model and associated test apparatus were essentially the same as during the previous test (Ref. 17). The instrumentation system included static pressure taps on the model surface, inside the slot collector grooves and in the plenum chambers, as well as boundary layer sensors such as hot film turbulence probes, elevated pitot-probes and one traversing boundary layer probe, all located along the 30% chord line just downstream of the last slot.

The surface imperfections were simulated by strips of self-adhesive tape running along the span parallel with the slots or spanwise rows of discs punched out from self-adhesive tape. The height, width (or diameter) and location of the disturbances as well as the intensity of suction and the tunnel speed were varied in order to determine the critical limits beyond which laminarization of the test surface was no longer possible. Off-design pressure distributions were simulated by changing the model incidence angle and flap deflection. Since the incidence change required the removal, adjustment and reinstallation of parts of the wall fairings, thus being quite laborious, only one change was made. However, changing the flap deflection angle was simple and convenient, permitting the testing of several configurations.

The baseline configuration, with an incidence of $\alpha = 0.5°$ and incremental flap deflection of $\delta_F = -4°/-1°/+2°$ (top/center/bottom) closely reproduced the nominal test condition of the previous entry (BRWT 106). Laminar flow over the controlled area of the model was again achieved without much difficulty. Some fine tuning of the slot-flow control valves was made, however, resulting in a smoother suction distribution than was achieved during the previous test.

The state of the boundary layer at the downstream edge of the suction surface (x/c = 30%) was monitored by two hot-film turbulence sensors and eight elevated pitot-static probes covering about 80% of the span. The primary means of transition detection were the hot film sensors whose indications were displayed on two oscilloscopes. The elevated pitot probes were mainly used for indication of the spanwise extent of laminar flow. Indications of these probes were displayed on a manometer board. The threshold suction level for laminarization of the test surface was, in general, established by the following procedure: first, the tunnel speed was stabilized with suction off; then the suction manifold pressure, ΔP_M was gradually increased to the point where the hot film sensors begin to indicate intermittent bursts of turbulence instead of the characteristic random fluctuations associated with turbulent flow. A slight additional increase in the suction manifold pressure then usually eliminated the intermittent bursts and led to steady laminar flow. The suction level at which turbulent bursts occurred only sporadically (at about 2 to 4 second intervals) was taken as the threshold value, ΔP^*_M. By repeating the above procedure at several tunnel speeds a relationship between ΔP^*_M and q was established which served as a baseline suction level for the subsequent phases of the test, namely, the evaluation of sensitivity to surface protuberances, off-design pressure distributions and imposed noise. The pressure in the manifold (referenced to the free stream static pressure) was a simple and very repeatable indicator of the suction flow rate, which could be read directly from a digital voltmeter and could be used very conveniently for establishing repeat conditions. It should be noted that, while the threshold value of suction manifold pressure required for laminarization increased with the tunnel dynamic pressure, the corresponding suction flow coefficient, C_Q did not vary with q.

In connection with task (2), a total of 26 different surface protuberance configurations were evaluated including 15 cases with two-dimensional ridge type protuberances and 11 cases with sparsely spaced three-dimensional "disc" type protuberances. The size (height, diameter or width) of the protuberances and their location on the test surface were selected to permit the exploration of critical limits through a relatively small number of configuration variations that could be tested during the limited time available.

The geometric details of the various surface protuberance configurations tested are shown in Figures 5.1-75 and 5.1-76. Normally, the protuberances were placed midway between two neighboring slots, except for configurations #9, #17, #18 and #19, in which cases a ridge type disturbance was located either immediately upstream or downstream of a given slot. Also, configurations #20 and #26 are a similar departure where either ridge or disc type protuberances were placed right on the leading edge. The purpose of the latter arrangements was to simulate the effects of surface discontinuities due to embedded leading edge cleaning devices.

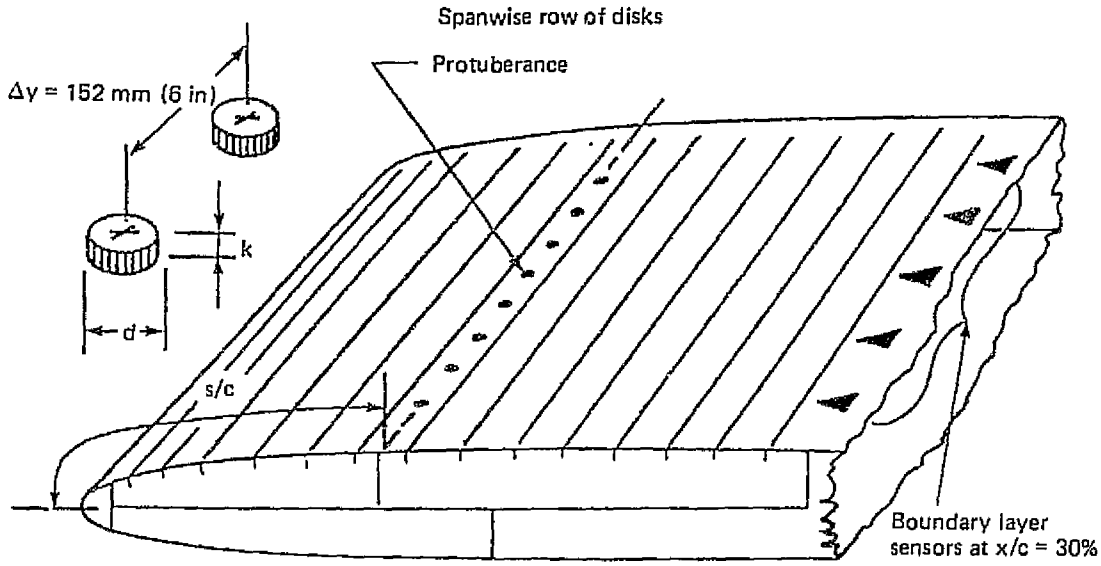

Config	k mm (in)	d mm (in)	d/k	s/c	θ mm (*)	k/θ	q_{crit} kPa (lb/ft^2)
10	0.254 (0.01)	1.0 (0.04)	4.0	0.21	0.233	1.09	≈ 1.43 (30)
11	0.127 (0.005)	1.0 (0.04)	8.0	0.21	0.233	0.54	> 2.63 (55)
12	0.190 (0.0075)	1.0 (0.04)	5.3	0.21	0.233	0.82	≈ 2.63 (55)
13	0.152 (0.006)	1.0 (0.04)	6.6	0.14	0.197	0.77	≈ 2.39 (50)
14	0.127 (0.005)	2.54 (0.10)	20	0.065	0.127	1.00	< 0.96 (20)
15	0.127 (0.005)	1.52 (0.06)	12	0.065	0.127	1.00	≈ 0.96 (20)
22	0.05 (0.002)	2.54 (0.10)	50	0.065	0.127	0.40	≈ 1.20 (25)
23	0.10 (0.004)	2.54 (0.10)	25	0.065	0.127	0.80	≈ 0.96 (20)
24	0.05 (0.002)	2.54 (0.10)	50	0.016	0.047	1.08	≈ 1.43 (30)
25	0.05 (0.002)	2.54 (0.10)	50	0.029	0.724	0.70	≈ 1.91 (40)
26	0.10 (0.004)	2.54 (0.10)	25	0	NA	NA	> 2.63 (55)

(*) Calculated, using experimental c_p and c_q distributions

Figure 5.1-75. Three-Dimensional Surface Protuberance Configurations Tested

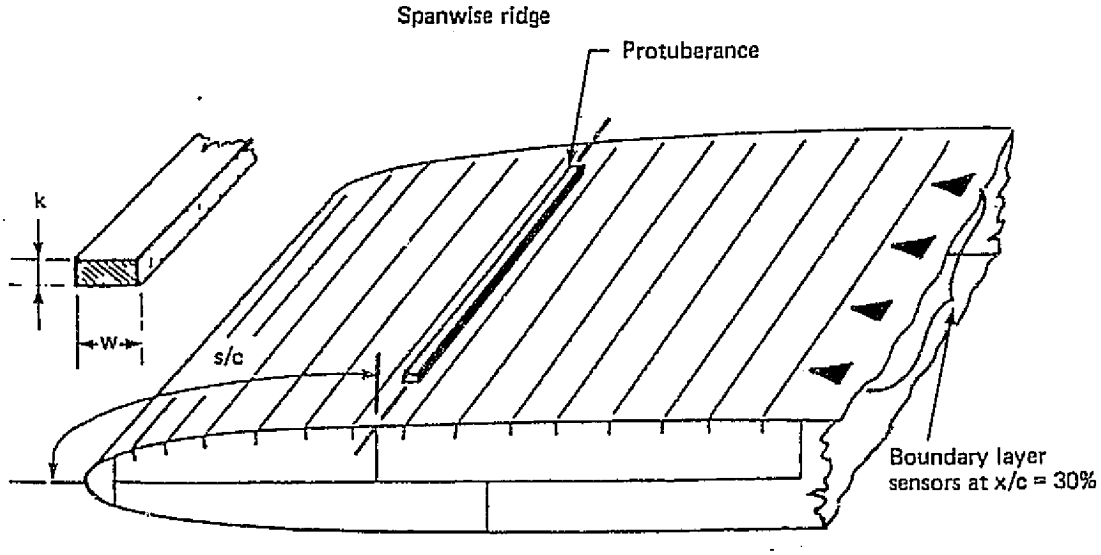

Config	k mm (in)	w mm (in)	w/k	s/c	θ mm (*)	k/θ	q_{crit} kPa (lb/ft^2)
1	0.127 (0.005)	0.762 (0.03)	6	0.250	0.245	0.52	> 2.63 (55)
2	0.127 (0.005)	0.762 (0.03)	6	0.147	0.202	0.63	> 2.63 (55)
3	0.127 (0.005)	0.762 (0.03)	6	0.065	0.127	1.00	≈ 2.63 (55)
4	0.127 (0.005)	0.762 (0.03)	6	0.028	0.071	1.78	≈ 2.63 (55)
5	0.127 (0.005)	0.762 (0.03)	6	0.016	0.047	2.70	≈ 2.39 (50)
6	0.254 (0.010)	0.762 (0.03)	3	0.016	0.047	5.40	< 0.96 (20)
7	0.254 (0.010)	0.762 (0.03)	3	0.100	0.164	1.55	≈ 1.91 (40)
8	0.254 (0.010)	0.762 (0.03)	3	0.25	0.245	1.02	≈ 1.67 (35)
9	0.127 (0.005)	0.762 (0.03)	6	0.0125	0.038	3.29	≈ 1.18 (25)
16	0.127 (0.005)	3.05 (0.12)	24	0.016	0.047	2.70	≈ 2.39 (50)
17	0.127 (0.005)	3.05 (0.12)	24	0.020	0.056	2.27	≈ 1.67 (35)
18	0.127 (0.005)	3.05 (0.12)	24	0.021	0.057	2.22	≈ 1.67 (35)
19	0.127 (0.005)	3.05 (0.12)	24	0.0125	0.038	3.16	≈ 1.18 (25)
20	0.127 (0.005)	3.05 (0.12)	24	0	NA	NA	> 2.63 (55)
21	0.127 (0.005)	3.05 (0.12)	24	0.0075	0.025	5.0	≈ 0.96 (20)

(*) Calculated, using experimental c_p and c_q distributions

Figure 5.1-76. Two-Dimensional Surface Protuberance Configurations Tested

Figures 5.1-75 and 5.1-76 also include a brief statement of the principal results pertinent to each configuration, quoting the dynamic pressure at which the given protuberance became critical or indicating that critical conditions were not encountered; i.e., the flow remained either turbulent or laminar throughout the available q range.

The test procedure for evaluating the effects of surface protuberances was the following: After a given protuberance configuration was installed on the model (with the boundary layer monitoring instrumentation permanently emplaced at the downstream edge of the suction surface), first an intermediate speed level, usually q = 1.67 kPa (36 lb/ft^2) was established; then the suction was turned on and its intensity was increased to the threshold level, ΔP^*_M , required for laminarization in the clean configuration. At this point, the boundary layer monitoring instrumentation was checked to see whether or not the flow was laminar at the measuring station; if not, an attempt was made to achieve laminar flow by increased suction. If laminar flow was achieved during the initial sounding test run, the routine was repeated at progressively higher speeds until either critical conditions were encountered or the tunnel speed capability, q = 2.63 kPa (55 lb/ft^2) was reached. The criterion for critical conditions was the occurrence of intermittent turbulent bursts at less than about 2 seconds intervals. If laminar flow could not be achieved at the initial speed level, the tunnel velocity was reduced gradually as far down as q = 0.95 kPa (20 lb/ft^2) to see if laminarization would be possible at lower Reynolds numbers. The test routine also included raising the suction intensity well above the threshold value required for laminarization to see if oversuction would have any adverse effect.

The basic ovservations regarding the effects of surface protuberances can be summarized as follows:

1. The two-dimensional (ridge type) protuberances were, in general, more tolerable than the three-dimensional (disc type) protuberances, as could be expected on the basis of previous results. The tolerable protuberance height, of course, was strongly dependent on the chordwise location, and the tunnel velocity. For two-dimensional disturbances, the critical height varied between 0.127 mm and 0.254 mm (0.005 in and 0.010 in) and for three-dimensional disturbances k_{crit} varied between 0.05 mm and 0.20 mm (0.0002 in and 0.008 in). These tolerance limits will be expressed later in non-dimensional terms.

2. Increasing suction intensity (C_Q) was not effective in making the model more tolerant to surface protuberances. In other words, the model could tolerate a given size of protuberance at the suction rate established for the clean condition but once the critical limit was reached, added suction could not extend the tolerance limit. This observation is consistent with previous data regarding three-dimensional protuberances but not so in the case of two-dimensional disturbances. The tests described in Reference 6, for example, showed that the admissible surface waviness could be significantly increased by suction. The above tests, however, were conducted on an unswept wing which precludes a direct comparison with present results. It is, in fact, quite conceivable that the effects of two-dimensional protuberances in a three-dimensional (swept wing) boundary layer are different than in a pure two-dimensional flow.

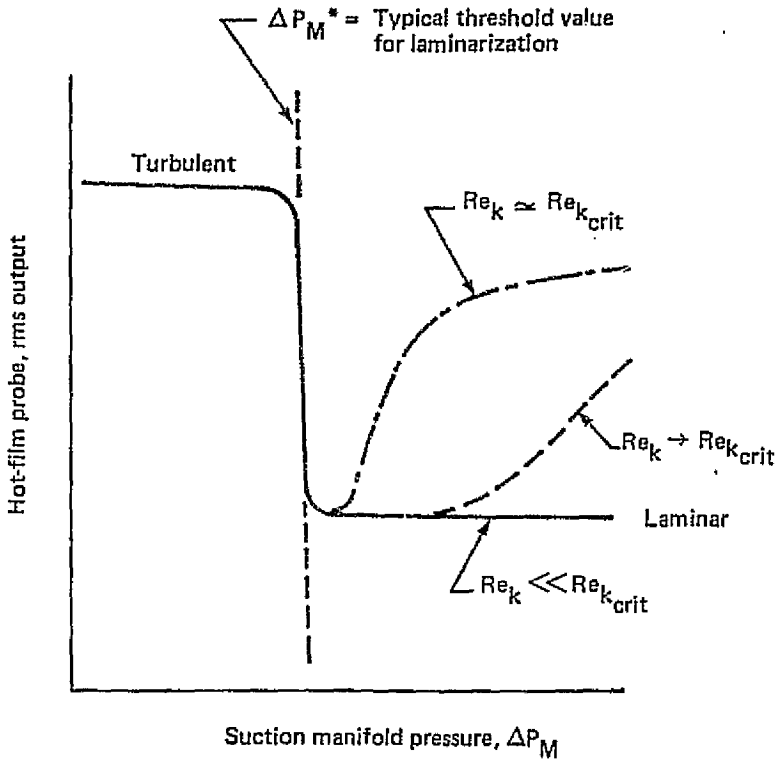

Figure 5.1-77. Effects of Roughness on Sensitivity to Oversuction

3. With protuberances approaching the critical height, the laminar flow on the model became increasingly more sensitive to oversuction. Thus, in the case of the smooth model and also with protuberances that were well below the critical limits, the threshold suction flow rate could be significantly exceeded (at least 50%) without any adverse effects. However, when the protuberances were near the critical height laminar flow could be maintained only within a narrow range of C_Q and oversuction would cause turbulent flow. Figure 5.1-77 illustrates this showing the typical indication of the hot-film turbulence sensor as a function of suction manifold pressure, as recorded by an X-Y plotter.

4. The location of a protuberance relative to the neighboring slots was also found to be quite important. For example, a given ridge (#16) was tolerable up to q = 2.39 kPa (50 lb/ft^2) when placed at s/c = 0.016, midway between the first and second slots, but the same size of ridges (#17, #18 and #19) could be tolerated only up to q = 1.67 kPa (35 lb/ft^2) when placed nearby, either ahead of or aft of the slot. At the adjacent forward slot location, only a q of 1.18kPa (25 lb/ft^2) could be tolerated when the ridge was located nearby. It must be noted, however, that the suction distribution was not altered during these test runs, and it seems quite possible that increased suction just downstream of a disturbance might have been effective in maintaining laminar flow.

5. The flow at the very leading edge was quite tolerant to surface protuberances. Neither a ridge of k = 0.127 mm (0.005 in) height nor a row of disks of k = 0.10 mm (0.004 in) height caused premature transition. This is regarded as a very encouraging result indicating that small protuberances due to the presence of certain types of leading edge cleaning devices might be tolerable on an LFC wing.

For generalization of the test results, the limits of permissible surface protuberances were expressed in terms of the so-called "roughness Reynolds number," Re_k. The customary definition of this term is:

$$Re_k = \frac{u_k k}{\nu}$$

where k is the height of the protuberance and u_k is the local velocity within the boundary layer at a height of z = k. For convenient numerical evaluation, the above relation is put in the following form:

$$Re_k = Re_1 \sqrt{1-C_p}\ u_k/U_e\ \ k$$

where Re_1 is the unit Reynolds number, C_p is the local pressure coefficient and u_k/U_e is the velocity ratio in the boundary layer at z = k.

Appropriate values of u_k/U_e were determined from theoretical calculations of the boundary layer profiles based on the experimental pressure distribution (C_p vs s/c) and suction inflow distribution (C_q vs s/c) required for laminarization.

Figure 5.1-78 presents a summary of the test results obtained with three-dimensional disc type protuberances. The format of the plot of Re_k vs d/k is the same as used in Reference 8 in order to make a direct comparison between the present results and the previous data. For any given disc configuration, characterized by the shape parameter, d/k, the range of test data, due to the variation of q, is represented by a bar. The q range within which laminarization of the test surface was not possible is indicated by blackening of the bar, whereas the open portion corresponds to laminar flow. Thus, the changeover between the blackened and open portions of the bar represents the critical condition and marks the corresponding value of the critical roughness Reynolds number, $Re_{k_{crit}}$.

The data band of previous test results on $Re_{k_{crit}}$, as compiled in Reference 8, is indicated by the two shaded boundaries. It is evident that some of the present results corresponding to lower d/k values of d/k, tend to indicate lower $Re_{k_{crit}}$ limits. Interpretation of these results in a somewhat subtle problem. One could simply conclude that the new data tend to indicate a steeper decline for the lower boundary of the Re_k band with increasing d/k than the previous data. However, it is probably significant that the data points corresponding to lower d/k values, were taken at locations further away from the leading edge where crossflow effects were minimal, whereas the data points associated with higher d/k values were taken within the forward region of the model where crossflow effects were important. Accordingly, the present results can be interpreted as consistent with the previous data under conditions when the crossflow is weak, but as indicating a lower

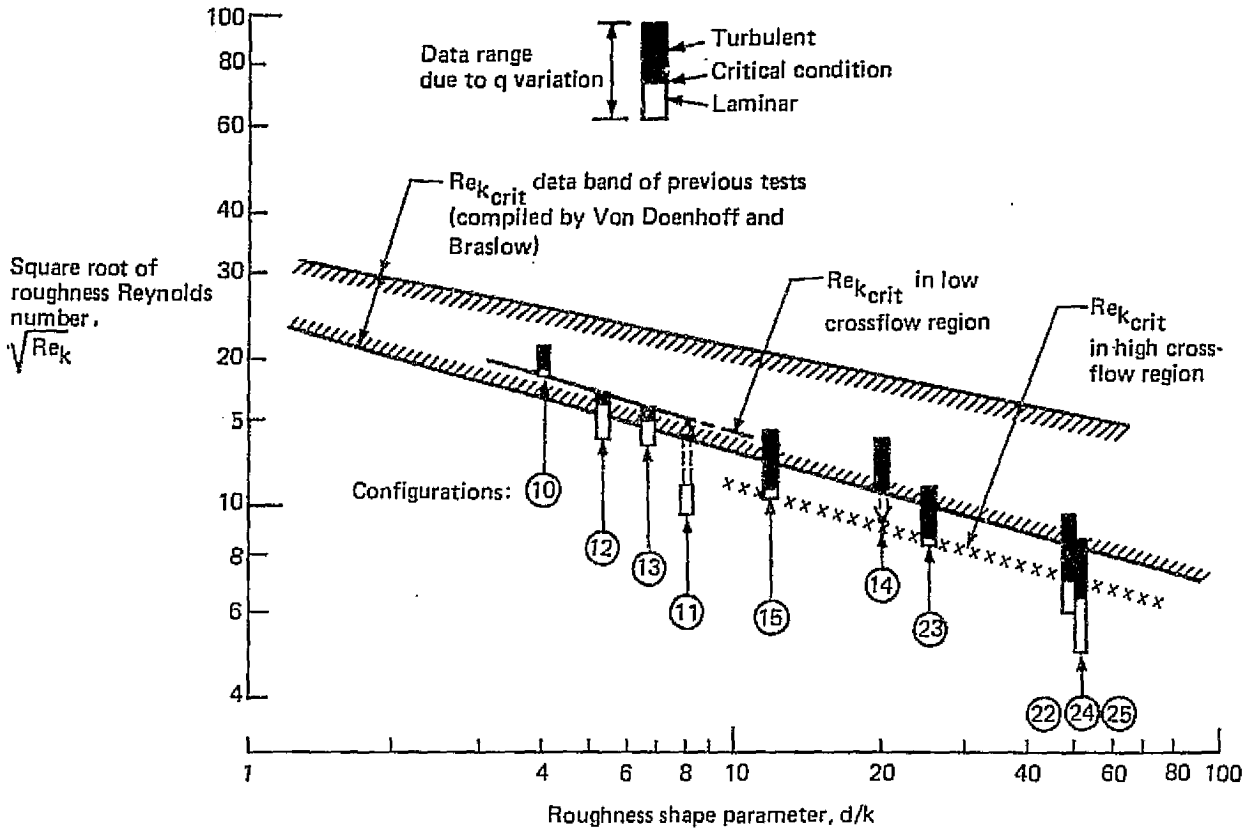

Figure 5.1-78. Comparison of Present Reslults on Critical Roughness Reynolds Number With Previous Data—Three-Dimensional Protuberances

$Re_{k_{crit}}$ boundary for the high crossflow region. It is unfortunate that there is not sufficient overlap between the two sets of data, i.e., discs of high d/k in the low crossflow region and discs of low d/k in the high crossflow region, which would permit a more definite interpretation of the results.

At any rate, it is quite conceivable that the critical roughness Reynolds number is not a simple function of the shape parameter (d/k) alone, but that it is also dependent on the location of the disturbance, and thus, the characteristics of the surrounding boundary layer, including its stability. This question deserves further investigation.

Figure 5.1-79 presents a summary of the test results obtained with two-dimensional ridge type protuberances. The format of the presentation is similar to that of Figure 5.1-78 to provide consistency. Re_k are plotted here in terms of k/θ, the ratio of the ridge height to the local momentum thickness.

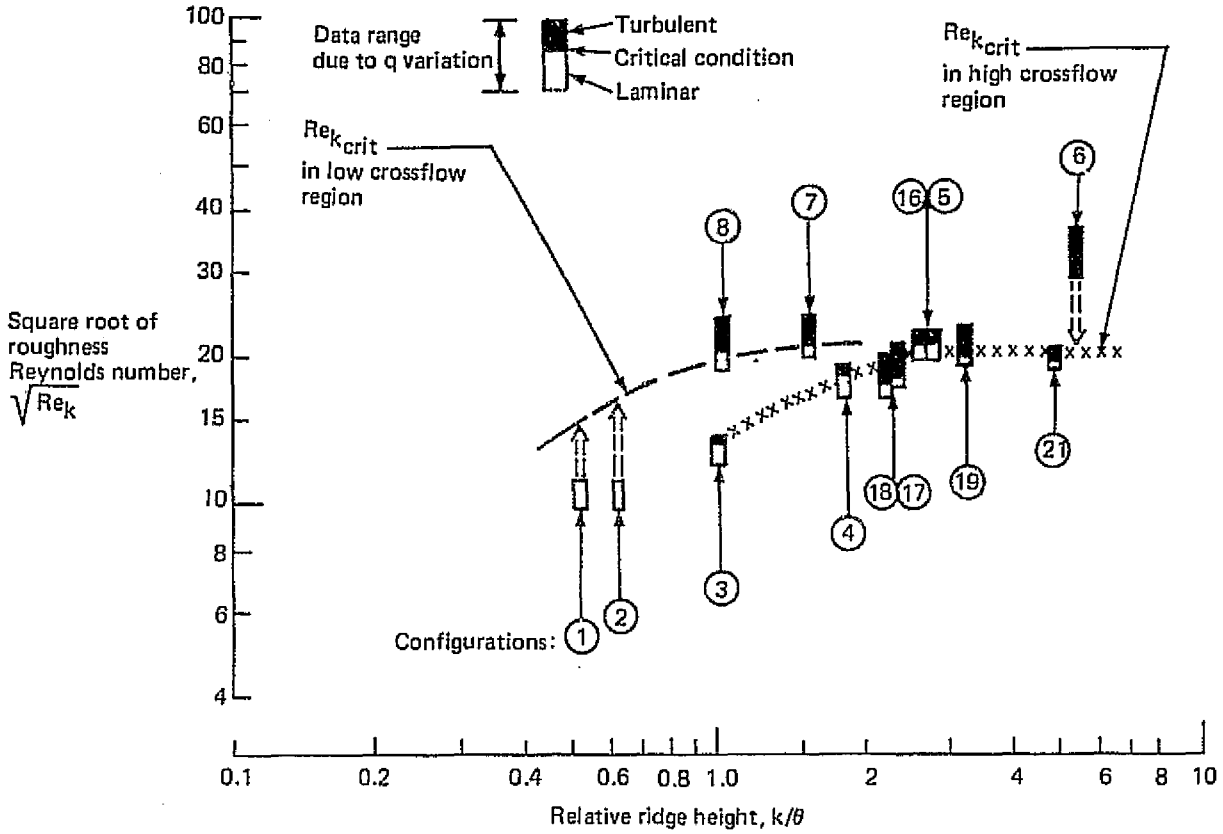

Figure 5.1-79. Summary of Present Results on Critical Roughness Reynolds Number for Two-Dimensional Protuberances

At first glance it appears that the critical values of Re_k tend to cluster around $Re_{k_{crit}} = 400$ regardless of k/θ. However, considering the test data for configurations #3 and #8, in which cases the k/θ ratio was the same, but $Re_{k_{crit}}$ was markedly different, one could again postulate the existence of two $Re_{k_{crit}}$ boundaries, one representing the data that correspond to the low crossflow regions and one that corresponds to the high crossflow regions. In the latter case, the $Re_{k_{crit}}$ limits are apparently somewhat lower than in the case of low crossflow. Here again, more data is necessary to establish definite trends and so this interpretation must be considered as somewhat speculative.

The concluding portion of the test was devoted to exploring the effects of off-design flow conditions. The intent was to simulate a low C_L flight condition with extended region of negative pressure gradient (accelerating flow) which also produces increased crossflow over the forward region of the wing. The model incidence angle for this test series was reduced by 0.5°, (from $\alpha = 0.5°$ to $\alpha = 0°$) which, according to estimates, should have given the desired pressure distribution. The test however, showed that the above change in α was not quite adequate, but since changing the model incidence required the removal, adjustment and reinstallation of certain portions of the wall fairings and thus was quite time consuming, no attempt was made to test another incidence angle. Changing the flap

angle, however, was quite simple and expedient so that several alternate flap settings were tested in an attempt to achieve the desired pressure distribution. Figure 5.1-80 illustrates the results showing the effects of the incidence change and flap angle variations on the centerline pressure distribution. It is apparent that the flap angle variations did not change the shape of the pressure distribution but only shifted the C_p level.

Laminarization of the test surface at the off-design conditions, that could be produced, presented no problem. The suction requirements, in terms of total C_Q, were actually somewhat lower than in the baseline condition. This is understandable, because of the reduced pressure peak and lower C_p level.

In this series of experiments, the tuning of the suction system deliberately was not changed in order to see the effects of variations in the external pressure distribution on the suction flow characteristics once the system has been tuned for a given design condition. The results indicated that changing external pressure distributions did alter the suction inflow distributions and certain portions of the model did receive more than adequate suction while others received only a marginal amount. Figure 5.1-81 illustrates this showing the distribu-

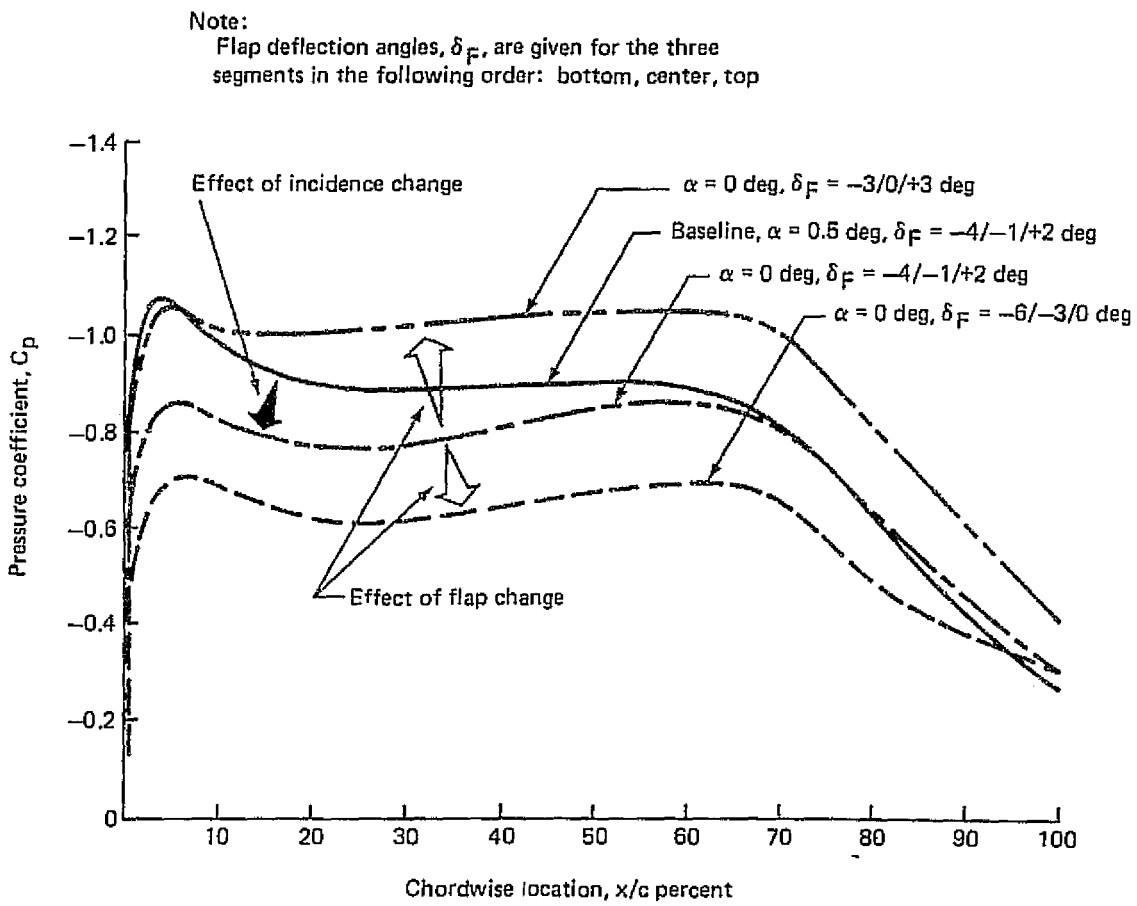

Figure 5.1-80. Off-Design Pressure Distributions Tested

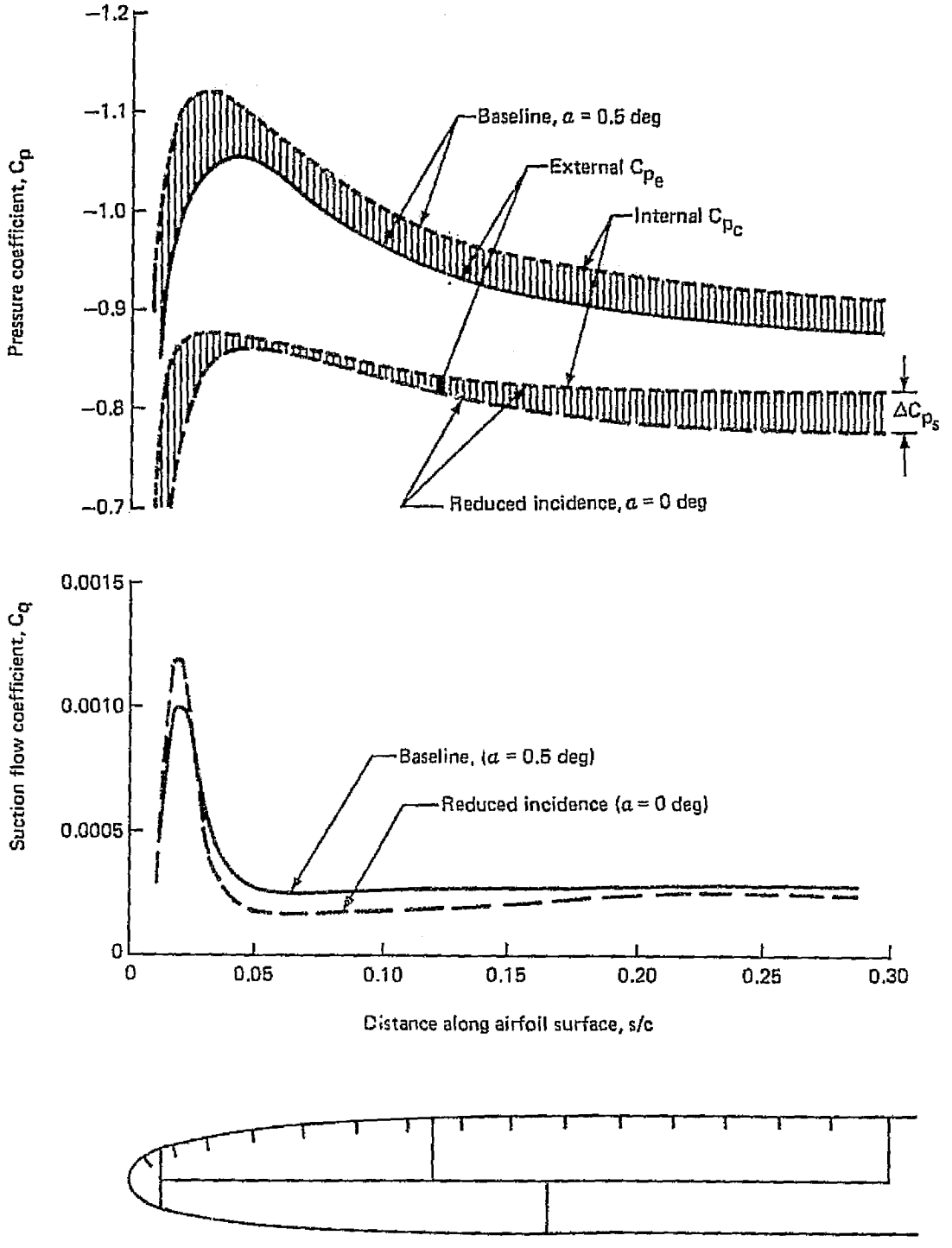

Figure 5.1-81. Suction Flow Characteristics at Reduced Incidence

tion of the suction pressure differential, ΔC_{p_s}, and corresponding suction flow coefficients, C_q, for a typical off-design condition in comparison with the baseline condition. It can be seen that the area between s/c = 0.03 and s/c = 0.10 received reduced suction, while ahead and aft of that region the suction was probably more than adequate. An LFC airplane would probably have to deal with a similar situation although some provision for suction flow adjustment by area would be provided.

Because of the extensive nature of the noise sensitivity tests conducted in the third test period, that activity is reported separately in the following paragraph.

5.1.8.2 Noise Sensitivity Tests

As part of the wind tunnel study of LFC aerodynamics, the opportunity was taken to acquire some engineering data on the effects of applied noise fields on the stability of a laminar boundary layer with suction. It was also an excellent opportunity to utilize a well developed LFC test model (described in Paragraph 5.1.8.1) to gather information on test procedures, unknowns in the wind tunnel test environment and measuring techniques needed to conduct a more extensive acoustical test program at a future date.

(a) Introduction

The quantity of boundary layer suction required to maintain laminar flow is known to be increased by high sound intensities imposed on the boundary layer (Reference 18). Air particle fluctuating displacements caused by the impinging sound waves add to displacements caused by flow turbulence, and the resulting disturbance velocities characterizing the vorticity modes undergo the well-known Tollmien-Schlichting and crossflow amplifications. This amplification has been shown theoretically and experimentally to occur only for the fluctuating disturbance velocity components in a limited frequency range corresponding approximately to critical frequencies in the vorticity modes.

The Sound Pressure Level (SPL) outside the boundary layer is the normal measure of sound intensity; however, the associated velocity fluctuation is the parameter most directly related to the breakdown of laminar flow. In the semi-reverberant environment of the wind tunnel, the ratios of sound pressures and disturbance velocities (i.e., the acoustic impedance) vary widely due to standing wave effects. It was, therefore, an important part of the test to measure disturbance velocities in the boundary layer as well as SPL, which was done by means of hot-wire anemometry probes within the boundary layer.

(b) Objectives

The primary objective of the test was to relate the acoustic environment to the suction requirements needed to maintain a controlled laminar boundary layer. The first step in this process is illustrated in Figure 5.1-82, which shows a typical variation of acoustically generated disturbance particle velocity, u_H inside the boundary layer corresponding to the applied noise velocity field, u_M outside the boundary layer that can be tolerated as a function of frequency without causing transition. This is designated

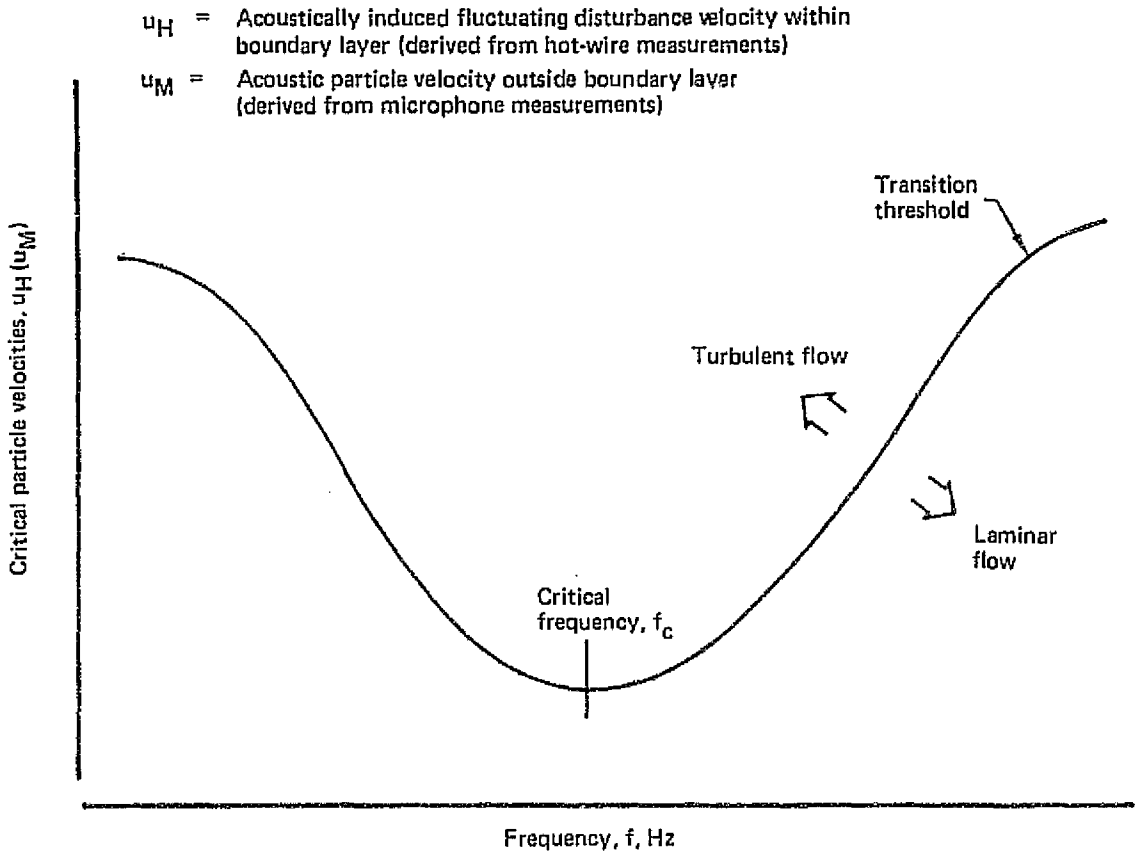

Figure 5.1-82. Illustration of Disturbance Velocity and Critical Frequency at Transition Threshold

the transition threshold curve, for a given rate of suction. Detailed measurements are required to determine the character of this curve and the frequency corresponding to the lowest level of u_H (or u_M) that will cause transition (i.e., the critical frequency). This information is essential to establish the sensitivity of the laminar boundary layer to applied noise fields and to determine the effectiveness of added suction in delaying transition.

A secondary objective was to investigate the transfer function which defines the relationship between the acoustical particle velocity, u_M outside the boundary layer and the disturbance velocity, u_H within the boundary layer. This function is determined by the energy transfer between the external acoustical field and the disturbance induced within the boundary layer.

The detailed objectives of the current investigation are given in Table 5.1-4 and compared with those of previous studies. A summary of the tests, principal results and conclusions are discussed below. Full details of the study are provided in Reference 18.

Table 5.1-4. Wind Tunnel Acoustical Investigation Objectives

Boeing investigation	Previous investigations
• Test model subjected to oblique sound field simulating wing-mounted engine noise	• Test model subjected to chordwise and spanwise grazing sound fields
• Investigation of transition with variations in sonic intensity, spectral content (narrow band and third-octive band), and suction rate	• Similar tests conducted with grazing sound field but with limited acoustical measuring techniques; detailed survey not previously made
• Investigation of vorticity disturbances amplification induced by applied sound field	• Limited tests and data available
• Obtain critical noise criteria as a function of frequency spectrum and sound intensity	• Existing critical noise criteria function of sound intensity only (i.e., overall SPL)
• Comparison of current LFC model with Northrop 1960 model	• Comparison of transition criteria, fluctuating disturbance velocity, sonic intensity, and LFC suction rate
• Development of guidelines and recommendations for future studies	

(c) Study Approach

The following discussion outlines the basic approach used for the exploratory acoustical work, conducted during the second laminar flow control wind tunnel test program.

An initial exploratory investigation was conducted as described below, to establish the range of interest for detailed studies. Sonic environments of various spectral content and intensity were imposed on the upper section of the model with suction over 30% of the chord. Laminar flow transition thresholds were then determined by two approaches: First, holding the suction flow rate and the imposed sonic spectral shape constant, and varying the sonic intensity. Second, by holding the sonic intensity and spectral shape constant, and varying the LFC suction flow rate. Transition was detected at the downstream edge of the suction surface by observing the boundary layer total pressure profiles and hot film traces on oscilloscopes. The above procedure was repeated with sonic inputs in a range of third-octave band frequencies. Each critical test condition was established by varying either the sonic intensity or the suction rate until transition was detected.

A detailed sound environment survey was then made as follows: After identification of a critical test condition, the sonic environment was surveyed with microphones. The wind tunnel flow speed, suction rate and sonic level were maintained constant during the above survey. On-line plots of approximately 15 narrow band spectra and the corresponding overall levels were required for each sonic survey.

After completion of the sonic surveys, the response characteristics of the boundary layer were evaluated to provide an insight into transfer functions, disturbance amplifications, and other phenomena of interest. Fluctuating disturbance velocities were measured in the boundary layer by use of a hot-wire anemometer. Measurements were made at a number of chordwise stations (one spanwise position only), and at three locations within the boundary layer, where spectral distribution of the fluctuating components was determined. The sonic environments consisted of third-octave band spectra and were selected from the conditions already evaluated in the initial exploratory sonic environment surveys. Conditions included one of zero sonic input and one of very high sonic intensity. The suction conditions were set by first establishing the sonic environment, then increasing suction until the hot-wire output, located at the chordwise downstream station being investigated, ceased to reveal intermittent bursts of turbulence. Great care was taken to repeat test conditions closely as the hot-wire was moved to other locations.

Figure 5.1-83 illustrates the method used to establish the transition threshold curve shown in Figure 5.1-82. The variation of the critical velocity ratio was obtained experimentally by directing a third-octave band noise field of a given center frequency toward the surface and measuring the fluctuating velocity spectrum, u_{η} generated in the boundary layer. This was measured at a number of noise levels until the transition threshold was reached for a particular frequency input. The critical velocity ratio was obtained, as in licated in Figure 5.1-83 by integrating the fluctuating velocity, u_{η} over the critical range of frequencies to obtain u_H and then forming the ratio with free-stream velocity, V_∞. This process was repeated for a sequence of applied frequencies so that the resulting variation of $u_{H(Critical)}/V_\infty$ was obtained thus forming the transition threshold curve. As expected, this is found to be function of the suction rate

(d) Test Program Outline

A schematic representation of the test setup is given in Figures 5.1-84, 5.1-85 and 5.1-86, showing the model and the two noise generator locations used in the test. Details of microphone and hot-wire locations corresponding to the listed test run numbers, are also given in the latter two figures.

The experimental investigation was conducted in four parts as follows:

(a) Exploratory noise survey, with acoustic field applied to the suction surface, for varying sound intensity, frequency spectrum, LFC suction rate and tunnel velocity.

(b) Survey of acoustic field over LFC surface of the model, with parametric variations shown in part (a).

(c) Hot-wire fluctuating velocity survey in the boundary layer over suction surface of model, with parametric variations shown in part (a).

(d) Repeat of parts (b) and (c) with a change of noise generator location.

A summary of the program test log is provided in Table 5.1-5.

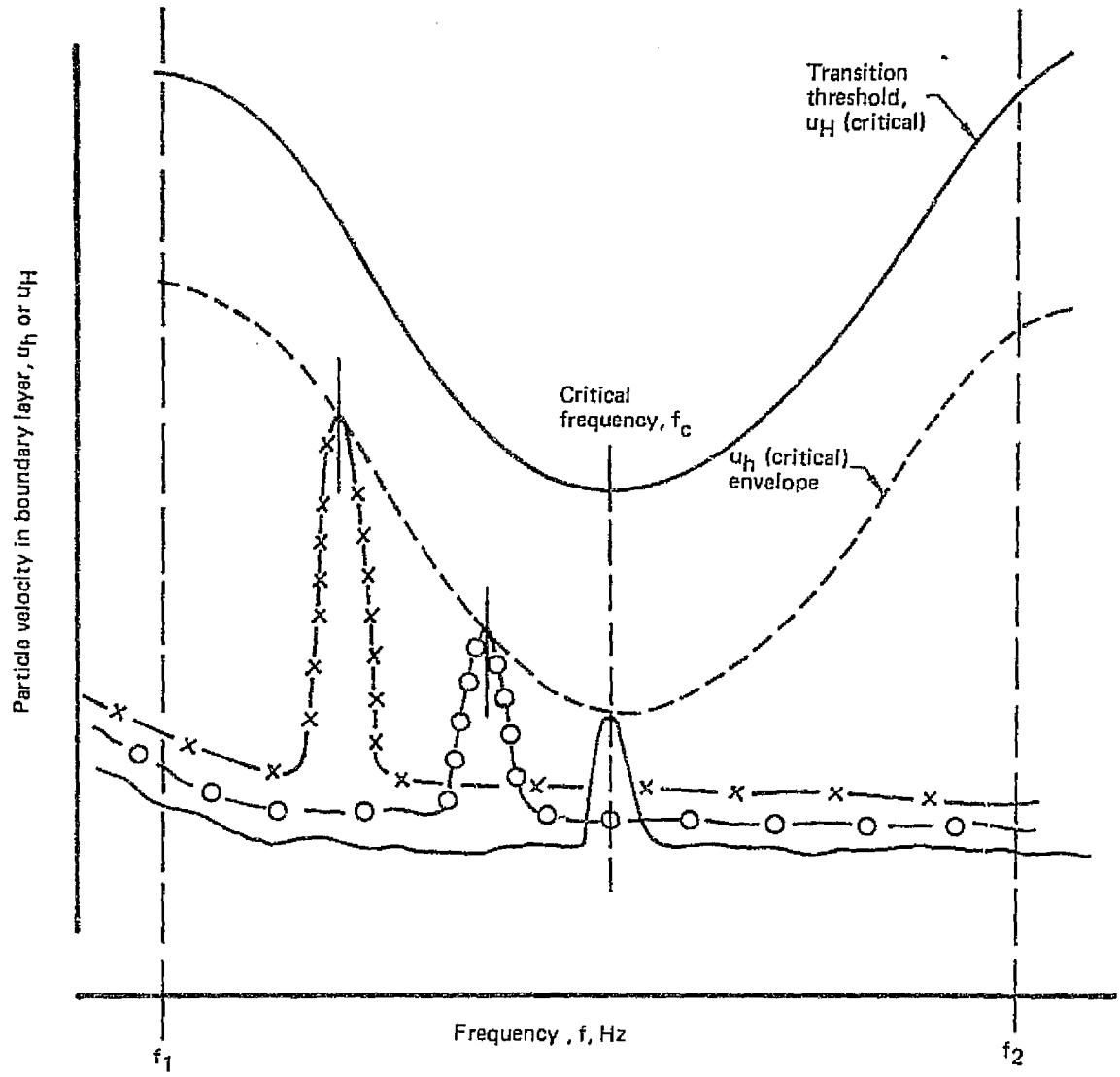

$$u_H = \int_{f_1}^{f_2} u_h(f)\, df$$

$u_h(f)$ = Fluctuating velocity over frequency range f_1 to f_2 associated with a third octave band applied field

Figure 5.1-83. Experimental Method for Determining Transition Threshold Curve

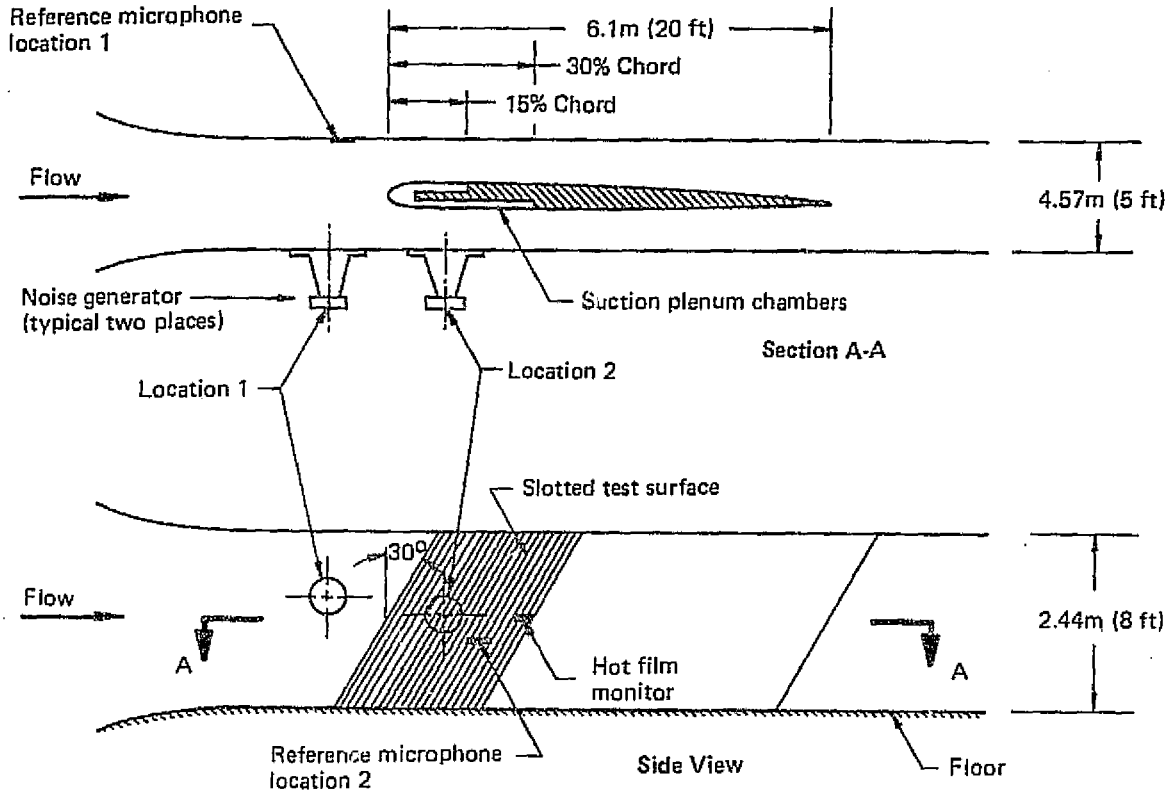

Figure 5.1-84. Test Arrangement for Acoustical Test on LFC Wind Tunnel Model

(e) Critical Features of the Test Method

The equipment used had some features which are critical to the understanding of the results. The acoustic source can be described as an air valve at the horn throat driven by a coil which was energized and modulated by an AC amplifier. When the noise generator was pressurized, a residual aerodynamic noise was generated by airflow through the valve which "homed" in an intermediate position in the absence of the driving signal for the flow modulator. When a drive signal, such as a third-octave band random signal was applied, a corresponding third-octave band random signal was applied, so a corresponding third-octave band acoustic signal was added to the residual acoustic spectrum generated by the airflow. Thus, the test included three basic acoustic conditions as exemplified in Figure 5.1-87; namely, tunnel residual (no contribution from the sound generator), noise generator residual (air valve background noise superimposed on tunnel residual noise) and band-passed random noise superimposed on the residual levels. In the results that follow, the intensity of the band-passed noise component will be referred to as the incremental acoustic input intensity.

(f) Summary of Test Results

The following is a brief summary of the principal results obtained in the exploratory study. More detailed results and analysis are provided in Reference 18.

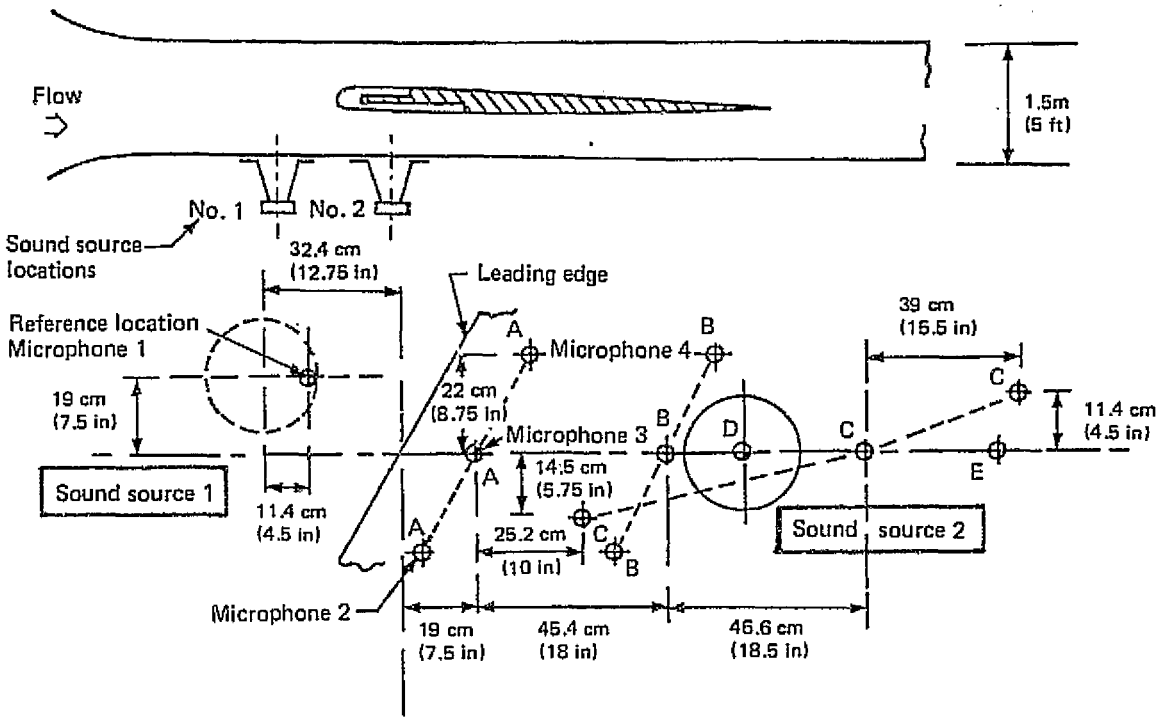

Microphone Locations:

Run 1 to 4—Reference location; microphone 1; source 1
Run 5—Array A; microphones 2, 3, 4; source 1
Run 6—Array B; microphones 2, 3, 4; source 1
Run 7—Array C; microphones 2, 3, 4; source 1
Run 18—Location A; microphone 2; source 2
Run 18—Location D; microphone 3; source 2
Run 18—Location E; microphone 4; source 2

Figure 5.1-85. Sound Survey on Model

Shown in Figure 5.1-88, are hot-wire fluctuating velocity spectra measured in the boundary layer resulting from applied acoustic disturbances at various frequencies, with a constant suction rate to maintain stable laminar flow. The results show the laminar boundary layer to be most sensitive to applied acoustic excitation in the 1.25 to 1.6 kHz frequency range. The acoustical input for condition 11.3 at a center frequency of 3.15 kHz was limited due to insufficient power of the noise source above this frequency. Therefore, the transition threshold level at 3.15 kHz is judged to be higher than shown in the figure. Test condition run numbers are included for identification of data and future reference. Full details of these are given in Reference 18.

It was noted in several test results that selective amplification phenomena were occurring in the boundary layer at frequencies above or below that of the applied acoustic field, and their origin has not been identified to date. For example, in Figure 5.1-88, a broad peak of amplification in fluctuating velocity occurs in the 2 to

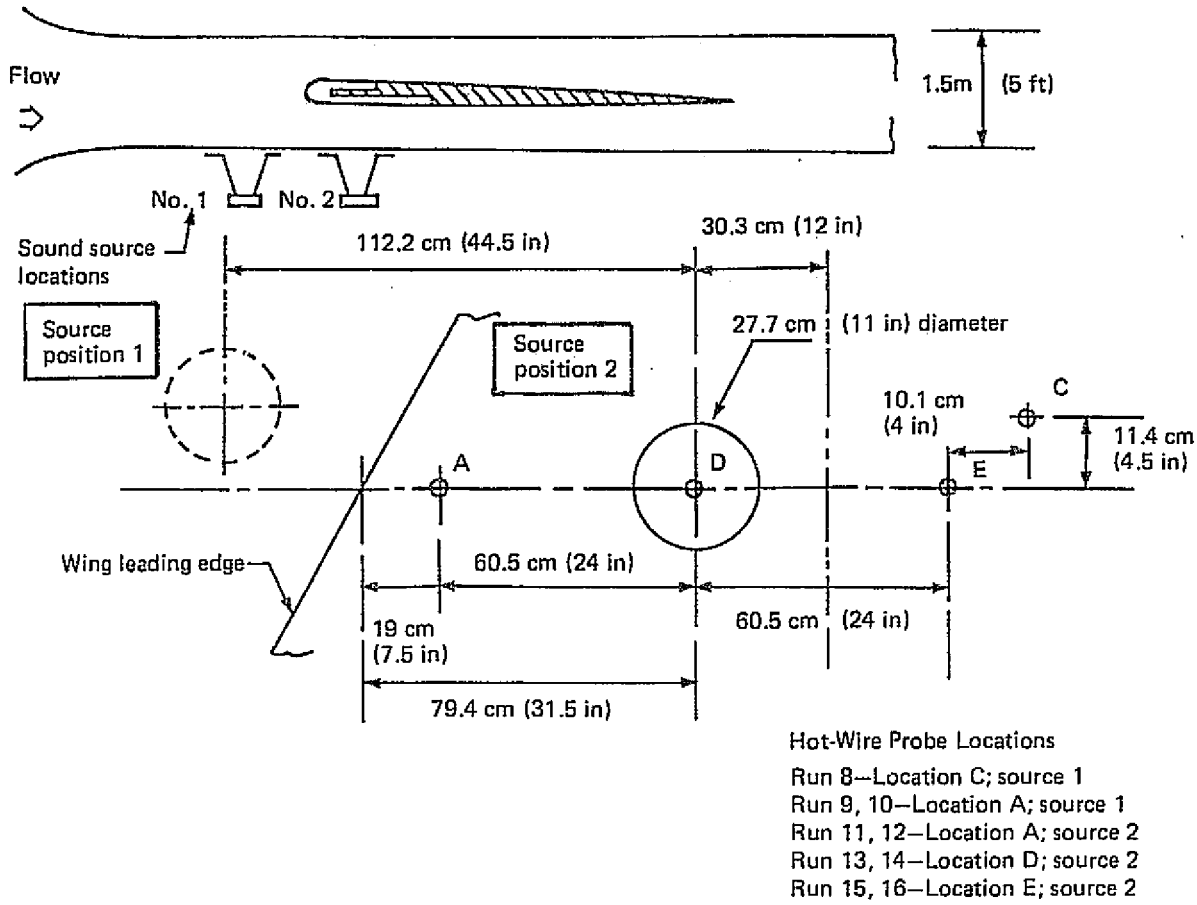

Figure 5.1-86. Hot-Wire Survey on Model

4.5 kHz range when only the residual sound fields are applied. When the suction rate is increased, however, these amplifications are substantially reduced or disappear, as seen in Figure 5.1-89. Similar amplifications occurred in several other tests, e.g., in Figure 5.1-92, where selective amplifications occurred in the region of 0.5 kHz as well as those in the 2.5 to 4.5 kHz region. In summary, these unidentified amplifications occurred in several frequency regions, are sensitive to the location inside the boundary layer and the chordwise location, and their amplitude is sensitive to the suction rate. It is unlikely that they are critical Tollmien-Schlichting amplifications because they are outside the expected frequency range for the tests. However, they could represent other unstable boundary layer disturbance modes.

Figure 5.1-89 shows the same type of test described previously repeated with an approximately 50% increase in suction rate. The results show a similar frequency sensitivity trend centered on 1.6 kHz maximum. The selective amplification effect in the 2.5 to 4 kHz frequency region in the noise generator residual spectrum of Figure 5.1-88 is not present in this case, which is attributed to the increased suction

Table 5.1-5. Wind Tunnel LFC Acoustical Test Program Summary

Run number	q lb/ft^2	Microphone location	Hotwire probe location	Description
1	50	Wall	—	* Exploratory acoustic survey (Vary SPL, spectrum, suction)
2	50	—	—	
3	35	Wall	—	Laminar flow transition
4	50	Wall	—	Frequency sensitivity
5	35/50	A	—	* Sound field survey on model (3 arrays of 3 microphones each and reference microphone on tunnel wall)
6	35/50	B	—	
7	35/50	C	—	Laminar flow transition
				Tunnel velocity variation
				Sound pressure sensitivity of LFC
8	35/50	—	C	* Hotwire velocity survey (two locations)
9	35/50	—	A	Laminar flow transition
10	35	—	A	Frequency sensitivity
				Relaminarization by increasing suction
11	35	—	A	**Hotwire velocity survey (two locations on model $\mathcal{C}_L$). new sound source location
12	35	—	A	
13	35	—	D	
14	35/50	—	D	
15	35	—	E	**Hotwire velocity and sound field survey on model $\mathcal{C}_L$. new sound source location
16	35	—	E	
17	50	—	E	
18	35/50	A,D,E	—	

* Sound source at position 1; reference microphone at position 1
**Sound source at position 2; reference microphone at position 2

rate. The results of Figures 5.1-88 and 5.1-89 are used to determine the critical fluctuating velocity amplitude and frequency, as explained in Figure 5.1-83.

Figures 5.1-90 and 5.1-91 show, at two tunnel velocities, a summary of LFC suction rates versus the incremental acoustic input intensity. The suction rates are those required to maintain a laminar boundary layer at conditions of intermittent threshold (minor bursts of turbulence at intervals of three to five seconds), and approximately fifty percent turbulent threshold (alternating turbulent and laminar flow at several seconds interval, observed on an oscilloscope). Velocity, u_M is calculated from the sound pressure measured at the model surface and the characteristic acoustic impedance, (i.e., $u_M = p_M/\rho a$) where p_M is the measured acoustic pressure.

The data were generated in the following manner: The tunnel was operated at constant stream velocity starting with a suction rate at the minimum level required to maintain a stable laminar flow. With the noise generator pressurized, but without a modulating

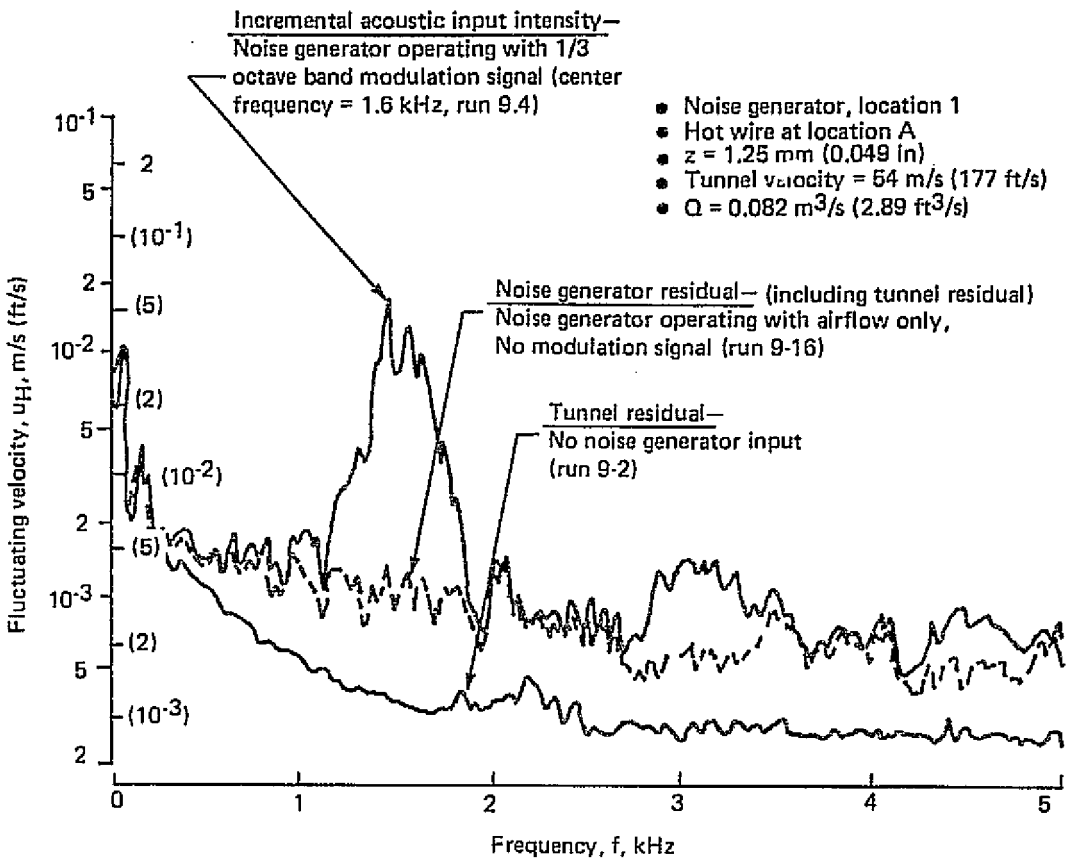

Figure 5.1-87. Hot-Wire Response Spectra—Three Basic Acoustic Conditions

signal (noise generator residual) the suction was increased until turbulence (as detected by the hot-film sensor at the trailing end of the suction surface) was reduced to occasional bursts. A one-third octave signal at 1.6 kHz center frequency was then added and the acoustic intensity increased (horizontal arrows) until turbulence bursts occupied 50% of the hot film monitor trace. Suction was increased again to the point where only occasional bursts occurred as indicated by the vertical arrows shown in Figures 5.1-90 and 5.1-91, and the above process was repeated until the entire curve was generated.

The tests demonstrated that an intermittent laminar boundary layer resulting from an external acoustical disturbance can be re-stabilized by increasing the suction rate. However, the magnitude of the additional suction rate needed to stabilize the boundary increases with the sound intensity. It may be inferred from the shape of the curves that a limit will eventually be reached where re-stabilization by increasing the suction rate cannot be achieved.

In another investigation, as shown in Figure 5.1-92, hot-wire spectra were measured at several heights above the suction surface (z = 1.25 to 12.5 mm), using an external noise input in the 1.6 kHz third-octave band at location A close to the leading edge.

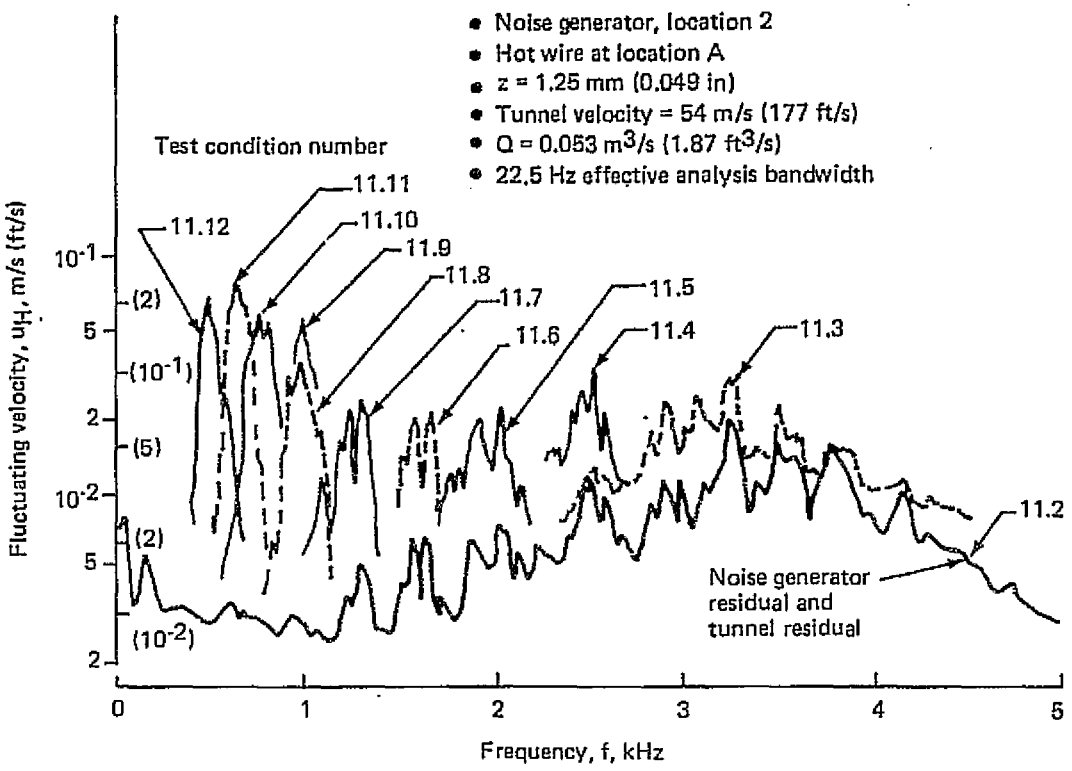

Figure 5.1-88. Hot-Wire Response Spectra at Transition Threshold Due to Applied Acoustic Signals of Various Frequencies –Q = 0.053 m^3/s

Results indicated that the fluctuating velocity due to the imposed acoustic signal did not vary appreciably in the laminar boundary layer profile. This result may be attributed to the fact that the profile was measured close to the leading edge where little amplification of induced disturbances would have occurred, so that the disturbance velocities were predominantly due to the acoustical input. A profile survey made further downstream, without an incremental acoustical disturbance present, revealed a substantial variation in fluctuating velocity profile, see Figure 5.1-93, and showed the largest disturbance amplification in the boundary to be close to the surface.

As in the case of the selective amplification at location A (near the leading edge), this phenomenon occurred only within the laminar boundary alyer, (z = 1.25 mm), at the condition of least laminar flow stability (minimum suction for laminar flow). A further example of selective amplification was observed at location E at frequencies between 0 and 1000 Hz. It existed over a broader range of suction values (Q = 0.065 to 0.147 m^3/sec) but was not evident at suction rates greater than Q = 0.147 m^3/sec; and again existed only within the laminar boundary layer, (z = 1.25 mm).

The relationship (i.e., transfer function) between the externally applied acoustic field and the induced fluctuating disturbance in the boundary layer was investigated by comparing the acoustic particle velocity, u_M derived from microphone measurements near the surface and the fluctuating velocity, u_H measured with the hot-wire in the

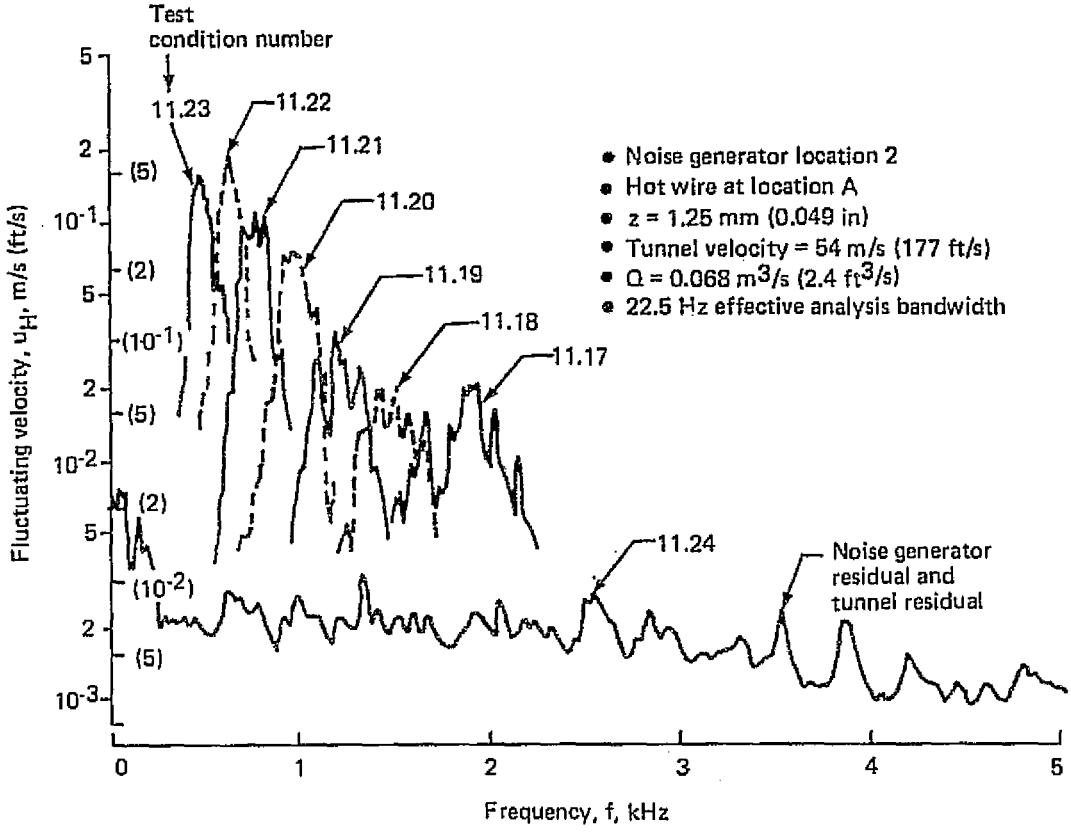

Figure 5.1-89. Hot-Wire Response Spectra at Transition Threshold Due to Applied Acoustic Signals of Various Frequencies –Q = 0.068 m^3/s

boundary layer. The transfer function can be used in conjunction with stability theory to calculate the fluctuating disturbance velocity induced in a boundary layer by a known external acoustic field, so that a preliminary estimate of the suction requirement to maintain stable laminar flow can be made. Alternatively, a transfer function can be used to estimate the permissible noise level outside a boundary layer when the allowable fluctuating velocity in the boundary layer is known.

Although it is recognized that the current tests can only provide limited insight into the energy transfer mechanism, typical results are presented in Figure 5.1-94. The acoustic particle velocity, u_M was calculated from the measured acoustic pressure by assuming the relationship, $p_M/u_M = \rho a$ using the characteristic impedance of sound in a free field. On this basis, the transfer function between the induced fluctuating velocity in the boundary layer to the external sound field velocity was found to be $u_H/u_M = 0.37$. Conversely, in order to obtain a transfer function of unity, a charac-

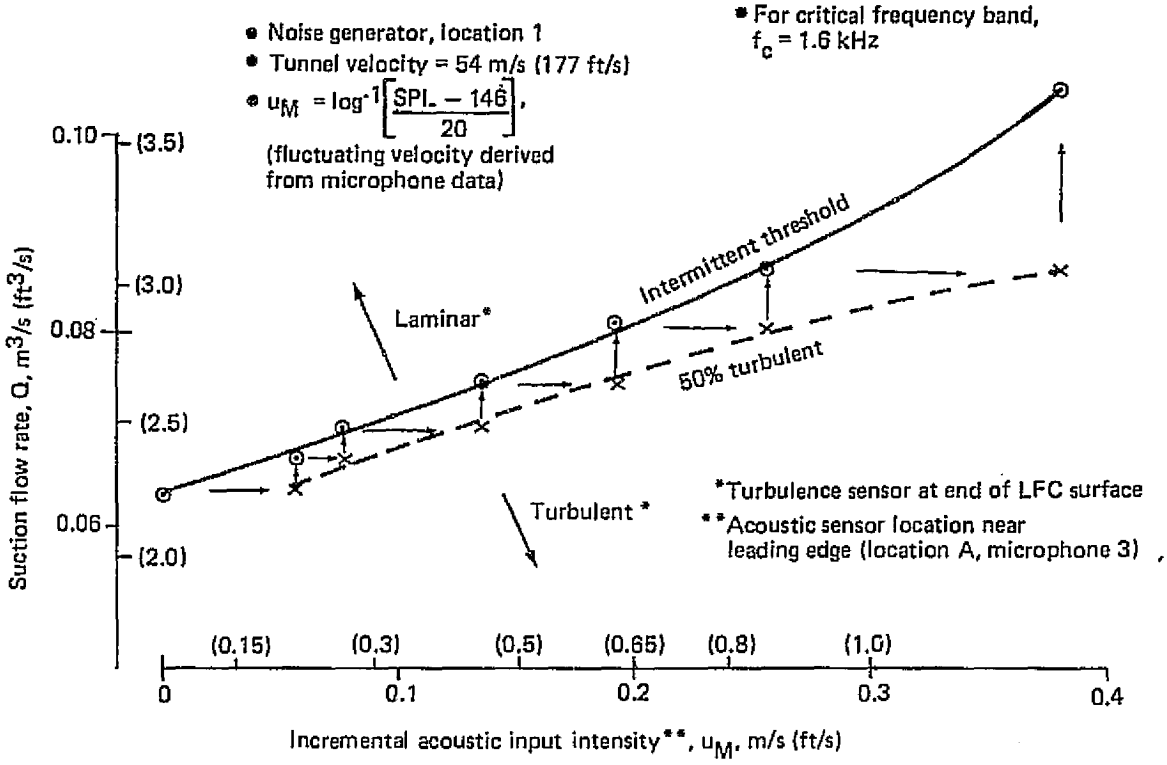

Figure 5.1-90. Suction Requirements Versus Incremental Acoustic Input Intensity —Tunnel Velocity = 54 m/s

teristic impedance of 2.7 ρa would be required (note, that near a hard surface, the characteristic impedance of sound may vary from 0 to ∞). Thus it is not unreasonable to expect the characteristic impedance to be substantially higher than 2.7 ρa since the response component of u_H would otherwise be zero (or less). It is apparent that much more data is necessary to establish the fundamental relationships involved in the energy transfer between an applied acoustic field and the vorticity mode associated with boundary layer instability.

Figure 5.1-95 shows critical velocity ratio values at a condition of stable transition threshold as a function of suction rate. These were calculated from hot-wire fluctuating velocities induced by sound in the critical third-octave band, i.e., 1.6 kHz center frequency in this case. The average suction rate used in the laminar flow aerodynamic studies was 0.07 m^3/s, which has a corresponding critical velocity ratio of 0.013. Critical velocity ratios were also calculated for cases with higher acoustic intensity levels, in which intermittent bursts of turbulence occurred at intervals of several seconds, which yielded values in the 0.03 to 0.05 range. The data in Figure 5.1-95 indicate that some level of critical velocity ratio occurs beyond which increasing the flow rate will not have a significant effect. This would pose a maximum limit to the permissible critical velocity ratio.

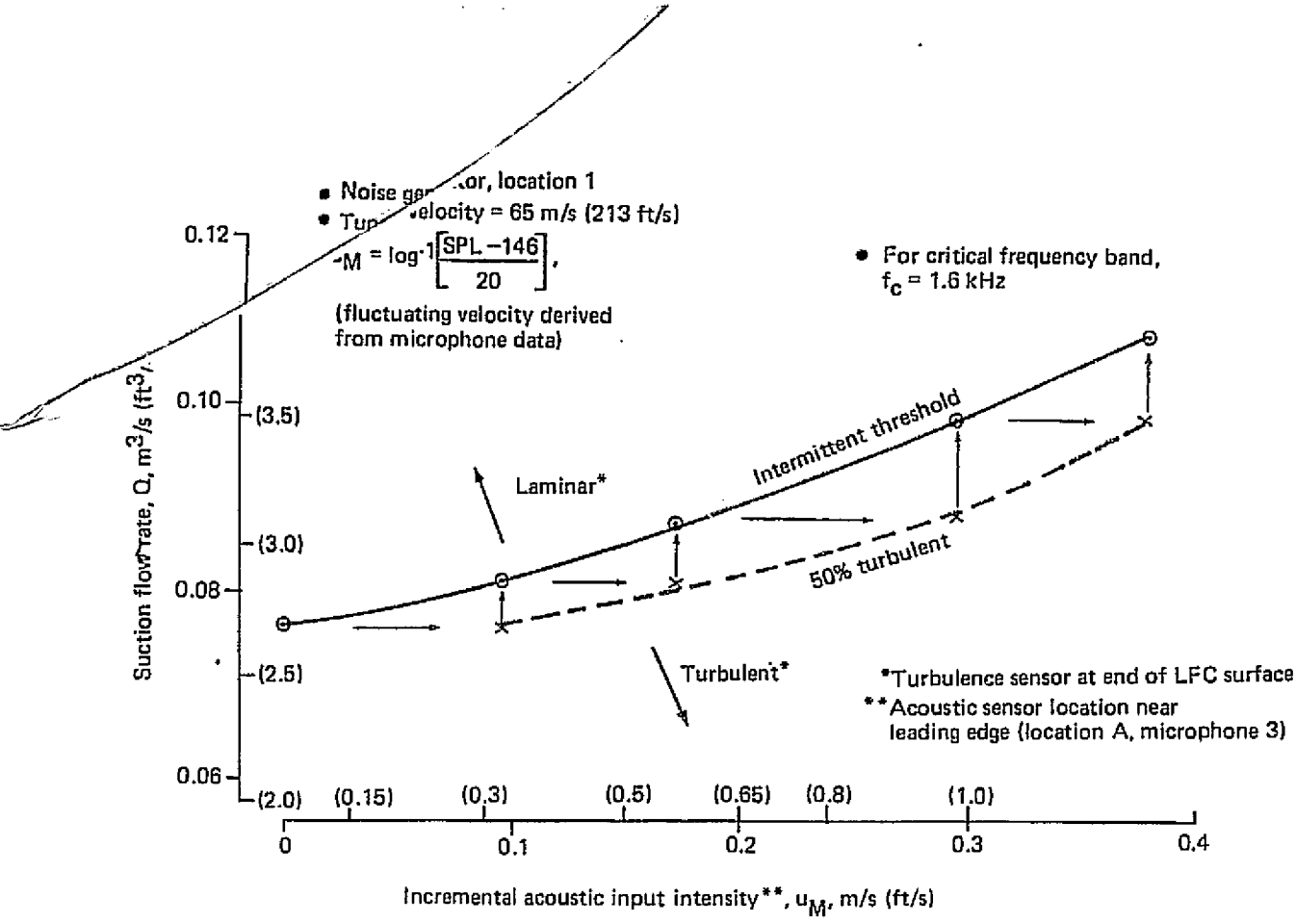

Figure 5.1-91. Suction Requirements Versus Incremental Acoustic Input Intensity —Tunnel Velocity = 65 m/s

(g) Conclusions

The following is a synopsis of the principal results obtained in the study.

1. The frequency sensitivity of a laminar boundary layer to acoustical disturbances was clearly established over a range of acoustic intensities and LFC suction rates, showing the existence of a minimum level of external acoustic intensity in a critical frequency range which will cause transition.

2. It was demonstrated that when an acoustical disturbance causes transition, increasing the suction rate will re-establish laminar flow. However, a further increase in sound intensity will again de-stabilize the flow, but laminar flow will be re-established by a further increase in suction rate. It is concluded, however, that a limit will probably be reached where re-stabilization by increasing the suction rate cannot be achieved.

3. Hot-wire measurements of fluctuating velocity due to an imposed acoustical disturbance, surveyed at several heights in a laminar boundary layer near the leading edge showed little variation in fluctuating velocity. However, a profile survey at a downstream location revealed a substantial variation in fluctuating velocity profile. It is concluded that the uniform profile near the leading edge

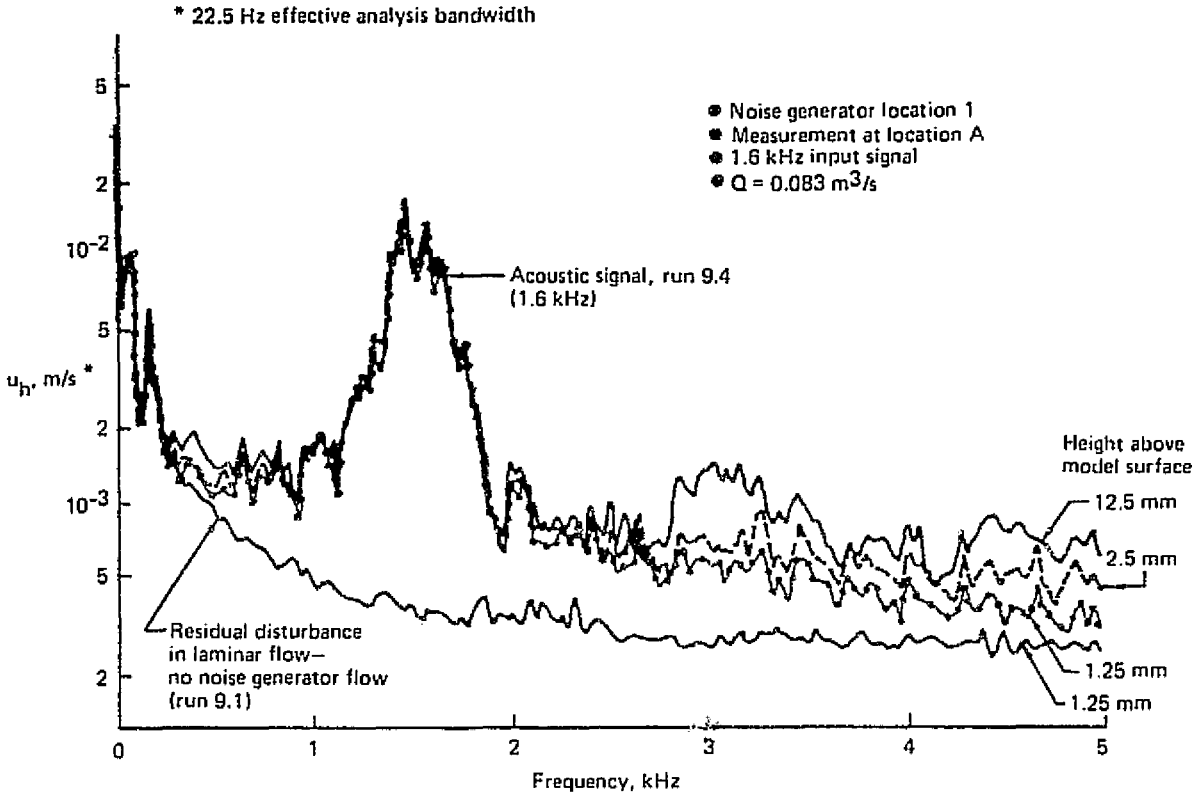

Figure 5.1-92. Hot Wire Profile Spectra at Various Heights Above LFC Surface

was due principally to the external acoustical disturbance, since little amplification of the induced disturbance is likely at this point. Conversely, the downstream profile reflects the presence of amplified disturbances in addition to the applied acoustic field.

4. It was noted in several tests that selective amplification phenomena were occurring in the boundary layer at frequencies above and below that of the applied acoustic field. These apparent amplifications occurred only at the location of measurement closest to the laminar flow surface (1.25 mm), and at the lowest suction rate possible to maintain laminar flow.

   Increased suction tended to eliminate these effects. The frequencies at which the apparent amplifications occurred differed widely for different chordwise locations of the measurements. Further analysis of this data is required to evaluate the relationship between these apparent amplification spectra, and the frequency spectra of critical incremental acoustic inputs.

5. The ratio of the fluctuating velocity in the laminar boundary layer to the derived acoustical particle velocity, (u_M/u_H) was found to be in the range of 0.25 to 0.40 in the most sensitive frequency region. Better definition of the transfer

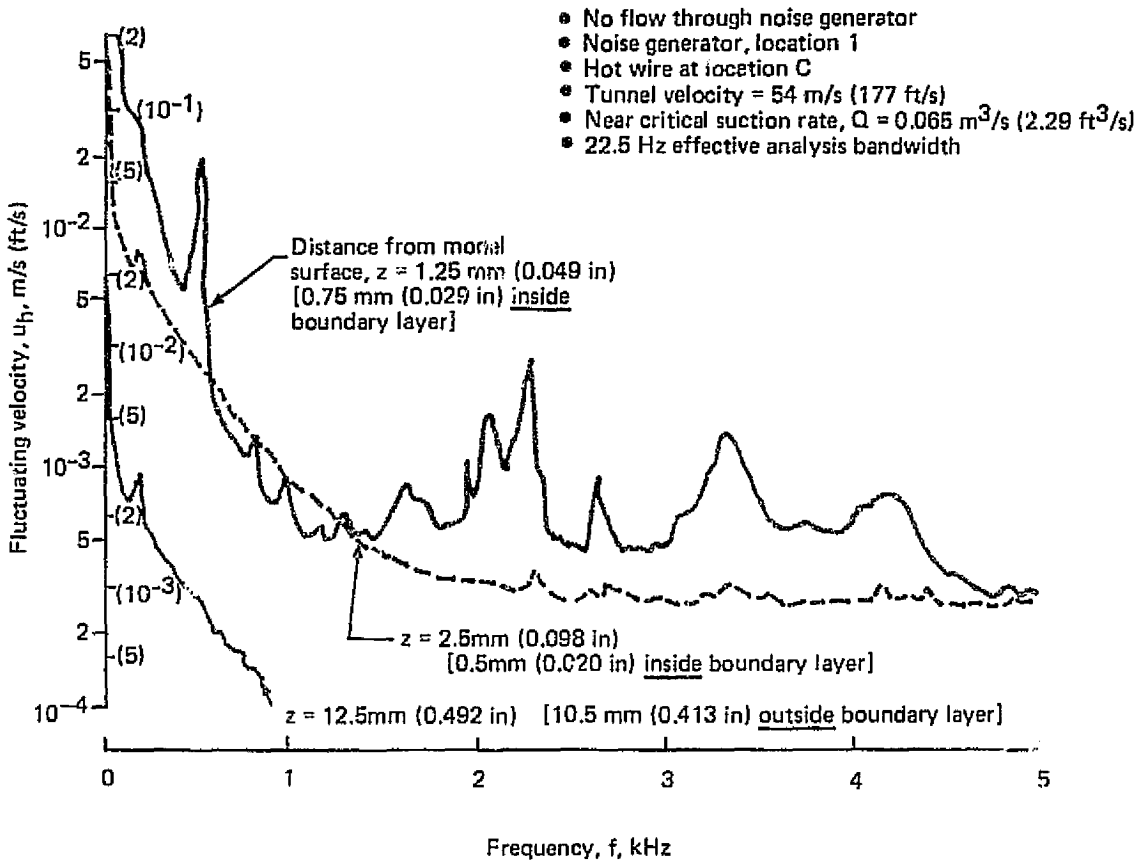

Figure 5.1-93. Hot-Wire Response Spectra at Locations In and Near the Laminar Boundary Layer

function requires the accumulation of more data and further analysis to establish this important relationship between the acoustical disturbance and the induced velocity fluctuations in the boundary layer.

6. Critical noise criteria at the most sensitive disturbance frequency have been developed from the test results, showing values of u_H/V_∞ between 0.010 to 0.015 depending upon suction rate at a condition of substantially laminar flow, near the transition threshold. Higher values (0.030 to 0.050) were noted for cases with intermittent bursts of turbulence. This tends to support the transition criteria used in the engine location study (see Figure 5.1-65). Critical velocity ratios will be higher for cases in which the acoustical disturbance spectra are composed of frequency components with energy predominantly outside the critical frequency range.

(h) Recommendations

The following suggestions are made for improving the test facility in order to investigate in further detail some of the results and trends found in the present exploratory

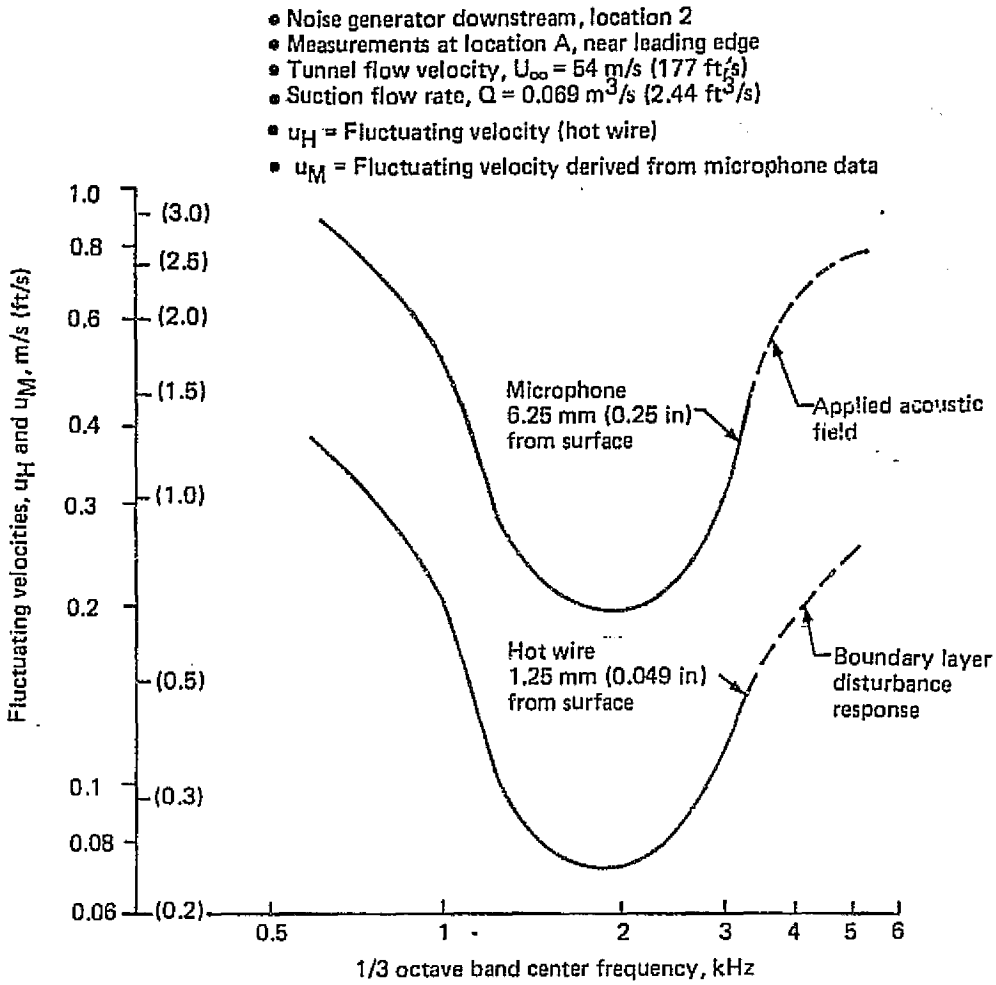

Figure 5.1-94. Critical Incremental Acoustical Velocities Versus Frequency— Hot-Wire and Microphone Sensors

study, to acquire better understanding of the physical phenomena, and to develop accurate design criteria.

1. The sound source used must provide sufficiently high acoustic intensity at frequencies well above the critical frequency in order to obtain better definition of the frequency response of a laminar boundary layer to an acoustical disturbance.

2. Modulated airflow sound generators, as used in the present test, are not considered suitable for narrowband frequency exploration. The airflow generates broadband noise which interferes with induced narrowband frequency modes.

3. The use of narrowband or discrete sound is recommended for identifying critical frequencies more accurately and for detailed exploration of boundary layer amplification of induced disturbance modes.

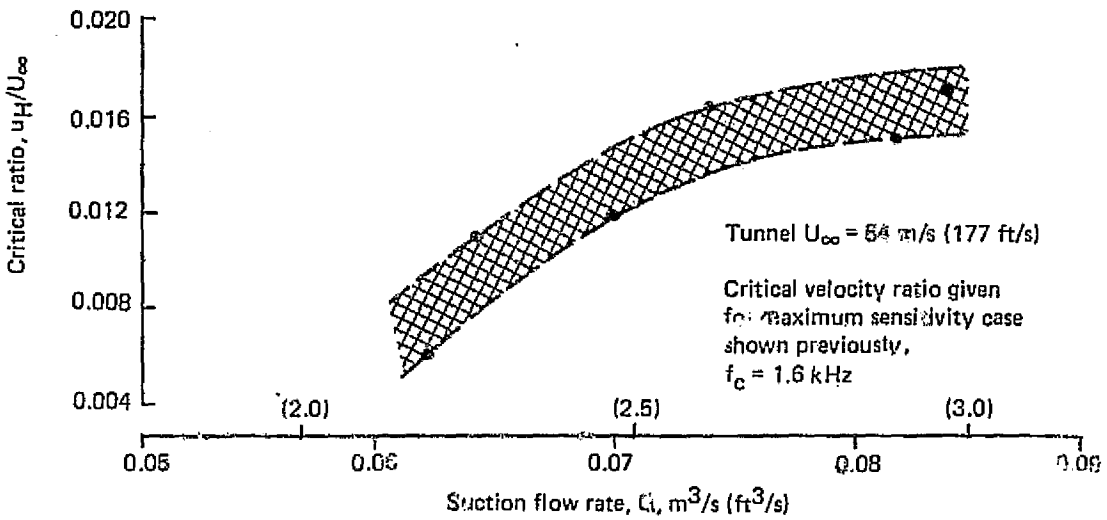

Figure 5.1-95. Variation of Critical Velocity Ratio With Suction Rate at Stable Transition Threshold

4. Acoustic reflections in the tunnel caused some ambiguity in interpretation of the data acquired. Although this effect was not a serious handicap when using a third-octave band sound source, acoustical reflections would pose a serious problem in the case of narrowband acoustic excitation. It is therefore highly recommended that more detailed studies should be conducted in an acoustically treated tunnel.

5. The use of a remote control traversing mechanism for both acoustical and hot-wire measurements would greatly improve data acquisition capability by minimizing the necessity of wind tunnel shut down to relocate instrumentation.

6. A substantial improvement in data management would be achieved by using computer techniques for reducing and plotting test results.

5.1.8.3 Suction System Laboratory Tests

The X-21A suction slot geometry concept does not allow for flow adjustment after installation and does not permit access to the internal duct system for inspection and repair. To use this concept on a commercial airplane, it is necessary to find a means to facilitate a one-time, as-installed adjustment capability to the suction system flow field area and to allow repair of potential internal duct problems. Studies to accomplish the required capability have identified several candidate geometries. However, before any of these candidates can be considered, their flow characteristics must be determined. This requirement results from previous Northrop work that showed that suction slot velocity fluctuations caused by internal flow disturbances could propagate back through the slot and cause premature transition of the boundary layer (Ref. 16). The candidate suction slot geometries differ considerably from the X-21A geometry and their internal flow characteristics are critical to slot flow stability. Therefore, it was decided that the flow characteristics would be evaluated by test.

Northrop had conducted a test evaluation of the X-21A slot/plenum/bleed hole arrangement to determine the effects of slot width and depth, plenum width and depth, and bleed hole arrangement on suction slot stability (Ref. 16). The parameters identified as critical to the test evaluation were slot velocity fluctuation with respect to average slot velocity and spanwise velocity gradients along the slot. Hot-wire anemometers were used to measure these parameters.

The candidate suction slot geometries were evaluated using a test setup similar to Northrop's. Modifications were made to the basic test setup to allow for continuous evaluation of the spanwise slot flow characteristics. The test hardware is shown on Figure 5.1-96. The detailed internal arrangement is shown on Figure 5.1-97.

Three basic slot configurations were tested. These consisted of a slot-plenum (3 bleed-hole variations), porous aluminum plenum (one density-one porosity) and the X-21A slot

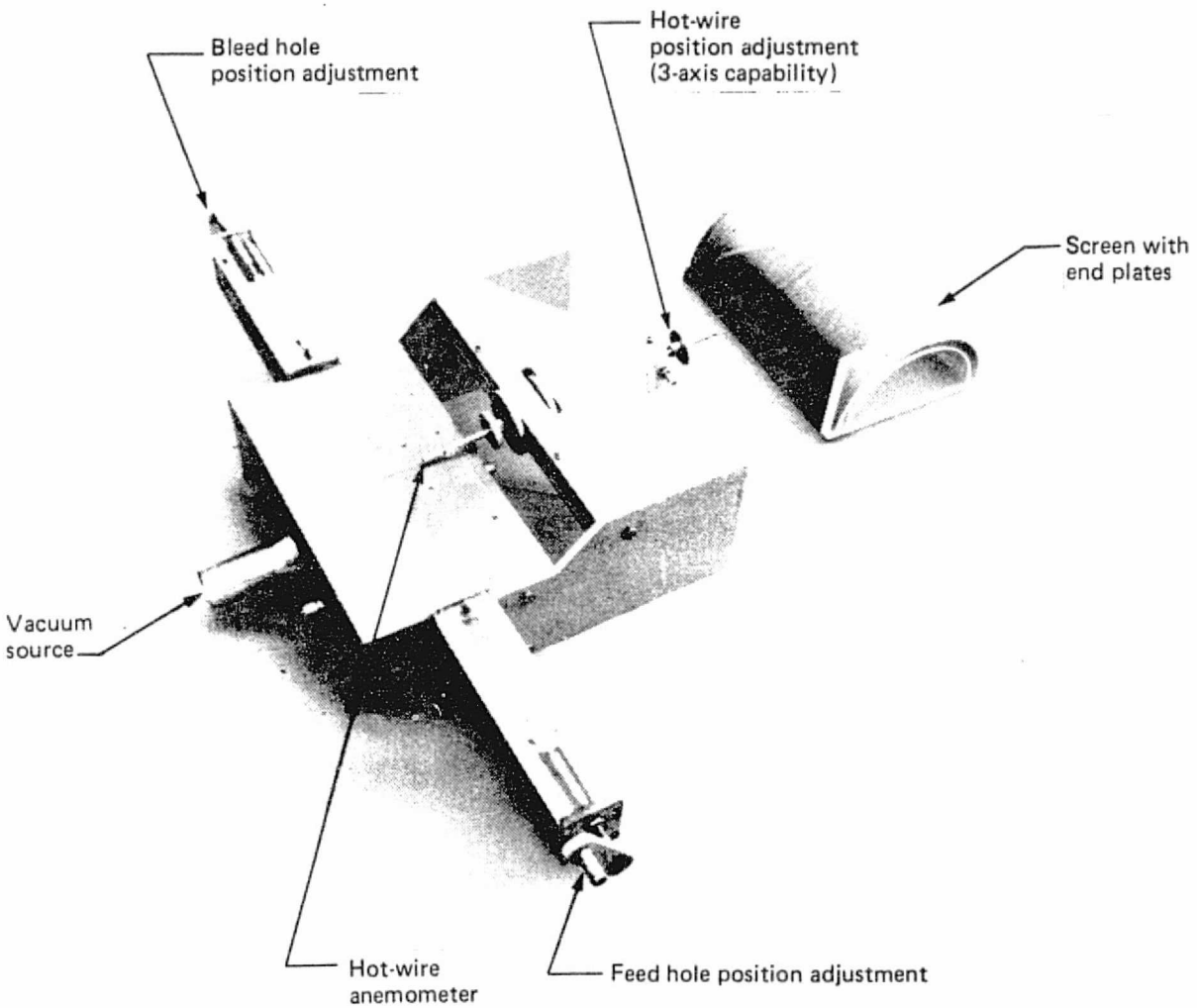

Figure 5.1-96. Suction Slot Geometry Laboratory Test Hardware

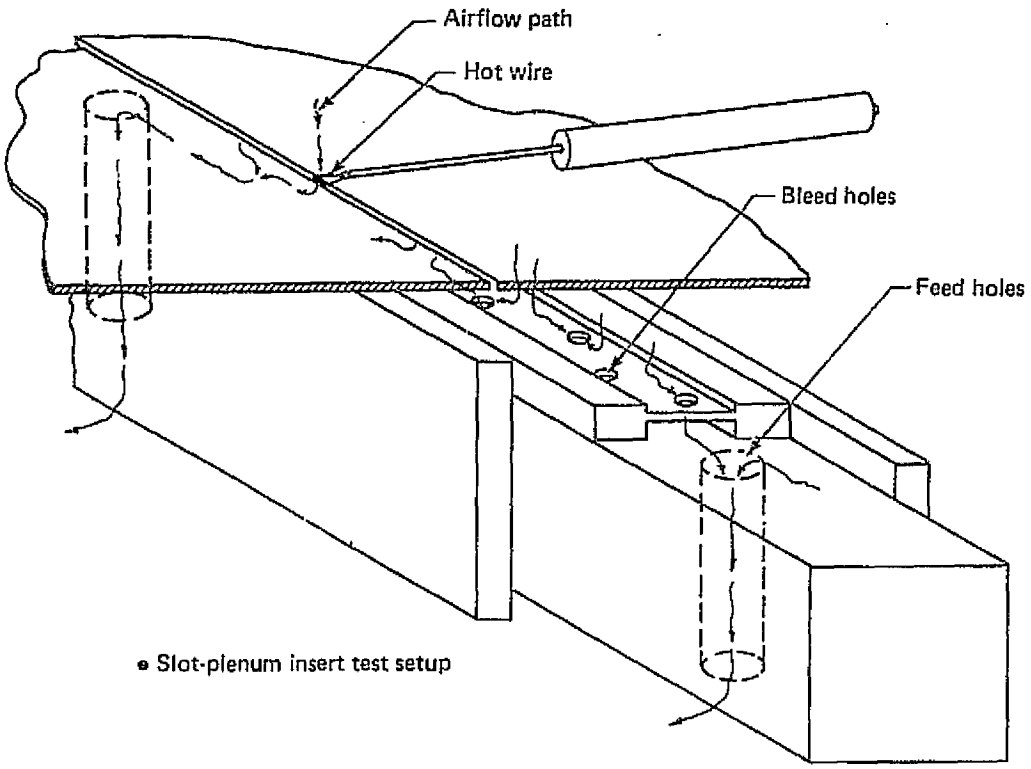

Figure 5.1-97. Test Hardware Arrangement for Slot-Plenum Evaluation

plenum (2 slot widths). The configuration arrangements are shown on Figure 5.1-98. The slot-plenums utilized a bleed-hole insert to provide a throttling pressure drop for flow control. With porous aluminum inserts the control function could be accomplished through variations in aluminum porosity. The X-21A slot plenum represented the configuration upstream of the tributary duct flow control adjustment. The test results are summarized on Figure 5.1-99, 5.1-100 and 5.1-101. A complete description and discussion of the flow evaluation test results is provided in Reference 19.

A supplemental test was conducted to determine the clogging characteristics of the porous aluminum plenum configuration. Procedures used were similar to those used under a previously conducted study (Ref. 20) except that the altitude effects were not evaluated. The test results showed that the porous aluminum clogged severely over a 34 day (approximately 2-year service equivalent time) continuous suction test at a representative operating slot Reynolds number of $Re_s = 150$.

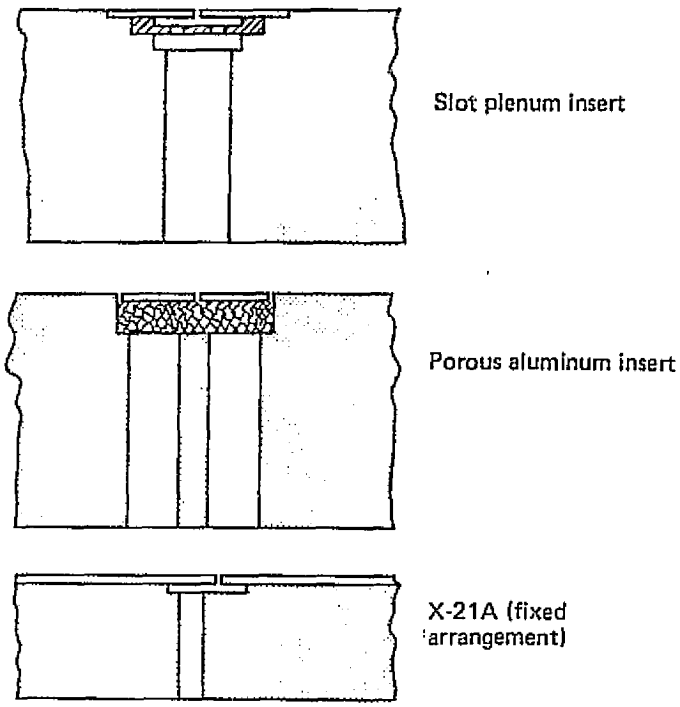

Figure 5.1-98. Slot-Insert Designs Tested

The conclusions from the test results are summarized as follows:

- All test configurations showed slot velocity fluctuations considerably less than those of the X-21 over the range of Reynolds numbers that would be used for airplane suction system design.
- Velocity variation along the slot would be within the recommended ±1.5 percent of maximum velocity gradient for all configurations except porous aluminum.
- The slot-plenum configuration bleed-holes can be used for slot airflow balancing.
- The use of porous aluminum in the slot plenums is unacceptable because of severe spanwise slot velocity gradients and excessive clogging characteristics.

Configuration	Bleed hole diameter mm (in)	Bleed hole area (% of basic)	Velocity variation along slot (Re_s = 150) (% of average)
Slot plenum 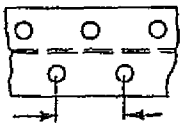 Basic config + Mod D 7.950 mm (0.313 in)	1.588 (0.0625)	100	±1.5
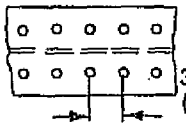 Mod E 3.96 mm (0.157 in)	0.794 (0.0313)	50	±1.3
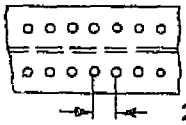 Mod F Mod G 2.007 mm (0.079 in)	0.338 (0.0133)	18	±1.0
	0.795 (0.0318)	100	±0.6
Porous aluminum 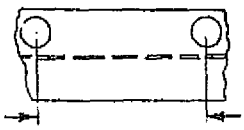 19.05 mm (0.75 in)	3.175 (0.125)	57	±7.5
X-21A 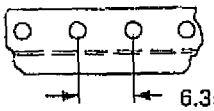 6.35 mm (0.25 in)	1.588 (0.0625)	63	±1.0

Figure 5.1-99. Comparison of Suction Strip Velocity Variation Along the Slot

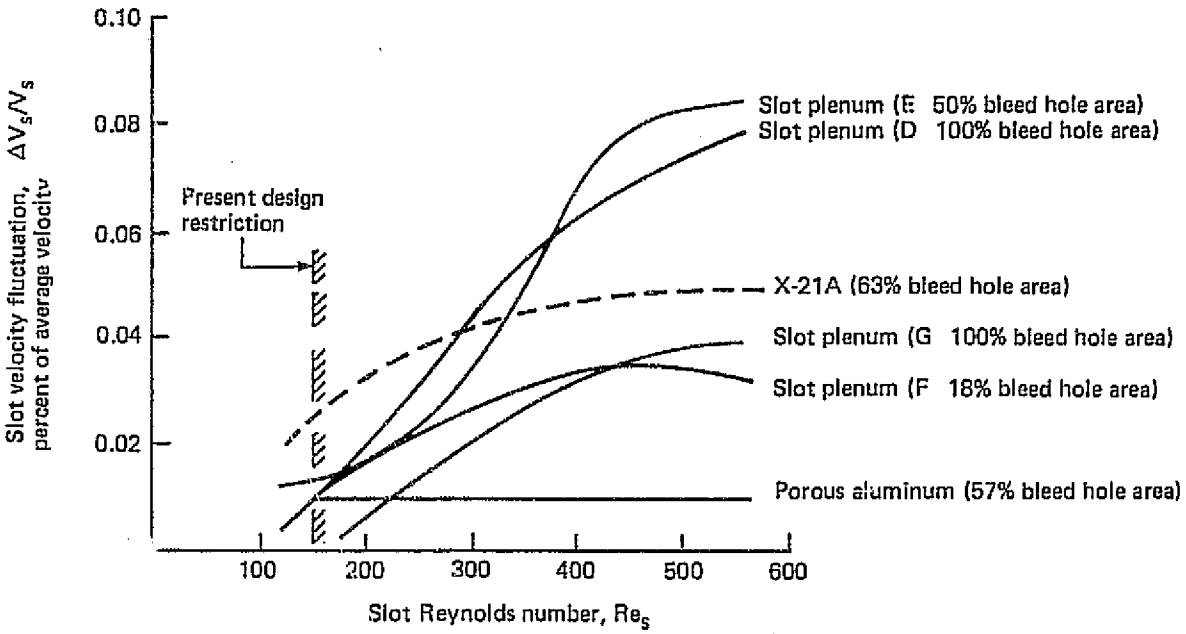

Figure 5.1-100. Suction Strip Slot Velocity Fluctuation Comparison

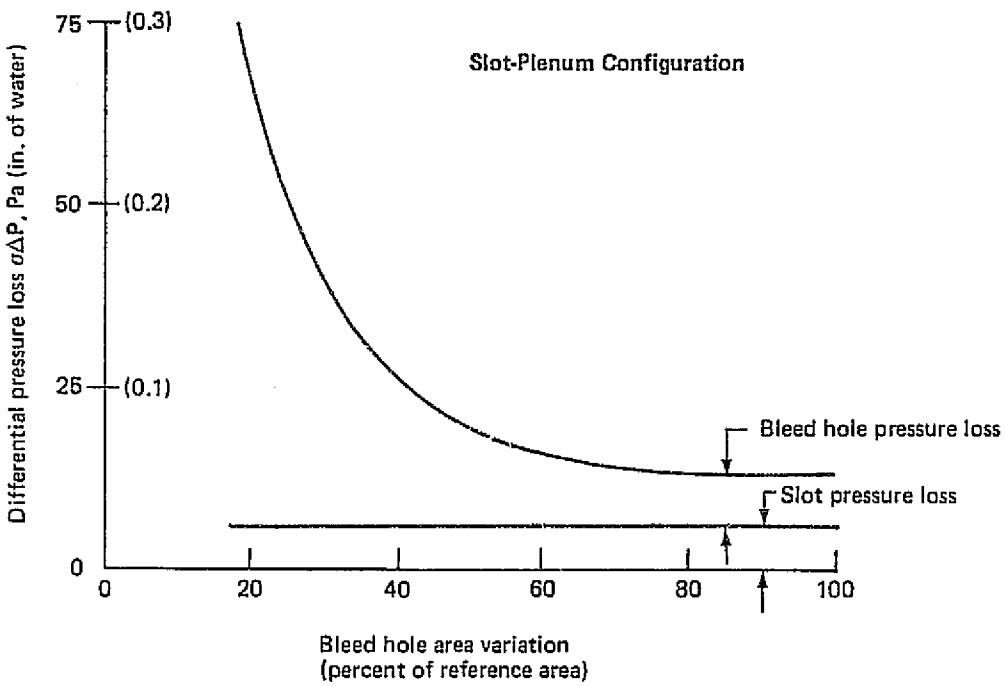

- Reference Reynolds number, $Re_s = 150$
- $\sigma = 1$ at standard sea level pressure and temperature. To correct for local pressures and temperatures use $\sigma = 2.84 \times 10^{-3}$ P/T where P = local pressure N/m^2 (psia), T = local temperature, °C (°R)

Figure 5.1-101. Slot-Plenum Insert Pressure-Loss Characteristics

5.2 STRUCTURES AND MATERIALS

Structures and Materials tasks were arranged to carry out a systematic evaluation of the structural design, materials selection and manufacturing alternatives in order to arrive at a viable LFC wing and empennage design. Many alternate design concepts using combinations of materials appropriate to each were developed and evaluated before arriving at the most promising design for application to an LFC transport in the 1990 time period.

For the final concept, a conventional structure with a fiberglass cover was selected. The cover incorporates suction slots (slot-plenum insert) and chordwise ducting to distribute suction airflow to spanwise trunk ducts. This concept permitted the selection of the most efficient structure and minimized parasitic weight. Stringer size, spacing and orientation are not affected by slot spacing and duct sizes. Fabrication costs of the wing box are reduced due to insensitivity of the basic structure to surface tolerance requirements for LFC. Tolerance buildup is avoided by machining the bonding surface prior to bonding on the prefabricated fiberglass cover. Other structural concepts or materials could be substituted whenever fabrication techniques or materials development warrant. As a result, a relatively low cost validator airplane could be constructed immediately without depending on or waiting for further advances in construction techniques or materials.

The concept development and evaluation activities leading to the above selection are discussed in the remainder of this section.

5.2.1 DESIGN REQUIREMENTS AND OBJECTIVES

The overall requirement of the structural design was to create a practical wing capable of maintaining laminar flow within the projected FAA and Boeing requirements for production commercial transport airplanes and the Aerodynamic requirements discussed in Subsection 5.1.1.

The major design objectives for this study were as follows:

1. Minimizing Weight: The weight of the LFC wing and the system weight must be kept to a minimum to prevent the added weight from offsetting the basic performance gains associated with the reduced wing drag.

2. Production Cost: The production costs must be kept to a minimum. The increase in production costs must be substantially below the decrease in operational costs derived from the fuel savings.

3. Maintenance Cost: Airplane inspection and maintenance costs also must be kept to a minimum in order to retain the operational cost benefits derived from fuel savings.

4. Crew Work Load: The structural concept should be configured to produce a self-balancing system. Control and operation of the system should not produce an appreciable increase in crew workload.

The above objectives are not totally independent of each other. In most designs a strict adherence to one jeopardizes another. The principles associated with the above must all be carefully applied, evaluated and traded to arrive at the most practical balance for each structural design. Since actual dollar values could not be assigned to represent the degree to which objectives 2, 3 and 4 were met, relative ratings for each competing design were determined on a judgmental basis largely by assigning relative complexities.

5.2.2 STRUCTURAL CONCEPT AND MATERIALS DEVELOPMENT

The Boeing Company has from time-to-time conducted research studies of LFC airplanes. These studies include NASA and Air Force contracts as well as Independent Research and Development (IR&D). An in-house study underway at the onset of this program had examined two types of structural concept; a removable glove and one with separate ducts.

Several attempts were made to design a rational removable glove arrangement. The very critical surface smoothness requirement for LFC created severe problems at joints and attachment areas. Removable fasteners require clearance holes and this in turn would result in some relative movement between the wing box and the glove. This movement would be expected to open and close gaps between the glove segments and tend to cause transition in the boundary layer. Since no satisfactory solutions were found for this and all the associated problems, the separate duct concept appeared more promising. Therefore, work on the removable glove concept was stopped.

The separate duct concept is illustrated in Figure 5.2-1. It used sandwich construction with laminated skins and spanwise tributary ducts buried in the core. Chordwise collector ducts,

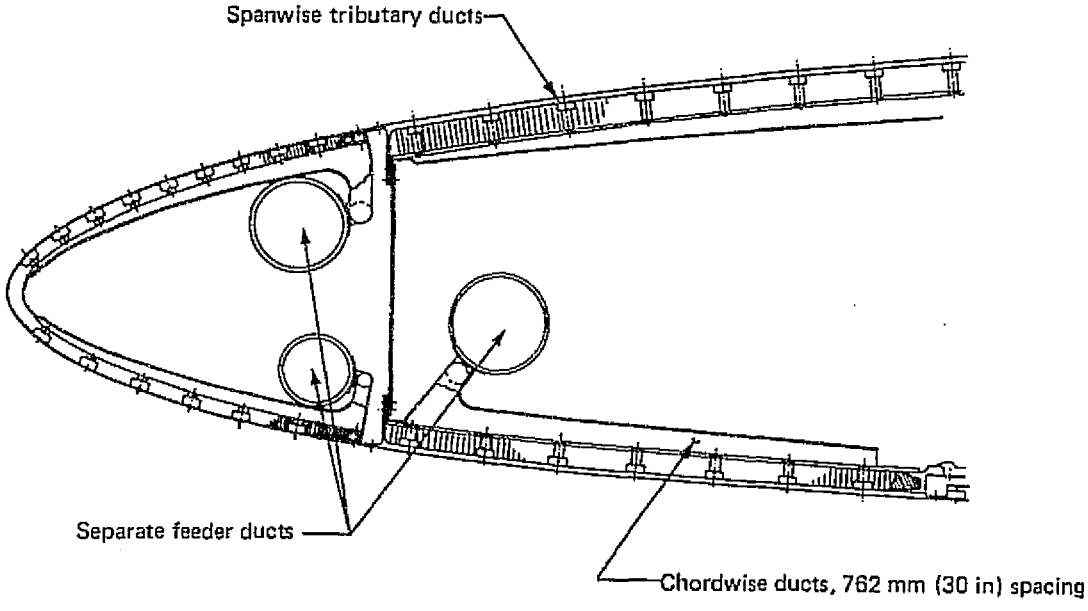

Figure 5.2-1. Initial Structural Concept—Separate Ducts

spaced at .762 m (30 in), were located inside the wing to collect air from the spanwise tributary ducts embedded in the sandwich skin panels. Spanwise feeder ducts, also located within the wing envelope were used to route air collected from the chordwise ducts to the suction units. This concept was under development at the beginning of this program and was the initial study configuration. After a period of development, the separate duct concept was found undesirable for several reasons: 1) Weight of ducts, 2) Sealing of suction ducts inside the fuel tanks, and 3) Structural compromises to allow large ducts to pierce the wing primary structure. All proved to be major stumbling blocks and the concept was dropped.

The concept development activity accomplished during the contract took place in two major phases; the exploration phase and the development phase. These phases were sequential and each lasted about a year. Wing geometry, suction requirements and structural loading play major roles in determining the workability at each concept. These parameters are different at all locations on the wing but the structural concept and materials used must generally be the same throughout a wing surface. However, a material and arrangement combination established as most desirable for a given wing at one particular location may be quite different at another location. Thus it became apparent that concept application to the complete wing of the baseline airplane was necessary for evaluation.

Development in the structures area took place simultaneously with aerodynamic development of the wing geometry (see Subsection 5.1.2). However, it was necessary to use the same wing and design ground rules on all candidate structural concepts in order to provide a rational comparison. Therefore appropriate wing geometries were chosen at different stages of the study corresponding to the then-current state of development. The wing used during the exploration phase had a quarter chord sweep of 25°, incorporated an advanced airfoil and had an area of 339 m^2 (3650 ft^2). The development phase took place approximately a year later and utilized the wing most current at its onset. This wing had the same area but the wing quarter chord sweep was changed to 15° and the cross section and the spanwise variation of wing thickness to chord length (t/c) were updated as discussed in Section 5.1.

5.2.2.1 Exploration Phase

The exploration phase began with a screening of a very broad group of materials and conceptual ideas.

The following concepts survived this screening and were developed further:

- Laminated Aluminum (Figures 5.2-2, 5.2-3 and 5.2-4)
- Laminated Titanium (Figure 5.2-11)
- SPF/DB Titanium (Figures 5.2-13 and 5.2-14)
- Graphite/Epoxy (Figures 5.2-15 and 5.2-16)
- Graphite/Epoxy Titanium Hybrid (Figure 5.2-17)

In order to provide a point of reference, a conventional turbulent wing with standard skin stringer construction was developed and weighed. The reference wing and all of the above candidates were developed with the same ground rules, design conditions, box geometry and technology level.

(a) Laminated Aluminum Concept

This concept incorporates spanwise ducting into the core area of the sandwich panels. Suction slots and ducts follow constant chord lines and sandwich thickness increases toward the wing root as the airflow requirements increase. The face sheets consist of multiple layers of 0.51 mm (.020 in) thick aluminum. Two major advantages are provided by the "Laminated" skins. First, each lamina will drape form over the mold to the required shape thereby eliminating the necessity of more costly fabrication procedures. Second, structural fail-safety has been achieved by using relatively narrow width pieces of aluminum and appropriately staggering the butt splices chordwise to provide many edges to stop crack progression. This concept eliminates the usual spanwise splices with the multitude of exterior flush fasteners. The shear material, ribs and secondary structure weights were not significantly different from those of a turbulent wing. Total wing weight increased by 9% over the reference turbulent wing. This increase was due to the use of honeycomb structure, and the incorporation of suction slots and ducts into the honeycomb panels.

The initial design of this concept, as shown in Figure 5.2-2, was dropped because of manufacturing difficulties. The revised concept as shown in Figure 5.2-3 resulted in fewer manufacturing problems but added weight. This approach uses a dense honeycomb core at the duct boundary to provide the necessary structural integrity and

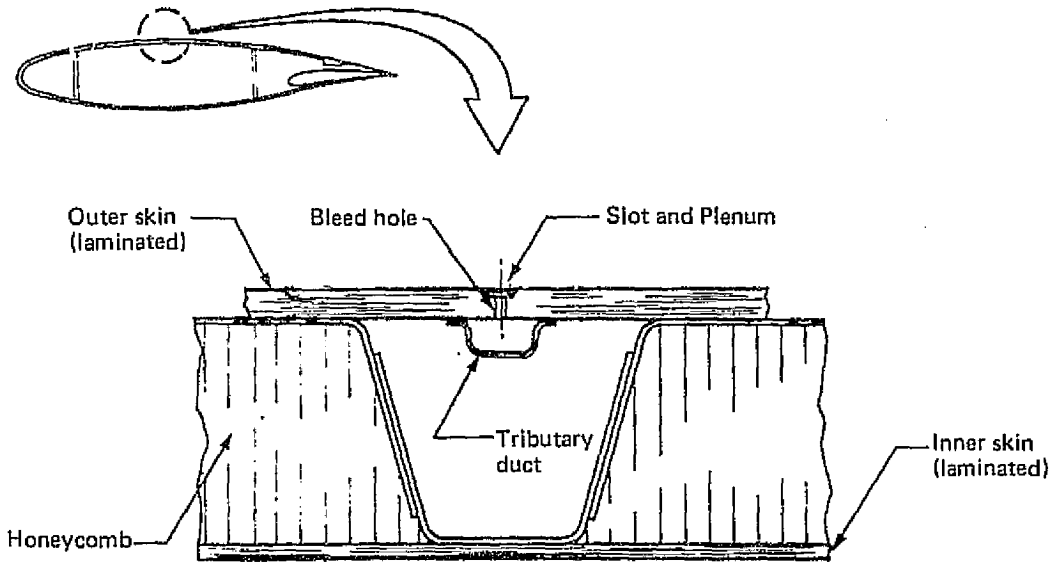

Figure 5.2-2. Initial Laminated Aluminum Concept

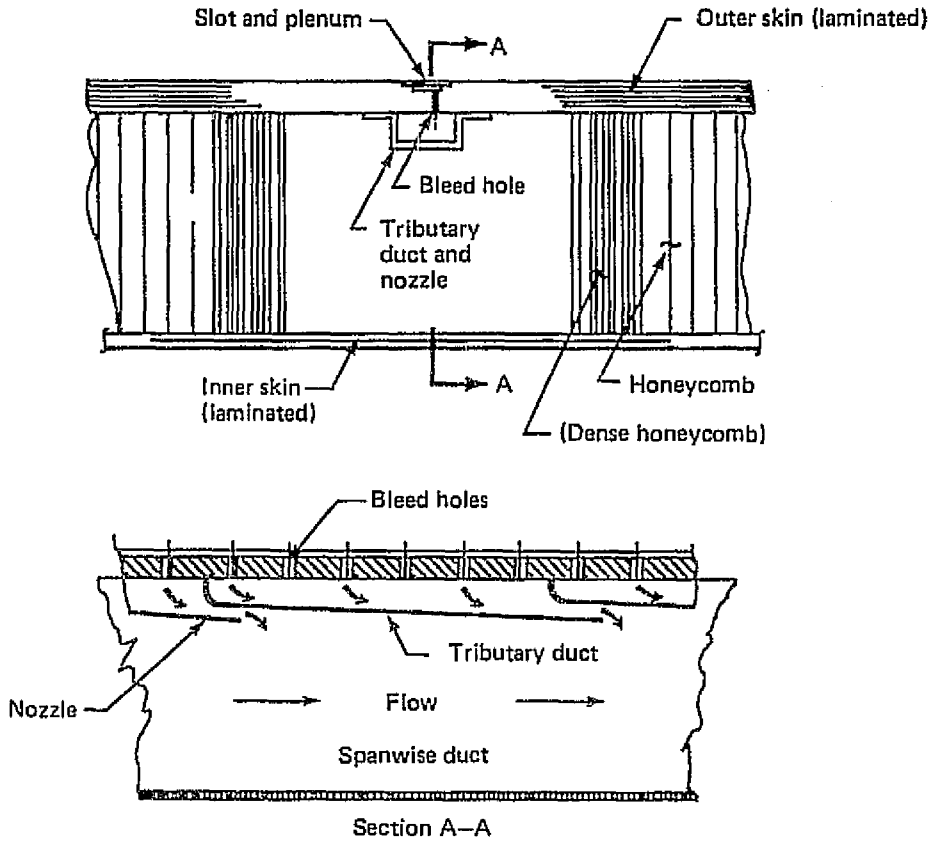

Figure 5.2-3. Revised Laminated Aluminum Concept—Tributary Duct Diagram

improve manufacturability. The spanwise ducts are integrated into the honeycomb core with 6.35 mm (.25 in) wide strips of dense core forming the walls of the duct. The initial laminated aluminum designs had tributary ducts bonded to the inner face of the outer skin. The tributary ducts helped to throttle and control the direction of the sucked air. The tributary ducts were a cost problem since there would be over 6000 per airplane; also, there appeared to be no reasonable method of replacing one in the event that it became disbonded. For these reasons the tributary duct was omitted from further designs and the required throttling was provided in the suction surface. The resultant concept, as shown in Figure 5.2-4 had an increase in bending material weight of 7.5% over the initial laminated aluminum honeycomb design. The increase in total wing weight over the reference turbulent wing was 14%. Based on the results of work done during the exploration phase, this version of the laminated aluminum honeycomb concept was selected for the baseline airplane and used as a reference during the development studies.

A typical side of body joint, as shown in Figure 5.2-5 requires that the ducts be vented into a dry bay. The inner skin is cut away locally and the material is replaced by bonding a fitting into the honeycomb panel. This fitting in effect turns the panel at the side of body joint into a skin-stringer configuration thus allowing the wing center section to be low cost conventional skin-stringer design. Details of spars and

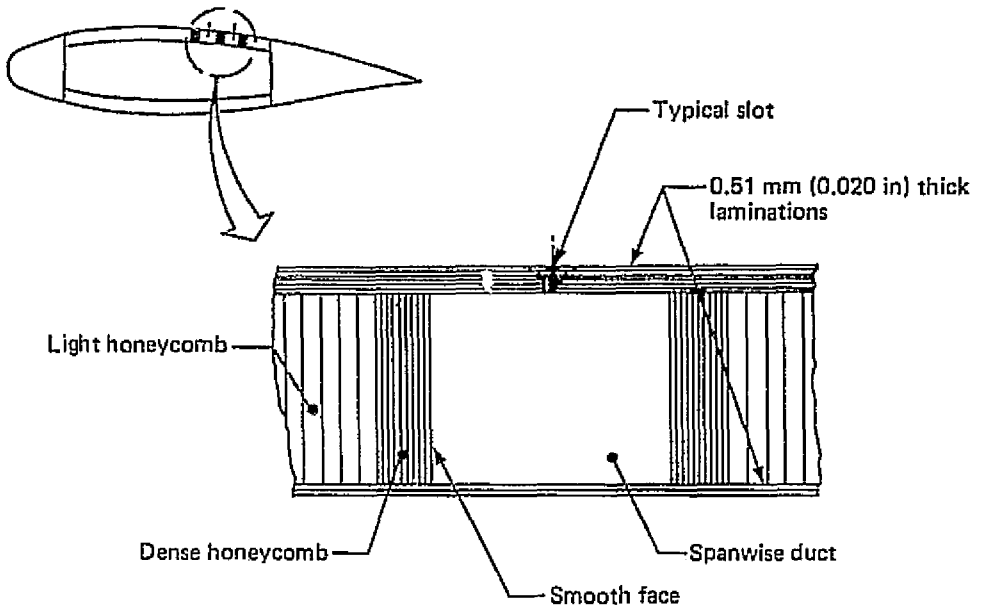

Figure 5.2-4. Laminated Aluminum Concept—Revised Core

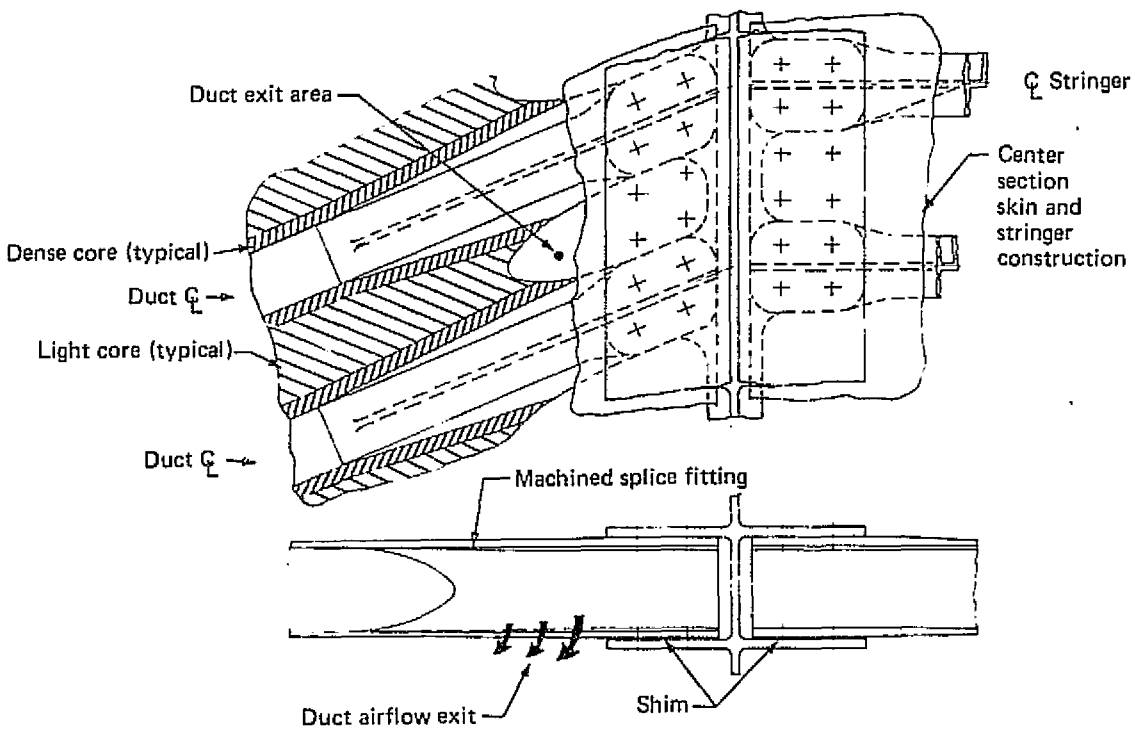

Figure 5.2-5. Laminated Aluminum Concept—Side of Body Joint

leading edge structure are shown in Figure 5.2-6. External joints are kept to a minimum in this design, but joints are still required. Joints at the leading edge must be very smooth and Figure 5.2-7 shows a method of obtaining that smoothness. The outer skins are milled down approximately .38 mm (.015 in) along the joint and the fasteners are slightly overcountersunk. After fastener installation, a cover strip .254 mm (.010 in) is bonded into the milled groove to provide a smooth surface.

Accessibility is a problem with all LFC designs. Figure 5.2-8 shows the access plan for the 25° swept wing. Removable external panels interrupt the suction slots, and make it very difficult to guarantee adequate smoothness. The approach taken was to minimize the number of external access doors in the wing box by providing entry into the fuel tank through the rear spar. Where the spar is not deep enough to accommodate an access door, the doors are located in the lower panel as near the rear spar as possible. No method was established that would allow laminarization across the access holes with this concept, therefore the external access holes reduce the laminarized area. The 15° sweep wing that was examined during the development phase (see Figure 5.2-9) lost even more laminarized area because it was a thinner wing and therefore more access holes were required in the lower surface.

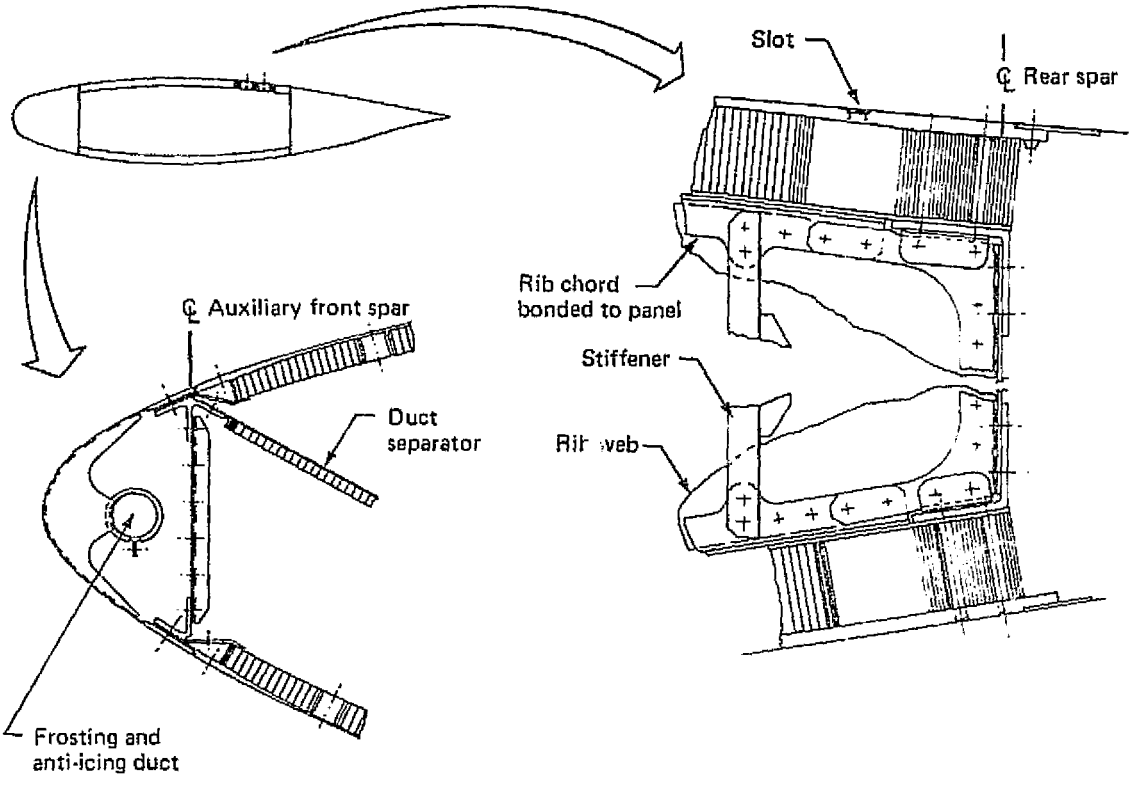

Figure 5.2-6. Laminated Aluminum Concept—Assembly Details

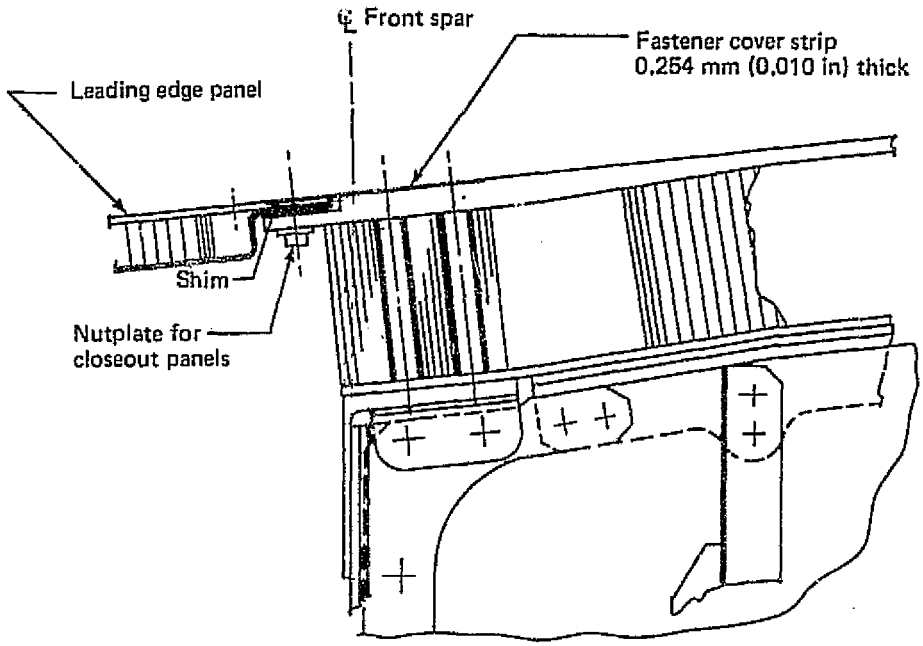

Figure 5.2-7. Fastener Installation for Skin Smoothness

A major problem with the laminated aluminum concept was not apparent until several slot-spacing and duct-sizing studies had been completed. Aft of 55% chord on the upper surface and 60% chord on the lower surface the slot spacing became very close and the duct area increased to the point where the honeycomb sandwich design was no longer practical. This problem is illustrated by Figure 5.2-10. Another problem was the number of skin laminations. High aspect ratio, thin wings have relatively high end load in the surfaces due to wing bending. The number of layers of the .51 mm (.020 in) aluminum laminae required to adequately react this load became unreasonable when viewed from the standpoint of inspection. Not only is it difficult to verify structural adequacy during fabrication but inspection for cracks, disbonds, etc. during routine inspections is much more complex. A potential resolution of this problem is to use fewer but thicker layers as discussed in Paragraph 5.2.2.2.

(b) Laminated Titanium Concept

This design, shown in Figure 5.2-11, is similar to the initial laminated aluminum design shown in Figure 5.2-2. Laminae thickness was selected as .25mm (.010 in.) on the assumption that this thickness could be drape-formed in a manner comparable to the .51 mm (.020 in) aluminum. The major advantage which prompted studying this concept is the superior properties of titanium in resisting corrosion and erosion.

Changing from aluminum to titanium did not change the duct sizes. As a result the compression surface of the wing encountered local instability problems at less efficient stress levels. Thic caused the weight of bending material to be 21% greater and the total wing weight to be 15% greater than the reference turbulent wing.

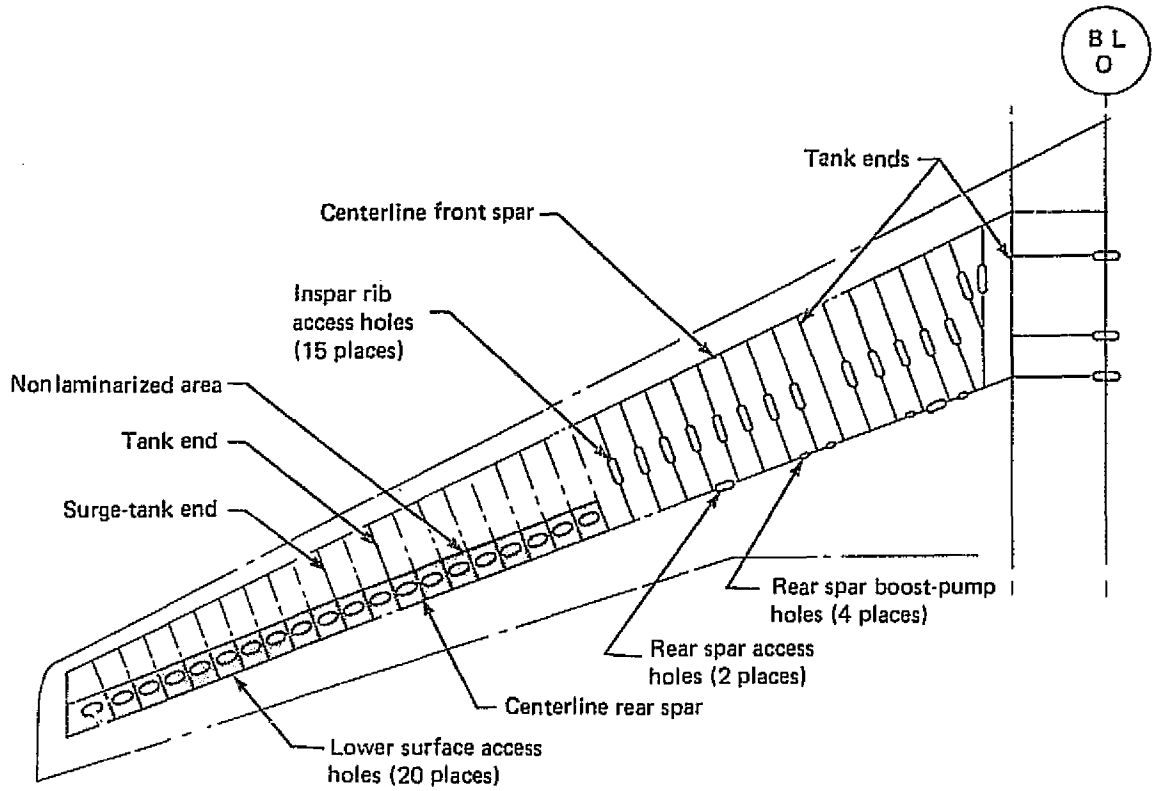

Figure 5.2-8. Wing Access Plan—25-Deg Sweep

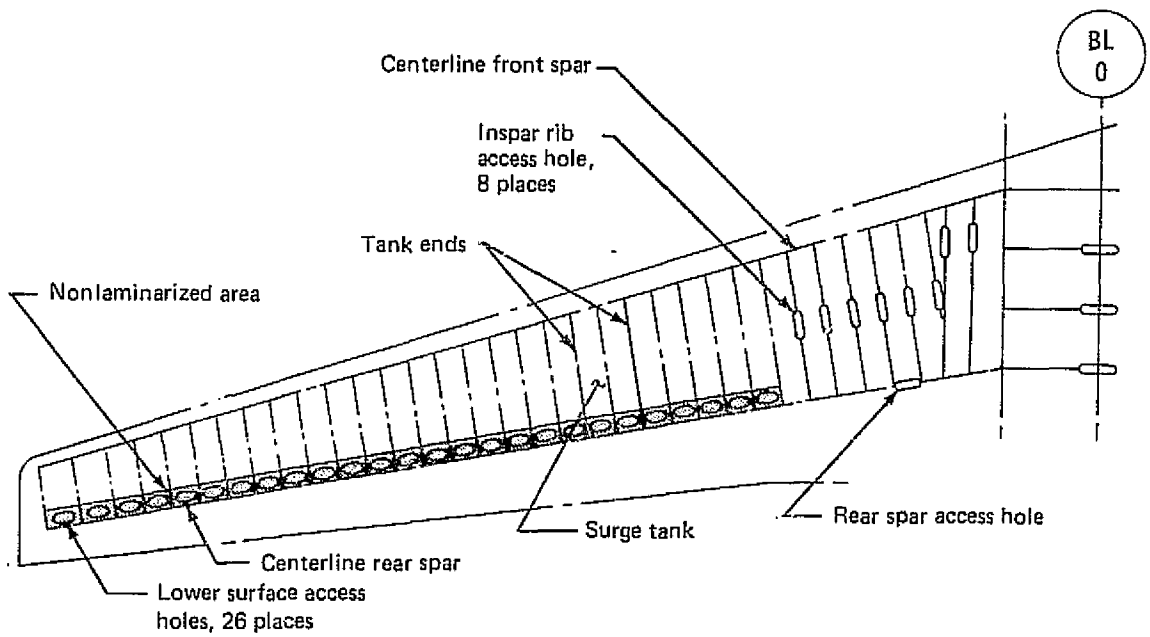

Figure 5.2-9. Wing Access Plan—15-Deg Sweep

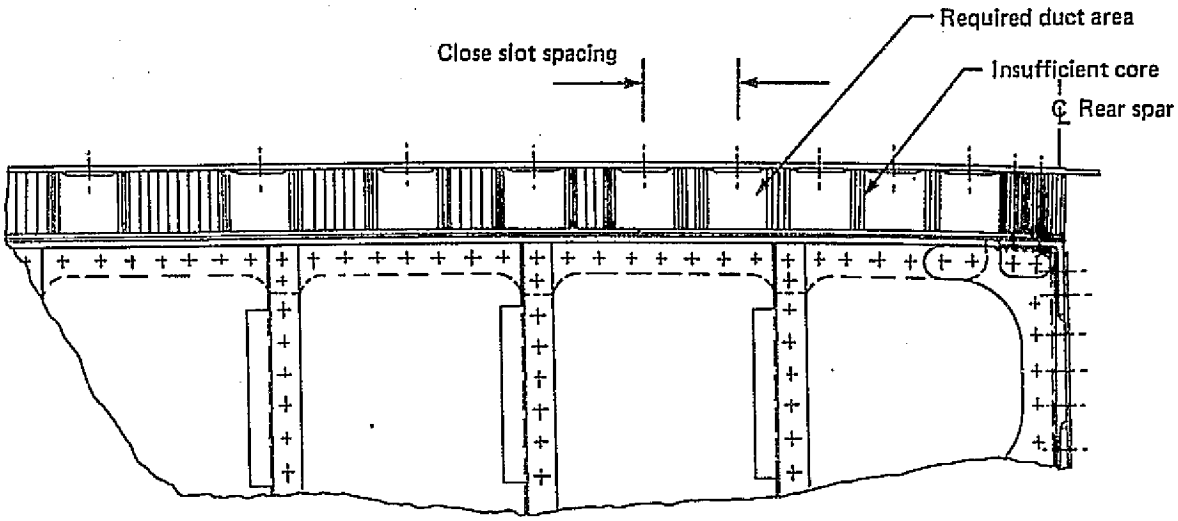

Figure 5.2-10. Laminated Aluminum Concept, Showing Core Space Constraint

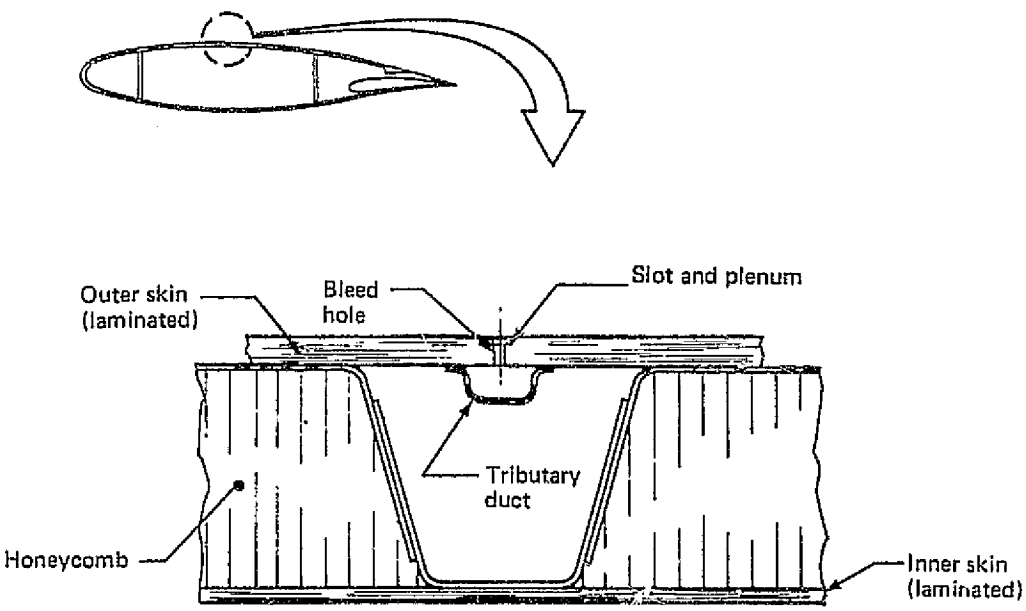

Figure 5.2-11. Initial Laminated Titanium Concept

The same manufacturing problems and other concerns existed with this concept as with the aluminum concept of Figure 5.2-2. It was assumed that the same changes could be made to this concept as were made to the aluminum concept. However, it would still be heavier and more costly than the aluminum concept of Figure 5.2-4 and was therefore dropped from further development.

(c) Super Plastic Formed/Diffusion Bonding Titanium Concept

Super Plastic Formed/Diffusion Bonding (SPF/DB) is a comparatively new fabrication process. Heat and pressure are used to make shapes and attachments that would be very difficult, if not impossible to make by any other process. Because of the intricacies of LFC wing structure this process showed potential for increased producibility and cost reduction.

A design concept was developed using this process in which the spanwise ducts and tributary ducts were all integrated into the structure. Figure 5.2-12 is a schematic showing the basic process applied to this design. In theory, a complete wing skin could be made in one piece. Initial facility costs would be high but the wing skins would have very low recurring costs. In practice however, wing structure must be fail safe, and therefore, spanwise joints must be incorporated into the design that adequately provide crack-stopping capability and sufficient residual strength to carry the loads after the crack stops. The close spacing of the ducts in some areas and the smoothness requirements create severe manufacturing problems which tend to make this concept unworkable. Figure 5.2-13 shows two suggested spanwise joint concepts to provide crack stopping capability while satisfying the other requirements.

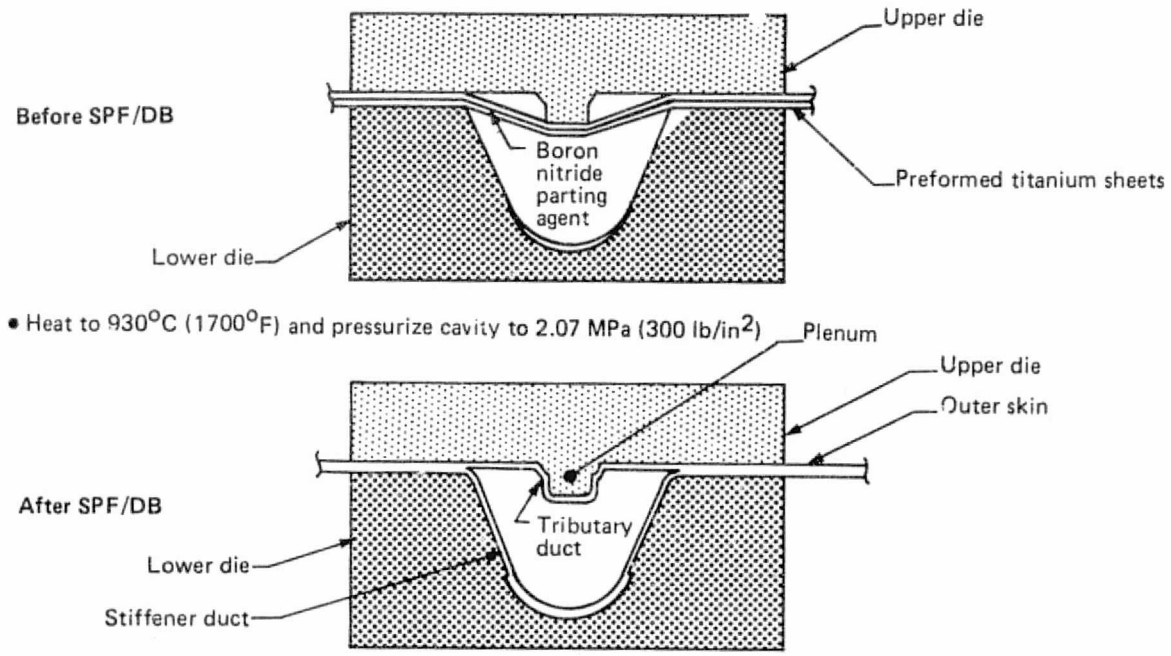

Figure 5.2-12. Superplastic-Formed/Diffusion-Bonded Titanium—Process Schematic

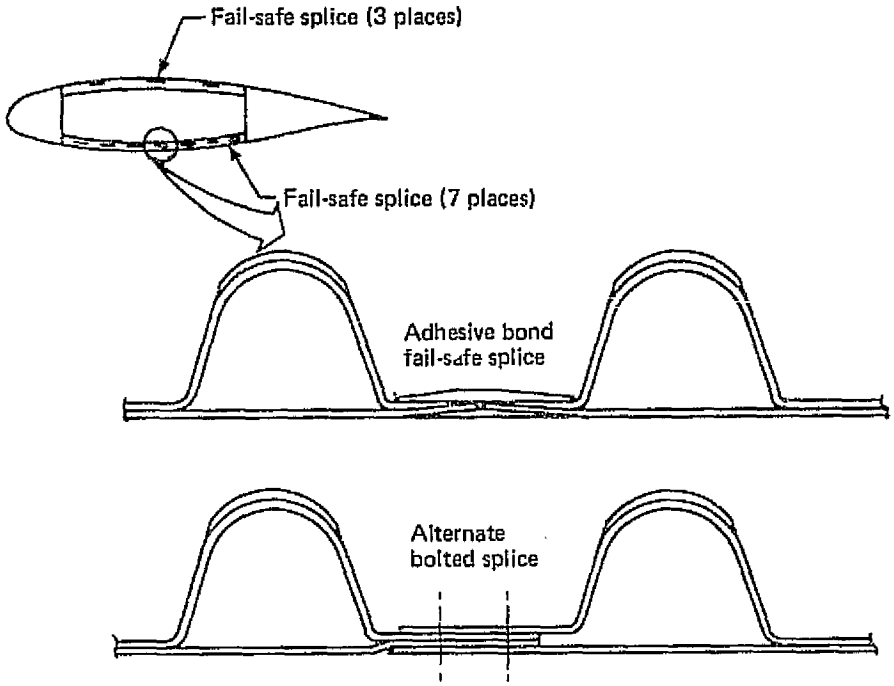

Figure 5.2-13. Titanium Concept (SPF/DB)—Typical Fail-Safe Splices

Figure 5.2-14 shows a proposed application of this concept to a typical rib at the front spar. Rib shear ties are diffusion bonded to the upper and lower panels during the SPF/DB process. Assembly of the wing box is accomplished by mechanical fastening skin panels to the ribs with closeout at the front and rear spars. This sequence avoids excessive tolerance buildup and provides wing contour control.

Although there is very little parasitic weight, this concept turned out to be heavy. Large duct size causes the duct walls and the skin to be sized for local instability. As a result the bending material is 23% heavier and the total wing weight is 17% heavier than for the reference turbulent wing. The primary reason for the increased weight of this concept is the poor compression load carrying capability. A weight reduction effort was undertaken and the final weight of this concept included savings realized by chem-milling between ducts. This weight savings was realized at the expense of manufacturing complexity and therefore increased cost.

(d) Graphite/Epoxy Concept

Graphite/epoxy shows a great deal of promise for use in 1990 and beyond because of its weight savings potential. To explore this application to LFC wing structure, two graphite/epoxy concepts were investigated. Figure 5.2-15 illustrates the skin-stringer concept at a rib location. Shear transfer from the rib to the skin is a serious problem with this concept. Further discussion of the merits of this concept will be taken up in a following paragraph on the closely related Graphite/Epoxy Titanium Hybrid Concept.

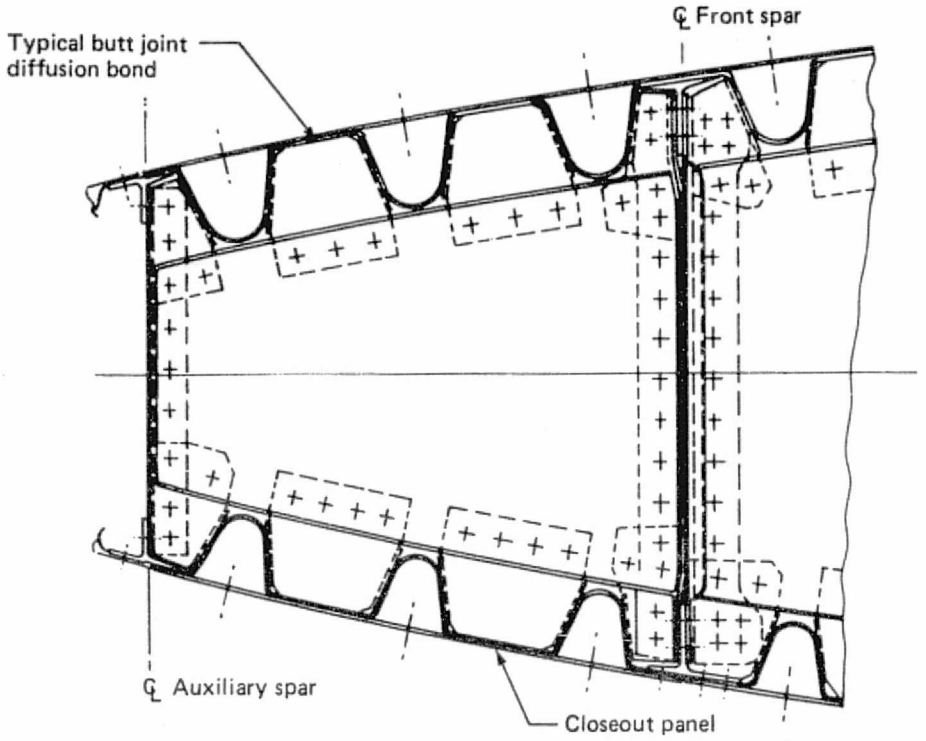

Figure 5.2-14. Titanium SPF/DB Concept—Rib and Shear Tie

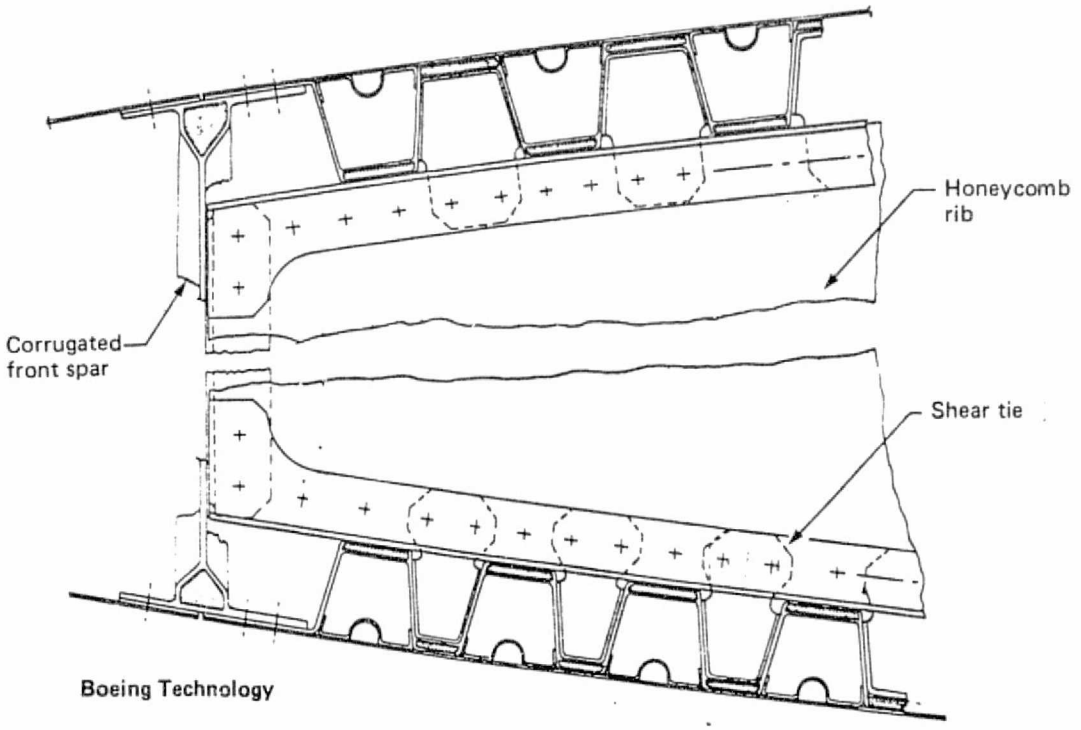

Figure 5.2-15. Graphite/Epoxy Concept—Inspar Area at Front Spar

Figure 5.2-16 shows the sandwich concept. It is patterened after the laminated aluminum concept of Figure 5.2-4. The use of metal honeycomb along with graphite skins is not recommended because of the adverse effects of lightning strike. Projections of strength and stiffness available in non-metal honeycomb cores are disappointing so it appears that some weight penalty must be accepted in the core in order to achieve the weight savings in the skins of composite honeycomb panels. This penalty was considered when weighing this concept. The bending material weight was reduced 15% when compared to the laminated aluminum concept of Figure 5.2-4 and increased 1% when compared to the reference turbulent wing concept. Total wing weight increased by 1% over the reference turbulent wing due to the compensating factors discussed above and because of differences in the leading and trailing edge areas.

(e) Graphite/Epoxy Titanium Hybrid Concept

Both titanium and graphite/epoxy as materials have distinct advantages over aluminum and they are compatible. Titanium used as an outer layer over a graphite/epoxy structure will provide excellent resistance to erosion and damage due to lightning strikes. Slots and perforations are not compatible with graphite/epoxy so some combination of these materials with titanium is logical. Figure 5.2-17 shows one of the concepts that was reviewed which is quite similar to the graphite/epoxy concept of

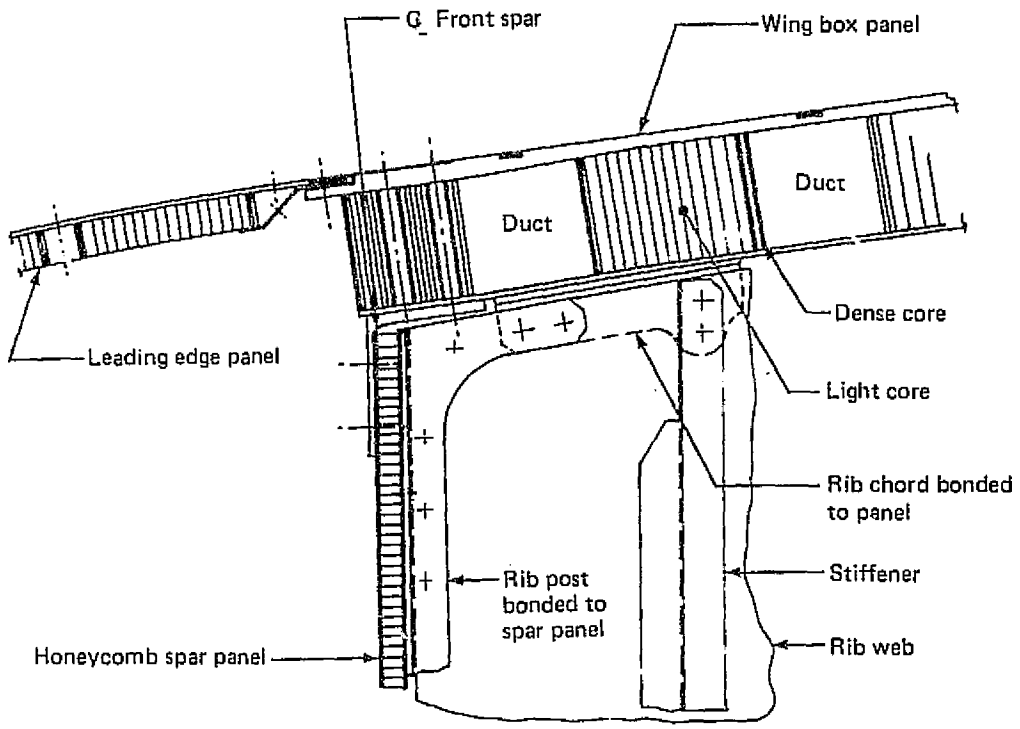

Figure 5.2-16. Graphite/Epoxy Honeycomb Concept

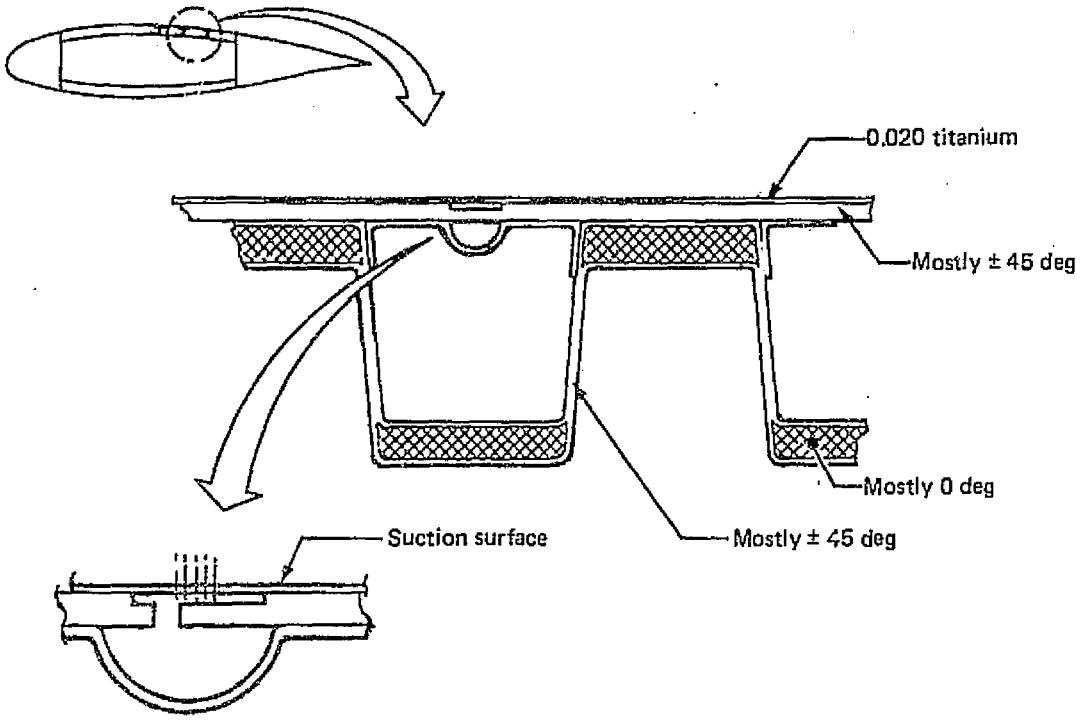

Figure 5.2-17. Graphite/Epoxy Titanium Hybrid Concept

Figure 5.2-15. It will be noted that this concept is not shown with suction strips but has the perforations or slots cut directly into the outer sheet. Variations of the concept could use suction strip inserts instead. This concept was not strength-sized but its weight is judged to be comparable to that of the similar graphite/epoxy concept. However, based on separate in-house studies of graphite/epoxy structural concepts for turbulent wings, the weight saving potential for the concepts shown in Figures 5.2-15 and 5.2-17 is attractive. There appear to be no features of these concepts which would preclude their use for LFC wings.

In spite of the favorable aspects, it is recognized that there are many unresolved questions related to the use of composites; some of the more important being lightning strike, erosion, radiation, crack growth, and manufacturing cost. These questions are considered beyond the scope of the LFC Program and are being studied in depth by the ACEE Composites Program. Thus it was decided that further effort on composites for LFC was not justified at this time and that their application should await further progress in the mainstream composites effort.

5.2.2.2 Development Phase

The results of the exploration phase were carefully reviewed following completion of competitive designs. Producibility, maintenance, repair, cost etc. were qualitatively analyzed and the results were unsatisfactory in some areas. The best of the designs was the laminated aluminum concept but it had two unresolved problems; 1) inspectability was

unacceptable and 2) it was structurally inadequate aft of 50% chord because of duct size and slot spacing problems as previously discussed in relation to Figure 5.2-10. It did, however, have significant potential so the task of solving these problems was undertaken while simultaneously investigating alternate aluminum concepts.

As previously noted, a revised wing geometry was introduced since it was judged to be the most likely candidate at that time. The reduction in wing sweep from 25° to 15° caused a reduction in effective wing thickness as well as an increase in the already critical gust load factor. Both caused skin load increases in the wing. However, along with the change in sweep, a change in the suction requirements took place. This permitted a duct-size and slot-spacing compatible with the laminated aluminum concept but it restricted suction to 70% chord on the upper surface and 60% on the lower surface.

A proposed solution to the inspection problem associated with the large number of plies, was to limit the maximum number of plies to four in each skin of each surface. This requires ply thickness as high as 3.17 mm (.125 in.). A minimum number of three plies was established for the inboard 80% of the wing span in order to provide fail-safety in the skin panels. Also achievement of reasonable weight efficiency dictated spanwise tapering of each ply.

Fatigue tests of laminated aluminum with cold-worked holes were completed, as discussed in Subsection 5.2.4, and improvements in allowable stresses were permitted for the laminated aluminum concept. The updated arrangement was strength sized for the revised wing geometry and the new weight was established to serve as a reference LFC wing concept for development of the alternate aluminum concepts.

Many new concepts were investigated. To illustrate the scope of this activity, Figure 5.2-18 shows four which were rejected after limited study because they were judged not practical. However, three new concepts were considered promising enough to study in further detail. These are identified in Figures 5.2-19, 5.2-20, 5.2-21 as 1) Inverted Stiffener/ Fiberglass Cover concept, 2) Hat-stiffened/Fiberglass Cover concept and 3) Conventional Construction/Fiberglass Cover concept.

These three concepts are similar in that they have a series of sacrificial spacers on the outer surface that allow fabrication of the primary wing box using conventional methods and tolerances consequently permitting significant reduction in production costs over other candidates. The manufacturing tolerances are compensated for by final machining of the sacrificial spacers to LFC smoothness requirements before bonding on the outer panel. Since the outer panels strain with the wing, they must not buckle or deform significantly throughout the spectrum of loads anticipated during laminarized flight. In addition, they must not fail during any portion of the anticipated load spectrum. A discussion of each of the above structural concepts follows:

(a) Inverted Stiffeners/Fiberglass Cover Concept (See Figure 5.2-19)

This concept utilizes an inverted skin-stringer basic structure with a fiberglass honeycomb outer panel. The slots and stringers follow constant percent chord lines and the stringers are tapered. Minimum stringer height is established by duct size requirements.

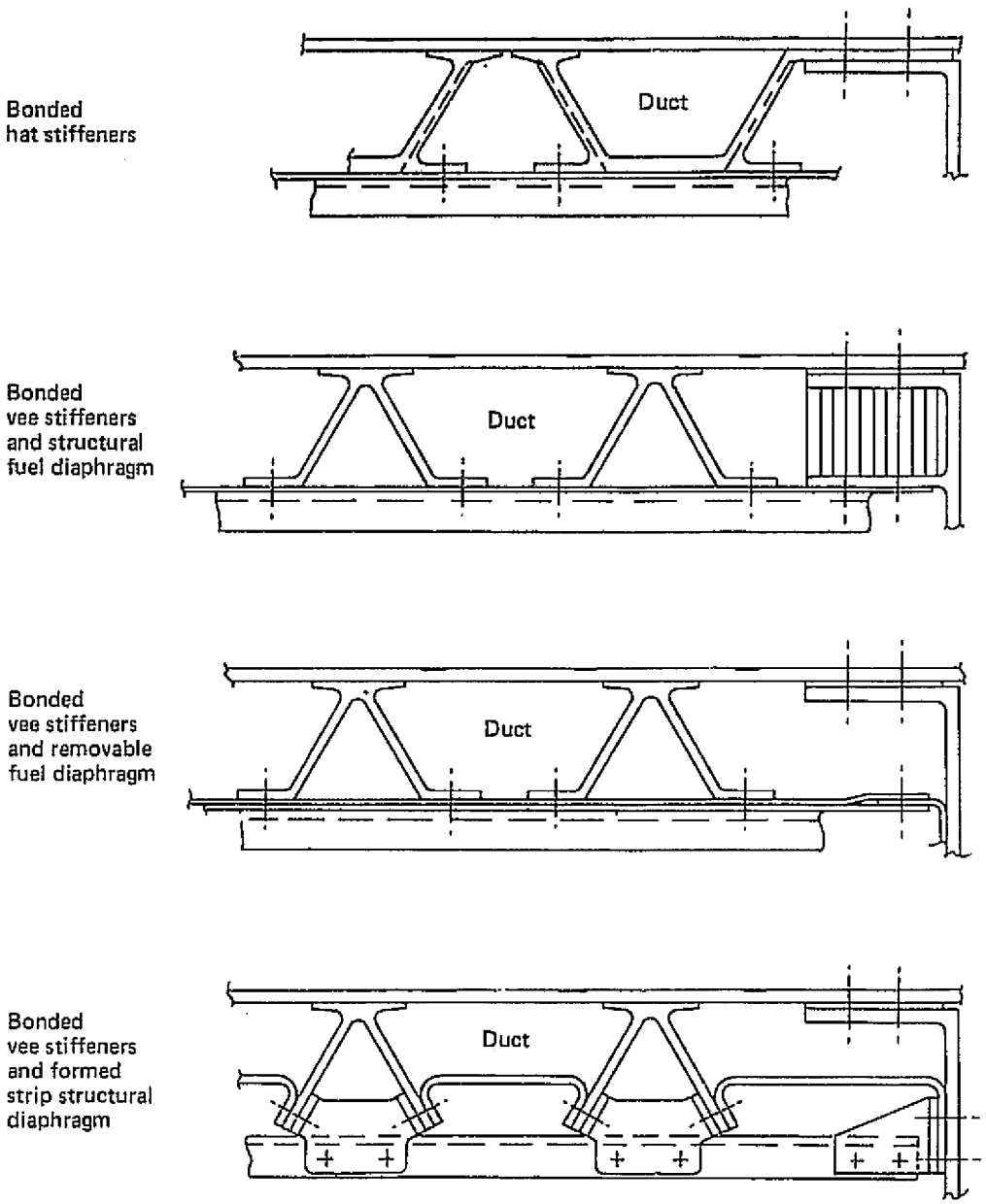

Figure 5.2-18. Alternative Aluminum Concepts

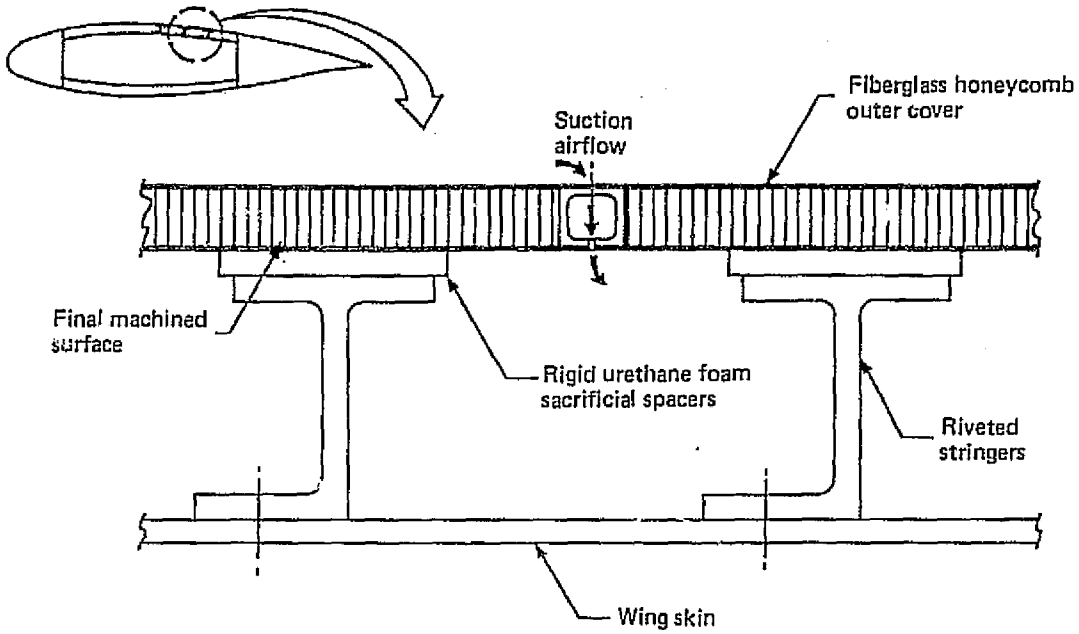

Figure 5.2-19. Inverted Stiffeners and Fiberglass Cover Concept

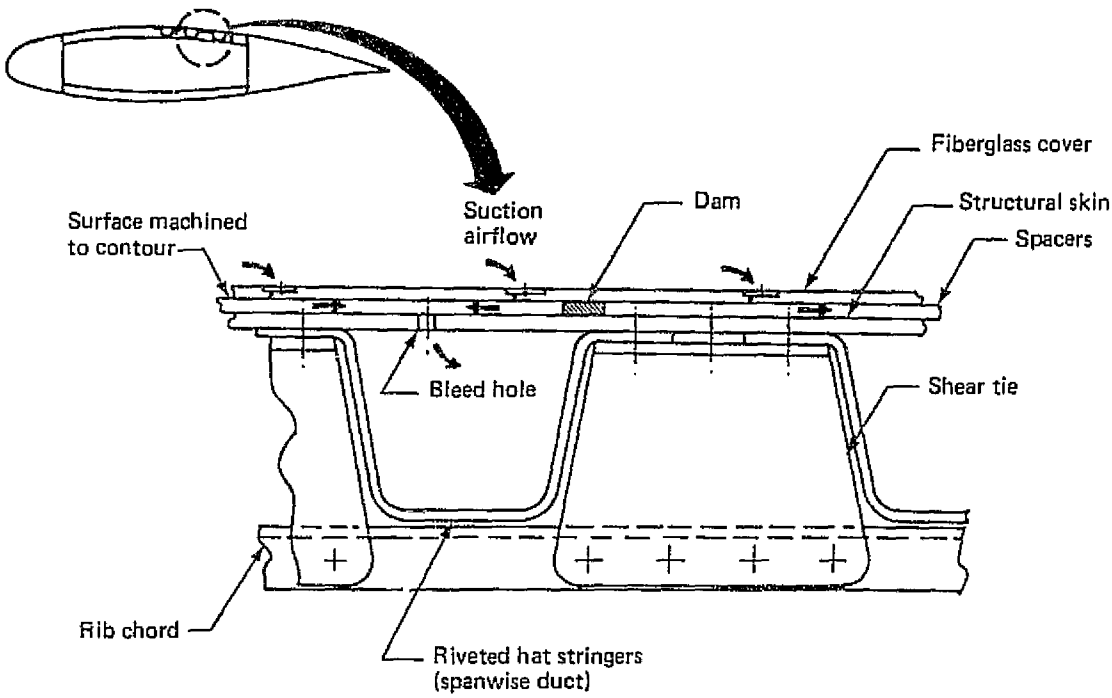

Figure 5.2-20. Hat-Stiffened/Fiberglass Cover Concept

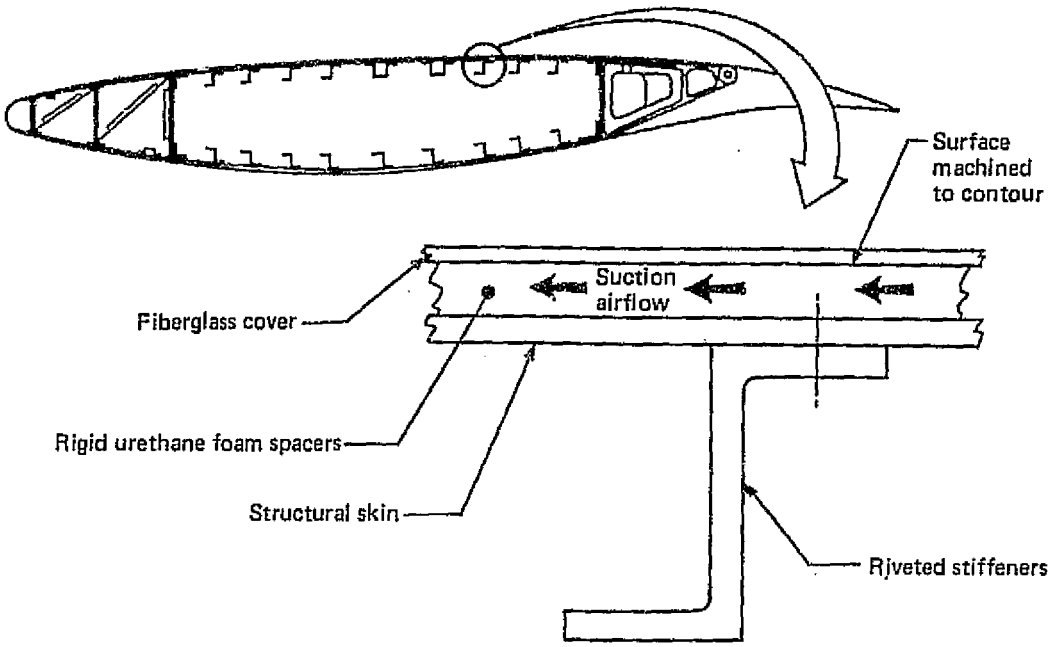

Figure 5.2-21. Conventional Construction/Fiberglass Cover Concept

A substantial disadvantage is that this structure loses efficiency because the centroids of the wing surface panels are moved closer together, in effect making the wing structurally thinner. The surface material of this concept (bending material plus fiberglass panel) was 15% heavier than for the reference LFC wing. The increase in total wing weight over the laminated aluminum concept (reference LFC wing) was 9%.

(b) Hat-Stiffened/Fiberglass Cover Concept (See Figure 5.2-20)

For this concept, the suction slot spacing was independent of the stiffener spacing. The passages formed by the spacers and the outer fiberglass cover constitute chordwise ducts which carry the air from the slots to the hat stringers which act as spanwise ducts. Figure 5.2-22 shows a better view of this feature and illustrates the suction airflow paths for this generic type of structural arrangement. Unfortunately the hat stringers had to be sized for the required air volume rather than structural efficiency. This created a severe weight penalty due to lower allowable stress levels.

An alternate approach was investigated in an attempt to reduce this penalty. A nonstructural air/fuel diaphragm was added, as shown in Figure 5.2-23, to enable use of the space between the hat stringers for air flow. Since this eliminated the shear ties, an attempt was made to transfer rib shear to the skin by "truss action" through the duct walls. This was found to be not very satisfactory. The complexities of installing and sealing the diaphragm coupled with the weight and cost penalties of the arrangement dictated that the concept be dropped from further study.

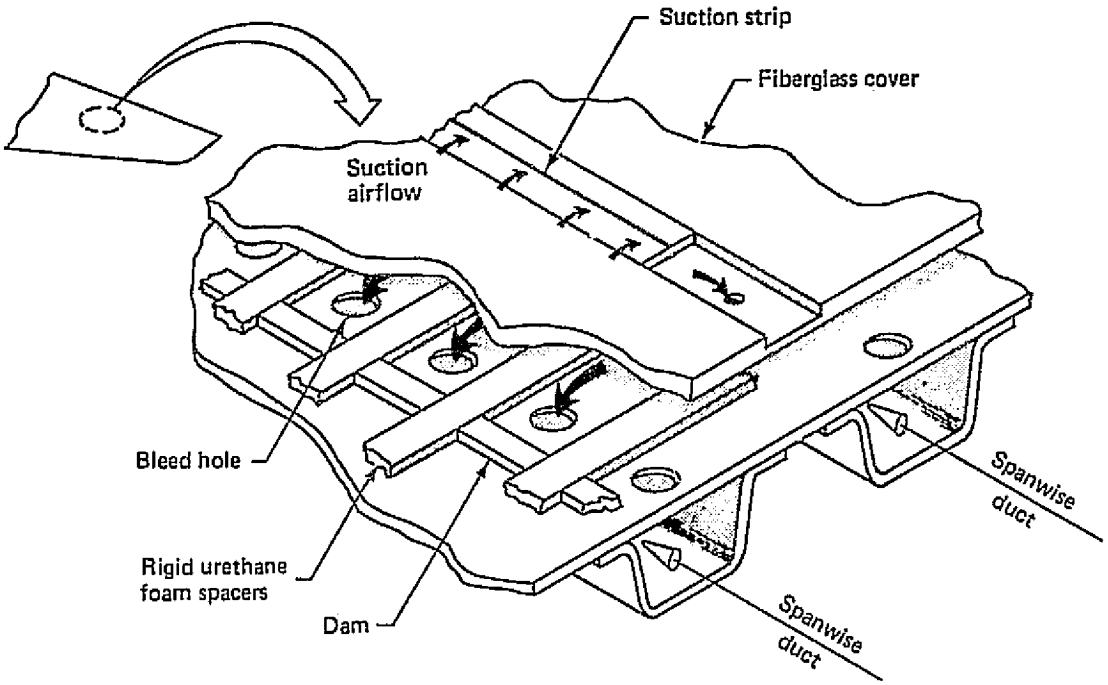

Figure 5.2-22. Separate Suction Surface Concept

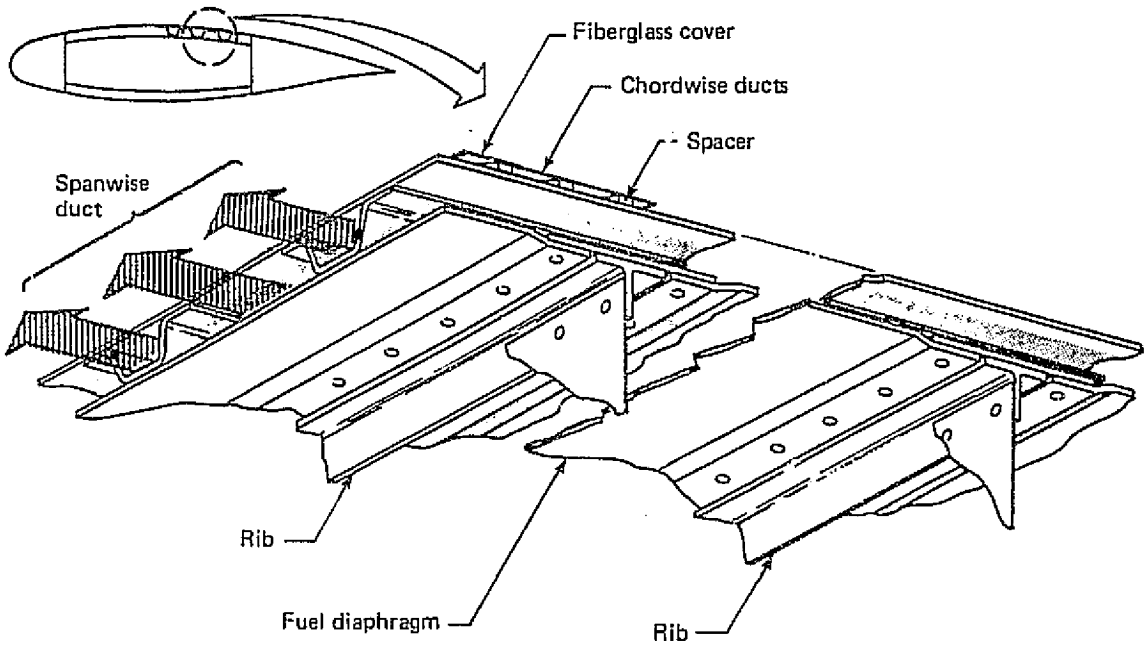

Figure 5.2-23. Hat-Stiffened Concept With Nonstructural Fuel Diaphragm

(c) Conventional Construction/Fiberglass Cover (See Figure 5.2-21)

The short chordwise ducts used in the hat-stiffened concept provided the inspiration for the chordwise ducts used in this concept. The principal difference is that the chordwise ducts carry the air completely over the primary wing box and into trunk ducts forward of the front spar. This eliminates all LFC-related holes through the primary structure and thereby relieves potential fatigue and sealing problems.

This concept uses conventional structure and a fiberglass/urethane foam cover in an arrangement that provides chordwise ducting. The front spar was moved back to about 14% chord to accommodate the volume of air now directed into the leading edge space. The first conventional construction design had two trunk ducts in the leading edge area. One duct served the upper surface and one the lower. With only two ducts forward of the front spar the structure could be kept very simple. Lack of diagonal members means that the panels must work in bending but the simplicity of the design, and the elimination of additional rows of external fasteners, made this approach attractive.

A problem with using only two ducts is in balancing the suction air distribution for different areas of the wing since the external air pressure over the wing is not constant from leading edge to trailing edge. Although it may be possible to balance the system for one flight condition, preventing oversuction or undersuction for the "off-design" conditions makes a two-duct design impractical. To give more control over the suction air distribution the design was changed to a five duct system (see Figure 5.2-24). The upper surface is divided into three areas, leading edge to 12% chord, 12% to 65% chord and 65% to 80% chord. The lower surface has two areas, leading edge to 12% chord and 12% to 70% chord.

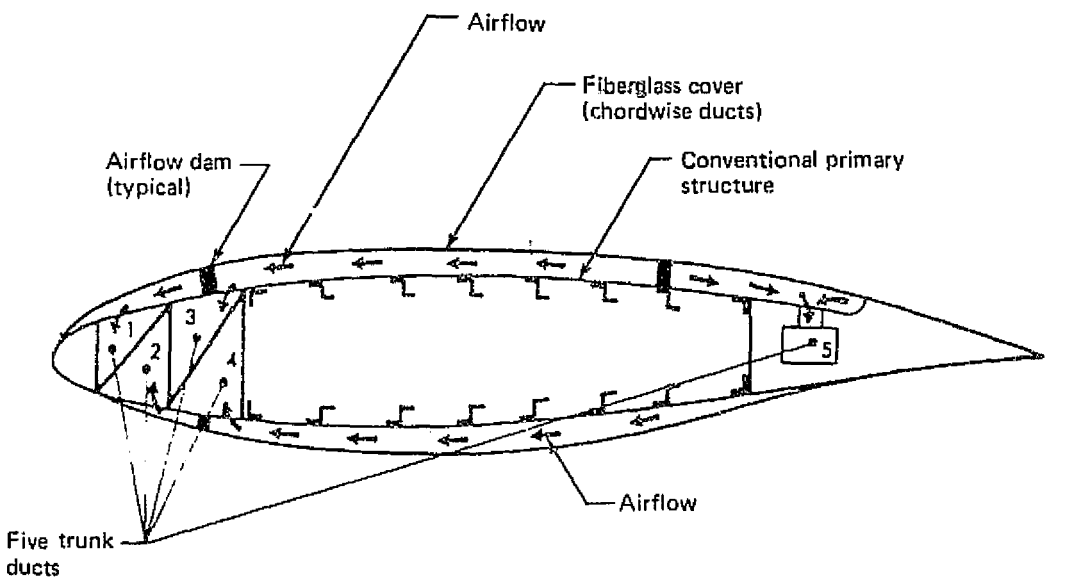

Figure 5.2-24. Conventional Construction/Fiberglass Cover Concept (Five-Duct Configuration)

The bending material of this concept is 9% lighter than for the reference LFC wing, i.e., laminated aluminum concept. Total surface material weight (bending material and fiberglass cover) is 1% less. The reduction in total wing weight over the reference LFC wing was less than 1%. Although this weight advantage was not really significant, other favorable characteristics of this concept ultimately led to its selection for incorporation in the final LFC airplane design.

5.2.3 SUCTION SURFACE DEVELOPMENT

The surface of a production airplane wing is subjected to many hazards not encountered in laboratory or wind tunnel environments. Foreign object damage is all too common on conventional airplanes. An LFC airplane wing surface will be more fragile and at the same time the smoothness requirements are much more severe. The objectives in design of the suction strips were to minimize the fragility, minimize production costs and minimize maintenance and repair costs. Because it is obviously impractical to replace an entire surface of a wing every time local damage needs to be repaired, it is apparent that surfaces should have multiple replaceable segments. The development of replaceable suction strips therefore became a requirement. However, the fact that the airplane would have over 4.8 km (3 miles) of suction strip warranted a great deal of design effort.

The suction strip concept more commonly used in early LFC studies is designed around a continuous spanwise slot. This suction slot is between .013 mm (.005 in) and .584 mm (.023 in) wide and must be held to a tolerance of approximately ±.025 mm (.001 in). Although expensive, it is possible to fabricate the structure to within this tolerance band. Further testing will be required to assure that the slot dimensions will remain within tolerance when subjected to continual fluctuations of stress and temperature.

The suction strip design is an area where inventiveness and ingenuity can pay large dividends and much time and effort was spent in search of features to assure low maintenance and reliable operation. Self-cleaning concepts, or designs with moving parts to provide desirable operating characteristics, were dropped because of cost, complexity and undependability reasons. Spring-retained or "snap-in" designs proved impractical because wing deflection causes enough movement to put the suction strip out of tolerance. The machining tolerances that would be required for a "snap-in" design would be impossible to obtain for the entire length of the many strips required per aircraft. Six concepts survived initial evaluation and are described in the following paragraphs:

5.2.3.1 Controlled Gap Insert

The controlled gap concept is shown in Figure 5.2-25 and appeared to be extremely simple and inexpensive. No precision sawing of slots was necessary. Two separate pieces were made and bonded to the structure at the proper spacing. In practice it did not work as the strips tend to move during the bonding operation leaving the slot width out of tolerance. There may be satisfactory solutions to this problem for production but no further work was done on this concept.

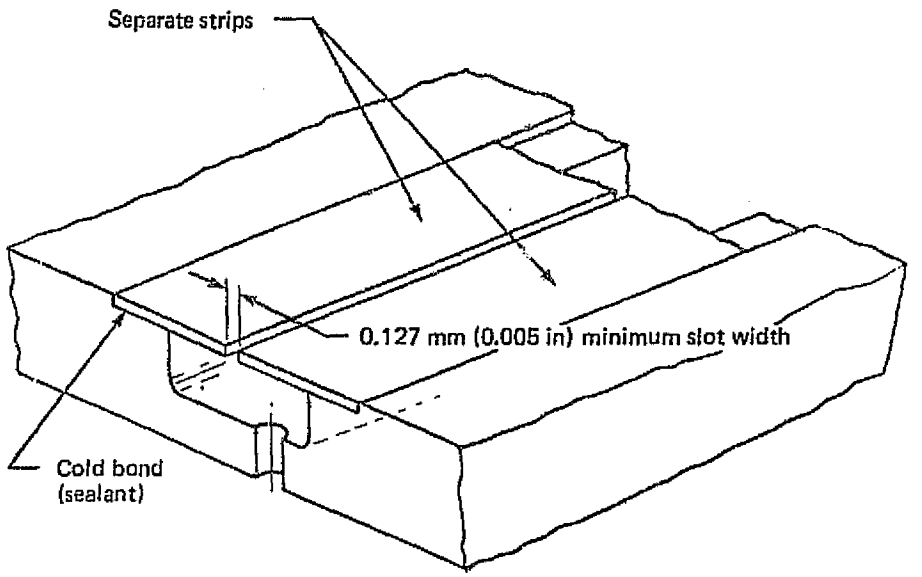

Figure 5.2-25. Controlled-Gap Insert

5.2.3.2 Bridged Slot Insert

The bridged slot concept was designed to overcome the problem of holding the slot width during the bonding operation but retaining the prefabricated unit feature. This concept was far more costly than others discussed here because it required precision chem-milling as well as precision sawing. Figure 5.2-26 shows the principal features of this insert.

Parts made for structural testing utilizing the bridged slot insert had insufficient bond area for attaching the insert to the skin. However, a minor change to the design can be expected to solve this problem. Also, the "bridges" may cause excessive disturbances in the suction airflow which would require flow test evaluation. No further work was done on this concept following the structural tests.

5.2.3.3 Aluminum Foam Base Insert

The aluminum foam base concept as shown in Figure 5.2-27 was developed to minimize precision machining and simplify achieving smoothness on installation. It uses "Duocel" foam aluminum as the carrier for the slotted strips. A single piece of aluminum and a slightly oversize strip of foam are bonded in the plenum. A hand roller can be used to crush the foam to provide a smooth flush surface (see Figure 5.2-43). The slot is then cut in the strip. However, this concept has unsatisfactory air flow characteristics and clogged during flow testing. It was therefore, considered unsatisfactory and eliminated as a candidate.

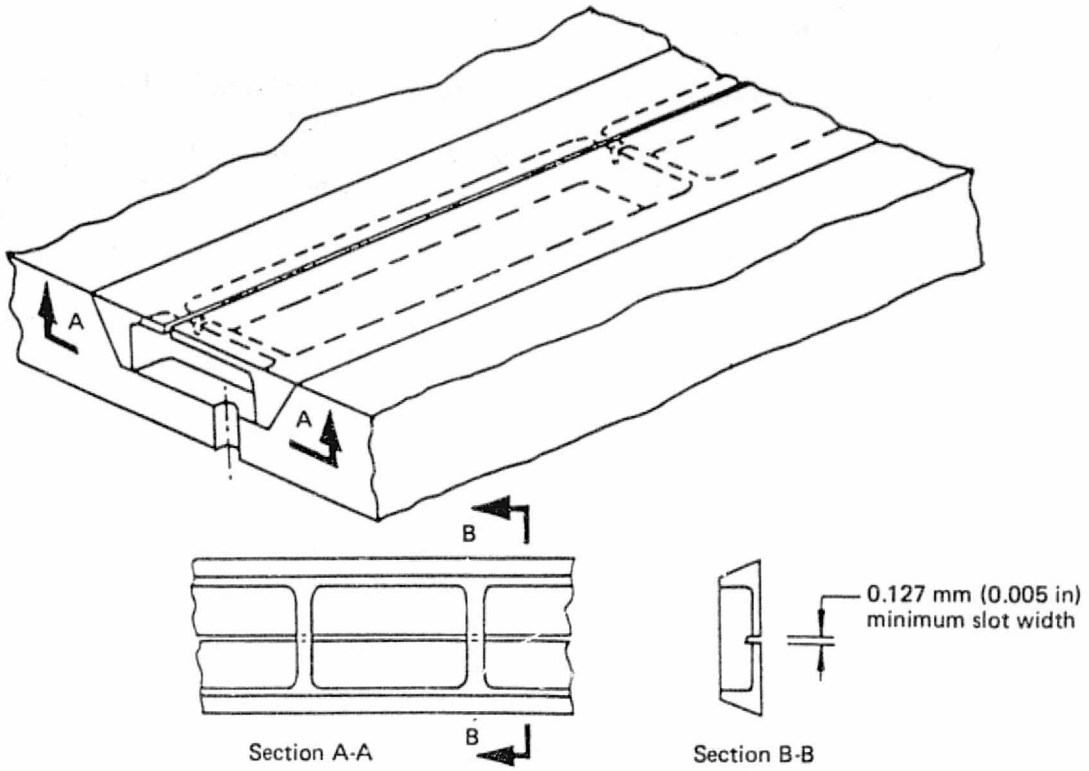

Figure 5.2-26. Bridged-Slot Insert

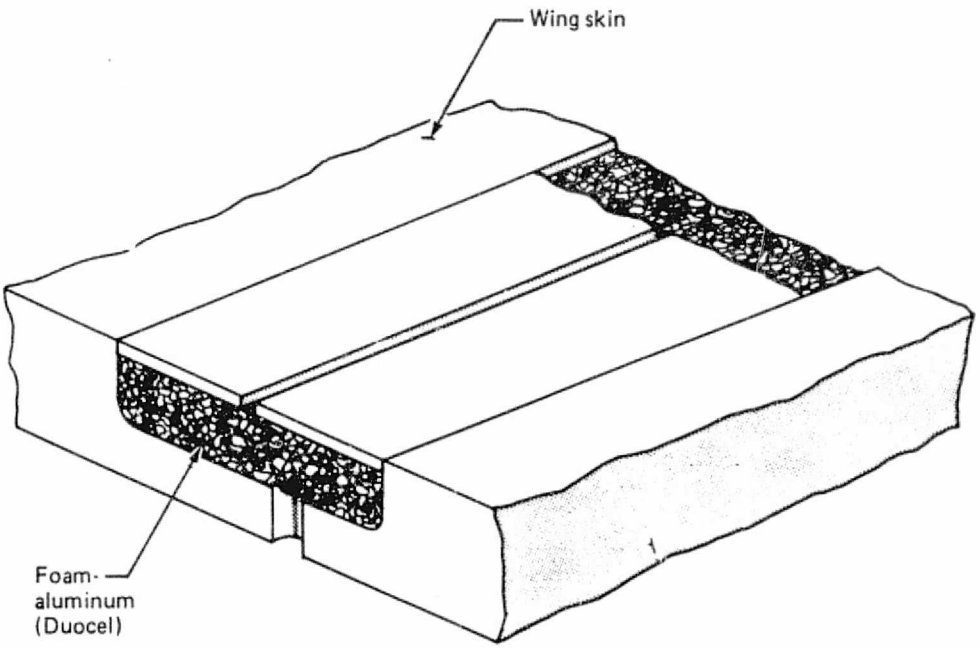

Figure 5.2-27. Foam-Aluminum Insert

5.2.3.4 Corrugated Base Insert

The corrugated base concept was intended to overcome the shortcomings of the foam aluminum design while retaining the "compression on installation" aspect. Figure 5.2-28 shows this insert. The outer slot strip is supported by a corrugated, perforated foil. Installation procedure is similar to that of the foam aluminum concept. The corrugations are deformed slightly by a roller to give a smooth flush surface. The amount of perforation can be varied to give added air flow control. No parts were built so no testing was accomplished on this design.

5.2.3.5 Perforated Strip Insert

The perforated strip concept (See Figure 5.2-29) is the cheapest arrangement of those inserts investiaged. The perforations are made by an electron beam (Steigerwald) process. Hole diameter and pattern can be held to a high degree of accuracy and holes can be produced at a rate of 250 holes/sec. This corresponds to a linear production rate that is faster than a slot can be saw cut. The manufacturing process gives holes that have a "built-in" taper. When the insert is installed as shown in Figure 5.2-30, this taper ensures that dirt particles entering the hole do not get jammed inside the hole. The holes can be made in titanium and aluminum but there may be a corrosion problem with the unfinished

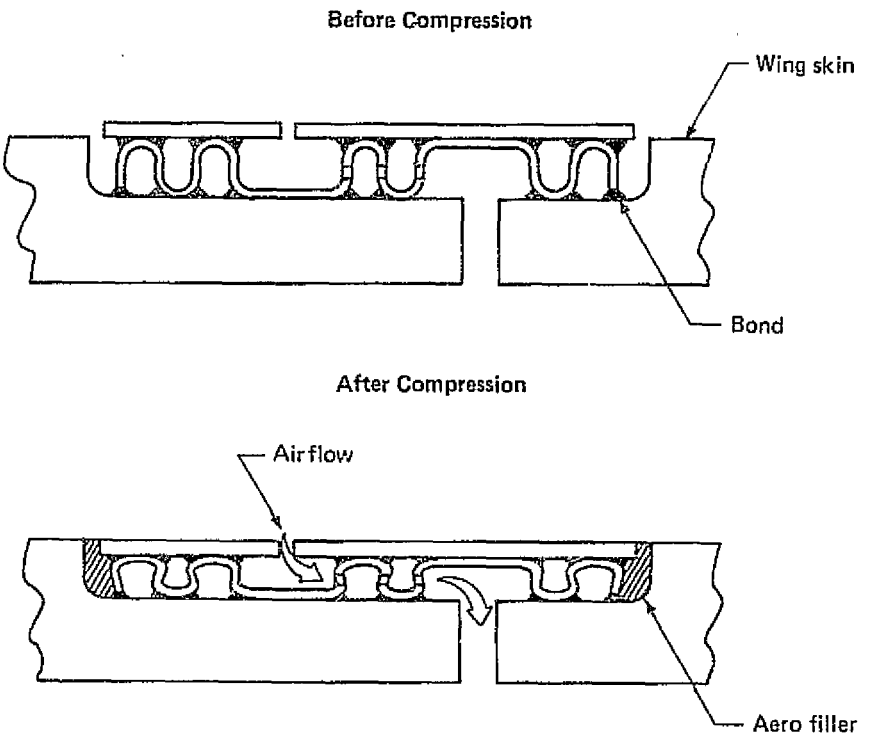

Figure 5.2-28. Corrugated Base Insert

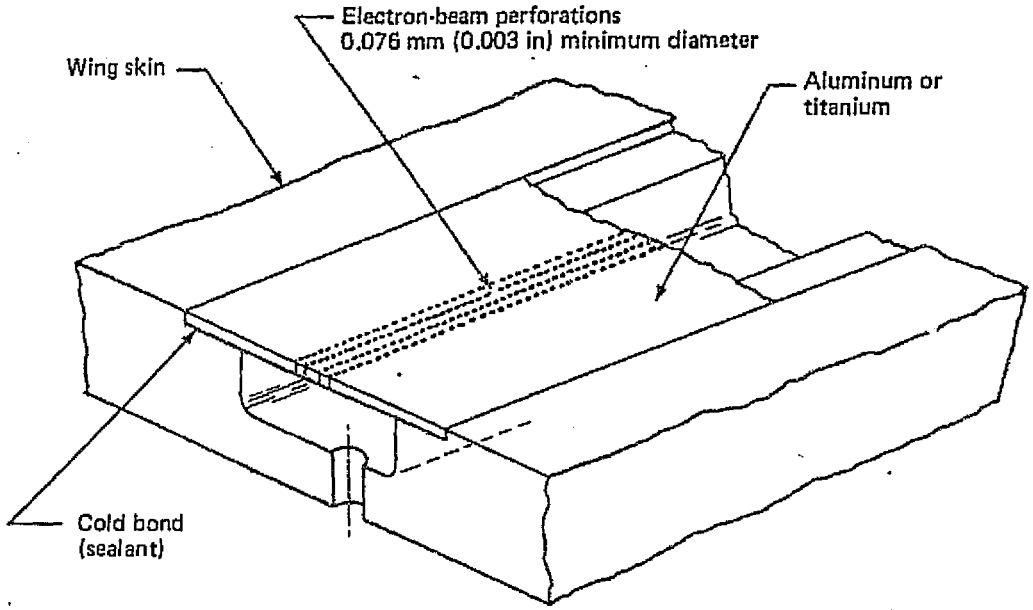

Figure 5.2-29. Perforated Strip Insert

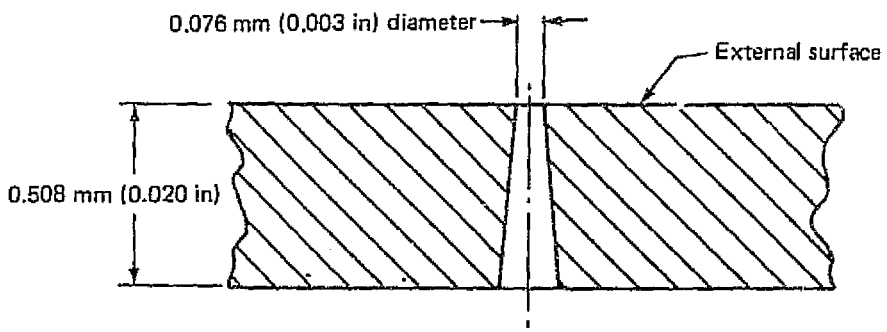

Figure 5.2-30. Perforated Strip Insert—Section Through Perforation

holes in aluminum. However, this may be controllable by a process that has been developed to apply primer inside the holes for corrosion control. Primer thickness can be controlled so that after the primer is applied the holes are within tolerance.

Preliminary fatigue testing was performed as discussed in Subsection 5.2.4 and the fatigue life of the perforated strip failed to meet the goal in highly loaded areas. Cracks are initiated at the holes and propagate across the insert. With pliable adhesives the insert stays in place and this may allow operation for some period without insert replacement. Testing is required to check airflow characteristics with cracks. The strips are not a safety of flight item and are replaceable.

5.2.3.6 Slot Plenum Insert

The slot plenum concept shown in Figure 5.2-31 incorporates the advantage of the bridged slot, obtains the theoretical advantage of the controlled gap concept and simplifies flow control. Fatigue cracks may develop through the small holes between the two plenums in less than the design life of the airplane but they are not flight critical and will not significantly affect air flow. The inserts are replaceable at an appropriate time. This concept has been flow tested successfully and appears adaptable to any area on the wing.

5.2.4 STRUCTURAL AND ENVIRONMENTAL TESTS

During the early portion of the exploration phase it was recognized that limited structural tests using small samples would be needed. The purpose of the developmental testing was to identify the severity of the major problems, investigate proposed solutions to these problems, establish design guidelines and identify areas needing further study so that concept development could proceed in an orderly, efficient manner.

Ideas had to progress to the point that hardware could be designed and samples fabricated for testing. The testing was divided into two general phases corresponding to the exploration phase and the development phase of the concept and materials development study.

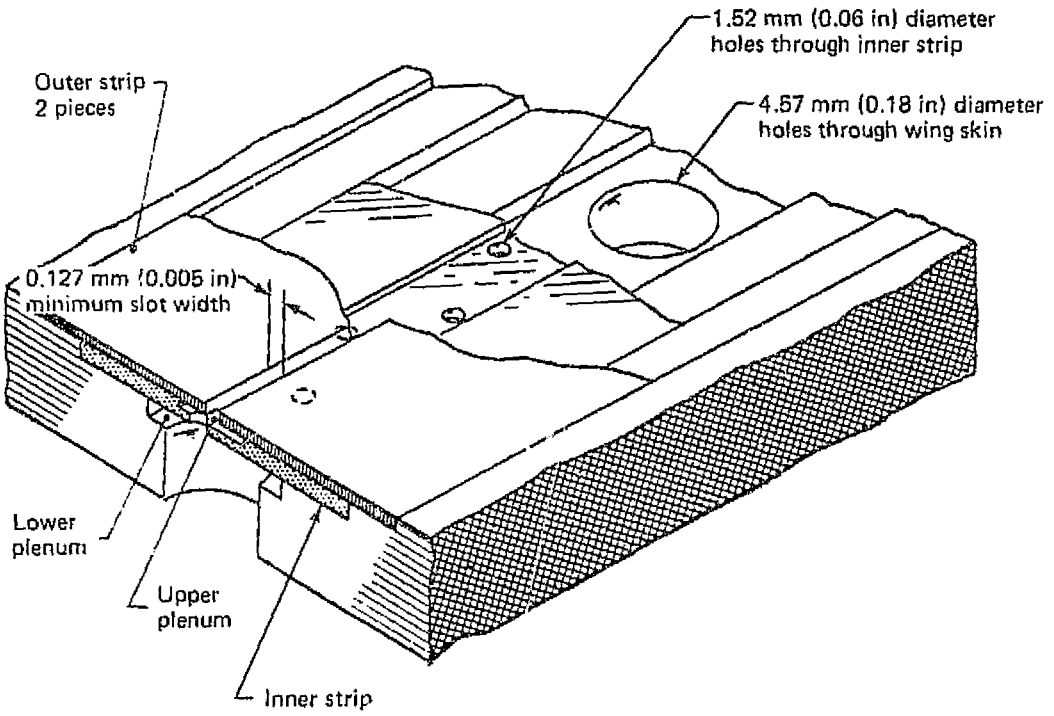

Figure 5.2-31. Slot-Plenum Insert

5.2.4.1 Exploration Phase Testing

Developmental testing accomplished in this phase consisted of fatigue and lightning strike testing and demonstrations of the deformations related to cold-worked holes and installing fasteners. A detailed description of these tests can be found in Reference 21. Fatigue testing was performed with standard dog bone specimens as shown in Figure 5.2-32. The structural concept investigated was the laminated aluminum concept. The primary concern was the effectivity of cold-working holes in laminated aluminum structures. Three of the candidate suction surface concepts were incorporated into the test specimen; a standard single plenum slotted design, a bridged slot design, and a perforated strip design. The standard slot design was intended as a comparison to the other designs which had structural discontinuities suspected of being fatigue critical.

Fatigue testing indicated that the existing data on fatigue life of single-element skins with cold-worked holes can be used for multiple-layered designs. If all open holes on the LFC wing are cold-worked, no fatigue penalty would exist for the upper surface and only a modest penalty would exist for the lower surface. Open holes that are drilled but not cold-worked must be treated as holes that have not been deburred. This would cause a significant fatigue penalty for the upper surface and a very large penalty for the lower surface.

Of the three insert designs tested, only the perforated strip failed to meet the target fatigue life. To increase the life of the strips to meet the target goal would require a reduction in stress level which would result in substantial weight penalties for both wing surfaces.

The use of tank sealant in place of the cold bond to install the suction surface inserts prevented rapid progression of insert disbond immediately after they failed in fatigue. A significant number of loading cycles occurred after insert failure before the surface smoothness appeared to be degraded enough to cause loss of laminar flow.

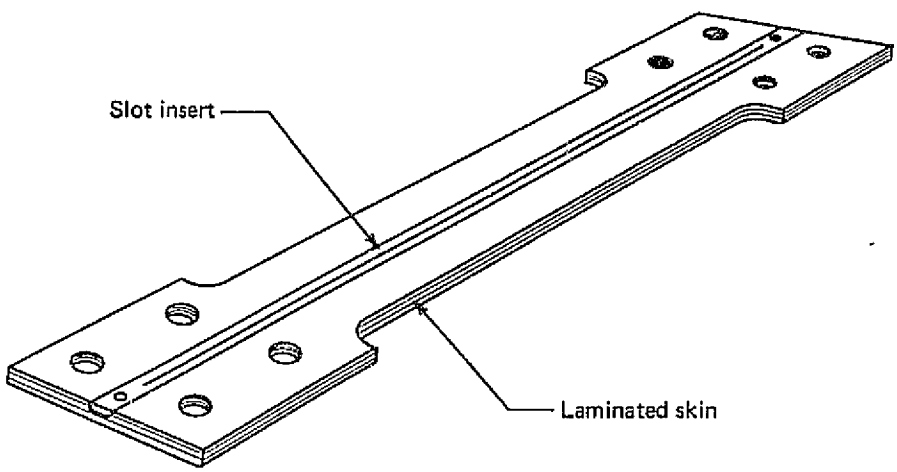

Figure 5.2-32. "Dog Bone" Fatigue Test Specimen

The buckling of the bridged slot insert during compression testing indicated that insufficient bond area existed to allow use of that specific configuration with the cold bond. A modified design incorporating additional contact area could provide a satisfactory solution to this problem.

Preliminary type lightning strike tests were conducted on the laminated aluminum concept primarily to investigate the effect on the laminations. The tests cannot be considered conclusive, but the indications are that structural problems will be minimal. The functional problems induced by lightning strike, as related to maintenance of laminar flow, require more investigation. The intensity of the lightning strikes used in the tests represents all but 1% of the lightning strikes to be expected in service. This level would be exceeded only once in every 300,000 flight hours. This is, of course, well within an acceptable range provided that suction strips are not frequently blown off by less severe lightning strikes.

Because of the stringent surface smoothness criteria for LFC surfaces, tests were conducted to determine the effects on surface condition due to cold-working holes and installing fasteners in laminated skins. Drilling, reaming and countersinking holes in laminated structure caused no distortions but installation of non-hole-filling countersunk fasteners caused noticeable in-plane and out-of-plane distortions. Cold-working of holes produced additional growth and distortion and the largest effects were observed with interference-fit countersunk fasteners. Concepts covered with a fiberglass cover after the structure has been assembled will not be adversely affected by this problem.

5.2.4.2 Development Phase Testing

During this phase, three additional test programs were conducted to answer questions relative to potential environmental damage. A detailed description of these tests can be found in Reference 22. They consist of freeze testing, clogging testing and additional lightning strike testing.

Samples were subjected to freeze testing to determine the extent of damage to the suction surfaces from water accumulated internally and subjected to a freezing environment. Four concepts were tested: The bridged slot, the aluminum foam base, the perforated strip, and the slot plenum. The samples were filled with water and frozen and repeatedly subjected to this test cycle. The test conditions were more severe than can be expected in actual service. None of the specimens were damaged.

Pressure loss and clogging tests were performed on the foam aluminum base concept. The foam adversely affected the airflow distribution and was susceptible to clogging. It was therefore considered unacceptable.

Lightning strike tests were conducted on a simulated conventional construction/fiberglass cover concept with the aluminum foam base suction surface. Figure 5.2-33 shows the details of this panel and Figure 5.2-34 shows the test set-up. The panel survived damage from strike magnitudes far beyond that to be expected in service on the laminarized areas of the wing surfaces.

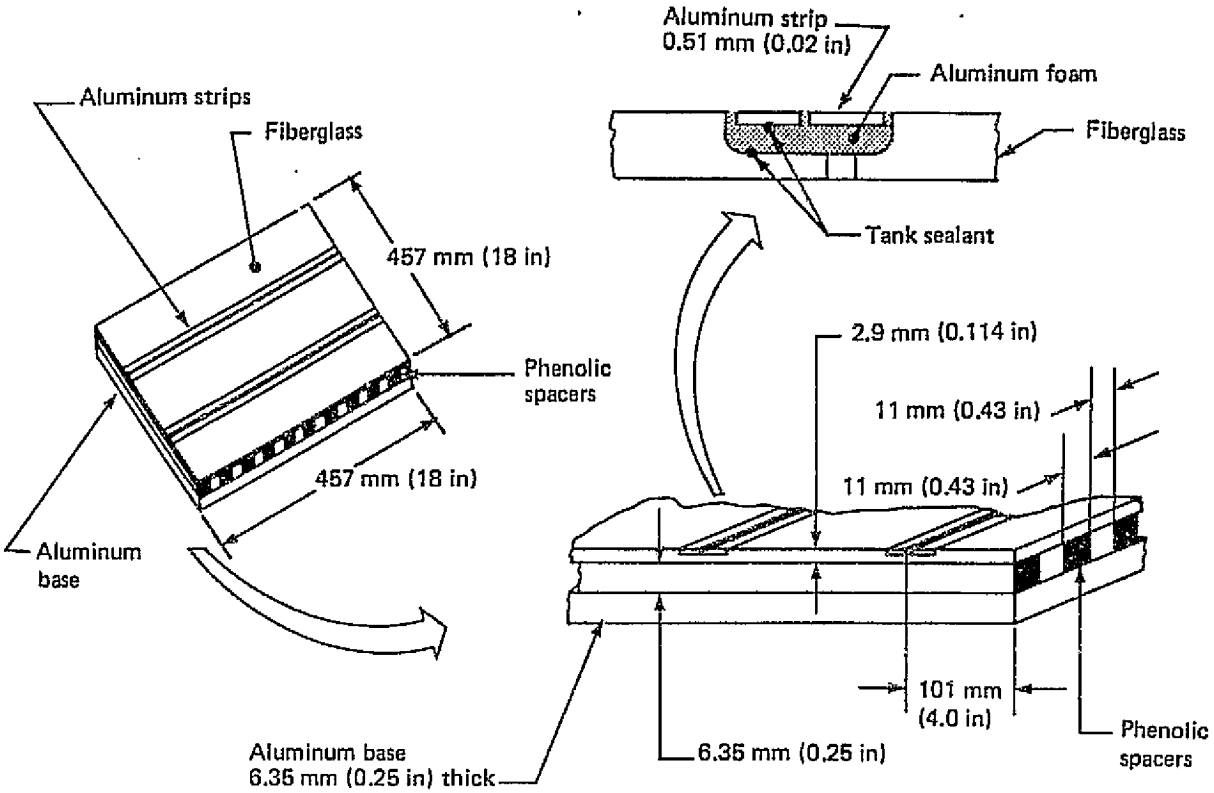

Figure 5.2-33.. Lightning Strike Specimen

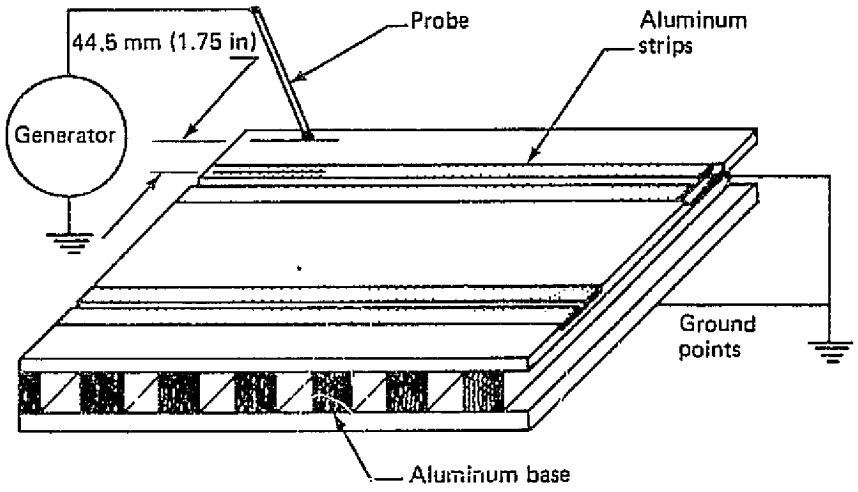

Figure 5.2-34. Lightning Strike Test Setup

5.2.5 STRUCTURAL WEIGHT EVALUATION

Weight evaluations of the various wing structural concepts were conducted in order to determine the effects of design details on wing structural weight. These evaluations were used to assist in the selection between alternate designs and to assess the weight impact due to various approaches in existing designs.

5.2.5.1 Wing Analysis Techniques

The wing structural concept weight evaluations were conducted using a computerized beam analysis program (ORACLE) to determine the load sensitive weight of the wing box structure. Utilization of ORACLE provided an accurate accounting of the amount of structural material required for the strength design of the various structural concepts. The effects of maneuver and gust design conditions on the required structural material were included in the designs to provide realistic evaluations.

The weight of non-load sensitive items and secondary structure (e.g., leading edge and trailing edge) were developed using a combination of statistical and parametric techniques taking into account applicable design parameters. These techniques are based on previously developed methodology and design studies, as well as past Boeing experience with production airplanes.

5.2.5.2 Wing Structural Concept Evaluation

As stated in Subsection 5.2.2, two phases of concept development were undertaken during the course of the LFC contract. These phases were the exploration and the development phases.

(a) Exploration Phase

The concepts evaluated during the exploration phase (i.e., the first year of contract) have been discussed in Paragraph 5.2.2.1. These concepts were evaluated using the baseline airplane configuration (Model 767-807) having the following characteristics:

- Wing Quarter Chord Sweep — 25°
- Wing Aspect Ratio — 10.0
- Wing Trapezoidal Area — 340 m^2 (3650 ft^2)
- Taper Ratio — 0.35
- Trailing Edge Break — 30% Semi-Span
- Design Gross Weight — 170 100 kg (375 000 lb)

These concepts incorporated spanwise suction ducts that were integral to the structure. This approach tended to minimize the weight penalties to incorporate LFC into the structure, but required the selection of structural designs that are not as efficient as conventional skin-stringer structure for this airplane configuration. Figure 5.2-35 compares the surface panel weight and total wing weight of the various

Concept	Structural weight of		
	Cover panel, kg (lb)	Upper panel, kg (lb)	Total wing, kg (lb)
Reference 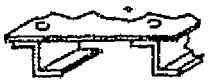	6454 (14 230)	5588 (12 320)	20 797 (45 850)
Concept No. 1 Laminated aluminum concept 	7135 (15 730)	6209 (13 690)	22 697 (50 040)
Concept No. 2 Laminated titanium concept 	7888 (17 390)	6650 (14 660)	24 013 (52 940)
Concept No. 3 SPF/DB titanium concept 	7800 (17 190)	7071 (15 590)	24 330 (53 640)
Revised concept No. 1 	7865 (17 340)	6477 (14 280)	23 686 (52 220)
Concept No. 4 Graphite/epoxy concept 	5905 (13 020)	6241 (13 760)	21 046 (46 400)

116120-122

Figure 5.2-35. Initial Weight Comparison—25-Deg Wing Sweep

concepts that were evaluated. The weight of LFC systems (i.e., compressors, turbo-shaft drives, etc.) are not included in the total wing weight but are separately accounted for and assumed constant for the various concepts. The revised laminated aluminum concept was chosen as the preferred alternative at the completion of this phase.

(b) Developmental Phase

The concepts evaluated during the developmental phase (i.e., the second year of the contract) have been discussed in Paragraph 5.2.2.2. A different wing planform was used in the evaluation of these concepts. This approach was taken because, at this juncture, critical design considerations were being studied intensively, which appeared to dictate a wing sweep reduction. The applicable airplane configuration (Model 767-809) had the following characteristics:

- Wing Quarter Chord Sweep — 15°
- Wing Aspect Ratio — 10.0
- Wing Trapezoidal Area — 340 m^2 (3650 ft^2)
- Taper Ratio — 0.35
- Trailing Edge Break — 40% Semi-Span
- Design Gross Weight — 165 500 kg (365 000 lb)

The concepts evaluated during this phase were generally designed to incorporate LFC into more efficient structural concepts than in the previous study. Although this resulted in a larger parasitic weight level, the overall weights tended to be lower. Figure 5.2-36 compares the two concepts fully developed in this phase and the updated laminated aluminum concept, designated the reference LFC wing.

(c) Evaluation

As a result of this study, it was shown that LFC wing concepts tend to separate into two categories:

1) Concepts with less efficient structural designs and relatively small parasitic weight penalties due to LFC.

2) Concepts with efficient structural designs and relatively large parasitic weight penalties due to LFC.

The Laminated Aluminum concept is an example of the first category and the Conventional Construction/Fiberglass Cover concept is an example of the second category. As can be seen in Figure 5.2-36, the total wing weights of the two concepts are nearly the same. However, due to the changes in wing geometry, suction requirements, and secondary structure design, a direct comparison between the concepts shown in Figure 5.2-35 and Figure 5.2-36 cannot be made.

Concept	Laminated aluminum, kg (lb) (Reference LFC wing) 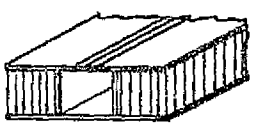	Inverted stiffeners fiberglass cover, kg (lb) 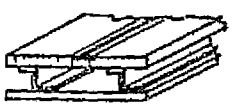	Conventional construction fiberglass cover, kg (lb) 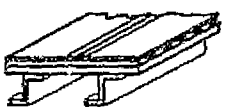
Lower panel	8133 (17 930)	7892 (17 400)	7289 (16 070)
Structure	8133 (17 930)	7008 (15 450)	6700 (14 770)
Cover	— —	884 (1950)	589 (1300)
Upper panel	7439 (16 400)	9956 (21 950)	8105 (17 870)
Structure	7439 (16 400)	9072 (20 000)	7475 (16 480)
Cover	— —	884 (1950)	630 (1390)
Total wing	24 980 (55 070)	27 201 (59 970)	24 788 (54 650)

Figure 5.2-36. Final Weight Comparison—15-deg Wing Sweep

5.2.6 CONCEPT SELECTION AND DEFINITION

For each of the structural candidates studied in detail the qualitative requirements and criteria have been met to a level required for final concept selection. While various cost-related factors were considered, no detailed manufacturing cost figures were obtained. Because of this, the manufacturing cost was judged purely on a manufacturing complexity basis. Resolution of questions on maintenance and repair is also judgmental and the candidates were all given numerical ratings relative to four categories, namely: Periodic inspection of primary structure, Corrosion prevention and repair, Isolation and repair of fuel leaks, and Repairability of structural damage. The ratings as shown in Figure 5.2-37 are not all on the same value scale so they cannot be totaled to give a definitive numerical answer. Thus the final selection was based on structural weight (obtained by analysis) and judgments of the relative risk associated with each concept.

The Conventional Construction/Fiberglass Cover has been selected as the best overall choice for a relatively near term application to an LFC transport and to support construction of a validator aircraft in the 1985 time period. The concept has the potential of being used with new structural materials as they develop, but for near term application uses familiar materials, and requires only the final development of inspection techniques to provide a low-cost workable design adaptable to existing production processes. In the final analysis, the advantage in cost, maintenance, and repairability of conventional structure concepts and the difficulties of incorporating the latest suction requirements into the laminated aluminum concept resulted in the selection of the Conventional Construction/Fiberglass Cover concept, as depicted in Figures 5.2-21 and 5.2-24, for application to the selected final LFC transport configuration.

The development of replaceable suction strips which have a flow control feature can still benefit from further design studies. With only limited testing complete, the most promising candidate is the slotted plenum design. It is, at present, the only design that has demonstrated the ability to adequately control the suction air flow and so it was selected for the final LFC configuration.

Concept			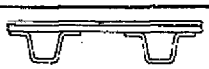	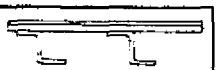
Periodic inspection of primary structure	3	4	2	1
Corrosion prevention and repair	4	4	2	2
Isolation of fuel leaks	2	2	4	4
Repairability of structural damage	4	3	2	1

● Judgmental comparisons. The lower the number, the less detrimental to maintainability.

Figure 5.2-37. Structure Concept Selection—Maintenance and Repair Evaluation

5.2.6.1 Wing Concept Definition

The following paragraphs discuss the definition of the selected structural concept. More detailed discussion and applicable drawings can be found in Reference 23.

(a) Air Collection System

As noted previously and shown in Figure 5.2-24 the wing surface is divided into five areas. The air from each area is sucked chordwise across the wing box to one of the trunk ducts. Air collected in the trunk ducts is routed as shown in Figure 5.2-38 to the suction unit located at the wing root. The flow balance in the suction system is maintained by appropriately and selectively sizing the bleed holes in each suction strip and by valves in the trunk ducts. Figure 5.2-39 is a schematic representation of a typical portion of the wing surface, the flow passage and control elements and a single trunk duct serving a section of the upper surface. The essential features associated with operation and control can be adjusted as required to yield an appropriate suction air distribution throughout the flight envelope.

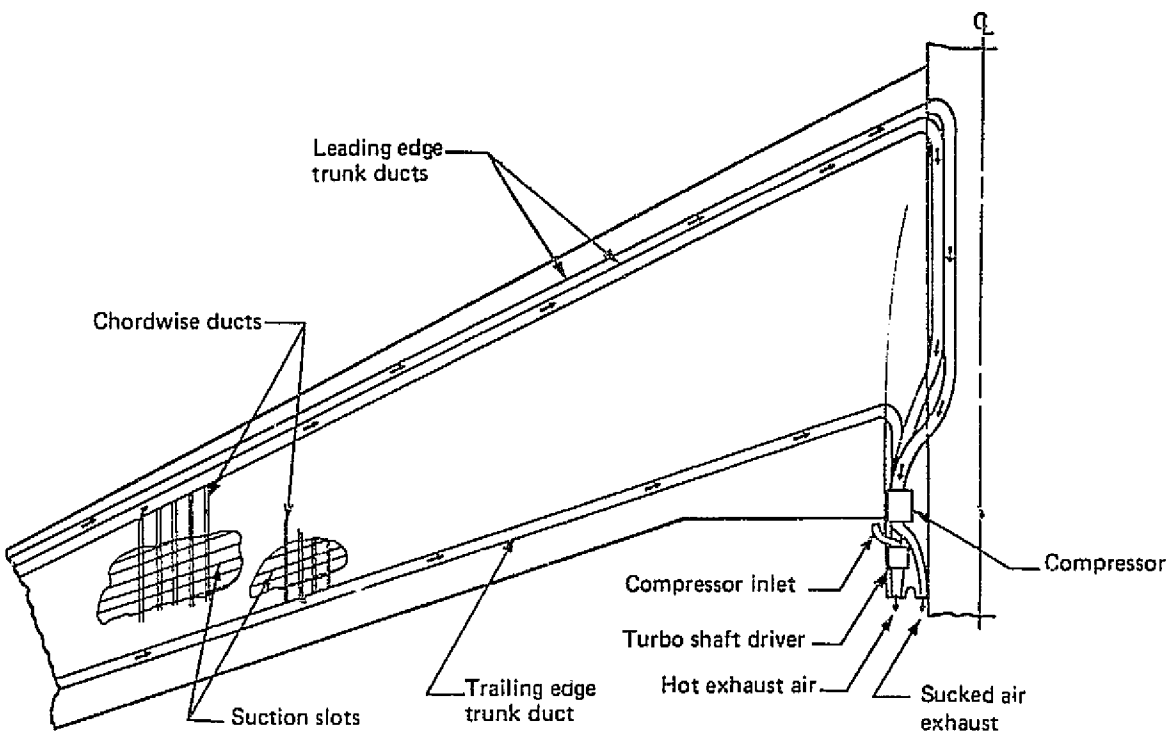

Figure 5.2-38. Conventional Structure--Air Collection System Schematic

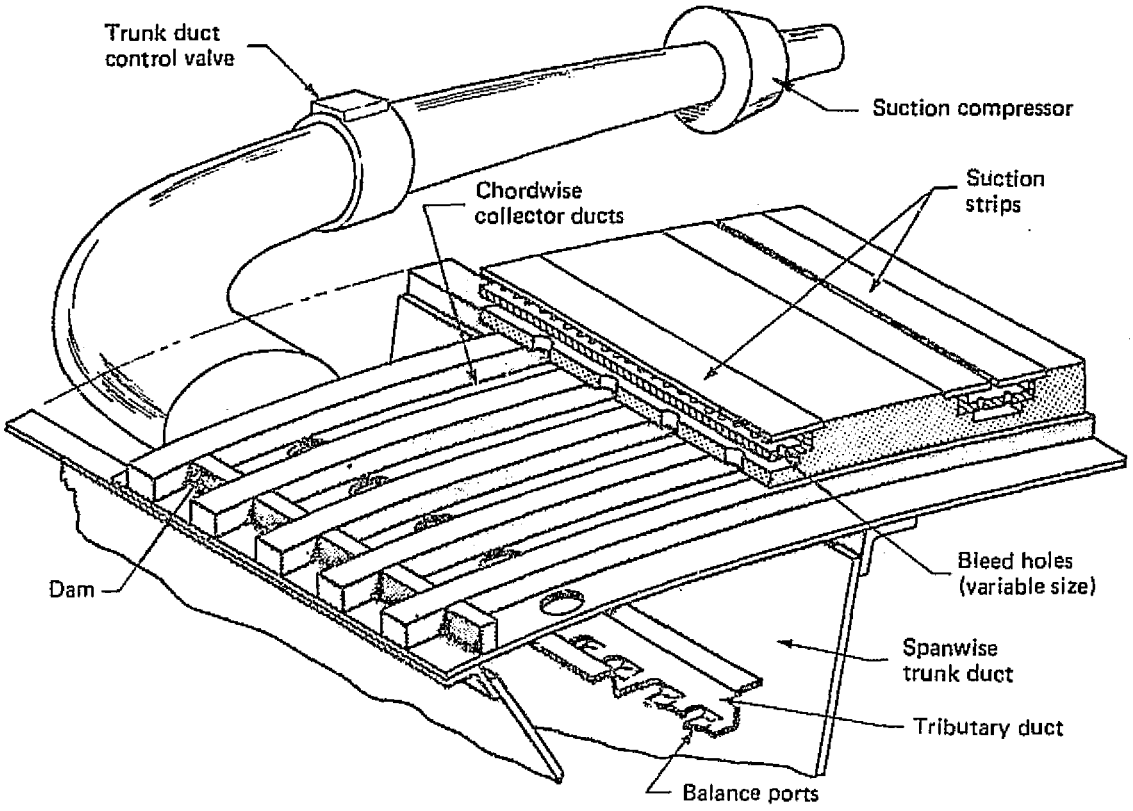

Figure 5.2-39. LFC Suction Control System

(b) Wing Box

The wing box is of conventional design and construction with upper and lower panels having stringers running parallel to the rear spar. Structural sizing was based on estimated properties of advanced aluminum alloys. The upper panel skin and stringers are made of an aluminum alloy with material characteristics projected from the 7075 aluminum data base and the lower panel skin and stringers are made of an aluminum alloy with material characteristics projected from the 2024 aluminum data base. The lower panel has four splices to provide fail-safety. The front spar has a honeycomb panel web to give a smooth wall for the leading edge trunk duct. The rear spar and the ribs are of conventional stiffened sheet construction.

(c) Wing Box Suction Surface

The suction surface panels are made of fiberglass and urethane foam and the spacers are made of self-skinning urethane foam. Figure 5.2-40 is of a typical section showing these elements and the slot plenum insert. The self-skinning sides of the spacers form non-absorbent walls for the chordwise ducts. The outer panel is a constant thickness fiberglass and urethane foam sandwich the external surface of which will be designed for durability. The outer face as shown has three plies of .114 mm (.0045 in) fiber-

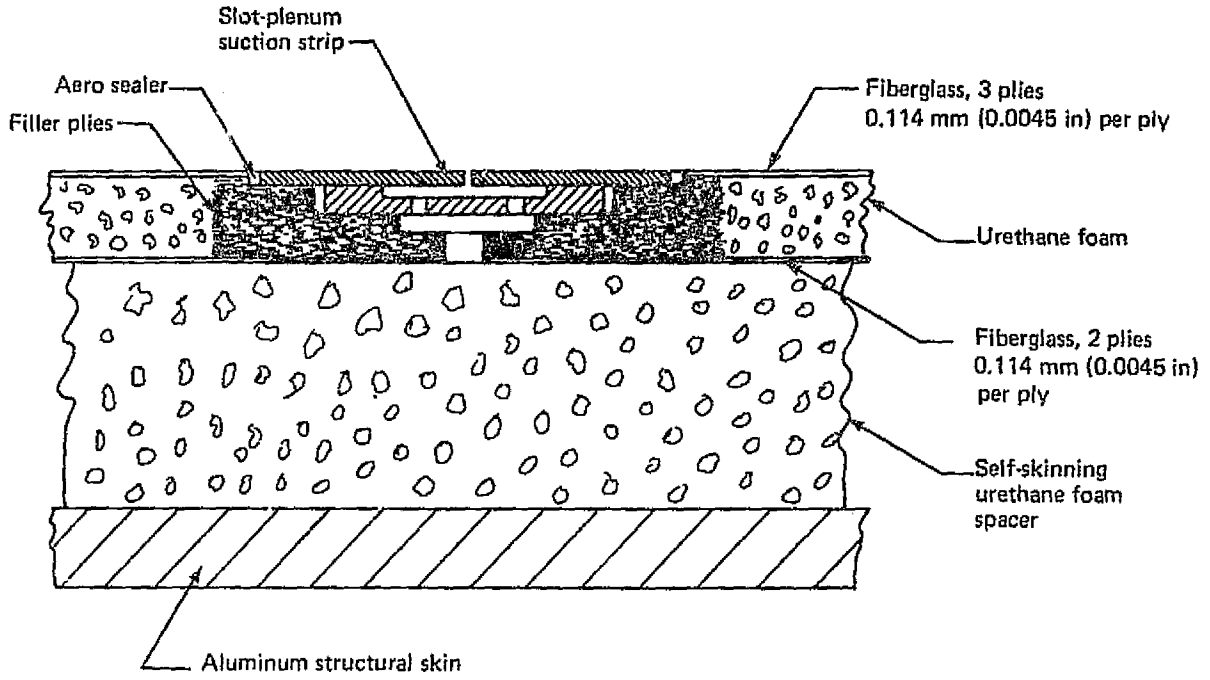

Figure 5.2-40. Wing-Box Suction Surface

glass cloth. This is the same thickness as the trailing edge panels on the 747 airplane. However, developmental testing is necessary to ensure a 20-year life span. This may ultimately show that additional plies are required. The outer panel is solid fiberglass at the suction strip locations, the grooves for the suction strips will be machined after the panel is removed from the mold. The rigid urethane foam is a closed cell type and is not exposed to moisture except in the event of surface damage. If the self-skinned wall surfaces or the fiberglass skins are damaged some moisture can be absorbed. The closed cell nature of the foam limits the water absorption to the immediate area of the damage. The percentage weight gain of the foam in this area could be up to 8% for a 321 kg/m^3 (20 lb/ft^3) foam.

(d) Leading Edge

The leading edge assembly consists of an upper and lower panel, duct separators, the auxiliary front spar and the nose assembly. Figure 5.2-41 illustrates the structural arrangement. The upper and lower panels are fiberglass and urethane foam sandwich panels of which the outer surface is very similar to that of the outer panel over the wing box. The core of the panel is made from strips of self-skinning urethane foam and the inner skin is five plies of fiberglass. The duct separators and the auxiliary front spar are bonded aluminum honeycomb to give smooth surfaces to the trunk ducts.

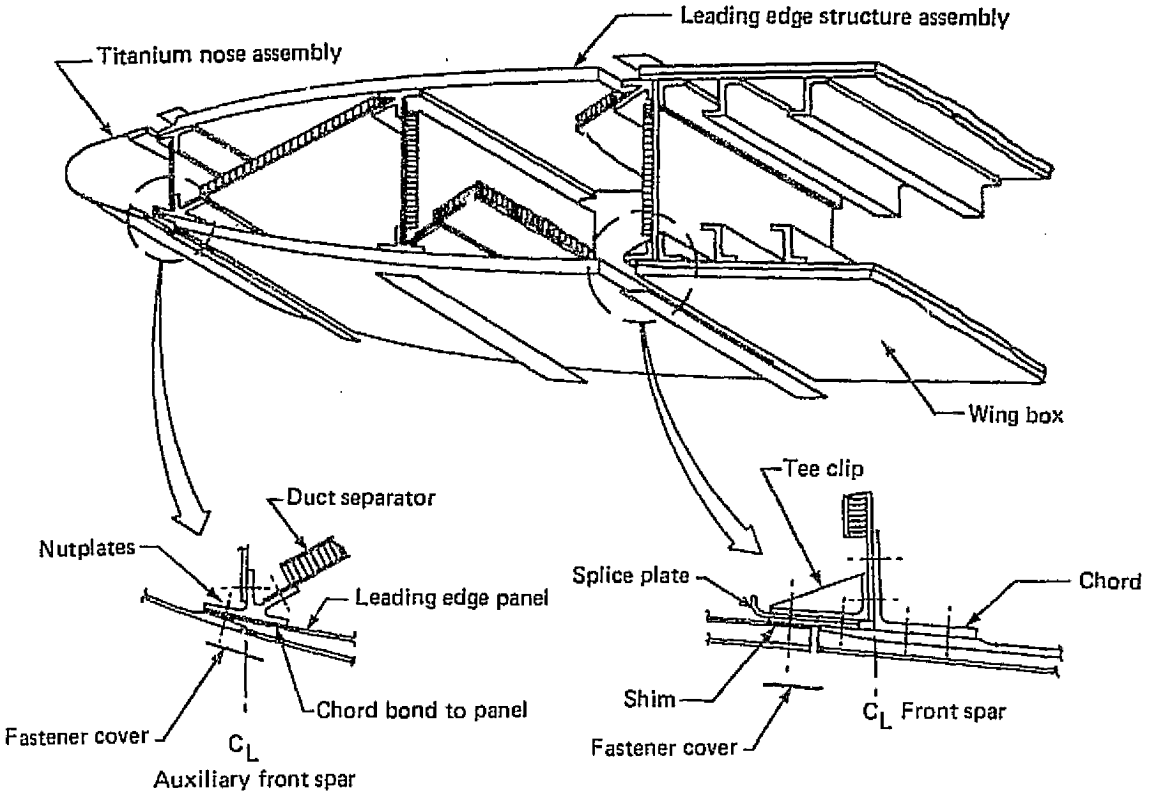

Figure 5.2-41. Leading Edge Structure Assembly Sequence for Conventional Structure/ Fiberglass Cover Concept

The nose assembly is shown in Figure 5.2-42. The nose skin is made of titanium for good erosion resistance and is manufactured in 6.1 m (20 ft) lengths. It is designed to be readily removable for ease of maintenance and repair.

Although no final selection of leading edge systems has been made, a candidate system is included for illustration in Figure 5.2-42. The leading edge contains the ducting and flow passages required for the appropriate combination of anti-icing, frosting, and suction systems.

(e) Trailing Edge

The trailing edge is laminarized on the upper surface back to 80% chord. The remainder of the trailing edge structure including flaps, spoilers and ailerons is similar to conventional turbulent airplane design. Only the laminarized part is detailed in this report.

The upper panel is the same construction as the leading edge panels but, because of the many support ribs for flaps and spoilers etc. and because reasonable access is required to the rear spar for servicing, the sucked air is carried along the rear spar in a separate

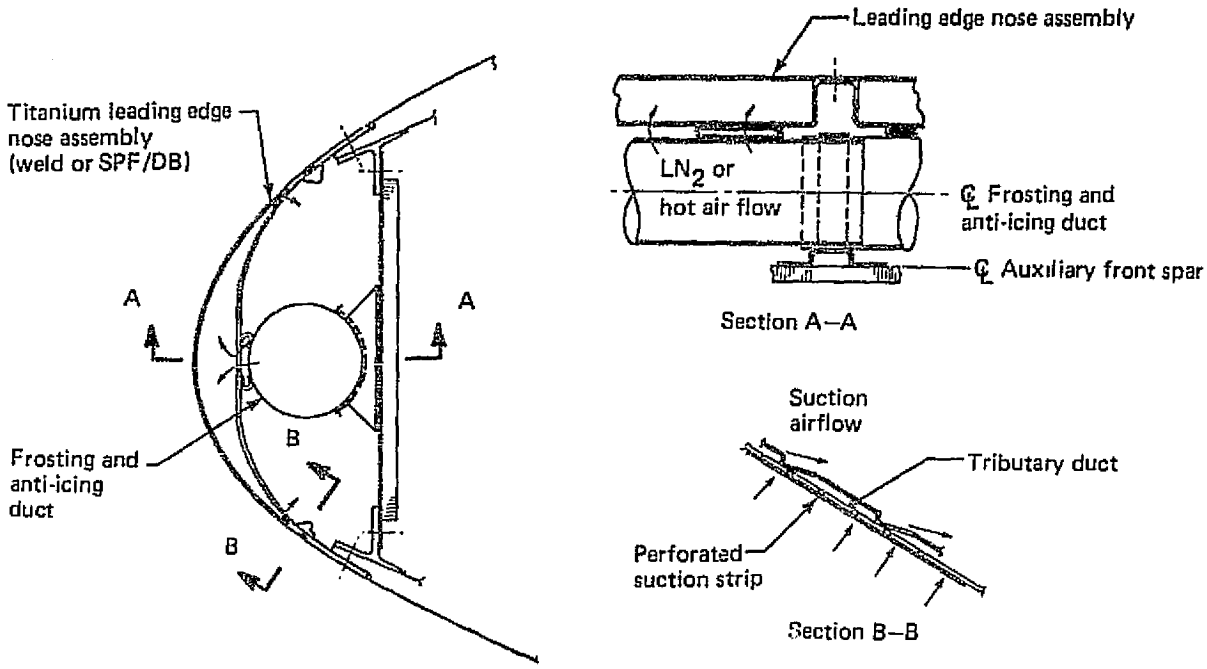

Figure 5.2-42. Leading Edge Nose Assembly

duct as shown in Figure 5.2-24. The duct is of filament-wound fiberglass and foam sandwich construction.

(f) Access Openings

An additional benefit obtained from the selected concept is laminarization across the access holes in the wing lower surface. These holes use a standard door and become unique items only after the foam spacers are attached. The spacers will be machined in the same operation as those on the wing box. After the external panel is attached a ring-shaped cutout is made to allow access to the clamp ring fasteners on the door. A clamp ring cover is installed in the cutout to give continuity to the suction surface. The cover consists of a fiberglass and foam outer panel similar to the main box outer panel. Instead of being supported with self-skinning urethane foam spacers it is supported by "Duocel" foam aluminum spacers. These spacers line up with the wing box spacers to form continuous ducts. They are used as compressible shims with no springback to ensure that the outer surface is smooth and flush after the ring is rolled into place. This method of installation allows the clamp ring cover to be a standard item. The compressible foam spacers also allow the ring to be pushed down to suit the differences in contour for various parts of the wing. The final stage of the installation (not illustrated) involves machining an insert groove continuously through the rings and door covers during the strip installation process for the wing. Emplacement of a continuous strip insert across the rings and door covers is accomplished in

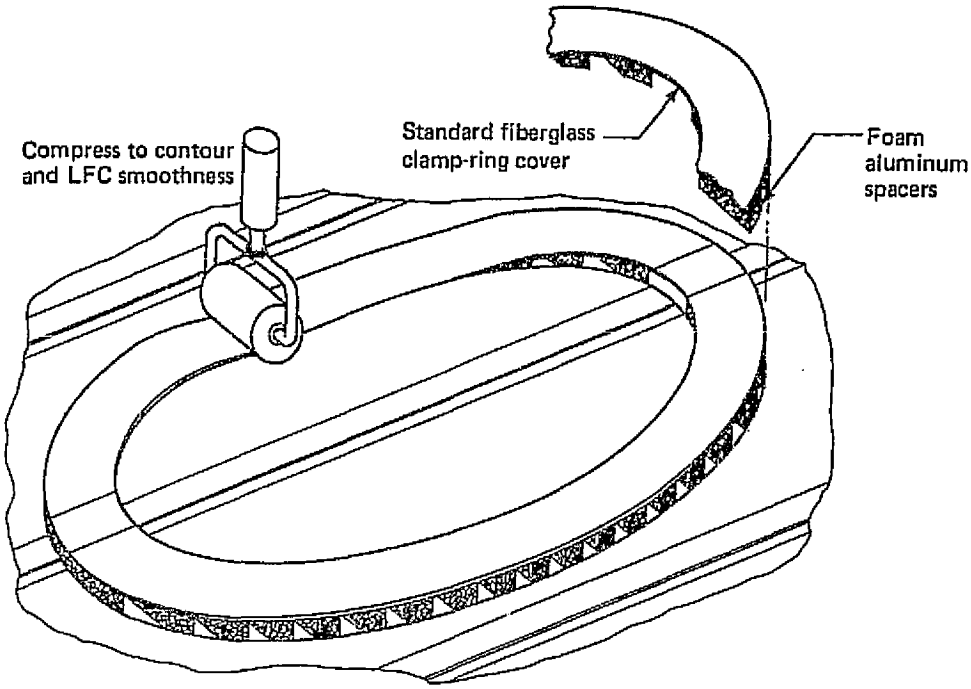

Figure 5.2-43. Clamp-Ring Cover Installation With Suction Across Access Holes

the same manner as in other areas. It should be noted that to remove an access door the clamp ring cover must be destroyed, but, as they are all standard, replacing with a new one should not be a significant problem. This concept will require further study and testing to ensure that deflections built into the clamp ring cover on installation plus operational deflections and vibration do not cause the foam aluminum to expand and put the surface out of tolerance. The concept is illustrated in Figure 5.2-43 where the basic arrangement and the installation approach are shown.

(g) Drainage and Corrosion

Water can be expected to enter the suction system at some time during airplane operation although the greatest exposure is expected on the ground. While tests have demonstrated that no structural problems will exist from freezing, a drainage system is provided. Drainage for the chordwise ducts of the upper wing surface is accomplished by locating entry holes to the trunk ducts at the lowest points of the chordwise ducts. That this can be done is apparent from Figure 5.2-24. The current arrangement shows a dam at 65% chord which is a flow-restrictor type allowing water to drain to the rear trunk duct as necessary and still serve to maintain the required airflow distribution at the suction surface. Overboard drains for the trunk ducts are located near the wing tip and at the side of body outside of the laminarized areas. The wing lower surface requires no special drainage provisions in the chordwise ducts. The trunk ducts for

lower surface air have the same drainage provisions as those for the upper surface air. Check valves are provided at each drainage point to prevent air inflow during operation of the LFC system.

Corrosion inside the wing box will present no new problems. The external surface of the wing structural skin will be treated per BAC 5555 prior to bonding on the spacers, and coated with corrogard after the spacers are bonded on. This is the same finish that is now used inside the air conditioning ram air ducts on the 727 airplane and no corrosion has been detected in these areas since this type of protective system was introduced. The environment inside the ram air ducts is more severe than that expected in the chordwise ducts of a LFC airplane since suction airflow will remove most of the moisture. The presence of corrosion, if it should occur, can be detected by NDT methods long before it becomes structurally critical.

(h) Lightning Strike Protection

The wing has a low probability of being struck by lightning except at the tips. Figure 5.2-44 shows the major lightning strike zones indicating that the laminarized portion of the wing is in a low probability zone. The wing tips are not laminarized and their surfaces are aluminum. The metal suction strips are grounded to the tip

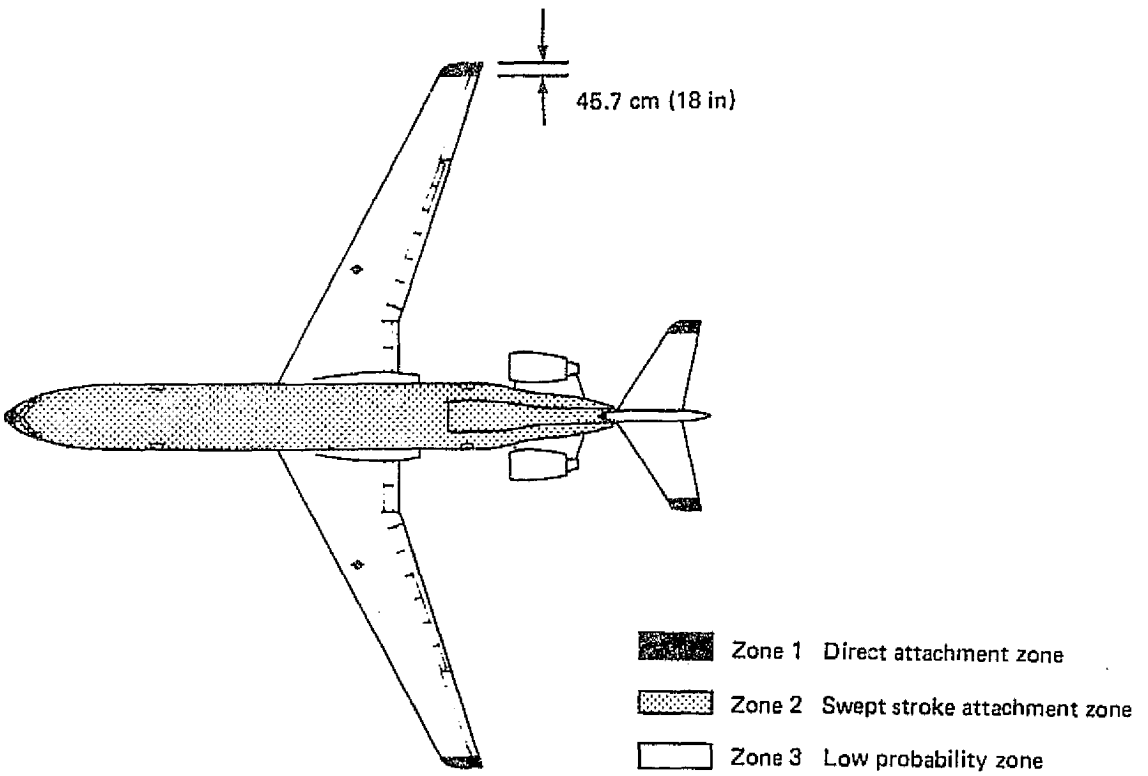

Figure 5.2-44. Lightning Strike Zone Definition

and at the side of body to minimize the possibility of damage to the suction surface. Figure 5.2-45 shows the elements of the wing tip design. More details of lightning strike testing, supporting the conclusion that damage is unlikely, can be found in Subsection 5.2.4.

5.2.6.2 Horizontal Tail Design

Application of LFC to the empennage was not considered in detail until a structural concept for the wing had been selected. The decision was made to use a concept similar to the wing in virtually all respects except for the structural box. Conventional skin-stringer construction for the horizontal stabilizer was not suitable for LFC because the lightly-loaded skin is normally allowed to buckle at low loads. Adding thickness to the skin to prevent buckling was too much of a weight penalty so aluminum honeycomb was selected for the basic structure. The suction surface, leading edge and trailing edge designs closely parallel those of the wing design.

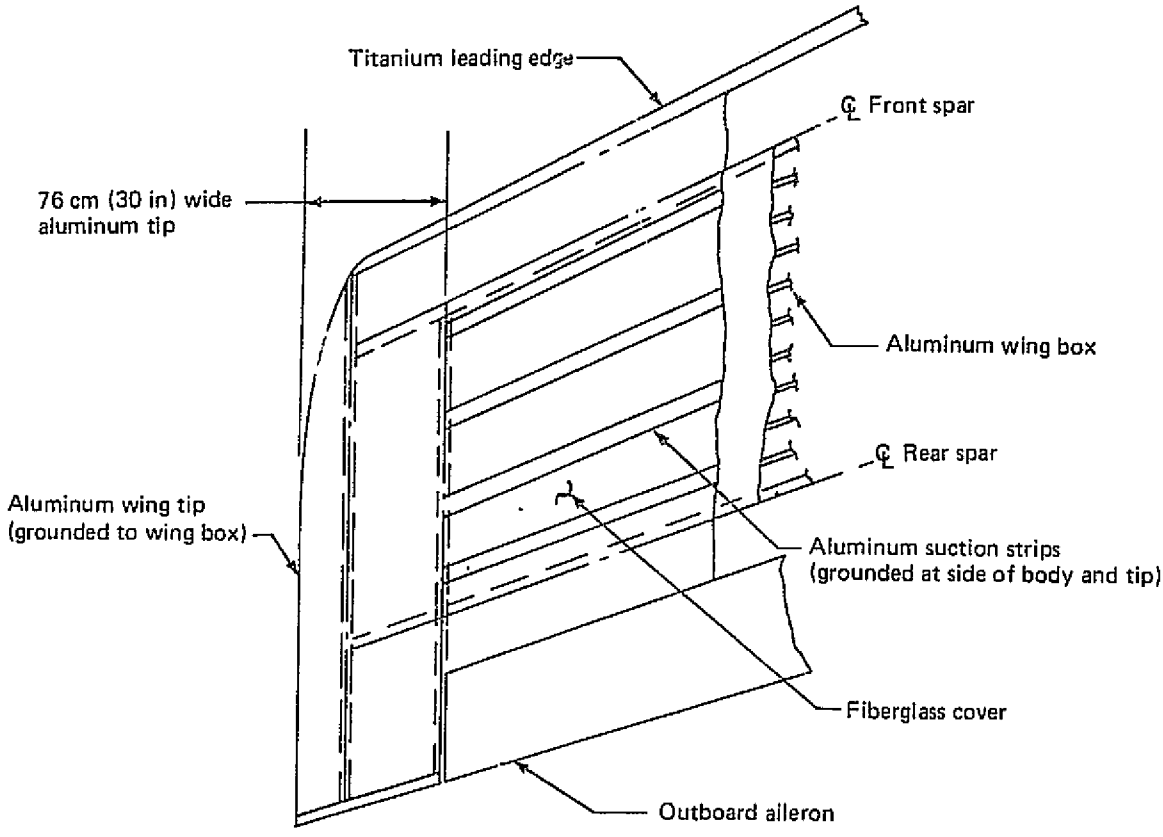

Figure 5.2-45. Wing Tip Design for Lightning Strike

5.2.7 MAINTENANCE AND REPAIR (SELECTED CONCEPT)

The study airplanes incorporating LFC capability are substantially more difficult to inspect, maintain and repair than a conventional turbulent airplane. The conventional construction/ fiberglass cover concept minimizes many of these problems.

Routine maintenance inspections are normally conducted to locate structural cracks, corrosion, erosion, fuel leaks, system leaks, etc. Typical wing damage to current commercial aircraft consists of the following:

- Cracks–(fatigue and stress corrosion)
- Corrosion
- Ground Incidents–(collision with service vehicles, other aircraft, and fixed objects while towing)
- Jacking Incidents–(puncture and/or scoring)
- Engine Rupture–(puncture by flying parts)
- Falling Objects
- Bird Strikes
- Lightning Strikes–(puncture and etching)
- Hail Damage–(inflight and on the ground)
- Tire Treads Separation–(puncture and denting)

It is estimated on the basis of extensive service experience that cracks and corrosion repair account for 90% of the structural repair work on the wing. Repair of cracks in the primary structure would be accomplished in essentially the same manner as for a normal turbulent airplane except for the removal and replacement of portions of the outer glove and foam spacers. Figure 5.2-46 illustrates a repair procedure for the spacers and outer panel when damage is in an area of high strain and is large in size. The cover and spacers would be cut away to permit repair of the aluminum structure. Following this repair, the spacers would be replaced. Either foam or foam aluminum can be used. Using foam aluminum may be easier as it can be crushed to the proper thickness. The pre-made repair panel would then be bonded in place. Epoxy filler and sanding to contour would be used to smooth out mismatch. The groove would then be machined to receive a replacement segment of the suction strip. Small repair areas and areas in regions of low wing strain would not require the overlap of the cover and a simple butt joint repair would suffice.

Many forms of damage can occur to the outer surface of an LFC wing and no historical data is available to evaluate the extent and frequency of damage to be expected. New operating procedures will be required to minimize damage to the wing surfaces from such things as fueling hoses, dropping tools, walking on the wings, hail, snow removal, etc.

The external structural surface, using the selected concept, would generally be well-protected against corrosion. After the foam spacers are bonded in place, the entire surface would be completely covered with Corogard (or a Skydrol resistant equivalent). Machining of the spacers to meet LFC smoothness requirements, before bonding on the

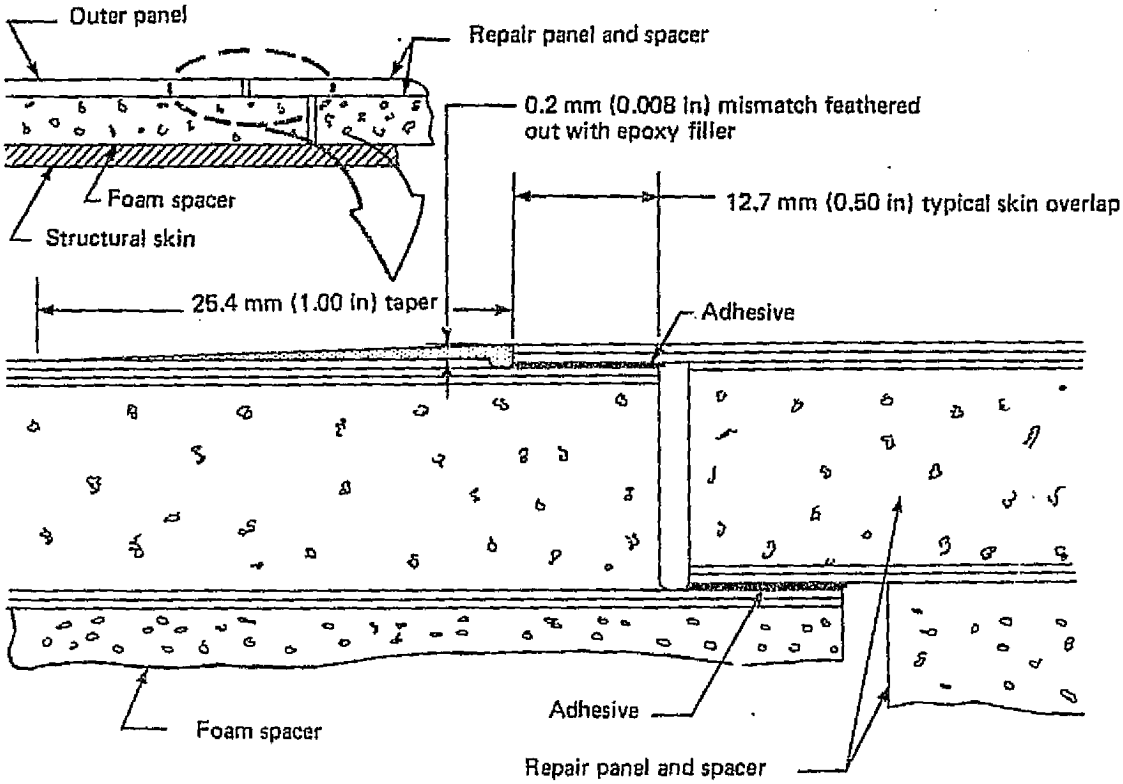

Figure 5.2-46. Cover Repair Scheme

outer cover, would not damage the Corogard covering the aluminum skins. No subsequent exposure to scratching, denting, or eroding would normally be expected. Boeing's experience with fuel vent lines and airconditioning ram air ducts has indicated that this design will eliminate the necessity for frequent corrosion inspection and repair on the outer surface of the structural skin in laminarized areas.

The leading edge structure is fiberglass from the front spar to the auxiliary front spar and has a titanium nose cap. Therefore, no corrosion or significant erosion problems are expected.

The trailing edge structure and the internal surface of the main wing box are today's conventional state-of-the-art and pose no new problems.

5.2.8 MANUFACTURING REQUIREMENTS (SELECTED CONCEPT)

The current Manufacturing Plan is to fabricate and paint complete wing box assemblies prior to the wing-body-join. All wing LFC Features will be incorporated in the manufacturing sequence prior to the paint operation. The exterior surfaces of LFC wing boxes differ from conventional wings in that these surfaces are phosphoric acid anodized to enhance integrity of subsequent bonding operations. In order to attain the surface regu-

larity necessary to support laminar flow, the wing covers must be laid-up as a single part. While this poses some formidable problems in tooling and assembly, it appears to be the manufacturing approach which has the greatest probability of success. The covers will have their outer surfaces laid up against a caul-plate contoured to airfoil surface shape. Spacer strips, bonded to the outer surface and machined prior to assembling the outer skin, become the tolerance payoff members. The manufacturing process is illustrated in Figure 5.2-47 showing the essential operations and performance sequence.

5.2.8.1 Subassembly of LFC Components

The subassembly requires a number of unique facilities, machines, processes and tools:

(a) Suction strips will be fabricated as continuous subassemblies from coil stock which has been anodized prior to use. Two strips and an extrusion will be machine joined following roll straightening and adhesive roller coating. Development of a production joining machine is a requirement.

(b) Spacer blocks fabricated of extruded self-skinned foam will have excess height dimensions. Prior to bonding to the aluminum wing, the bonding surface of the spacers require milling for which a feed-through milling machine will be required.

(c) The outer panel (fiberglass/foam) will be laid up in a full wing surface female caul plate to control the exterior surfaces to critical contour and smoothness dimensions. This process requires expanded Numerical Control (NC) machining capability as well as increased handling capacity. Accurately locating the suction strips will require the use and development of a production laser scribing system.

(d) Curing of the laid-up exterior skin assemblies requires a new, very large autoclave. (Approximately two and one-half to three times as large as any now existing at Boeing.)

(e) Peripheral trim of the cured skin requires the development and use of an electronic measuring device coupled to an X-Y-Z manipulating mechanism for directing conventional cutters over the skin's surface.

5.2.8.2 LFC Suction Panel Installation

Attachment of the LFC panels to the wing box requires unique capabilities:

(a) Attachment of the spacer blocks to the wing-box skins necessitates the development of a mechanized layup machine capable of applying a series of spacer blocks to the surface during each sweep of the box surface.

(b) Machining of the spacer blocks to net height will require the development and acquisition of an extremely large surfacing machine with NC control and three axis capability. Provisions will have to be made for exhausting a considerable quantity of foam waste.

(c) Fitting of the exterior skins to the foam block machined contour requires the development of a non-destructive testing (NDT) system to verify acceptability of fitup prior

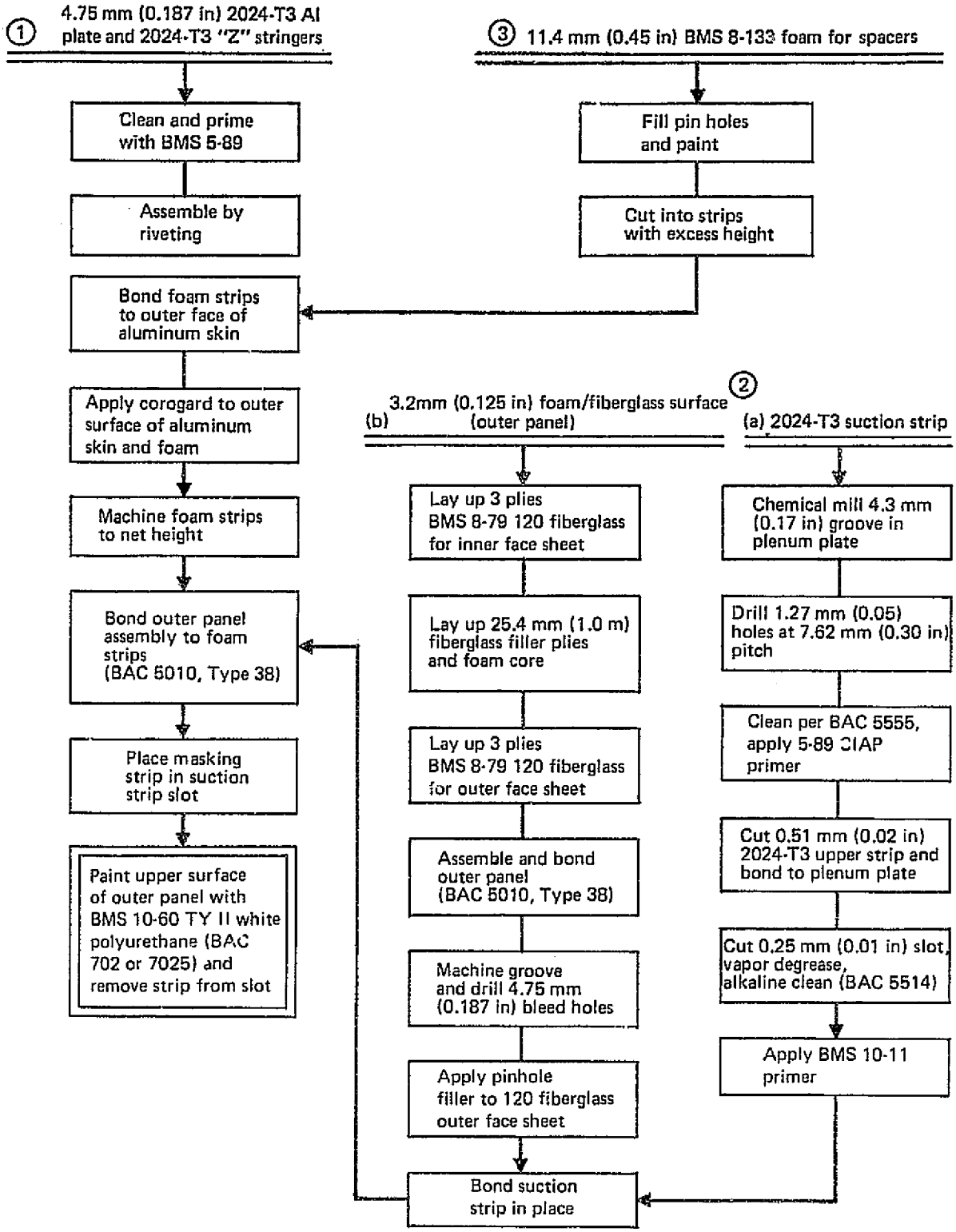

Figure 5.2-47. Manufacturing Sequence for LFC Surface Assembly

to, during and after bonding. Bonding of the suction strips in place will require an automated adhesive application system with alignment capability incorporating pressure application provisions.

(d) Milling of slots for suction strips necessitates the development of a magnetic following system to locate the buried reinforcements, that operates in conjunction with a vacuum-attached milling system and vacuum exhaust system. Drilling of through-holes from the outer surface to the between-spacer areas will involve a multi-spindle drill attachment to the NC controlled slot-milling apparatus.

(e) Wing painting requires a controlled air supply and duct-attach system to provide plenum pressurization for paint exclusion. Roll-over capability for access to both surfaces will be needed (see Figure 5.2-47).

Existing Aero-Space Production capabilities to support this preliminary Manufacturing Plan do not currently exist. All processes, tools and equipment have already been verified in the conceptual stages by small-scale hardware and laboratory testing. Full-scale capability for production would require an extensive developmental program leading to verification with full-size hardware for each process and/or concept. Manufacturing technology development will be required in support of each of the foregoing processes. Primarily in the bonding discipline, effort will need to be addressed to the maintenance of close-fitting joints and theidentification of gap-tolerant adhesives. NDT development will be necessary for verification of bond integrity during manufacture as well as inspectability of the covered wing during in-service use.

Existing airplane production facilities could not be used for fabrication and assembly of LFC components and for airplane final assembly. New facilities would have to be developed utilizing a clean room atmosphere similar to those utilized for fabrication of decorative passenger accommodations or Quality Control laboratory conditions for instrument calibration. To further protect the LFC components from contamination and damage, a massive training program would have to be instituted for personnel that would be working on these vehicles to condition them for the work environment and to instill the proper "Zero Defect" attitude and approach.

None of the foregoing complexity factors have been given a cost impact for this program. Nevertheless they must be considered as a substantial risk element in any program assessment.

5.3 SUCTION PUMP AND PROPULSION SYSTEM

This section discusses the process used in defining the suction pump system and the main propulsion engine. Selection and definition of the suction pump system and its location in the airplane was done through a series of trade studies. The main propulsion engine was selected on the basis of the expected technology level for the 1990 time period and the engine cycle was finally selected to be near-optimum for an LFC airplane based on a separate trade study. The results of these trade studies and the rationale used in the selection process will be presented in the following paragraphs.

These studies were conducted as a subtask of the concept evaluation task under Subtask 4.2.3. The concept development effort was conducted in relation to the LFC baseline aircraft, Model 767-807, which was also based on technology levels consistent with an airplane service entry in the 1990 time period. Pratt and Whitney Aircraft (P&WA) provided consultation and technical service for the main propulsion engine, and AiResearch Manufacturing Company of Arizona provided the same for the suction pump system. United Airlines (UAL) was also consulted on the maintainability aspects of the suction pump system.

5.3.1 DESIGN REQUIREMENTS AND OBJECTIVES

The main propulsion engines do not have a direct impact on the feasibility and viability of the LFC system; hence, the design requirements and objectives for defining the main engines were based on the airplane thrust requirements and technology level expected in the 1990 time period. Also, the selected engine bypass ratio was desired to be optimized for this particular airplane. These and other design requirements and objectives are consistent with those of any turbulent advanced technology transport which must conform to Boeing design practice and for which the applicable FAR regulations must be satisfied.

The design requirements for the suction pump system were to provide the necessary suction power at all flight conditions within the flight envelope while maintaining acceptable reliability, maintenance and flight safety characteristics. Design objectives included optimization of the system in terms of fuel consumption and consistency with acceptable weight reliability and maintainability. Considerations were also given to the possibility of interface with other systems and the location flexibility of the system selected.

5.3.2 MAIN PROPULSION SYSTEM

The laminar flow control (LFC) airplane studies and the energy efficient engine studies which are both part of the NASA-sponsored Aircraft Energy Efficiency (ACEE) Program are parallel efforts aimed at early 1990 entry-into-service. Thus, for the LFC airplane, it is appropriate that the main propulsion engine be consistent with an engine evolving from the Energy Efficient Engine (EEE) studies.

Since the LFC airplane studies began prior to the EEE definition, it was necessary to select a study engine that could be considered representative of an EEE baseline engine. Because of Boeing participation in continuing cycle studies by Pratt and Whitney of engines incorporating advanced technology, it was decided to use the P&W STF-482 study engine for the LFC airplane baseline configuration. This engine has the following nominal cycle characteristics:

Overall Pressure Ratio	40
Fan Pressure Ratio	1.65
Bypass Ratio	7.5
Maximum Combustor Exit Temp. °C. (°F)	1532 (2700)

Certain adjustments to the nominal engine performance were required to accommodate to sizing and system changes representative of an LFC airplane application. This was accomplished by parametric simulation of engine characteristics using the Boeing engine cycle analysis program, which was initially adjusted according to Pratt and Whitney inputs to provide performance data matching the STF-482 engine. This program was also used to provide final engine performance data for the LFC baseline airplane.

5.3.3 SUCTION PUMP SYSTEM

The interface between the duct system and the suction pump system is defined to be at the face of the suction compressors. The design of the suction duct system is discussed in Subsection 5.1.4 and will not be discussed here. However, it is important to note that the ducting system is separated into low pressure and high pressure elements corresponding to the upper and lower wing surfaces, respectively.

The suction pump system, therefore, consists of coupled low-pressure and high-pressure compressors and the pump drive system. Two separate suction units are required to provide the suction for the entire wing, one on each side of the body. This system was sized and conceptually designed to provide the desired suction air-flow at an initial cruise altitude condition of Mach 0.8 at 12 800 m (42 000 ft), which is shown on the operating envelope defined in Figure 5.3-1. The suction pump system must remove sufficient air from the wing surfaces to satisfy the boundary layer stability requirements over the slotted portions of the wing surfaces within the principal operating envelope. While the system will not normally operate below the operating envelope, it is assumed that system operation can be initiated prior to takeoff and continue until commitment to landing at destination. Operation of the system is also expected during checkout, maintenance and special situations on the ground.

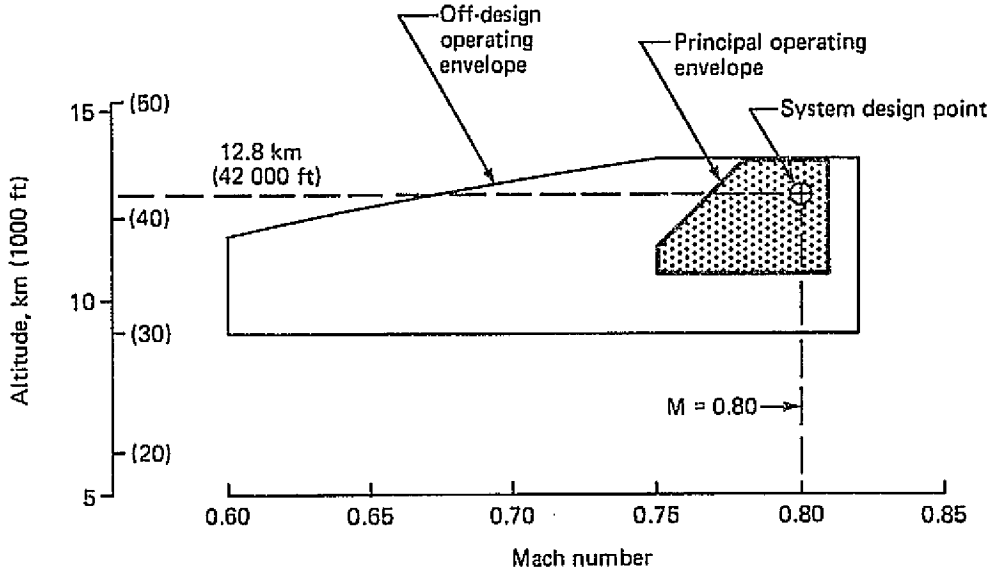

Figure 5.3-1. Suction Requirements

Initial requirements for the suction unit at the 12 800 m (42 000 ft), Standard Day, Mach .8 design point are shown in Table 5.3-1 below:

Table 5.3-1. Initial Suction Unit Flow Requirements

Suction surface	Corrected airflow, kg/s (lb/s)	Pressure ratio
Upper (0 - 70%)	11.7 (25.7)	1.44*
Lower (0 - 70%)	19.3 (42.5)	1.89

*Pressure ratio for first stage only.

It will be noted that the pressure ratio for the first stage only is given in the table opposite the upper surface. However, the upper surface flow requires an overall pressure ratio of 2.72 (i.e., the product of 1.44 by 1.89). This is apparent from inspection of Figure 5.3-2.

To arrive at a suction pump system configuration a trade study was necessary to evaluate the merits of alternative arrangements. Following an initial selection of number of pressure levels for the compressor based on expected wing pressures, the trade study considered different options in driving the suction compressors and the various location possibilities for the system. The options considered in driving the suction compressor were: 1) Turbo-shaft engine, 2) Bleed/burn turbine, and 3) Direct mechanical drive. These alternative drive concepts were all evaluated for an aft-body lower-compartment location since all the above concepts were possible due to the close proximity to the main engines. This permitted a comparison unclouded by location considerations. Once a system concept was selected, the other locations for the system were considered.

Suction unit location studies were conducted to determine where the selected suction pump concept could best be integrated into the overall airplane design. Consideration was given to operational problems, structural arrangement, aerodynamic drag and flow efficiency.

The following paragraphs cover the selected compressor design, the trade study to determine the best method for driving the system and the location study to select the location of the system on the airplane.

5.3.3.1 Compressor Design

Each suction pump consists of low-pressure (LP) compressor coupled with a high-pressure (HP) compressor. The LP compressor draws air from the low pressure area of the wing (wing upper surface) and raises the pressure to the HP compressor intake level. The HP compressor takes the air from the LP compressor along with the air from the high pressure area of the wing (wing leading edge and lower surface) and boosts all of the suction air to freestream

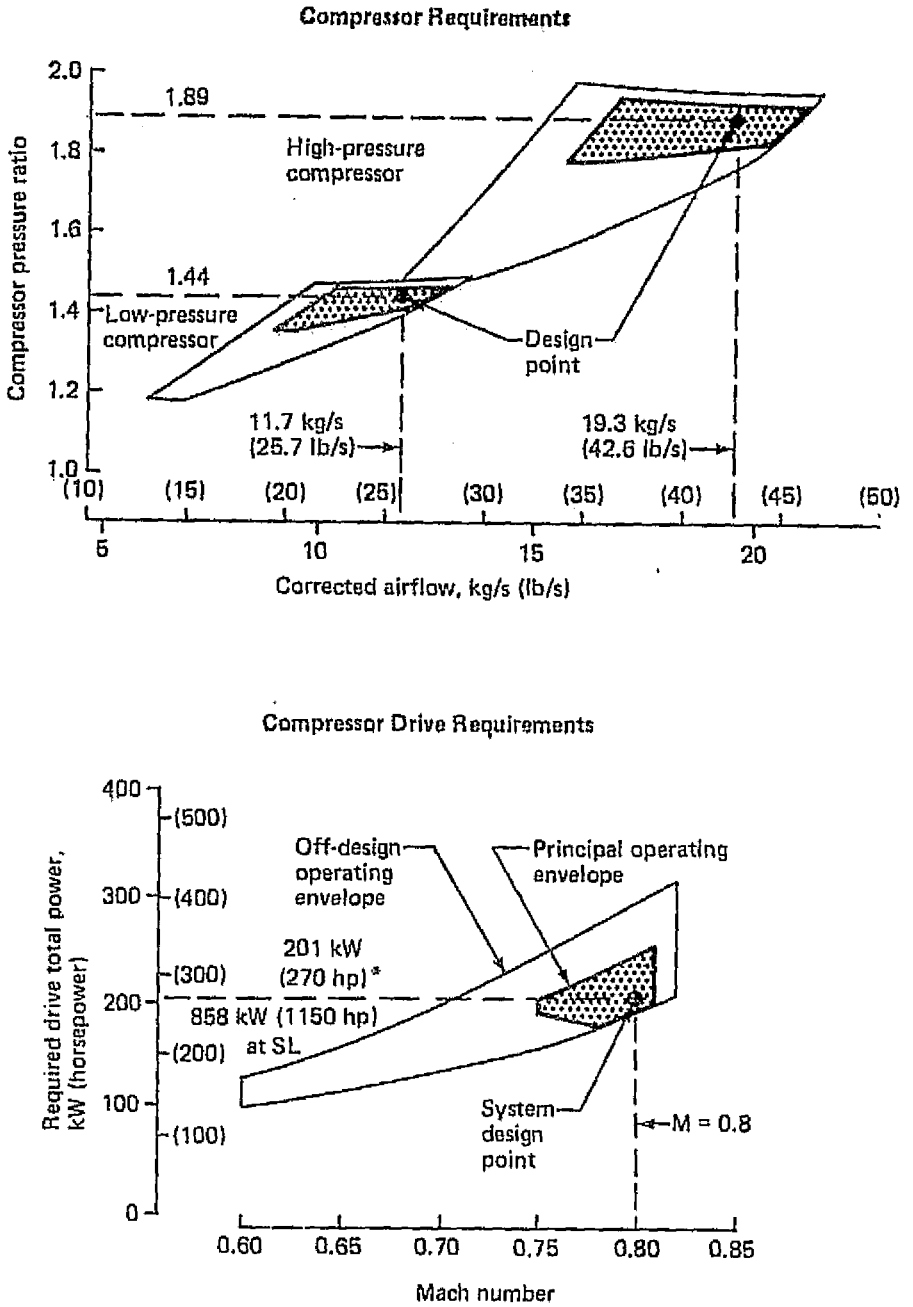

Figure 5.3-2. Suction Unit Flow and Power Requirements

total pressure. The LP compressor is a single-stage axial-flow compressor and the HP compressor is a two-stage axial-flow compressor. Both compressors require variable inlet guide vanes to provide efficient operation over the operating envelope shown on Figure 5.3-2. The two compressors are driven at the same rotational speed through a common shaft at approximately 14 800 RPM at the design point. For the design point condition, the LP compressor is required to provide 1.44 pressure ratio with 11.7 kg/sec (25.7 lb/sec) corrected flow and the HP compressor must provide 1.89 pressure ratio with 19.3 kg/sec (42.5 lb/sec) corrected flow. The above requirements correspond to laminarization back to the 70% on both upper and lower wing surface corresponding to the initial baseline airplane configuration.

Required compressor drive power has been determined for both the principal and the off-design operating envelopes as shown on Figure 5.3-2. As noted, the required power input to the compressor is 201.4 kw (270 horsepower) at the design point. With the drive power unit sized to this requirement, the potential horsepower output at sea level standard day conditions is 875.9 kw (1150 horsepower).

5.3.3.2 System Drive Options

Energy to provide power to drive the suction compressor is available from: 1) The main propulsion engine or, 2) A separate energy source in the form of a turboshaft engine. For this study, the alternatives selected for evaluation were:

1. Turboshaft Engine
2. Bleed/burn or Bleed-Drive Turbine
3. Direct Mechanical Drive

The Model 767-807 baseline airplane was configured with the suction pumps located on the wing trailing edge at the wing break. It had been concluded that with this configuration, the only practical drive method was a separate turboshaft engine. Therefore, to evaluate all of the above alternative drive methods and to provide information on alternate suction unit locations, an aft lower body location was selected for study purposes. In this location the suction system ducting back to the interface point is identical for all drive methods thus permitting an evaluation of the suction unit independent of the duct system. Figure 5.3-3 shows a typical arrangement of suction units below the cabin floor level in an unpressurized compartment in the aft-body area.

Safety considerations were an important element in the process of evaluating the operational suitability of alternative suction systems which is influenced by both system drive and unit location. Containment of fragments in the event of rotating machinery failure is a firm requirement for all suction unit locations although some installations are more sensitive than others. Of primary concern is the possibility, even though remote, that fuel or fuel vapors could be present in air entering the suction pump. This could come about through failure (e.g., structural cracks, sealant loss, etc.) at the interfaces between fuel tanks and suction ducting within the wing. Thus, to provide adequate safety it will be necessary to install multiple fuel/vapor sensors in the suction system ducting upstream of the compressor faces where a signal from any sensor would trigger an automatic system shut-down. In

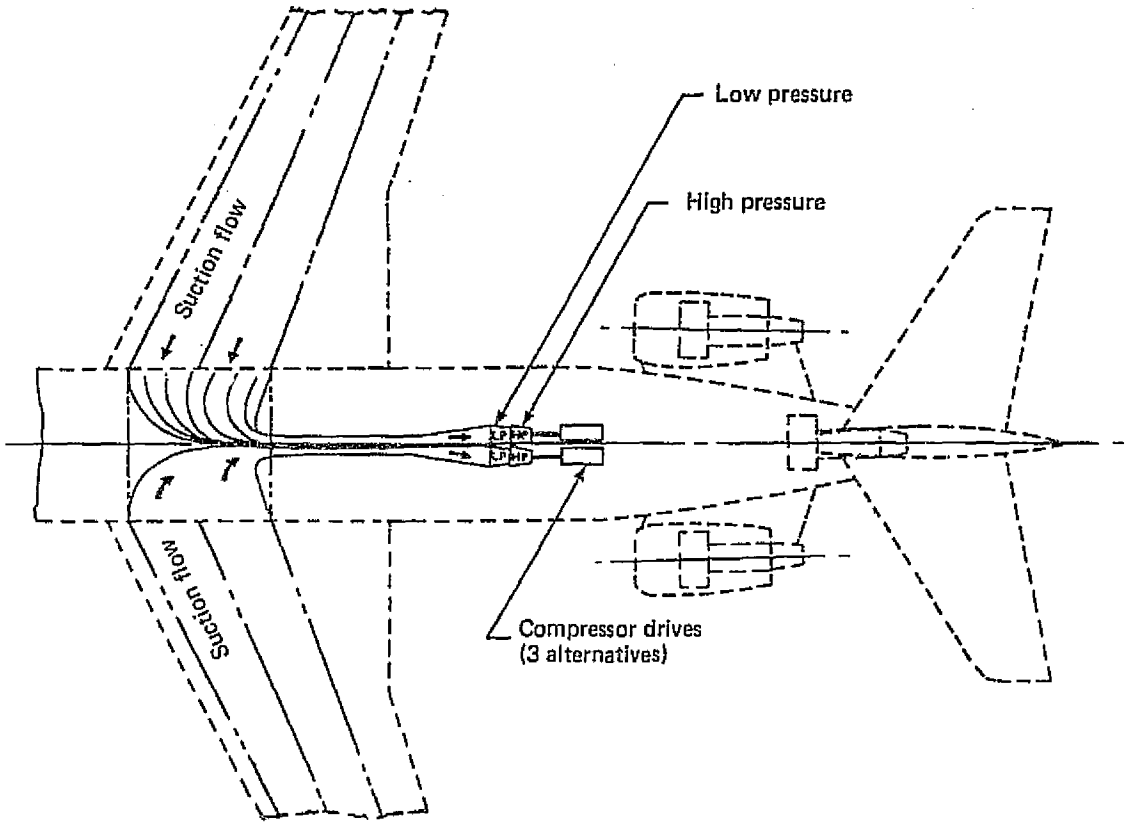

Figure 5.3-3. Suction System Alternatives—Aft Body Location

addition, bearing failure and over-temperature sensors were required on any bearing or gearbox located in the path of the suction airflow where a signal from these sensors would result in automatic system shutdown. This concept is shown schematically on Figure 5.3-4.

Further study showed that safety considerations were more demanding for suction units located in the aft-body areas. Additional design requirements included the provisions that all units be shock-mounted to minimize noise transmission and that all rotating equiment be fully contained in the event of failure. Proper orientation of nozzle exhaust and compartment fire-proofing were also given special attention.

The following discussion outlines the design approach and major concerns for each of the drive alternatives studied:

(a) Turboshaft Engine Drive

An advanced technology turboshaft engine with an overall pressure ratio (OPR) of 20 was utilized for this study. This engine is configured with two centrifugal compressors driven by a two-stage axial turbine in the gas generator and a two-stage axial free turbine in the power section to drive the suction pump. AiResearch has provided

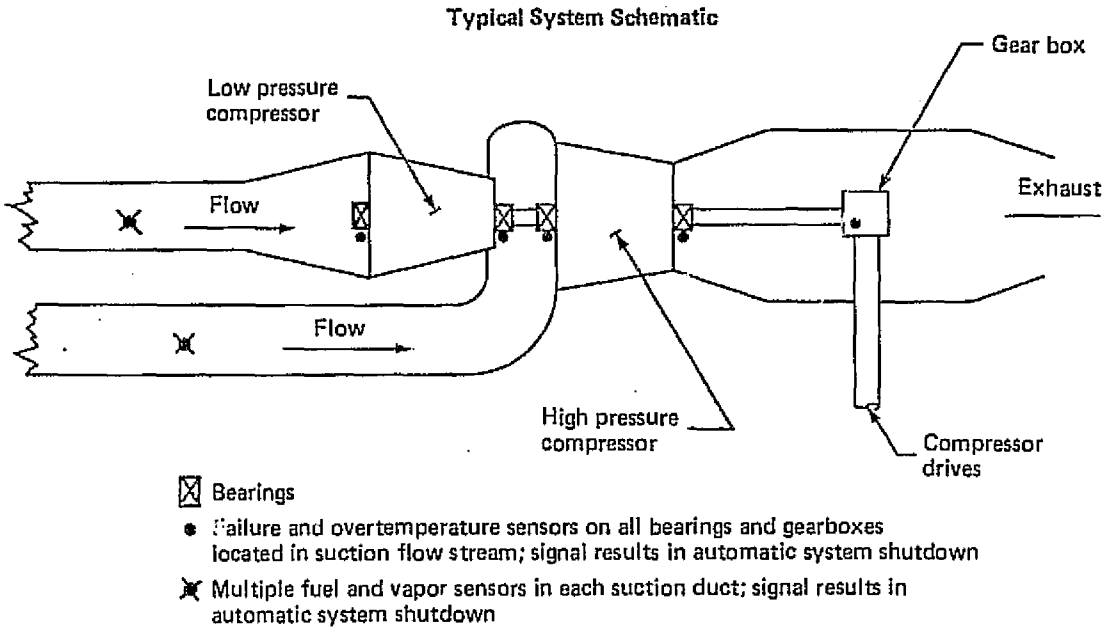

Figure 5.3-4. Suction Unit Safety Considerations

the above definition of the turboshaft drive engine and performance data to support its evaluation.

The installation for this drive method located the turboshaft engine under the aft-body floor at the side-of-body in a fire-protected zone. The installation criteria used was the same as for a standard engine installation. This configuration, which is shown in Figure 5.3-5, required two angle-drive gearboxes to transmit the power to the suction compressors which were located low in the keel beam area of the aft-body. During a special review of this configuration with United Airlines maintenance personnel, it was stated, on the basis of experience with similar equipment, that in-line drives would be preferred to the angle-drive gearboxes because of high maintenance predicted for the off-set drive.

The turboshaft drive system provided the most flexibility of operational control of the suction pump units since they were completely independent of the main engines.

(b) Bleed/Burn or Bleed-Drive Turbine

The bleed/burn turbine drive engine was located in the same area as the turboshaft drive engine and also required two angle-drive gearboxes in each drive train. Figure 5.3-6 shows the principal features of this system. Bleed air from all three main propulsion engines was manifolded together to supply the two bleed/burn units. The bleed/burn units were sized such that in the event of a single main engine failure both of the burn units could still be operated to provide the design point suction flow performance.

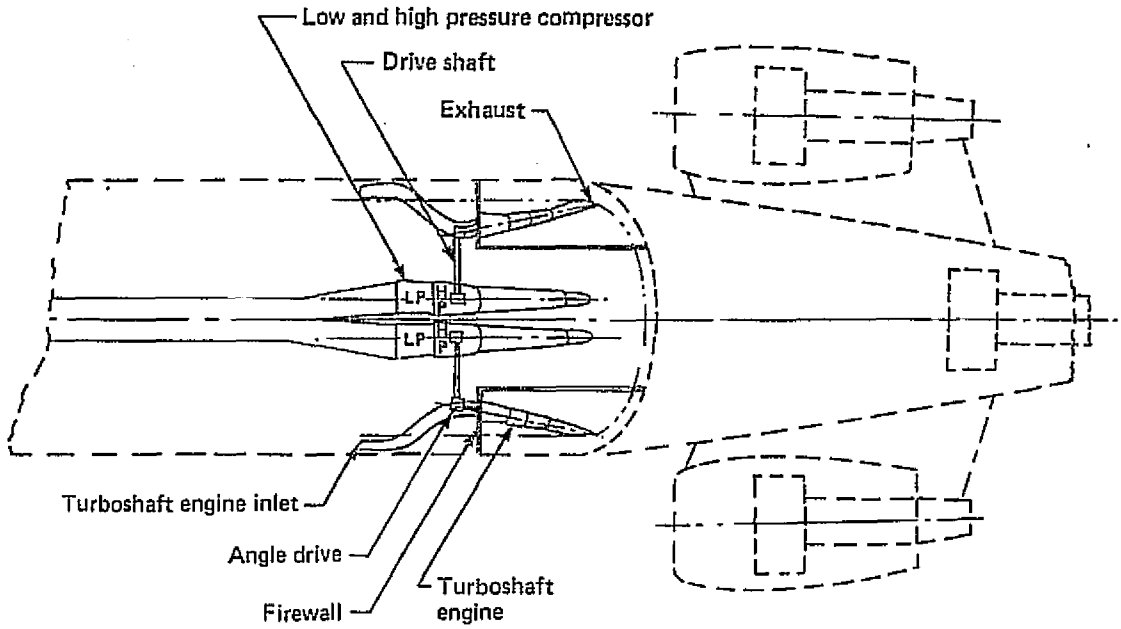

Figure 5.3-5. Turboshaft Engine Drive

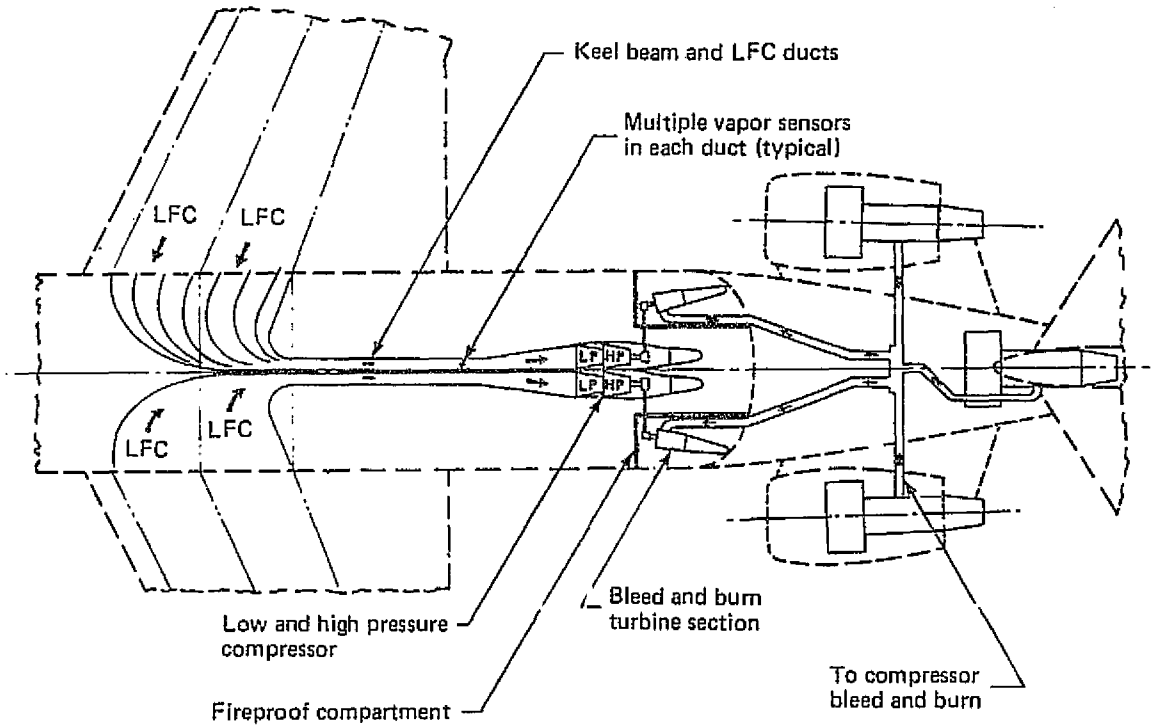

Figure 5.3-6. Bleed and Burn Turbine Drive

Studies were conducted to evaluate the best bleed air pressure from the main propulsion engine. Pratt and Whitney Aircraft have indicated that pressure ratio 10 was the lowest level which should be considered for extraction from the 40 OPR engine to avoid the variable geometry section of the engine. Therefore, pressure ratios of 10, 20, 30 and 40 were evaluated by utilizing a bleed/burn engine simulation program developed by Boeing. This study showed that on an airplane total fuel burned basis, the variation in fuel burned from the lowest extraction pressure level to the highest was less than 1% when pre-cooler airbleed from the main engine fan airflow was neglected. Since precooling would be required in order to use the higher extraction bleed pressure levels, a pressure ratio of 10 was selected to minimize the impact on installation problems associated with airbleed extraction.

The question of burn level (i.e., turbine inlet temperature) was raised early in the study where a preliminary assessment showed that low burn levels were inefficient because higher bleed requirements resulted in adverse effects on the main engine performance. This was also true for the Bleed-Drive case even though some saving in complexity and weight resulted from elimination of burner sections. Thus, a single burn level corresponding to a turbine inlet temperature of 944°K (1700°F) was used for the study.

AiResearch provided a conceptual design of a bleed/burn system with the drive turbine using a pressure ratio of 10 at the air extraction point with the main engine at its design operating point. Reduced engine power level associated with the end-of-cruise portion of the mission and a low payload were accounted for in sizing the drive unit.

(c) Direct Mechanical Drive

Direct mechanical power extraction from the high pressure rotor of the main propulsion engine was studied as an alternative to drive the suction pumps. Figure 5.3-7 shows a two-shaft drive arrangement although a three-shaft arrangement was also considered. These studies indicated that the expected RPM variation of the main engines was not compatible with that required by the suction compressors to cover the desired LFC operating envelope. Therefore, it was concluded that either variable speed capability in the drive train or additional features (e.g., variable area nozzles) on the suction compressors would be required. Restricting the operating envelope was not considered an acceptable option.

During the course of the study, both two-engine and three-engine drive concepts were evaluated. The three-engine drive concept offered the advantage of no loss in LFC suction performance in the event of a main engine loss but the resulting drive system was more complex with associated higher maintenance than the two-engine drive. In addition, a single failure in the three-engine mixer gearbox would cause loss of all LFC capability. Therefore, the three-engine system was dropped and only the two-engine concept retained for the balance of the study.

The two-engine system requires a 45° and a 90° gearbox in each system with multiple shaft supports to a variable-speed drive unit upstream of the suction compressor in the drive train. Speeds were limited to 10 000 RPM for the shafts between the main engine and the vari-drive unit.

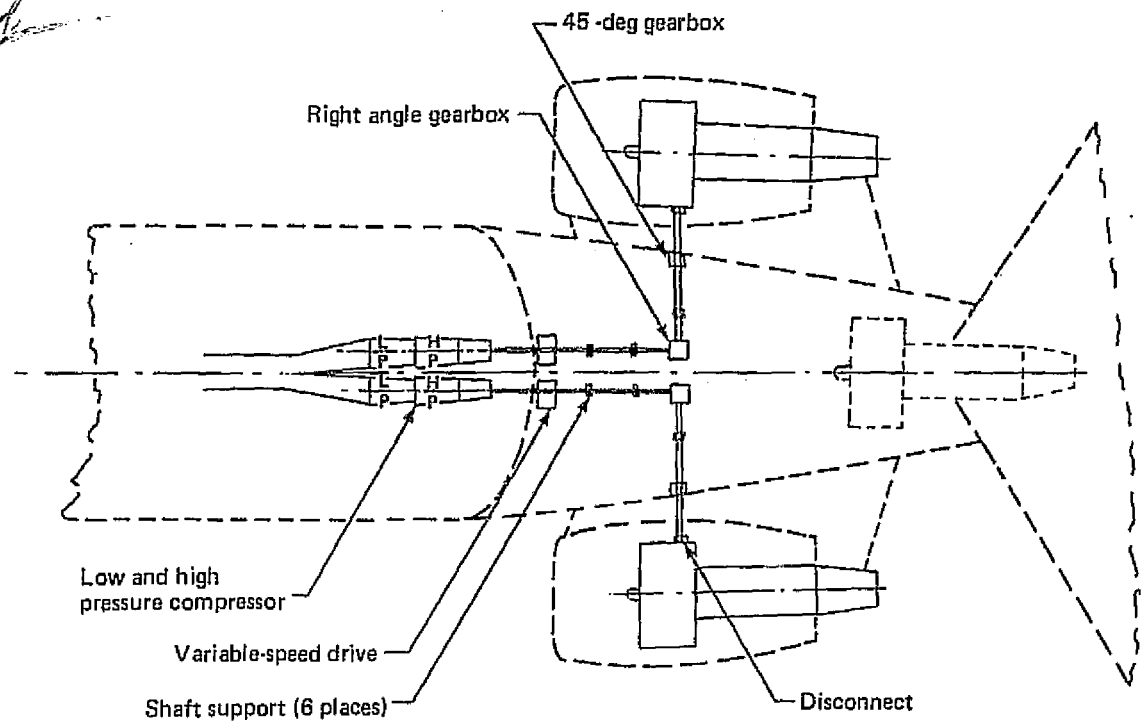

Figure 5.3-7. Direct Mechanical Drive

The direct-drive system was considered to be the most difficult system to provide means to cope with the suction compressor operational control problem.

The results of the drive alternatives study has shown that, of the practical options considered, all provided competitive fuel consumption performance (within 1%) whereas the weight advantage was significant for the turboshaft drive. Based on the qualitative considerations discussed above; namely, a) Reliability, b) Maintainability, c) Ease of control and d) Location and interface flexibility, the advantage was also clearly with the turboshaft drive. Table 5.3-2 shows a comparison of the three drive options based on the above factors. The turboshaft drive option, therefore, was selected as the basis for further design studies and ultimately, for the final LFC airplane configuration.

5.3.3.3 Suction Unit Location

Since the results of the drive alternatives study clearly indicated a selection of the separate turboshaft drive, the evaluation of suction unit location options was based on the above choice. Furthermore, Boeing IR&D studies had also shown that the turboshaft drive was the only practical alternative for the baseline configuration with wing-mounted suction units. Thus, the suction unit location study was based on a common turboshaft drive system and the evaluation conducted for four different locations; three mounted on the

Table 5.3-2. Evaluation and Selection Basis—Compressor Drive

Item	Aft body location		
	Turbo-shaft	Bleed and burn	Direct mechanical, 2 engines
Net fuel consumption at design point, kg/h (lb/h)	Base	+30 (+66) +0.7%	−18.6 (−41) −0.5%
System weight, kg (lb)	Base	376.5 (+830)	186 (+410)
Reliability and maintainability	High	Medium	Low
Ease of control for off-design operation	High	Medium	Low
Flexibility of interface with other airplane systems	High	Medium	Low
Location flexibility	High	Low	Low

116120-172

wing and one in the aft-body. The wing locations considered are illustrated in Figure 5.3-8 and listed below:

1. Under-wing mounted (aft, planform break)
2. Wing rear-spar mounted (aft, planform break)
3. Over-wing mounted (aft, wing root)

The two configurations at the wing break both posed structural problems associated with removal of the suction air to the suction pumps. Also, both configurations have significant drag penalties due to wing laminarized area lost and basic aerodynamic interference associated with the presence of the suction unit pod. In addition, the aft-spar mounted configuration poses a potential wing flutter problem which would result in increased wing weight.

The wing root location appeared to provide the most workable configuration of the three wing locations studied. However, there were still compromises associated with this location. This arrangement minimizes wing area lost to laminarization but it did cause concern about the drag impact and also introduces some safety concerns. However, further study indicates that these can be eliminated or minimized by appropriate design features.

Since the wing location is preferred over the fuselage location, the wing root location was selected as the best location overall for the suction pump system.

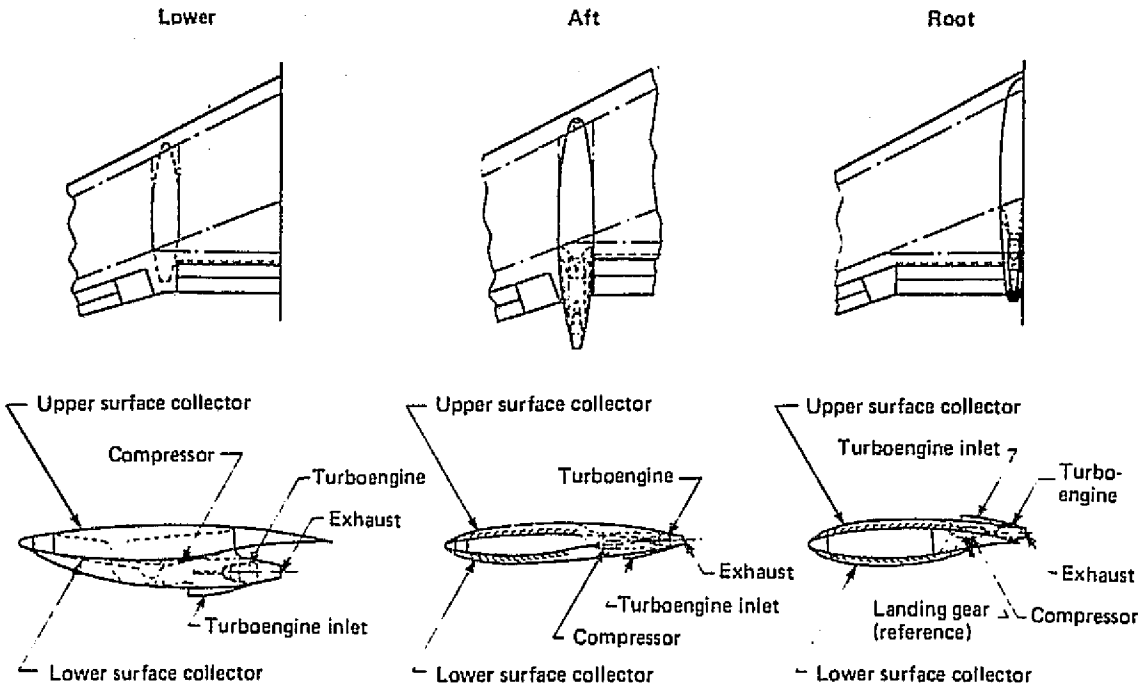

Figure 5.3-8. Options for Suction Unit Location

5.3.4 SUCTION SYSTEM CONFIGURATION SELECTION

Based on the above criteria of Section 5.3.3, the turboshaft drive was clearly superior and was, therefore, selected as the appropriate drive method regardless of suction unit location.

For the preferred turboshaft engine-driven suction unit, a comparative evaluation of wing location versus aft-body location showed unmistakable benefits favoring the wing root location. Thus, a final selection of the turboshaft-driven suction unit located in the wing root area was made for the baseline airplane configuration.

5.4 LEADING EDGE REGION CLEANING

Contamination of the wing leading edge by foreign particles such as insects or ice has been identified as a serious concern in all previous laminar flow studies and experiments where operational factors were considered. Of the two contamination problems, insect contamination has always presented the most formidable problem. Elimination of ice can be handled in a straightforward manner and will be mentioned only briefly in this section of the report. Elimination of insects is an entirely different matter. Many solutions have been proposed in the past and recommended solutions are included in this section of the report. However, no proposed solution is known that solves the insect contamination problem in a completely satisfactory manner without some adverse characteristic. A continued effort

in the area of insect contamination is necessary since a completely acceptable solution to this problem is required before LFC will be successful in the commercial airline environment.

5.4.1 DESIGN REQUIREMENTS AND OBJECTIVES

The primary design requirement for any leading edge cleaning or protection device is that it not cause premature transition of the laminar boundary layer. This requirement essentially eliminates any known type of mechanical device such as a scraper or deflector from being used. Any such device would have to be stowed with a resulting seam or joint in the leading edge. Tolerance on such a joint would be prohibitively small and would have to be maintained to close tolerance throughout the life of the airplane. Therefore, mechanical devices to either clean or protect the leading edge were not considered.

The design objective of a leading edge device to either clean or protect the leading edge is that it perform during both takeoff and landing approach and while operating within the insert layer, up to approximately 3000 ft above the terrain. It is also an objective that such a device or system not require significant expenditure of ground maintenance personnel time for servicing between flights. It should be essentially self-contained and activated as necessary by the flight crew.

5.4.2 PREVIOUS APPROACHES

Many schemes have been devised for either protecting the leading edge from insect contamination or cleaning the leading edge during flight. These schemes are well documented in Reference 24 and are summarized in the list following:

- Mechanical scrapers that travel along the wing leading edge.
- Flow deflectors that are stowed inside the leading edge when not in use.
- Fly-away fabric covers attached to the leading edge prior to takeoff.
- Soluable films applied to the leading edge prior to takeoff and washed off in flight.
- Thermally removable covers that are burned off in flight.
- Highly viscous fluids applied before takeoff and carried away by the airstream in flight.
- Continuously or intermittently discharged liquids over the leading edge.
- A layer of ice formed over the leading edge prior to takeoff.

All of the above approaches have some drawbacks or undesirable features. The best concept described appears to be that of discharging liquids over the leading edge. But, even this approach has the undesirable feature of holes in the leading edge, the significance of which to maintaining the laminar boundary layer has not been fully evaluated. The undesirable features associated with one or more of the above approaches can be summarized as follows:

- Penetration of the leading edge skin is required to incorporate the device, which results in a joint or hole exposed to the laminar boundary layer that may cause premature transition.

- Application of the device or material by the ground crew prior to takeoff is required resulting in excessive flight preparation time.
- Fly-away devices would litter the countryside and would probably be unacceptable to the public.
- Protection is not possible for landing approach as well as takeoff.
- The expendable fluid reduces the payload by a significant amount.
- The technique will not work.
- The technique presents a flying safety hazard.

During this program the attempt was made to identify a leading edge cleaning or protection scheme that either had no objectionable features or would otherwise minimize them.

5.4.3 RECOMMENDED SYSTEMS

Leading edge cleaning or protection systems were identified in this study based on previous studies as discussed above and contract efforts at design innovation. These systems are depicted in Figure 5.4-1 and are identified as the Liquid Film System, the Cryogenic Frost System and the High-Pressure Air Shield System. These three approaches have the highest potential for success of any identifiable at this time. All three systems have some point of disadvantage but these approaches are, nevertheless, considered promising and worthy of additional study and development. Significant disadvantages are: 1) The liquid film and the high pressure air shield require penetration of the leading edge with bleed holes to supply the water or air, and 2) The liquid film system requires a significant amount of water to be carried, reducing the performance a small amount. However, both are self-contained and both should work equally well on approach and on takeoff.

A liquid film system has been demonstrated in flight as an effective means of protecting the leading edge from insect contamination as discussed in Reference 25. It would require penetration of the leading edge surface to supply the water to the exterior surface. The success of such a system would depend on the ability to design and maintain flush or hidden nozzles that would not trip the laminar boundary layer during cruise flight.

The high-pressure air shield has had no flight or wind tunnel test evaluation and whether or not such a system will actually work is not known. Also, the success of such a system is dependent on the ability to design flush or hidden nozzles that would not trip the laminar boundary layer during cruise. However, since air is used, no payload penalty would result due to carrying the protection medium onboard. And, like the liquid film system, this approach would work on landing approach as well as takeoff which would essentially eliminate ground cleaning between flights.

The Cryogenic Frost System is an innovation. The system is presented in schematic form in Figure 5.4-2. In this figure it is seen to be combined with the hot air anti-ice system which is a very advantageous combination. The frost system operates on the principle of expanding liquid nitrogen into a mixing chamber to provide very cold air for distribution

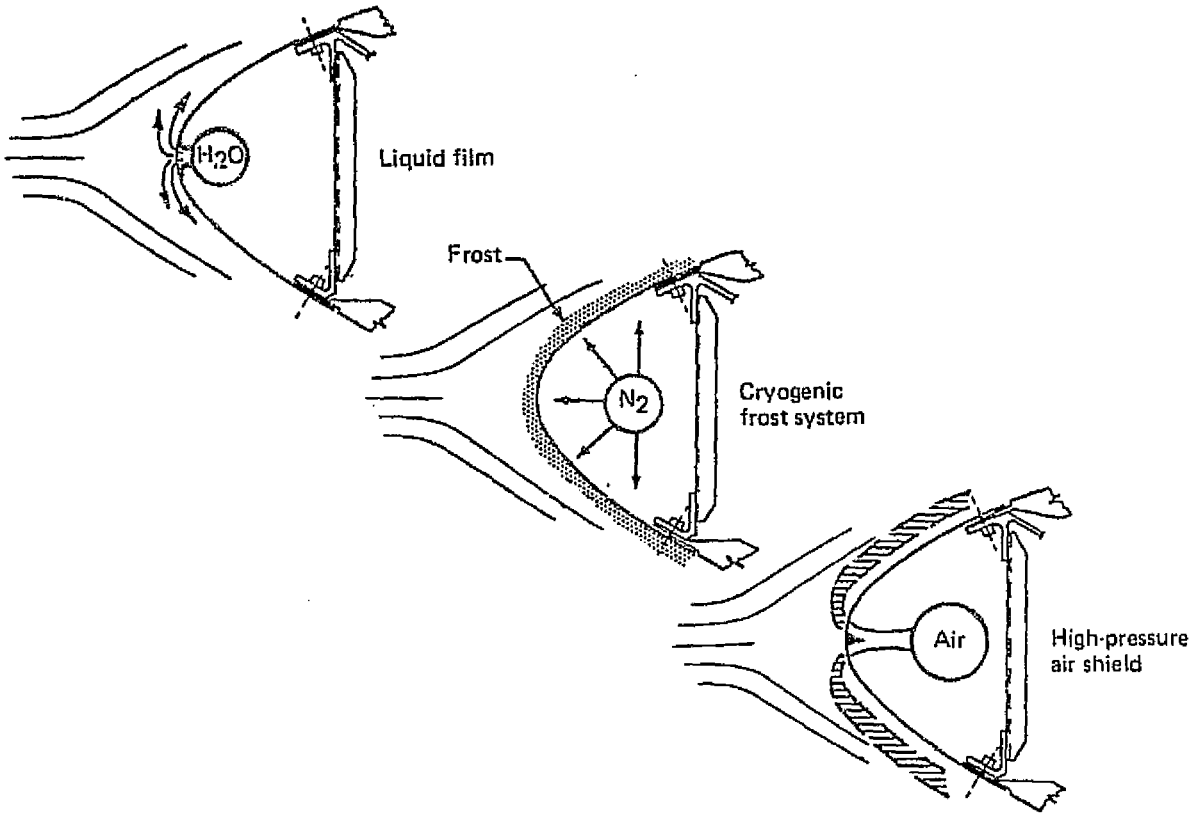

Figure 5.4-1. Leading-Edge Region Cleaning Concepts

along the leading edge. The formation of frost on the leading edge prior to takeoff would occur through the natural moisture in the air condensing on the cold leading edge. During takeoff and climb, adherence of impinging insects would be inhibited by the frost. With shut down of the system, the airstream would quickly melt the frost leaving a clean surface. Such an approach would work best on warm, humid days which correspond to the conditions of worst insect contamination. On cold or wintry days such a system would not produce frost well but it would probably not be needed since little or no insect problem would be expected under such conditions. Therefore, the system would only be used under favorable conditions for frost formation which should correspond to conditions when insect protection is needed. Under the unusual conditions when frost formation is not adequate and insect protection is needed, some insect contamination of the leading edge would be expected.

The disadvantages of such a system are a lack of actual test experience and the fact that such a system would not work on landing approach. This would require cleaning the leading edge between flights which is undesirable. However, no penetration of the leading edge surface is necessary and only a small quantity of liquid nitrogen is required to supply the cold temperature.

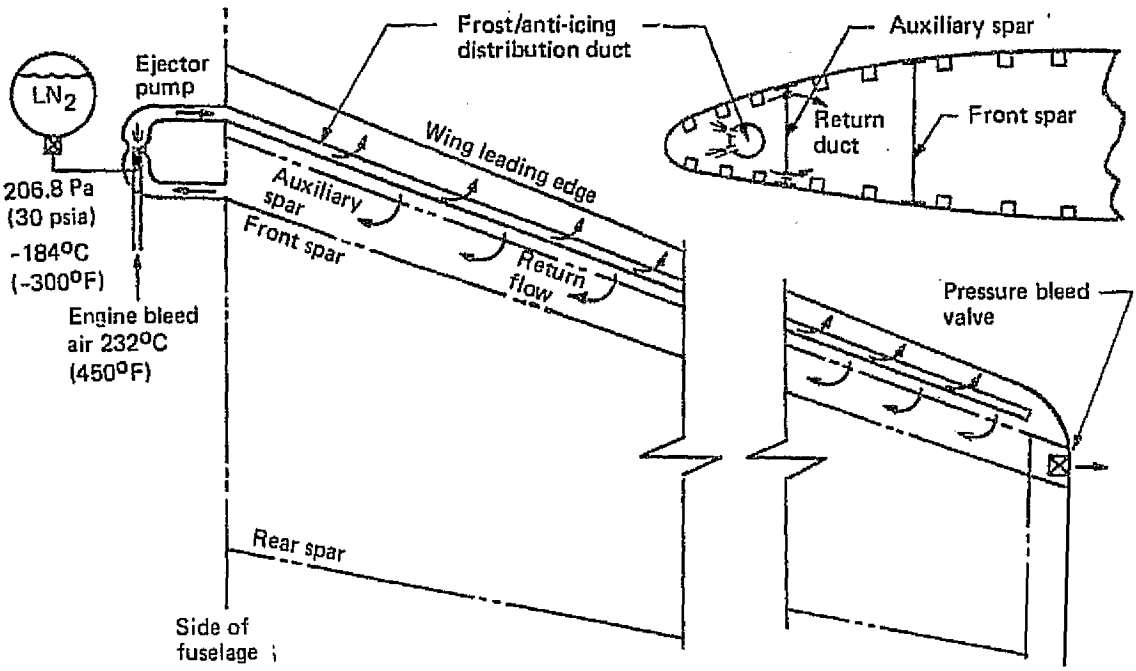

Figure 5.4-2. Wing Leading Edge Frost/Anti-Icing System Schematic

At this time no clear choice of leading edge protection system is apparent so further innovative design effort is highly desirable. As can be concluded from the above discussion, considerable additional development and testing effort is also needed before a satisfying leading edge cleaning or protection system can be chosen.

5.5 AUXILIARY SYSTEMS

Airplane auxiliary systems provide the functions other than propulsive thrust necessary to meet airplane operational requirements. Included are the hydraulic, pneumatic, electrical, electronic, environmental control systems, and high lift systems. The objective was to investigate the possible technical and economic benefits of integrating the LFC system with one or more of the auxiliary systems. Rationale for evaluation included improvement of performance and reliability, reduced maintenance, reduced cost, reduced weight and compatibility of installation space requirements.

Auxiliary systems and LFC systems integration studies are configuration dependent and must be conducted subsequent to final airplane configuration definition. However, preliminary airplane configuration studies have identified two areas where significant gain can be realized through combining auxiliary systems functions. In the leading edges, ducting systems and installation space are required for both hot air anti-icing and leading edge protection systems. Operation and control of both systems appears to present no incompatibilities since, for example, leading edge protection against insects would not be required

during anti-icing operation. Also, preliminary estimates indicate that the horizontal stabilizer suction unit power requirement would result in a power unit with sufficient capacity to meet the airplane ground APU requirement. However, provisions would be needed in the power unit design to match the compressor pressure ratio and airflow capabilities to meet both the LFC and ground APU requirements.

The auxiliary systems definition for the final LFC configuration is incomplete at this point since no final decision on type of leading edge protection from insects has been made among the candidates previously discussed. However, an integration of the anti-icing and leading edge protection system must be accomplished along with provision for one or two slots near the wing root. Such a combination would be used for the horizontal tail also but the tail will probably not require leading edge slots since the Reynolds number and leading edge radius are smaller than for the wing.

The LFC suction unit for the horizontal tail is combined with the airplane APU in the systems definition for the final LFC airplane configuration. Installation and performance details are discussed in Section 6.5.

6.0 CONFIGURATION SELECTION AND DESIGN

The study activity under the subject task culminated in the definition of LFC systems to be incorporated in an integrated transport design which would be technically feasible and economically attractive for introduction to service in the early 1990's. The rationale for selection was based on: 1) technical feasibility, 2) performance and economics-related benefits versus cost, and 3) operational suitability. The results of the extensive concept evaluation studies previously discussed were used as a basis for systems selection and evaluation of the final configuration design. The performance of the selected airplane design is presented in Section 6.6 to provide a basis for eventual economic assessment of the airplane in airline service A comparison of fuel efficiency with that of a representative current turbulent transport design is also shown.

As discussed in Section 4.6, a baseline LFC aircraft was defined early in the study to provide a valid basis for design development and evaluation of LFC system options. Figure 4.0-4 shows the baseline aircraft originally defined to meet mission and operational requirements given in Chapter 4.0. Further refinements were made during the course of the concept evaluation studies which resulted in the configuration shown in Figure 6.0-1. This configuration is the basis for development of the final LFC transport design and its performance presented at the conclusion of this section.

6.1 FINAL DESIGN REQUIREMENTS

Design requirements for the final LFC airplane fall into several categories.

Since the airplane is a conventional layout and similar in many respects to a turbulent airplane design, the normal Federal Air Regulations (FAR) requirements are considered to be applicable unless otherwise stated. The airplane features associated with laminar flow and the corresponding systems can be expected to introduce airplane characteristics which may require modification or extension of the FAR. At this stage of development, however, the potential impact of LFC on the FAR has not been studied, but the effects on design are anticipated to be relatively minor. Certification may involve special problems which cannot be anticipated at this time.

Prior to the definition of final design requirements, studies to resolve such items as cruise altitude and climb requirements and fuel reserves were undertaken to provide a rationale for defining these items. While these are influenced primarily by environmental considerations, their selection is also related to airplane operational factors. For a given cruise Mach number, high altitude corresponds to low unit Reynolds number which is of fundamental importance in reducing the sensitivity of laminar flow to disturbances of all types. It is well-established that the following types of operationally-related disturbances are of significance:

- Atmospheric ice particles
- Erosion/light impact damage
- Insect residues
- Noise
- Turbulence

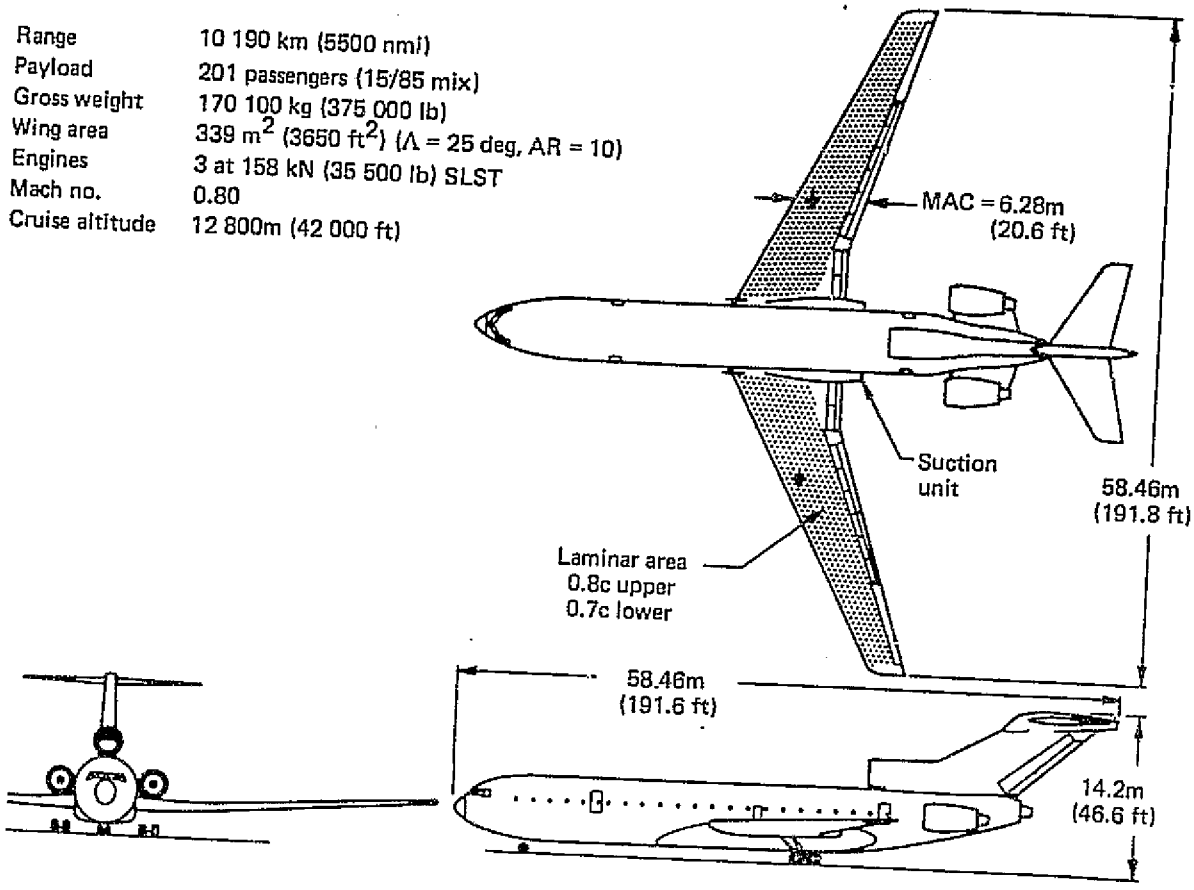

Figure 6.0-1. LFC Transport Configuration—Modified Baseline (Model 767-808)

Other types of disturbance are related to design or manufacturing tolerances and include steps, gaps and other surface imperfections. Suction slots in the leading edge region are particularly subject to damage and the incorporation of some types of insect protection scheme are potential disturbance sources in a particularly critical area of the wing. The allowable values for various disturbances are discussed in Subsections 5.1.1 and 5.1.8, and are applicable to the final airplane design. The data in Table 6.1-1 give the final design requirements and show that the performance and mission-related values are unchanged from those used originally. However on the basis of the studies discussed above, the cruise altitude has been reduced to 12 190 m (40 000 ft) partly in recognition of the substantial economics penalty associated with higher than optimum cruise altitude. This should still provide reasonable margins against ice crystal contamination effects most of the time. However, further assessment studies and experimental data not now available may ultimately show a need to adjust the cruise altitude requirement.

Table 6.1-1. Airplane Design Requirements

Item	Requirement
Design range	10 190 km (5500 nmi)
Payload	201 passengers
Cruise Mach number	0.8
Cruise altitude	12 190m (40 000 ft) (initial)
Turbulent climb capability	91.4 m/min (300 ft/min) at 10 670m (35 000 ft)
Takeoff field length	3566m (11 700 ft) (or less)
Approach speed	250 km/h (135 kn) (or less)
Fuel reserves	1967 ATA international rules (turbulent flow) or fuel to reach destination with LFC failure at halfway point

The fuel reserves requirement has been extended to include a provision that the reserves be sufficient to reach the destination with LFC failure at the halfway point in the mission and with sufficient fuel for 15 minutes operation thereafter. This is approximately satisfied if the updated 1967 ATA international rules are applied with the reserve segment flown under turbulent flow conditions. The flight profile and the applicable mission rules are shown in Figure 6.1-1. However, the first provision above takes precedence and will be satisfied in any case. The above reserve requirements are also approximately compatible with normal airline and FAR requirements for engine failure enroute.

6.2 AIRLINE CONCERNS AND RECOMMENDATIONS

Initially it was recognized that airline participation in the evolution of LFC design concepts could contribute substantially to the success of this effort. Thus the services of United Air Lines (UAL) were secured on a consultation basis to provide inputs, particularly on matters related to airline operations and economics. This participation has taken the form of periodic design reviews by responsible UAL personnel which have been reported during the course of the contract work. These reports have been furnished to NASA as received. Therefore, only the major concerns and observations, taken directly from these reports, will be presented (mostly verbatim) in this section.

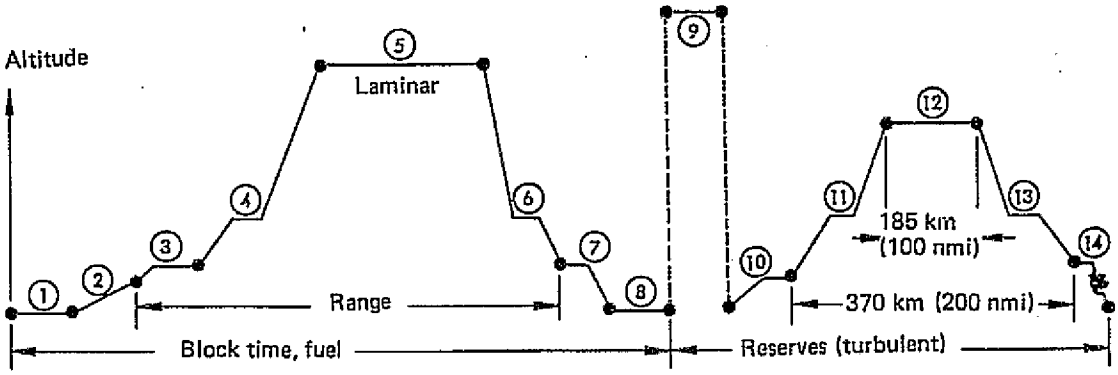

1. Taxi out (9 min taxi thrust)
2. Takeoff (1 min maximum thrust)
3. Climb to 457 m (1500 ft), accelerate to 463 km/h (250 kn)
4. Climb to 3048 m (10 000 ft), accelerate to 556 km/h (300 kn), climb to cruise altitude
5. Cruise, constant cruise altitude
6. Descend to 3048 m (10 000 ft), decelerate to 463 km/h (250 kn), descend to 457 m (1500 ft) decelerate to V_{APP}
7. ILS approach (2 min maximum thrust)
8. 5 min taxi in (from reserves)
9. 10% trip air time for end-of-cruise weight at LRC altitude and M
10. Missed approach (2 min maximum thrust)
11. Climb
12. Cruise
13. Descend

(11), (12), (13): 371 km (200 nmi) alternate mission

14. Hold for 30 min at 457 m (1500 ft) altitude, descend and land

Figure 6.1-1. Flight Profile and Mission Rules

6.2.1 GENERAL CONSIDERATIONS

In the opinion of the UAL staff, h'gh reliability and justifiable total life cycle costs are the prime hurdles facing development of a practical commercial laminar flow control system. Therefore, it is worth reciting several principal shortcomings that are often observed in early system development programs, viz:

- Insufficient emphasis, in concept stages, on maintainability in all its aspects
- Superficial simulation of environmental exposure, and inadequate environmental test experience
- Excessive reliance on cost formulas as criteria

Although the original Boeing proposal recognizes maintainability, durability, and cost as important design considerations, we can never be wholly confident that sufficient attention is given to these aspects.

Low speed performance, and stability and control considerations are included in the subjects to be investigated. In our view they remain principal criteria in design and there should be no compromise in what would otherwise be possible in order to optimize the LFC design. Put another way, LFC design options should be evaluated in terms of what further improvements in these flight characteristics they make possible.

The discussion on surface tolerances gives recognition to in-service contamination, and smoothness criteria for manufacturing tolerances and maintenance requirements. It should be recognized that a common criteria for manufacturing and maintenance is seldom tenable, and that the criteria have different objectives. It is useless to be concerned with manufacturing tolerances if unlivable maintenance requirements are associated with them. Both basic design and smoothness criteria must have enough cushion to tolerate a reasonable degree of in-service degradation and even minor defacement before remedial action is required. That action itself must be relatively simple and economical to pass the inevitable test of acceptable operating costs. The main thrust should be devoted to exploration and definition of the maintenance requirements and the effects of repair action as they pertain to corrosion, physical damage, and quality control in field repair.

Costs for development and production, though borne by the operator as investment, are external to his control and subject to some manipulation, whereas operating costs become "hard costs" that cannot be strung out or otherwise absorbed. Consequently, the operator's concern is that operating costs are frequently underplayed when assessing tradeoff benefits that are favorable to lower investment costs (viz., maintainability vs. manufacturing costs). A skeptical attitude regarding assessment of the various concepts in meeting requirements for reliability, maintainability and operational suitability in airline type operations is justified.

UAL's negative position regarding use of the ATA cost formula, particularly for evaluation of new technology, we believe is well known. The objection is not a matter of outdated coefficients, but rises from the manner in which the formula was developed to grossly describe the general characteristic of a relatively small family of airplanes, all of a fixed common design technology, but having quite different missions. Hence, to use it for evaluating or comparing new technology of airplanes at common mission points is not consistent with its formulation.

Updated coefficients do not resolve this fault. There are several obvious problems with the ATA formulation when applied to developmental studies. For example, though used for convenience in the formula to represent gross airplane size, airplane weight is not a determinant of crew pay. That is to say, savings in operating weight for a particular study airplane will not reduce crew pay, which is really a function of the design mission. It is recommended that the LFC study use a constant crew pay.

The simplistic determination of maintenance cost as a function of airframe weight and price, engine thrust and price, and flight time also is inappropriate for technology assessment. In estimating maintenance costs and evaluating various structural options, the UAL Structures Engineering group suggests that the costs should be developed in terms of repairs or modifications that might become necessary on an operator fleet basis.

Maintenance costs in an airline system for any given study mission are dependent on the overall system utilization (i.e., average stage length) of the airplane. There is some question whether the ATA equation is applicable for calculations using other than average stage lengths. The weight, thrust and price elements may or may not correctly reflect the impact of technology on maintenance costs. These effects must be examined directly by comparison with some known reference. The use of composite materials may or may not reduce maintenance costs, but this cannot be measured by the reduction in weight or the change in price. The same is true for advanced avionics. Similarly, if there are variances in airframe weight, and hence engine thrust requirements, for comparative LFC airplanes, it is questionable whether the variances can be translated into maintenance costs via the ATA equation.

6.2.2 OPERATIONS

6.2.2.1 Fuel Reserve Criteria

In conventional concepts, basic reserve fuel criteria focus simply on two notions—first, that a prudent quantity, additional to that anticipated to be used for events of the flight actually expected to occur, be carried to provide for routine, but contingent, extended operation; second, that the additional quantity must also cover, in some combination, higher than normal consumption occasioned by unfavorable deviations from ideal.

To identify realistic fuel reserve criteria, UAL envision four cases which should be examined for all stage lengths of the aircraft up to maximum range. It is expected that all four cases will exceed the basic minimum requirements (45 minutes domestic, 10% overwater) by large margins. In each case the first half of the total still air distance is traversed with all engines and LFC pumps operating. The fuel on board must permit flight from the midpoint to destination, and for 15 minutes thereafter, in all four abnormal modes, which are:

Case 1. All engines operating and all LFC pumps inoperative.

Case 2. One engine inoperative and all LFC pumps inoperative.

Case 3. Two engines inoperative and all LFC pumps operating.

Case 4. Loss of cabin pressurization, descent to 3048 m (10 000 ft), all engines operating and all LFC pumps operating.

The minimum "reserve" is the difference between the most critical of the four cases and the planned trip fuel. Anticipating a challenge that the engine inoperative cases represent double failures and therefore should not be used for basic reserve criteria, it is pointed out that Case 3 is nothing more than the existing operating rule, while Case 2 is a much more likely real probability.

6.2.2.2 Use of LFC System in Takeoff and Landing

It is generally inadvisable to operate the LFC system during takeoff and approach to take advantage of any available drag reduction, fuel savings, and propulsion benefits. These benefits are probably relatively small and not justified against the complications they create

in operating procedures and crew proficiency requirements. Even if it were possible to operate in such a full-time mode without the requirement of taking account for the LFC performance increment in complying with the regulatory requirements controlling performance in certification and operation, there would be a requirement for crew training and proficiency in flight procedures with LFC both on and off. The possibility of an LFC system shutdown during takeoff or landing, even if the performance decrement were negligible, would introduce an undesirable additional crew response requirement in a critical flight phase. If the differential performance in takeoff and landing between LFC on and off is in fact significant, then additional emergency operating procedures would be required, and the regulatory performance requirements would become even more complicated. These requirements would be reflected in increased training and also would compound operational support in ascertaining allowable gross weights. Standardization and simplification of operating procedures and reduction of workload in critical flight phases are keystones in all airline flight safety programs.

6.2.2.3 System Operation

No problems are anticipated with scheduling start-up of LFC pumps during climb outside of terminal control airspace, i.e., sometime after rising above 3048 m (10 000 ft). Similarly, shutdown shouldbe accomplished above 3048 m (10 000 feet), but preferably as soon in descent as LFC benefit becomes degraded, to exclude this item from the approach descent period. Suction pump startup should be under automatic control upon crew selection, with standby manual start only if it can be accomplished with the monitoring instrumentation that may be otherwise required. Only that instrumentation required to assure safe operation is desired, and it should be integrated into the aircraft instrumentation warning system. Fuel flow indication should be integrated with the aircraft fuel management system. If pump suction power required over the entire operating envelope requires variable fuel control, this control must be automatically scheduled or require not more than HI-LO switching by the flight crew.

Provisions for independent operation of pumps are desirable providing asymmetrical operation proves practical. The need for sensitive fuel vapor sensing in the suction ducting is again emphasized. This system will be exposed to severe environmental attack, and should have redundancy, self test, and automatic LFC shutdown features.

6.2.2.4 Cruise Control

It is not at all clear at this time that the LFC system design, either aerodynamically or in suction power, will have a sufficiently large operating envelope to make it even marginally useful in those situations in which the airplane is forced to lower altitude operation such as LFC failure or single engine shutdown.

Notwithstanding the desire to optimize in every way possible the design of the LFC system, it is imperative that the airplane performance with LFC inoperative is such that the airplane can be operated in a completely conventional manner. This requires the ability to operate efficiently at cruise altitudes from 10 670 m (35 000 ft) to 11 890 m (39 000 ft). It will be a requirement to include in the airplane's supporting instrumentation a cruise control director for speed/thrust and altitude management with LFC either on or off.

6.2.2.5 Laminar Flow Confirmation

It may be possible to provide direct cockpit indication that laminar flow is being developed, or the extent to which it is not, across the entire surface. It is difficult to conceive a system which could fully achieve this function without a multiplex of sensors, an elaborate display, and the attendant installation problems in a wing structure that is already constricted in accessibility and location of auxiliary equipment.

Figure 6.2-2 illustrates a concept that may be adequate, if it can be shown that the extent of laminarization on the surface can be confidently deduced from indications provided by an array of sensors mounted along an axis parallel to the rear spar. This would rely on empirical determination of turbulent boundary layer spreading and adroit sensor positioning to create a matrix coverage of the entire surface. If this concept is practical it could be used to provide input into the cruise control flight director, and location information for maintenance. The cockpit indication, however, must not be an elaborate display. Conceptually, it must provide an ATTENTION signal, numerical readout of some suitable performance degradation parameter such as range loss or fuel flow rate degradation, and provide either on-call identification or on-command flight data recording of fault source.

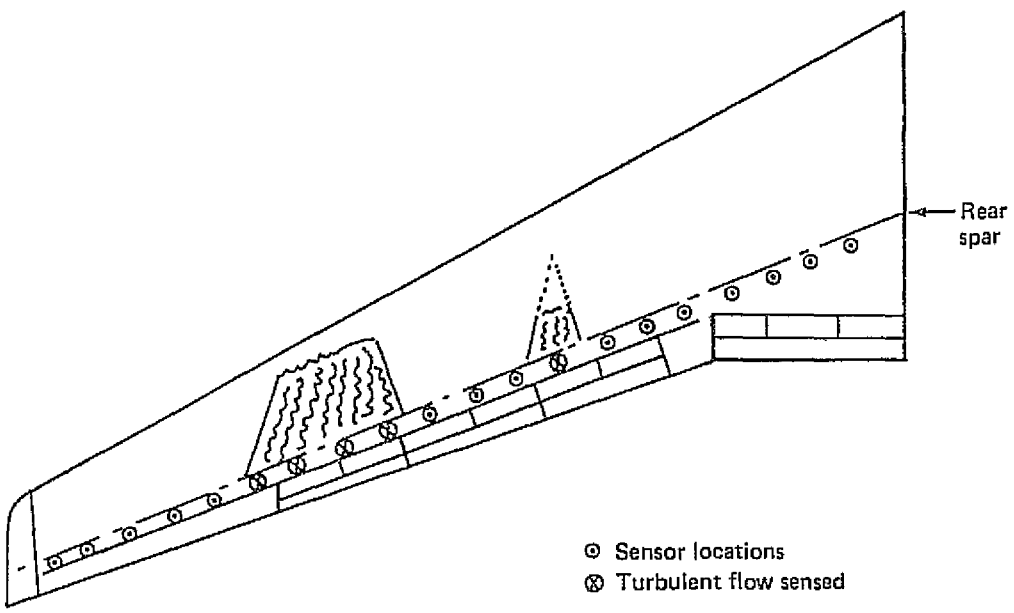

Figure 6.2-2. Laminar Flow Monitoring System

6.2.2.6 Meteorological Planning

Reviews so far have indicated that LFC is likely to become reduced in effectiveness in turbulence and in air masses containing crystalline water of certain particle size and flux. Present meteorological reporting and forecasting networks do not have the capability of detailing atmospheric conditions this finely and on the nearly mile-to-mile basis that would be required by LFC for flight planning and dispatching. It cannot be expected that such a network will become an integral component of future satellite based meteorological data systems, because of the specialized purpose for this data. If such a system can be established, its cost is likely to be prohibitive and would fall upon a limited number of airlines as users. This is another reason high fuel reserves will be normal practice for LFC airplanes. In addition, it appears that CAB Aircraft Servicing costs, which include flight planning and dispatching functions, will become significantly increased, because of the necessity for even greater application of computerized flight planning techniques and the more sophisticated planning required. To determine the extent of this impact it will be necessary to define in some detail the atmospheric conditions which will cause full or partial boundary layer transitions and the resultant performance degradation. Supporting studies of future meteorological forecasting capability will be necessary.

6.2.2.7 Scheduling

At this stage of development, the only characteristic of an LFC airplane that would appear to have possible impact on flight scheduling is the requirement for special turn-around ground servicing. Routine ground servicing of the laminar flow system, including charging, set-up, or other preparation of leading edge cleaning devices, should require no more than one-half manhour of labor and be non-interfering with other ground service activity. A 45 minute cycle is a commonly used ground servicing schedule for large, long-range aircraft. If continuing study indicates that more frequent maintenance/inspection checks will be required for the LFC system than are provided in current operation of conventional aircraft, there could be some impact on schedule flexibility. Current airline scheduling techniques are geared to recurrent check cycles typical of today's aircraft.

6.2.2.8 Pre-Flight Deicing

Reviews to date have not adequately outlined any design concepts devoted to preventing or disposing of ice formations in the slots, plenums, and ducting. We do not consider the use of ground covers to be a practical solution under any conditions. It should be noted that wing icing occurs not only in conditions of snow and freezing rain but also by condensation on cold soaked structure, even in the summer. It can be expected that ice will form not only on the wing surface but that accompanying liquid will also settle in the slots, plenums, and ducting, and thereupon become frozen. During snow and icing weather, treatment is usually applied in the form of heated glycol spray solutions under pressure. Recently, it has been found that more dilute solutions of glycol and hot water can be equally effective. Deicing solutions will also drain into the LFC system. A number of problems are foreseen. To dispose of entrained water from rain or melted ice, and deicing solutions, the LFC system will require automatic drains in the ducting. It may also be desirable to consider use of the suction pumps for purging if they can be designed to operate with large quantities of ingested liquid. If the pumps are used for purging, it will be necessary to incorporate suction relief

valves throughout the system to protect against ice blockage. However, suction purging could itself form ice in the system under certain conditions. This problem of possible ice formation in the system must also be considered with respect to flight operations. An investigation of the flight and atmospheric conditions which can cause ice formation in the system is needed.

6.2.3 MAINTENANCE CONCEPTS AND IMPACT

The environment and atmosphere in which commercial aircraft operate is very hostile in comparison to the pure medium in which the aerodynamicist works and the ideal conditions which the designer contemplates. Airline aircraft suffer contamination and physical abuse from climatic exposure heightened by the presence of reactive pollutants; from repetitive contact with foreign material, both natural and manmade; and from continual human mistreatment attendant to large-scale operations. Coping with these elements is far more determinant to ultimate success than so far has been recognized.

6.2.3.1 Wing Leading Edge Damage

Criticality of wing leading edge condition in establishing and maintaining laminar flow directs concern to the problem of potential damage and proper design provisions for its repair. It would be desirable to analyze in-service experience regarding frequency of occurrence, extent of damage, and source. Damage to the leading edge is typical of externally caused aircraft damage in general. Unfortunately, in-service damage of this type, though more widely suffered than is generally recognized, has not been systematically reported or investigated. With respect to the wing leading edge, the two principal reasons are the diverse nature of the kinds of major damage experienced (that requiring immediate repair) and the inability to effect repair of minor damage readily. In the latter case numerous dents and gouges that would be critical to LFC, are presently allowed to persist in routine operation. Prominent among causes, however, is the random occurrence of incidents involving ground servicing of the aircraft. The latter includes inadvertent contact by cargo, galley, fueling, and other service vehicles. Major aircraft damage from this cause and other reportable sources (such as bird and lightning strikes, ground scrapes, taxiing, etc.) is estimated to be incurred in United's fleet at a rate of slightly over 1 incident per day, equivalent to about 1 incident per aircraft per year, or 1 incident per 1500 departures.

6.2.3.2 Maintenance Requirements

Three major areas of impact upon maintenance, including servicing, are foreseen from the LFC system concepts being pursued. They are:

- Routine, non-routine, and periodic maintenance of the LFC system itself.
- Introduction of more extensive and elaborate inspection and repair of integral wing structure and fiberglass cover.
- Restrictions in accessibility, particularly as it affects line maintenance, to other wing mounted systems.

None of these areas are viewed as working towards reduction of conventional maintenance costs, and their cost must be fully charged against the fuel savings offered by LFC. Table 6.2-1 is an elementary listing of LFC system maintenance requirements. Considerably more concept development and analysis will be required before the frequency of periodic requirements can be projected. The listing is provided, however, to draw attention to the considerations that should be taken into account early in concept development.

Table 6.2-1. LFC Maintenance Requirements

Periodic Maintenance • Inspection and testing of LFC slots, metering orifices, and ducting for faulty flow, leakage and contamination • Inspection of suction pump installation for integrity of mounting, shielding, connections, and leakage; sampling of drain plugs and filters • Operational check of all safety subsystems that do not receive confirmation in normal operation • Restoration of leading edge cleaning system effectiveness (depending on concept) • Verification of laminar flow monitoring systems
Recurring Non-routine Maintenance • Replacement of damaged slots and orifices • Repair of LFC ducting • Replacement of suction pump or controls • Repair of leading edge cleaning system • Replacement of laminar flow monitoring system • Restoration of wing surface smoothness
Servicing • Replenishment or charging of leading edge cleaning system • Flushing or purging of system ducting • Application of anti-icing agents • Suction pump lubrication system

6.2.4 STRUCTURAL AND SYSTEMS DESIGN

It should be apparent from the preceding discussion that the impact of LFC systems on operations and maintenance will be substantially influenced by their characteristics which are to a large extent determined by design approaches. The practicality of LFC for commercial aircraft will ultimately hinge on the development of simple, reliable, rugged systems which provide trouble-free operation in the airline operating environment.

Regardless of the materials and structural concept finally selected, maintenance costs will be heavily leveraged by inspection requirements. The discussion which follows is directed primarily toward concerns which remain relative to the selected structural design concept. The conventional design with fiberglass cover concept represents the most acceptable of those which have been developed during the course of the study. Damage to the suction strip can occur from a variety of causes including walking on the wing surface during maintenance operations. Foreign object contact on the ground and hail are also sources of damage which must be recognized. Final design of these strips must be as rugged as possible and provide for easy repair and replacement in the event of damage.

Criticality of the leading edge smoothness and contour represents an increased maintenance burden. Service experience, as related to foreign object damage, will seriously affect the unattended service life of the leading edge. The development of a dent filler compound that is curable at standard temperatures within one hour and be readily workable to contour would largely offset these difficulties.

Concepts for leading edge protection and cleaning are obviously still in the conceptual development stage. Of the three concepts being seriously considered to date, the air shield system appears to have the most promise from an operational standpoint. Further development and testing under actual or simulated flight conditions is needed.

There are in every airline maintenance program requirements to inspect the primary and secondary structure at intervals using non-destructive test methods. These include visual, dyecheck, eddy current and x-ray. Visual methods are relied on heavily at present and other more sophisticated and indirect methods are more costly. Since the chosen concept involves a cover over the entire wing structural surface, visual inspections will be done internally which also involves additional cost.

Improved techniques and materials for corrosion protection will be required to minimize corrosion in the surface ducting areas. Additionally, better methods of inspection must be developed.

From a materials standpoint, the durability of the fiberglass cover can benefit from the development of less brittle resins and heavier prepregnated cloths. An extensive testing program simulating conditions anticipated in service during development will be required to assure acceptable durability characteristics.

The suction unit compressor and drive systems have been the subject of intensive study and involved consideration of several drive schemes and locations on the airplane. Based on experience with current state-of-the-art machinery, maintenance problems, etc., the

preferred combination is a wing-mounted suction pump driven by a turboshaft engine on a common shaft. One unit is required near each wing trailing edge behind a dry bay area for necessary ducting and controls. The above stated preference is based also on considerations of safety, noise, and access for inspection and servicing.

6.3 PARAMETRIC STUDIES

During the course of configuration development and optimization, studies were conducted to determine the relative importance of various configuration characteristics which impact the overall performance, fuel consumption, and economics of a LFC transport. The airplane design parameters selected for these studies included wing sweep, wing aspect ratio, and engine bypass ratio. Within each of the studies, wing loading, thrust-to-weight ratio, and initial cruise altitude were varied parametrically to aid in determining optimum configuration characteristics. Configuration evaluations were based on the mission and performance requirements and constraints specified in Table 6.3-1.

As noted in the table, an initial cruise altitude capability (ICAC) of 12 800 m (42 000 ft) or higher was desired. This is a particularly significant requirement because high values of ICAC, rather than takeoff field length, tend to size the engines. Nevertheless, high cruise altitudes are desired for the LFC airplane to minimize encounters with ice crystals which make laminar flow difficult to maintain. The subject of ice crystals is discussed at some length in Section 6.1.

The studies which led to the selected configuration took place over the duration of the contract and are illustrated schematically in Figure 6.3-1. The Initial Baseline Airplane wing was selected at 25° sweep to get the benefit of substantial sweepback (i.e., higher thickness and greater span for reasonable wing weights) without incurring the severe cross-flow instability and leading edge contamination occurring at higher sweepback.

Table 6.3-1. Mission and Performance Requirements and Constraints

Item	Requirement
• Payload	201 passengers
• Range	10 190 km (5500 nmi)
• Mach number	0.8 (LRC)
• Takeoff field length	3570m (11 700 ft) or better—SL, 29°C (84°F)
• Approach speed	135 kn or less at mission landing weight
• Initial cruise altitude	12 800m (42 000 ft) or better (desired)
• Cruise C_L	0.55 or less
• Turbulent rate of climb	Approximately 91.4 m/min (300 ft/min) at 10 670m (35 000 ft)

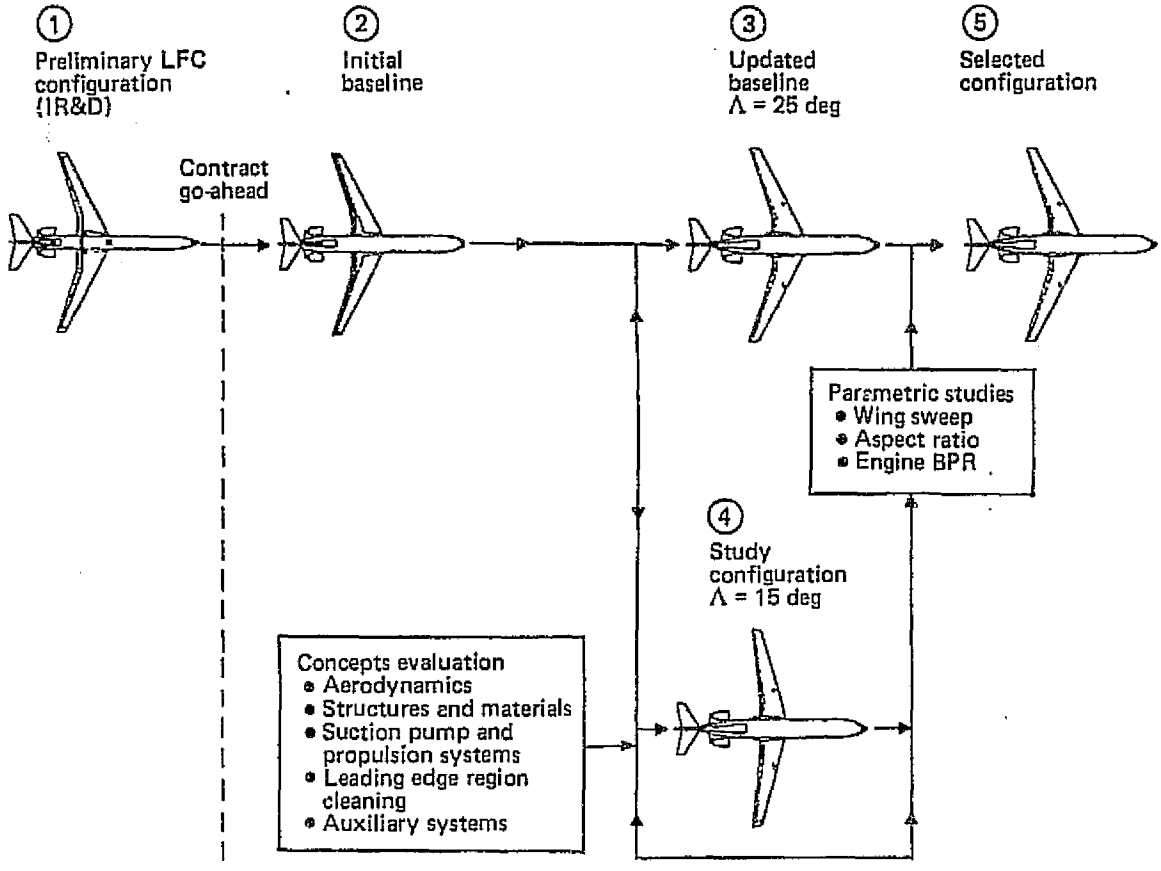

Figure 6.3-1. LFC Configuration Development

The standard flight profile and mission rules used for these studies are summarized in Figure 6.1-1. Reserves were calculated using international ATA rules with the airplane operating at fully turbulent flight conditions during the reserve portion of the mission (26% higher drag than under laminar flight conditions).

The parametric studies shown in this section required the calculation of size, performance and economic characteristics for numerous engine/airframe combinations, all of which satisfy the design mission payload/range. The parametric design method development used to obtain this data is shown in Figure 6.3-2. The initial airplane design definition (Step 1) described above was used to create a baseline configuration drawing (Step 2), with sufficient detail to enable analyses of the airplane's weight, aerodynamic, and performance characteristics (Step 3). These data were then used in the engine/airframe matching analyses (Step 4) to determine various combinations of engine size, wing size, fuel requirements, and gross weight necessary to achieve the design mission (201 passenger/10 190 km (5500 nmi)). The type of chart shown in Step 4 illustrates the effect of thrust (T/W) and wing loading (W/S) on the airplane gross weight and block fuel requirements. Various performance characteristics, such as takeoff field length (TOFL), mission landing approach

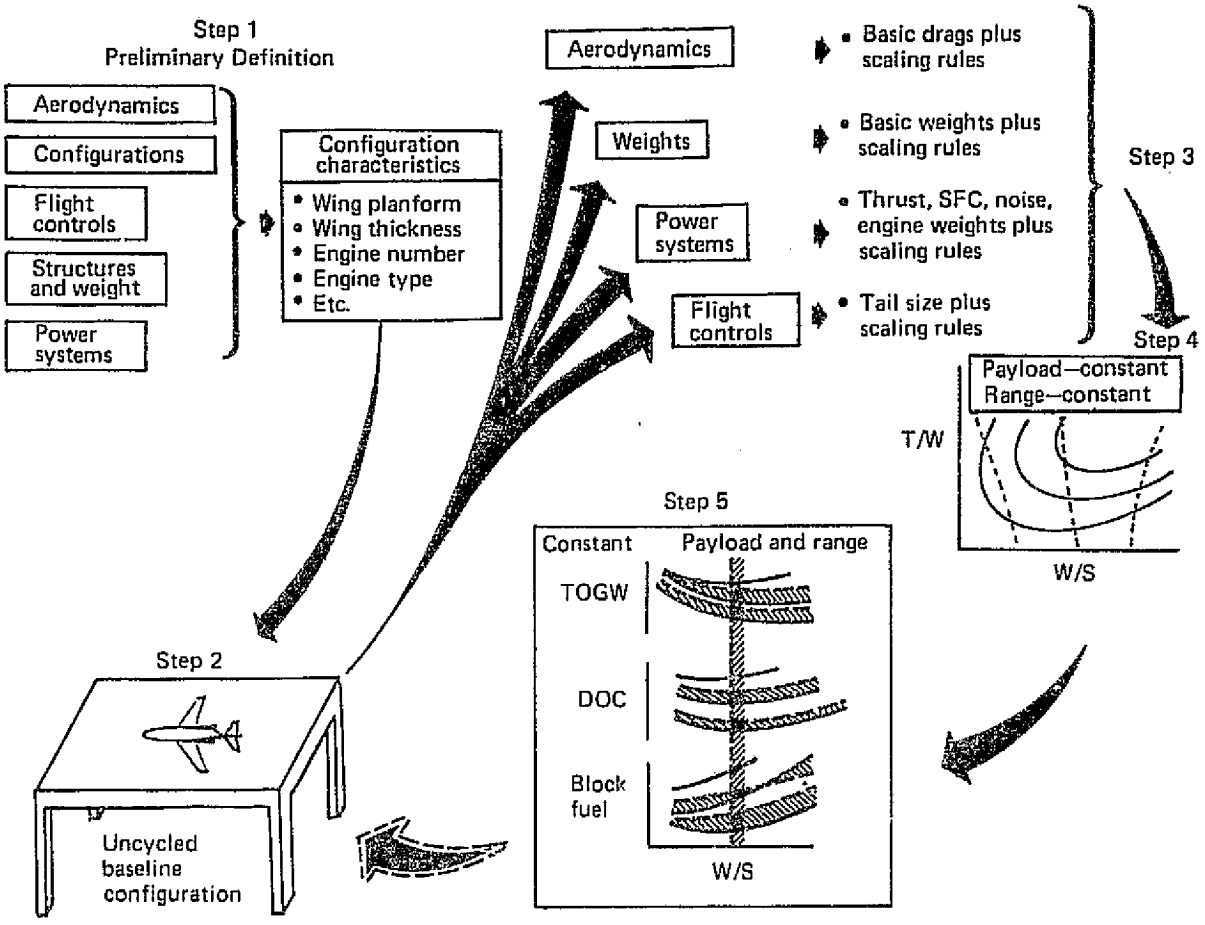

Figure 6.3-2. Parametric Design Development Method

speed (V_A), and initial cruise altitude capability (ICAC) are also included as well as direct operating costs as functions of T/W and W/S. Step 5 shows cross-plots of the pertinent design parameters along lines of constant ICAC and the mission constraints (V_A, TOFL, etc.). With these data a final analysis of the effect of the study parameters on airplane performance and economics was accomplished.

6.3.1 WING SWEEP STUDY

Several study configurations evolved from the initial Baseline Airplane as a result of the concept evaluation studies indicated on Figure 6.3-1. Among these studies, that for the suction system indicated that the 25° sweep wing would require suction slots so near the leading edge highlight (based on Northrop X-21 design criteria) that the wing manufacturing and maintenance requirements for a practical air transport could probably not be met. Consequently, a study configuration with a thinner wing and having 15° sweep (to maintain cruise Mach at 0.8) was established to explore the impact of reduced sweep on overall airplane characteristics and performance. This configuration which is shown in Figure 6.3-3, was also used in the wing aspect ratio and engine bypass ratio studies reported below.

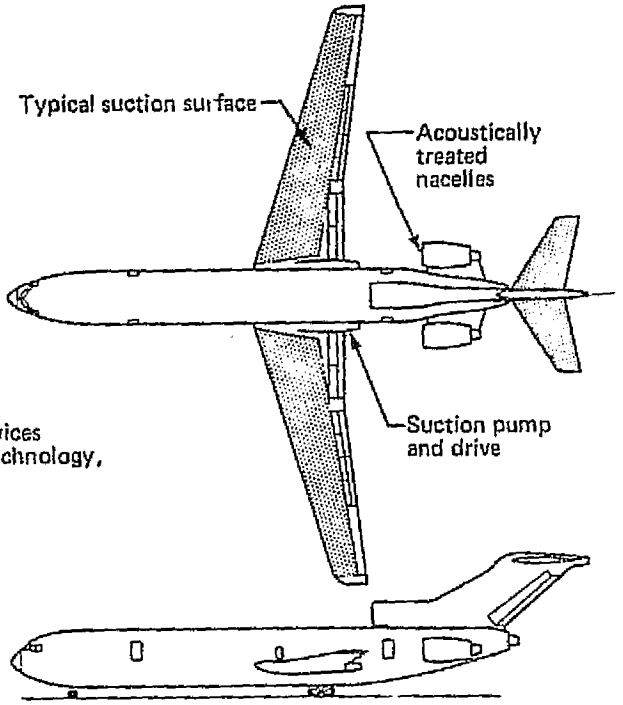

TOGW	165 561 kg (365 000 lb)
Payload	201 passengers
Wing area	340 m^2 (3658 ft^2)
Wing span	63.85m (209.5 ft)
Taper ratio	0.35
Sweep	15 deg
Aspect ratio	10
Flaps	TE single-slotted, no LE devices
Engine thrust	158 kN (35 500 lb),1990 technology, BPR = 7.3
Body length	50.3m (165 ft)
Body diameter	5385 mm (212 in)

Figure 6.3-3. Study Configuration—Model 767-809

The pertinent results of this study show that the 15° sweep airplane has a higher OEW because of increased wing weight. This weight increase occurs because of the thickness ratio reduction and increased lift curve slope which requires additional structural material to resist critical gust loads. Therefore, the 15° sweep configuration has a higher takeoff gross weight and block fuel requirement for the design payload/range mission.

Figure 6.3-4 shows the results of the wing sweep trade study as a function of the minimum wing loading required to satisfy the initial cruise C_L constraint of 0.55. For an initial cruise altitude capability of 12 190 m (40 000 ft) and wing loading of 4.8 KPa (100 lb/ft^2), the 15° sweep airplane has a 5% higher takeoff gross weight and 2.5% greater fuel burned.

To meet the initial cruise altitude capability objective of 12 800 m (42 000 ft), the engine size must be approximately 15% larger. Consequently, takeoff gross weight increases 4.2% and block fuel goes up by 2.1%.

In conclusion, the wing sweep study shows that reducing the wing sweep:

1. Significantly increases the gross weight and fuel burned.
2. Has no significant impact on wing loading or high altitude cruise trends.
3. Requires a thinner wing which reduces structural efficiency and accessibility.

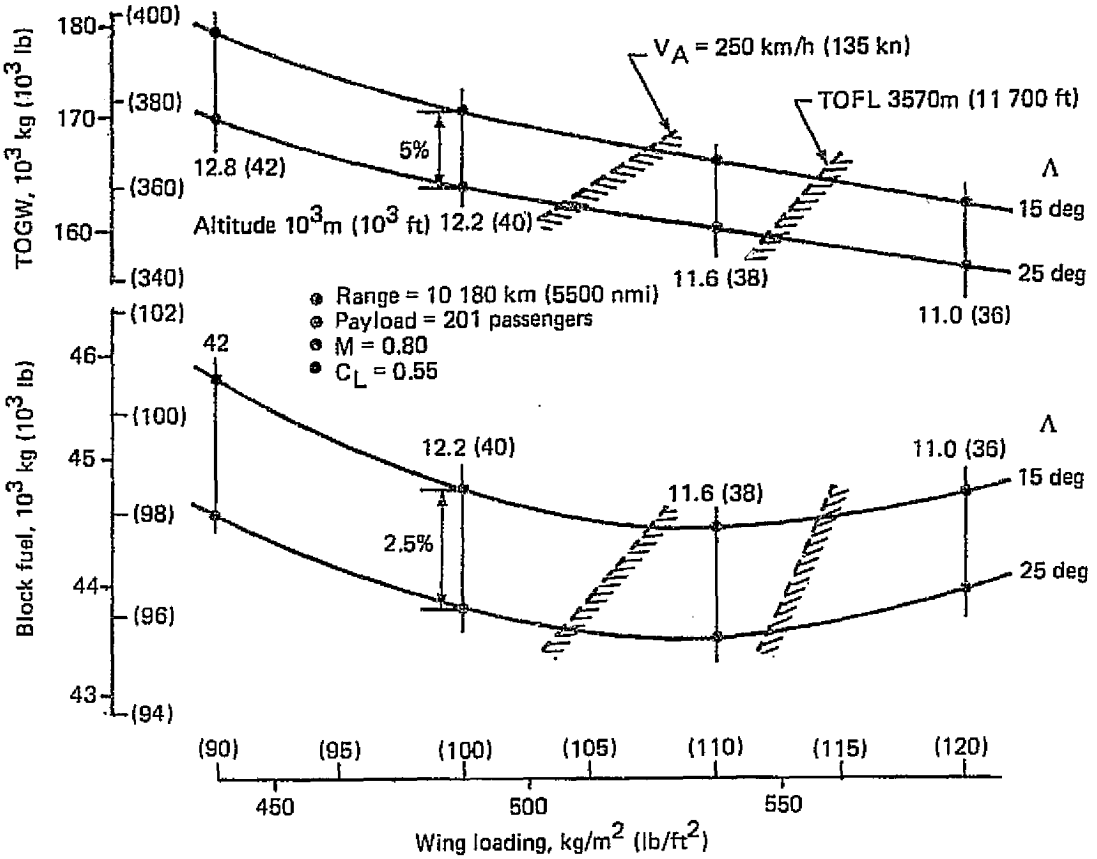

Figure 6.3-4. Wing Sweep Effects

6.3.2 WING ASPECT RATIO STUDY

Another of the LFC parametric studies investigated the effects of wing aspect ratio on airplane size, fuel efficiency, and economics. This study evaluated a series of three LFC transport airplanes having aspect ratios of 8, 10, and 12.

For each airplane, wing loading and initial cruise altitude capability were varied independently to determine their effects on size and performance characteristics. Figures 6.3-5, 6.3-6 and 6.3-7 show the resulting economics and fuel burned for aspect ratios of 8, 10, and 12, respectively. Studying the locations of the constraints on these charts reveals that the configurations are restricted to fairly small regions by the approach speed (V_A), maximum cruise C_L, and takeoff field length (TOFL) limits. The turbulent flow climb rate limit, 91.4 m/min (300 fpm) at 10 670 m (35 000 ft), is not a hard constraint and values exceeding 76.1 m/min (250 fpm) are generally attained within the regions defined by the other limits. It is also noteworthy that the 12 800 m (42 000 ft) cruise altitude objective is not attainable without either increasing the cruise C_L value or going to very light wing loadings. Moreover, either approach to increasing cruise altitude would result in a significant economic penalty for the LFC airplane at any aspect ratio studied.

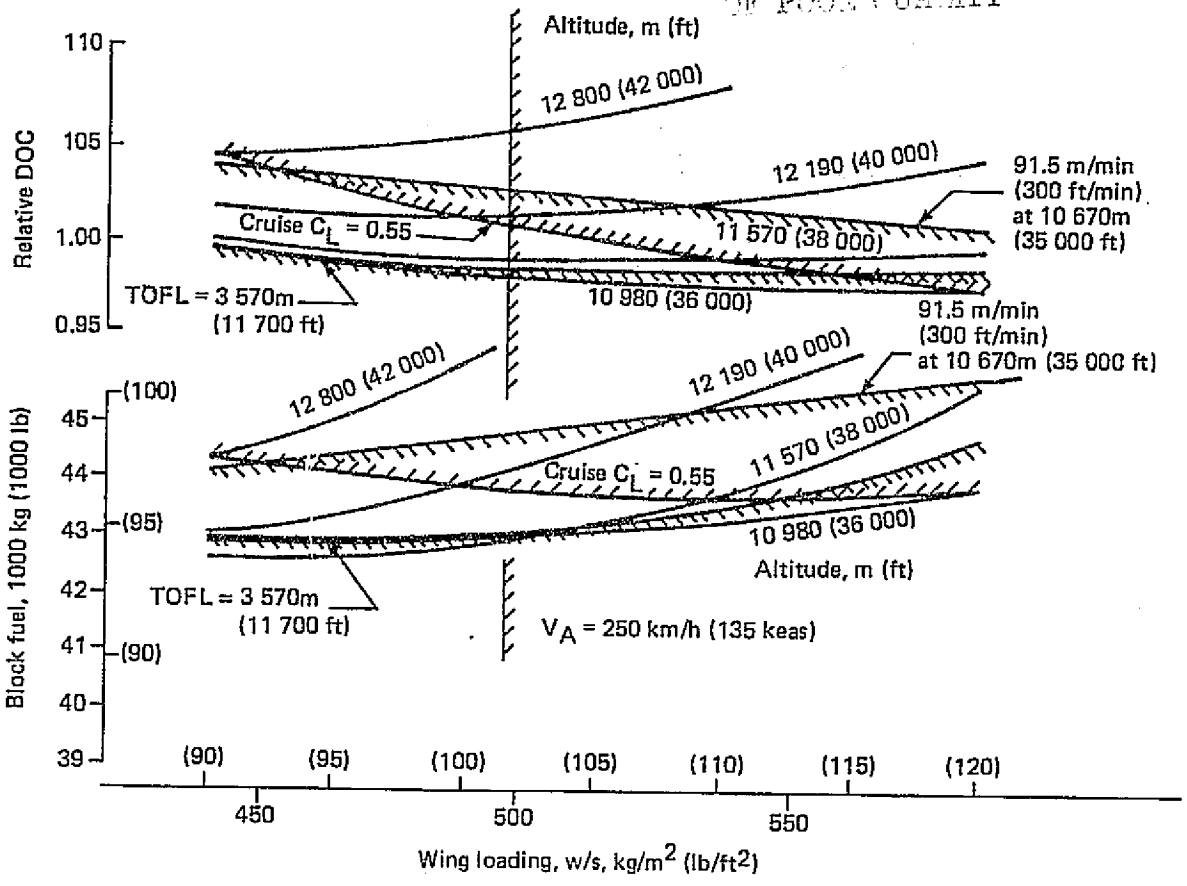

Figure 6.3-5. Cruise Altitude Effects--Aspect Ratio = 8

Figure 6.3-8 illustrates the effects of wing aspect ratio and initial cruise altitude on economics and fuel efficiency. The curves show the minimum values for relative DOC and block fuel at which the principal constraints (i.e., approach speed, takeoff field length, and maximum cruise lift coefficient) are satisfied. As noted earlier, the turbulent flow climb rate criterion of 91.4 m/min (300 fpm) is not treated as a hard constraint. The shaded area on each plot indicates the region where additional structural material might be required to prevent flutter. However, susceptibility of the higher aspect ratio configurations to flutter was not specifically evaluated in this study although Boeing experience indicates potential flutter impact on wing weight about AR = 10 or so. Increasing the aspect ratio from 8 to 12 provides substantial improvements (10%) in fuel efficiency at a small penalty in DOC, ignoring possible weight penalties associated with flutter. The original initial cruise altitude objective of 12 800 m (42 000 ft) has a substantial impact on the airplane economics; viz., lowering this requirement by 610 m (2000 ft) would improve direct operating costs by 4% and fuel efficiency by 2%.

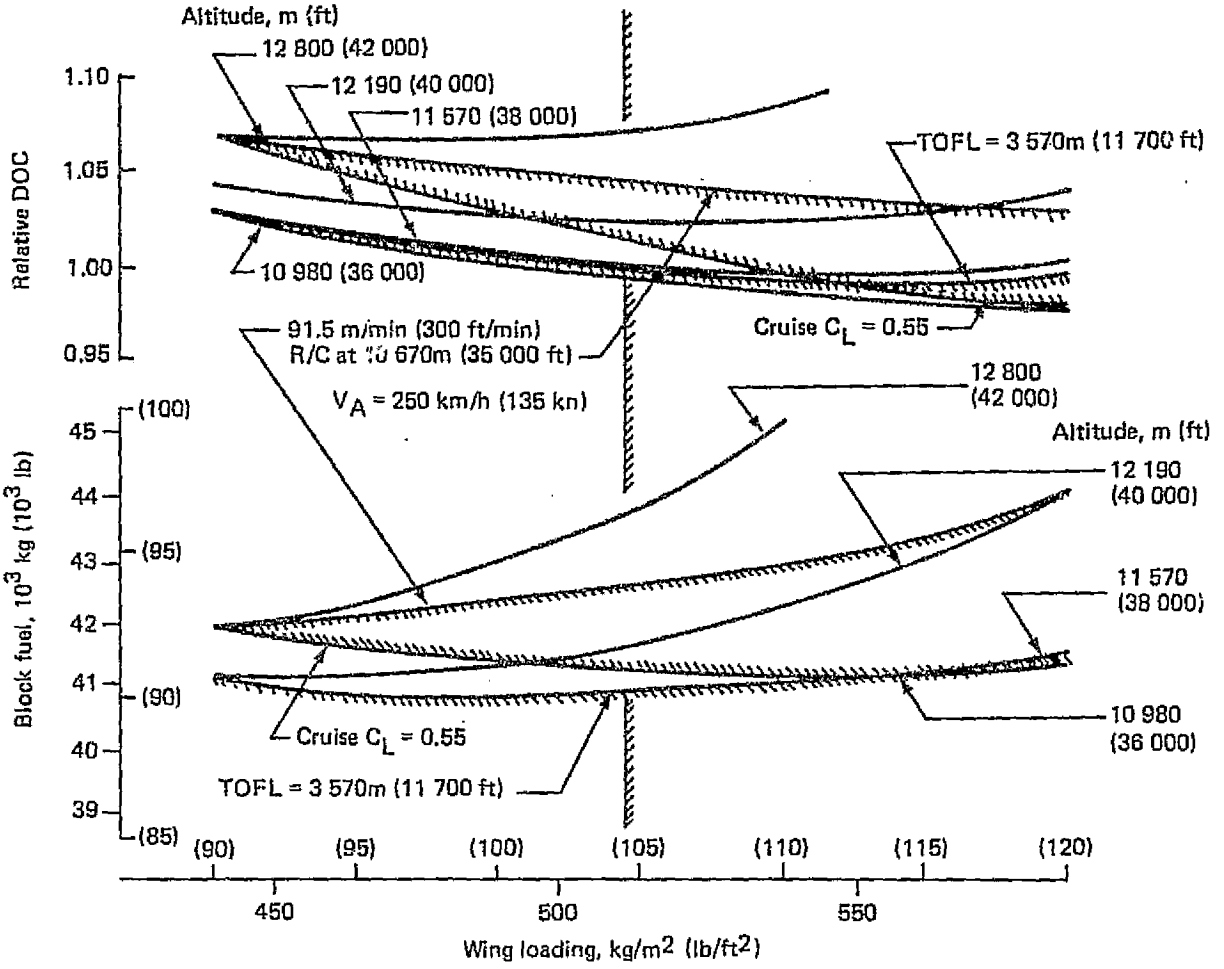

Figure 6.3-6. Cruise Altitude Effects—Aspect Ratio = 10

In summary, the wing aspect ratio parametric study results (ignoring potential flutter impact) indicate the following conclusions:

1. The choice of initial cruise altitude controls the economics and increasing aspect ratio slightly degrades DOC's.

2. The choice of aspect ratio has a substantial effect on block fuel with initial cruise altitude having a minor effect.

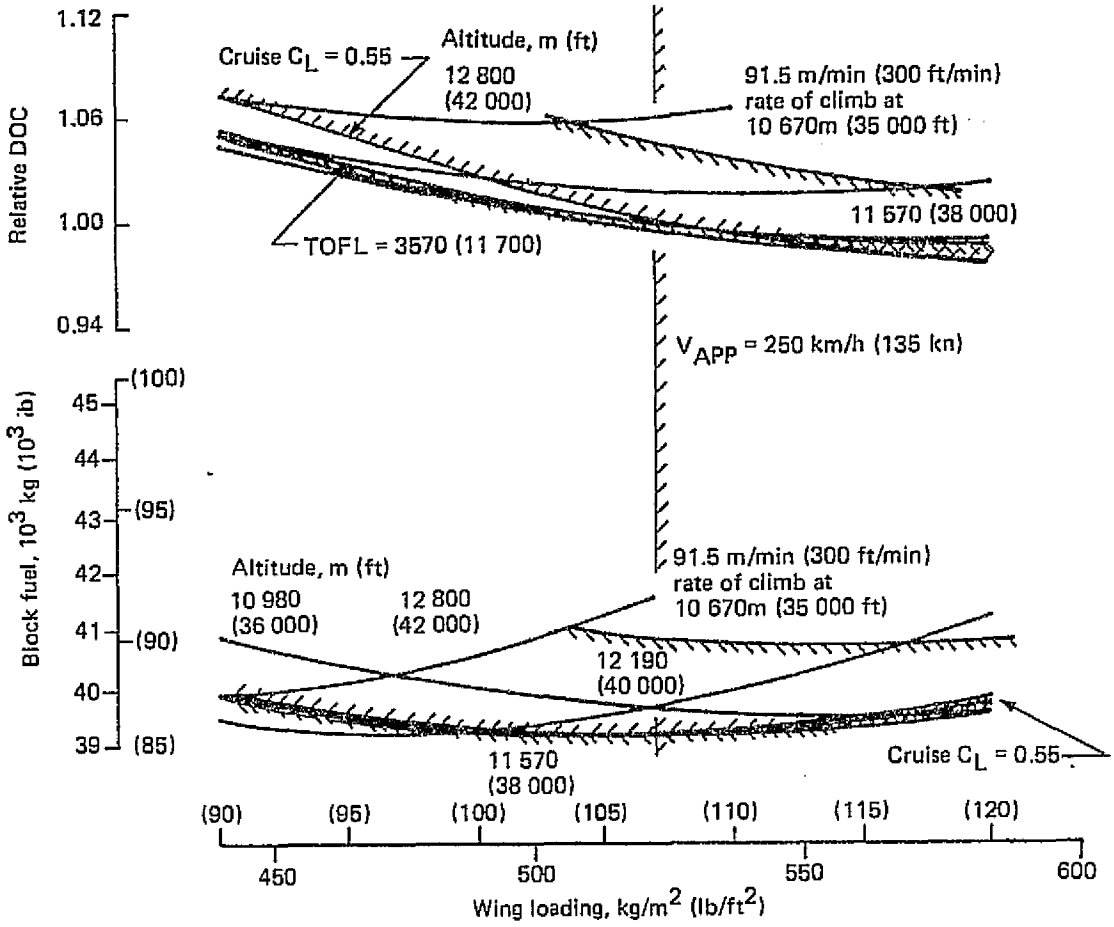

Figure 6.3-7. Cruise Altitude Effects—Aspect Ratio = 12

6.3.3 ENGINE BYPASS RATIO STUDY

The final phase of the parametric studies was directed to evaluation of the effects of engine bypass ratio on the performance of the LFC transport. The baseline airplane had an excess of takeoff performance capability as a result of the combination of a high bypass ratio (BPR = 7.3) and a high initial cruise altitude objective (ICAC = 12 800 m (42 000 ft)). Therefore, this study was initiated to determine if a lower bypass ratio engine might provide a better match for this airplane since, for a constant cruise thrust, a lower bypass ratio would produce less takeoff thrust which is not critical to meet the takeoff requirement. A lower bypass ratio also results in a smaller, lighter engine with, however, higher cruise fuel consumption.

Representative engine cycles incorporating technology advances available in the 1990's were simulated for design point bypass ratios of 7.3, 6.6, 6.0, and 4.5. Relative performance and size characteristics are shown in Figure 6.3-9 for the study engines. The engine characteristics used in this investigation were based on single-stage fans for bypass ratios

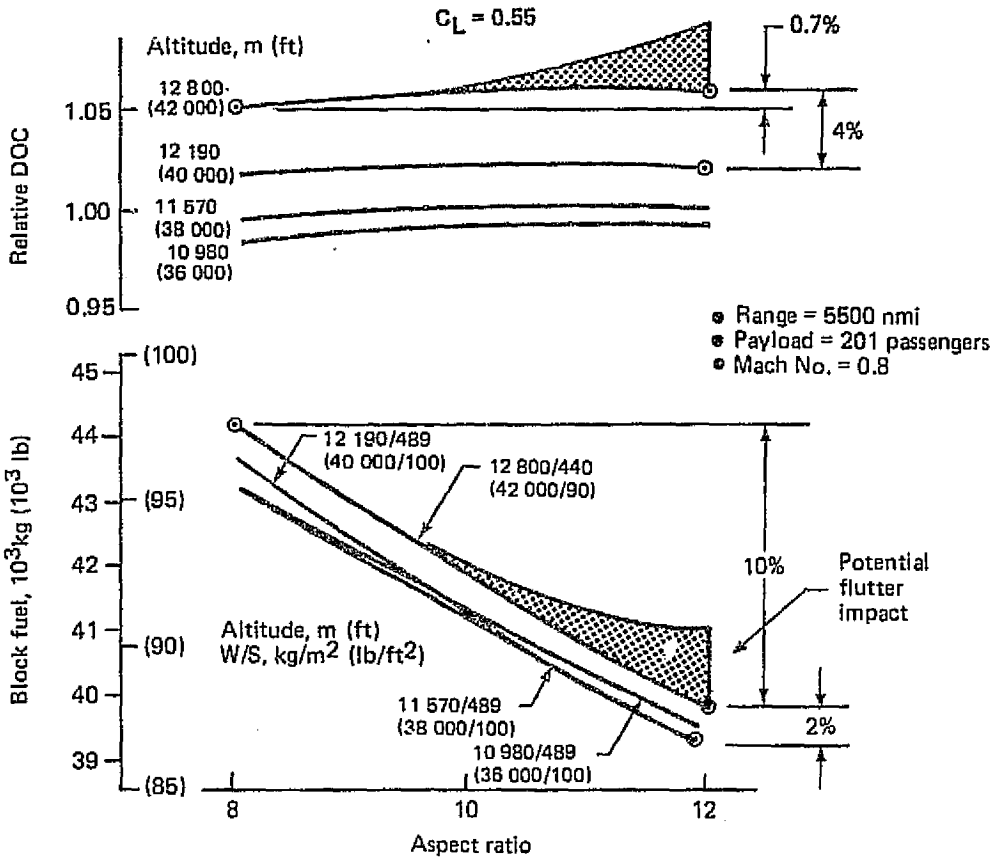

Figure 6.3-8. Wing Aspect Ratio Effects

above 6.0 and a two-stage fan at 4.5 bypass ratio. Because of better fan efficiency, the SFC trend line for the two-stage 4.5 BPR fan is about 2.5% below the trend line indicated for single-stage fans. At higher bypass ratios, this would give the two-stage fan a significant SFC advantage over the single-stage fan at the expense of about 750 lb/engine and 12 inches of additional length.

A summary plot of the study results, Figure 6.3-10, illustrates the effects of BPR on the direct operating cost (DOC) and block fuel at maximum cruise lift coefficient (C_L = .55) and an initial cruise altitude capability of 12 800 m (42 000 ft). These results indicate that the selection of engine bypass ratio does not have a significant impact on the fuel efficiency or economics of the LFC airplane. Reducing BPR from 7.3 to 4.5 causes a 1.5% decrease in DOC but, also, a 1% increase in block fuel. The airplane with a 7.3 BPR engine has maximum fuel efficiency for a small penalty in economics. These parametric data also suggest a two-stage fan would show a small improvement in fuel efficiency over the base-line single-stage fan but cause a small penalty in economics. Since the increments were small and an extensive study would be required to verify these trends, the baseline engine single-stage fan concept was retained.

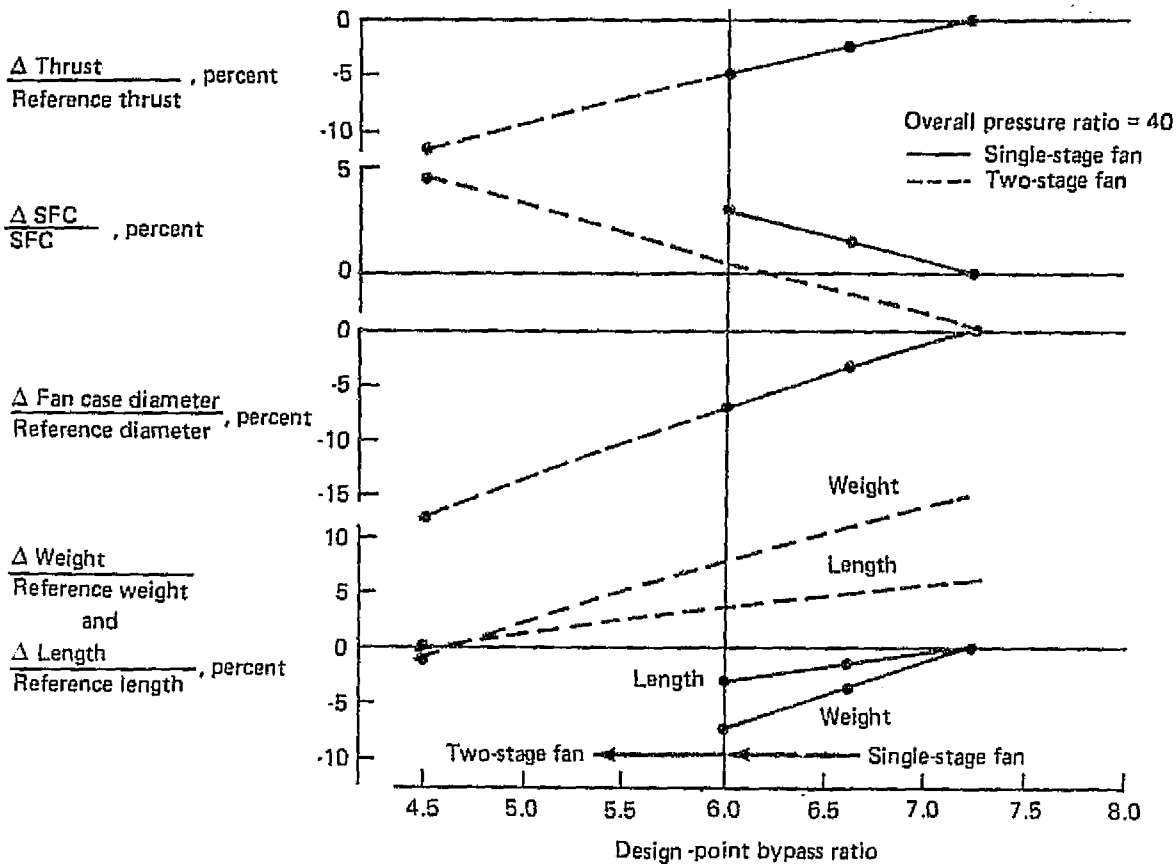

Figure 6.3-9. Characteristics of Study Engines

With respect to these trends, several items are worth noting. The DOC analysis in this study did not include any effect of reduced BPR on engine maintenance costs. In addition, the smaller diameter lower bypass ratio engines present an easier aerodynamic integration problem and this effect is not accounted for in these data. Finally, it should also be noted that all engines are high technology engines (high Overall Pressure Ratio (OPR) and Turbine Inlet Temperature (TIT)) and a study conducted at reduced technology levels could show different trends.

With the above in mind, it was concluded from the bypass ratio studies that:

- Bypass ratio does not have a substantial influence on fuel efficiency or economics.
- Aerodynamic integration and maintenance costs tend to favor low bypass ratio while fuel usage tends to favor high bypass ratio.
- A two-stage fan may show improved fuel efficiency over a single-stage fan.

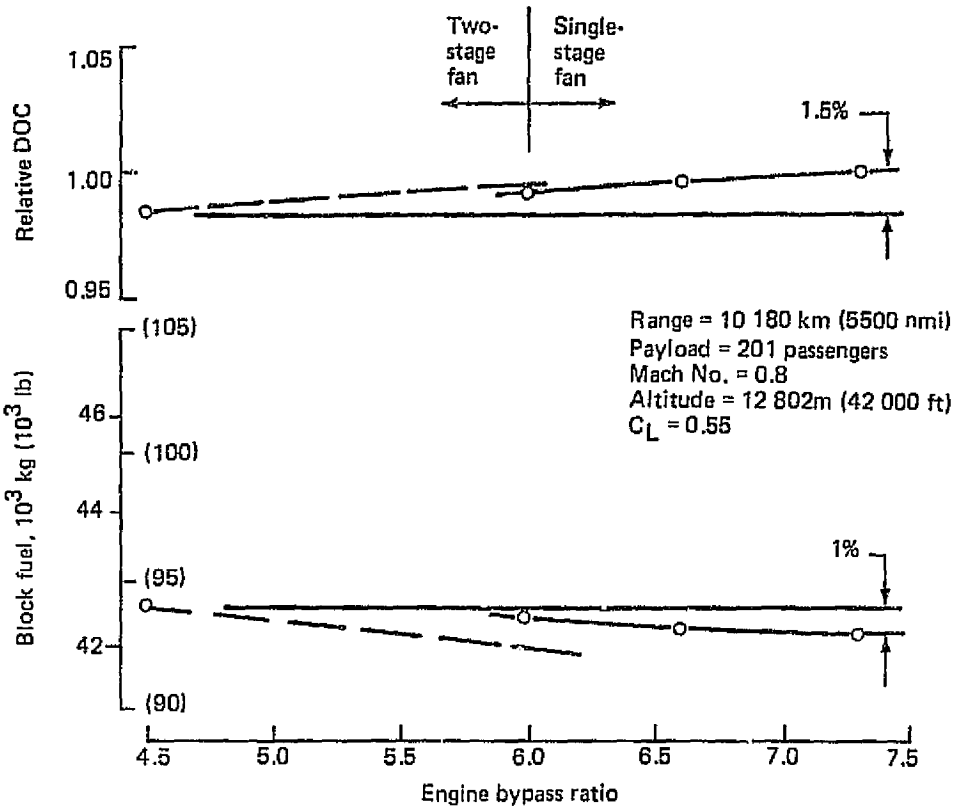

Figure 6.3-10. Engine Bypass Ratio Effects

6.3.4 PARAMETRIC STUDIES CONCLUSIONS

The results of the overall parametric studies indicate that the baseline wing geometry and engine bypass ratio should be retained for the final configuration. Therefore the parametric study design selections are:

- Wing Aspect Ratio — 10.0
- Wing Sweep — 25^o
- Engine BPR — 7.3 (Single-stage fan)

Relaxing the cruise altitude capability from the original objective of 12 800 m (42 000 ft) to 12 190 m (40 000 ft) at the design range-payload condition provides improvements in the airplane fuel efficiency and economics providing the current objective for turbulent rate of climb can also be slightly relaxed. This appears a reasonable choice since most flights in actual service would be conducted at reduced gross weight conditions where cruise altitude capability would meet the original objective of 12 800 m (42 000 ft).

6.4 TECHNOLOGY LEVEL AND IMPACT

Based on the current programs and projections for the development of laminar flow control technology, its application to a subsonic transport is a real possibility for the 1990 time period. Furthermore, advances in other technologies are also to be expected in this period based on existing programs in government and industry. Thus a combination of compatible advances can logically be projected. The final LFC airplane configuration presented in this chapter is therefore conceived for introduction into service in the early 1990's incorporating the currently projected technology advances appropriate to this time period.

The listing given in Table 6.4-1 defines the advanced technology elements incorporated in the final airplane configuration and provides an assessment of the gains to be expected for

Table 6.4-1. Advanced Technology Impact

	Δ Component weight	Δ (L/D)	Δ SFC
Aerodynamics			
Laminar flow control	To be determined	26% (33%)*	2.3% (2.7%)*
Advanced airfoil section	-14% wing box -8% empennage		
Reduced roughness		2% (3.5%)*	
Active controls			
Reduced longitudinal stability	-20% horizontal tail	3%	
Load alleviation	-6% wing box		
Propulsion			
Advanced turbofan (BPR = 7.3)	-13% engine		-14%
Advanced structures and materials			
Improved aluminum alloys	-7% wing box -4% fuselage -4% empannage		
Improved titanium alloys	-20% heavy fittings		
Bonded construction	-5% fuselage		
Graphite/epoxy composites	-25% trailing edge surfaces -27% wing box** -15% fuselage** -15% empennage**		
Carbon brakes	-10% landing gear		
Reference: Existing levels			

*Applicable for laminarized wing and empennage

**Applicable if composites used in place of improved alloys and bonded construction

each element based on application to the baseline airplane and without recycling the design. Of major significance, of course, is laminar flow control itself which provides a 26% gain in lift to drag ratio (L/D) when applied to the wing alone. When the horizontal tail is also laminarized, as for the final configuration, a 33% gain in L/D is projected. Partially offsetting this large gain is an equivalent increase in engine SFC of 2.7% which accounts for the fuel consumed by the suction units. Also a significant weight penalty occurs because of the basic need to provide viable suction surfaces in the laminarized areas and provisions for internal flow passages and distribution ducting to handle the suction air. The values shown in the table of Figure 5.2-36 correspond to unit weight penalties of slightly less than 4.79 Pa (1 lb/ft^2) for the wing. An additional increment of 2.15 Pa (.45 lb/ft^2) accounts for the weight of wing suction units and distribution ducting. A value of 4.06 Pa (.85 lb/ft^2) was used for the horizontal tail LFC structure penalty in the laminarization studies discussed in Paragraph 5.1.6.2. Since the horizontal tail suction is provided by a unit which also serves as an APU (only slightly oversized for suction) the added unit weight penalty for the tail suction system is only .72 Pa (.15 lb/ft^2). The area base in all cases is the actual laminarized area.

It is well-recognized that recent advances in airfoil design appear primarily as weight improvement since higher thickness ratios are permitted for given values of cruise Mach number and lift coefficient. These benefits are somewhat greater for an LFC airplane since it tends to optimize at higher aspect ratio and lower wing loading. Furthermore, the profile drag penalties associated with increased thickness for a turbulent airplane do not apply for the laminar airplane. Reduced roughness drag, which is possible because of the inherent smoothness of the LFC wing and the use of bonded construction on the fuselage and empennage, provides a significant gain in L/D as compared with today's turbulent aircraft.

The incorporation of active controls provides substantial improvement in both weight and L/D, through reductions in both tail size and trim drag. Load alleviation is effective for both maneuver and gust loads but studies show that the impact will vary considerably depending on airplane configuration. An adaptation of previous studies done for conventional transport configurations in which the outboard aileron is used as the active element, indicates that 6% of the wing box weight can be saved for the LFC final configuration. The increased systems requirement, however, reduces the saving to about 5%. The use of a flutter suppression system (FSS) is not projected for the final airplane because numerous studies on similar configurations have not shown this to be necessary for wing aspect ratios of 10 or less. Even a small weight penalty to provide adequate flutter margins is preferable to the added complexity and weight of a flutter suppression system. However, if the fuel saving benefits due to higher aspect ratio become increasingly important in time, the use of an FSS should be considered.

An advanced turbofan may be a reasonable possibility in the 1990 time period provided that ongoing studies (e.g., the EEE program) continue to support substantial performance and weight gains such as those shown in Table 6.4-1. Such gains would have to be achieved with high confidence that unfavorable maintenance trends with current high bypass ratio engines could be avoided. The results of engine cycle studies for LFC application tend to show significant gains for bypass ratios up to 7.5 with small effects on cost-related factors.

The discussion of Chapter 5.0 highlights various aspects of structural concept development in which favorable combinations involving different materials and types of construction have been sought. The application studies have primarily involved the wing structure where it is difficult to assess the impact of each technology element. While it is recognized that these developments can benefit the turbulent airplane as well as the laminar airplane, the overall effect is significantly greater on the latter since configuration studies continue to point toward higher wing area and span for LFC airplanes. The use of advanced materials and construction techniques is thus more effective in reducing weight for the LFC airplane. A definitive comparison of the relative impact of advanced structures and materials for laminar versus turbulent airplanes must be left for the time when final designs of each aircraft, both performing the same mission, are available. The listing in Table 6.4-1, with the exception of the asterisked items, define the use of advanced structures and materials in the final airplane configuration. Again the benefit projections correspond to the baseline airplane, but the final airplane weight statement reflects the applications listed to a level consistent with the values shown.

It is apparent from the table that extensive application of graphite/epoxy composites to the airplane would exhibit the greatest potential for weight saving. However, these gains are only applicable in the longer term whereas those for improved aluminum alloys and bonded construction are available sooner. Therefore the final airplane does not incorporate graphite/epoxy composite construction in primary structure even though this would be compatible with the structural arrangements and systems otherwise defined. If composites do achieve a state of technology readiness in the 1990 time period, no significant difficulties in application are anticipated. On the other hand application of composites to trailing edge surfaces is considered appropriate for the near term and their use is specified for the final airplane configuration.

6.5 FINAL CONFIGURATION DEFINITION

The final LFC airplane configuration incorporates the results of the entire series of tasks involved in the contract study. Of primary importance are those involving the alternative systems evaluations and selections and the parametric trade studies used to determine proper choices for airplane arrangement and component sizing; i.e., those which best suit the airplane to economically perform the design mission and meet operational requirements representative of the airline operating environment.

6.5.1 GENERAL CHARACTERISTICS

Figure 6.5-1 shows the concept finally selected, namely; a long range trijet of conventional layout incorporating laminar flow control on both wing and horizontal tail and the various advanced technology elements defined in the previous section. It is designed to meet the airline general operating requirements and the applicable FAR insofar as possible at this time. As previously stated, the mission requirements remain as originally defined for the baseline airplane and the final set of design requirements are as defined in Section 6.1. The passenger accommodations provide 7-abreast seating with 2-aisles and allow the use of 8-abreast for full economy configurations. Cargo is accommodated in two sections. The forward compartment is sized for 20 LD-3 containers while the aft compartment is available for bulk cargo.

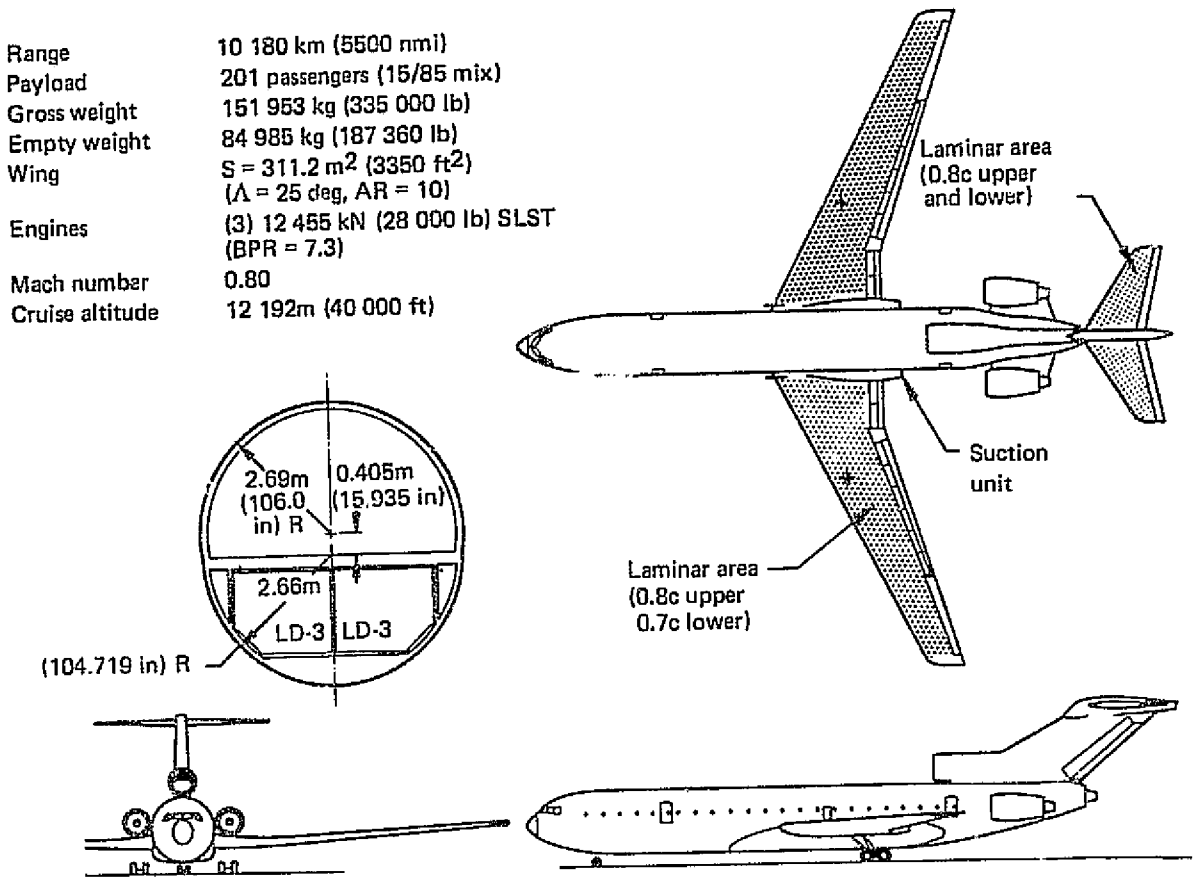

Figure 6.5-1. Final LFC Configuration—Model 767-811

The listing in Table 6.5-1 allows comparison between the final configuration (Model 767-811) and the baseline configuration (Model 767-807). While the overall arrangement is relatively unchanged, significant differences do exist which greatly improve the performance of the airplane. These differences are highlighted in the previous table whereas the rationale for selection of the various airplane features and the performance impact are discussed in appropriate sections of this report.

6.5.2 SYSTEMS DEFINITION

The following paragraphs provide a general definition of those systems in the airplane which are either specifically related or unique to an LFC transport. Unless otherwise noted, the remaining systems would be designed to provide the essential services and meet the general design and regulatory requirements as normally required for turbulent transports.

Table 6.5-1. Configuration Characteristics Comparison

	Baseline configuration model 767-807	Final configuration concept
Wing		
Sweep/t/c	25 deg/0.11	25 deg/0.11
Aspect ratio	10	10
Wing loading	103	100
Flap-chord ratio	0.25	0.20
Laminarization	0.70c (upper and lower)	0.8c upper/0.7c lower
Structural concept	Laminated aluminum honeycomb (spanwise ducts)	Conventional structure/fiberglass cover (chordwise ducts/spanwise trunks)
Empennage	T-tail (turbulent flow)	T-tail (horizontal tail laminarized to 0.8 chord)
Engines	Aft body-mounted (BPR = 7.3)	Aft body-mounted (BPR = 7.3)
Suction units		
Wing — Compressor	Two-pressure level	Two-pressure level
Wing — Drive	Turboshaft	Turboshaft
Wing — Location	Two, wing-mounted	Two, side-of-body
Empennage	None	APU
Leading edge		
Insect removal	—	Choice open*
Anti-icing	Bleed air	Bleed air

*Systems need evaluation and validation

6.5.2.1 Airplane Systems General Considerations and Selection

Conventional environmental control, hydraulic, pneumatic, electric and fuel systems are used. Modifications required to be compatible with the laminar flow control system are minimal and generally involve space routing provisions and flight control surface actuator locations. Airplane systems functions are integrated with LFC systems where performance requirements are similar.

The environmental control system utilizes a conventional air cycle cooling unit for cabin air conditioning. The leading edge anti-icing system is a conventional hot gas system that uses engine bleed air as the heat source. The air is ducted through a spray tube integrated with and located in the leading edge LFC suction duct cavity. The anti-icing air is directed on the surface to be anti-iced. The air then flows overboard through a vent located near the wing tip and a small amount through the leading edge slots. The hydraulic system operates at 20 690 k Pa (3000 psi). The plumbing is routed to be compatible with both the surface actuation and suction airflow collection requirements. The electrical system requires only minor wire routing provisions to be compatible with the laminar flow control system. The fuel system has added provisions required to supply fuel to the suction engines. Boost pump location and access areas require special provisions to ensure that the wing surface laminarized area is not compromised.

The APU power requirements are compatible with and are supplied by the empennage suction compressor drive unit. These include ground electric power and compressed air for cabin air conditioning and engine starting.

6.5.2.2 LFC Systems

Section 5.3 describes the location and system trade studies that were accomplished to select the location and type of suction unit best suited to the LFC application. These studies led to selection of turbine engine-driven axial suction compressors located in the wing root. The design conditions for these baseline studies were 12 800 m (42 000 ft) altitude, 0.8 Mach Standard Day, and $C_L = 0.5$. Size of the units were initially based on providing suction for slots located from 0 to 70% chord on both upper and lower wing surfaces.

As airplane studies progressed, performance requirements for the suction system changed. The upper wing suction surface was increased from 0 to 70% chord to 0 to 80% chord, and design altitude and C_L were also increased. Since horizontal tail laminarization was incorporated in the final configuration and since power requirements were compatible with APU functions, the concept of a dual usage APU/suction unit was introduced. The APU configuration was therefore changed to permit its use for suction during flight. Provisions are included to allow the suction compressor to be unloaded and shaft power supplied to the airplane accessories for APU operation. Table 6.5-2 compares the baseline and final suction unit requirements and size and gives the design performance of the final system. Installation of the two wing units in the wing root and the horizontal stabilizer unit at the base of the fin above the center engine is illustrated in Figure 6.5-2.

The wing and horizontal stabilizer leading edge protection systems (Section 5.4) power source will be provided by the airplane secondary power systems and will be determined by the protection system selected. A liquid film system will require electrical power for actuation control and fluid pumping. The high pressure air shield will require a compressed air source (e.g., engine bleed) and electrical power for actuation and control. The cryogenic frost system will require electric power for actuation and control and a circulating power source. Detailed trade studies are required to determine both power source selection and degree of systems integration required.

6.6 AIRPLANE PERFORMANCE CHARACTERISTICS

The final LFC configuration, Figure 6.5-1, is an engine-aft trijet with wing and horizontal tail laminarization. The design mission rules and flight profile used for this airplane are described in Subsection 6.1 and illustrated in Figure 6.1-1. The design requirements used to define this configuration are as listed in Table 6.1-1 with the additional constraints that 1) design cruise C_L can be 0.55 or less and 2) that wing loading be 49.1 kg/m^2 (100 lb/ft^2) as determined in the parametric configuration studies. The engine thrust and SFC characteristics are appropriate to the P&WA STF-482 engine cycle (BPR = 7.3) which incorporates an engine technology base projected to the 1990 period. These characteristics are presented in Figures 6.6-1 and 6.6-2 for standard day conditions.

Table 6.5-2. Suction Unit Requirements, Size, and Performance

	Wing Units		Horizontal Stabilizer Unit
	Baseline*	Final	
Design conditions	h = 12 800m (42 000 ft) M = 0.8 C_L = 0.5 Standard day	h = 13 560m (44 500 ft) M = 0.8 C_L = 0.55 Standard day	h = 13 560m (44 500 ft) M = 0.8 C_L = 0.5 Standard day
Suction surface data Extent of laminarization, $(x/c)_L$			
Upper	0.70	0.80	0.80
Lower	0.70	0.70	0.80
Suction unit Corrected airflow, kg/s (lb/s)			
Upper	11.7 (25.7)	23.4 (51.6)	5.5 (12.13)
Lower	19.3 (42.54)	28.9 (63.74)	5.5 (12.13)
Suction engine shaft power,			
kW/unit (hp/unit)	246 (330)	383 (514)	112.9 (151.4)
Sea level equivalent power	1029 (1380)	1603 (2150)	546 (732)
Unit size (Dia.)			
Low pressure compressor	baseline	1.41 x baseline	Single stage suction compressor
High pressure compressor	baseline	1.224 x baseline	0.686 x baseline (low-pressure compressor)
Drive engine	baseline	1.33 x baseline	0.60 x baseline
Performance data (one unit)	h = 12 190m (40 000 ft) M = 0.8 C_L = 0.5 Standard day		h = 12 190m (40 000 ft) M = 0.8 C_L = 0.5 Standard day
Shaft power per unit, kW (hp)	177.5 (238)		117.4 (157.4)
Shaft power—total airplane, kW (hp)	355 (476)		117.4 (157.4)
Specific fuel consumption, kg/h/kW (lb/h/hp)	0.608 (0.5)		0.487 (0.4)
Fuel consumption, kg/h (lb/h)	108 (238)		47 (53)
Total fuel consumption (including 20% allowance), kg/h (lb/h)	315.5 (423) (all units)		

*Units sized for model 767-803

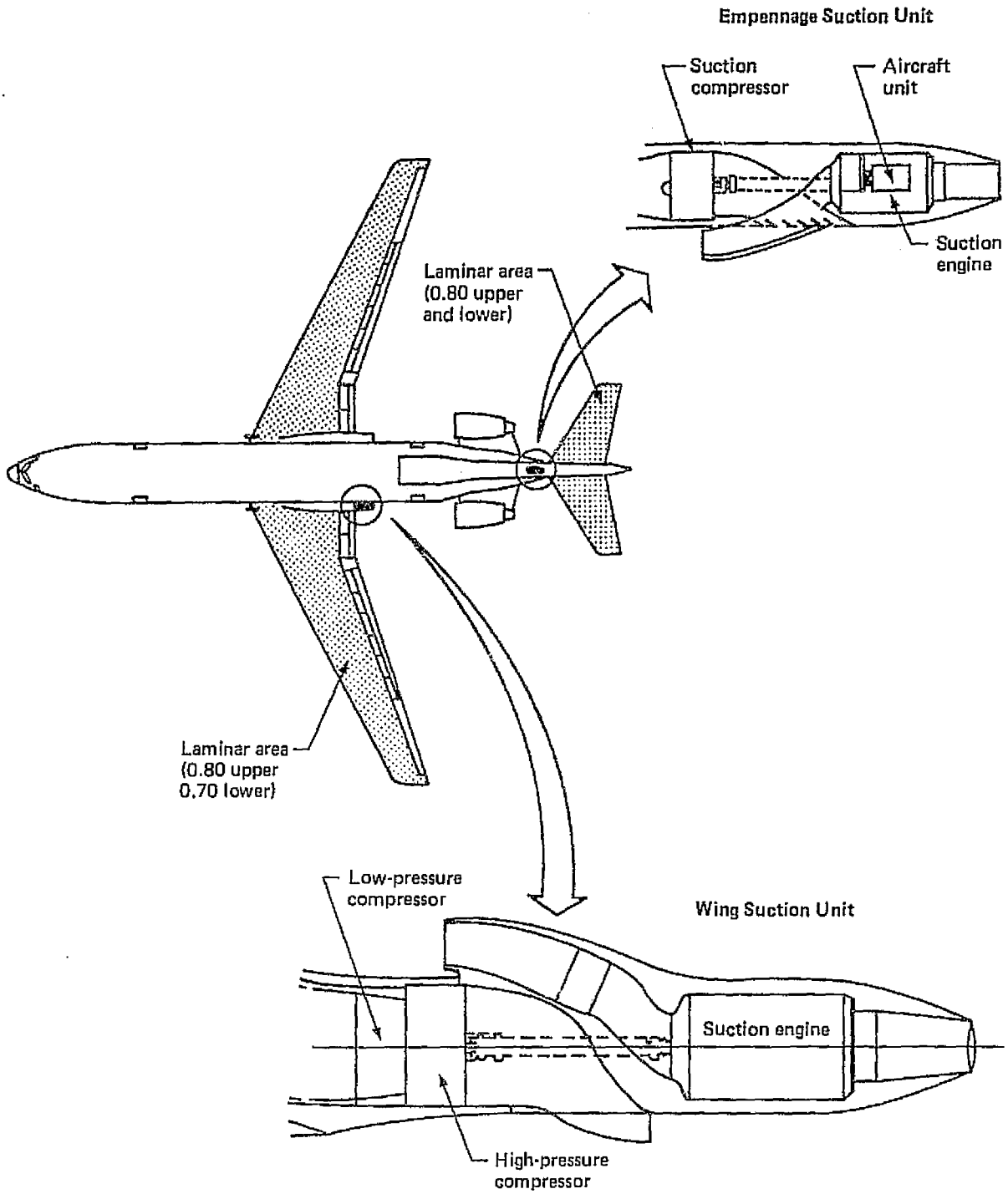

Figure 6.5-2. LFC Suction Unit Locations

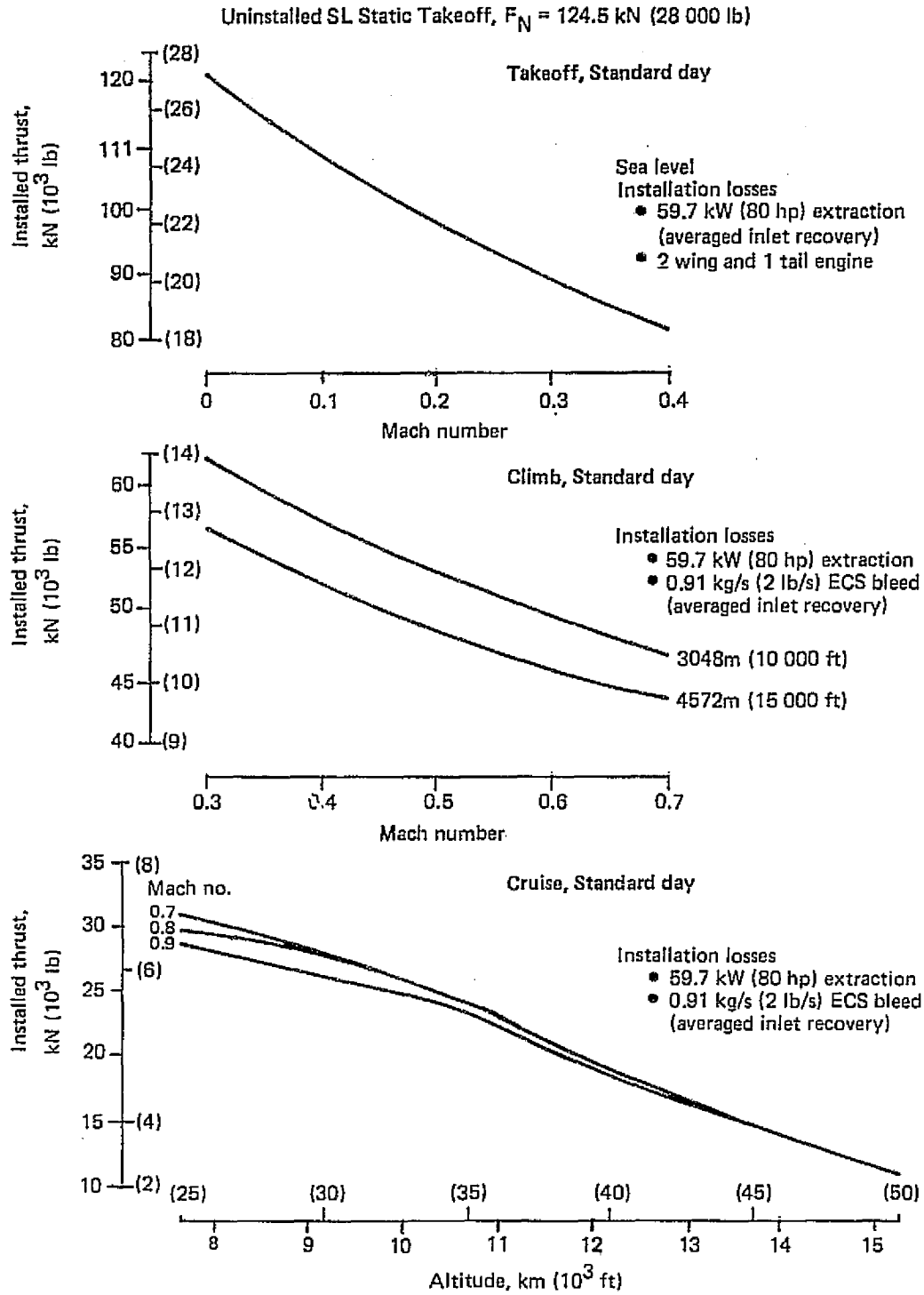

Figure 6.6-1. Engine Thrust Characteristics P&WA STF-482 (7.3 Bypass Ratio)

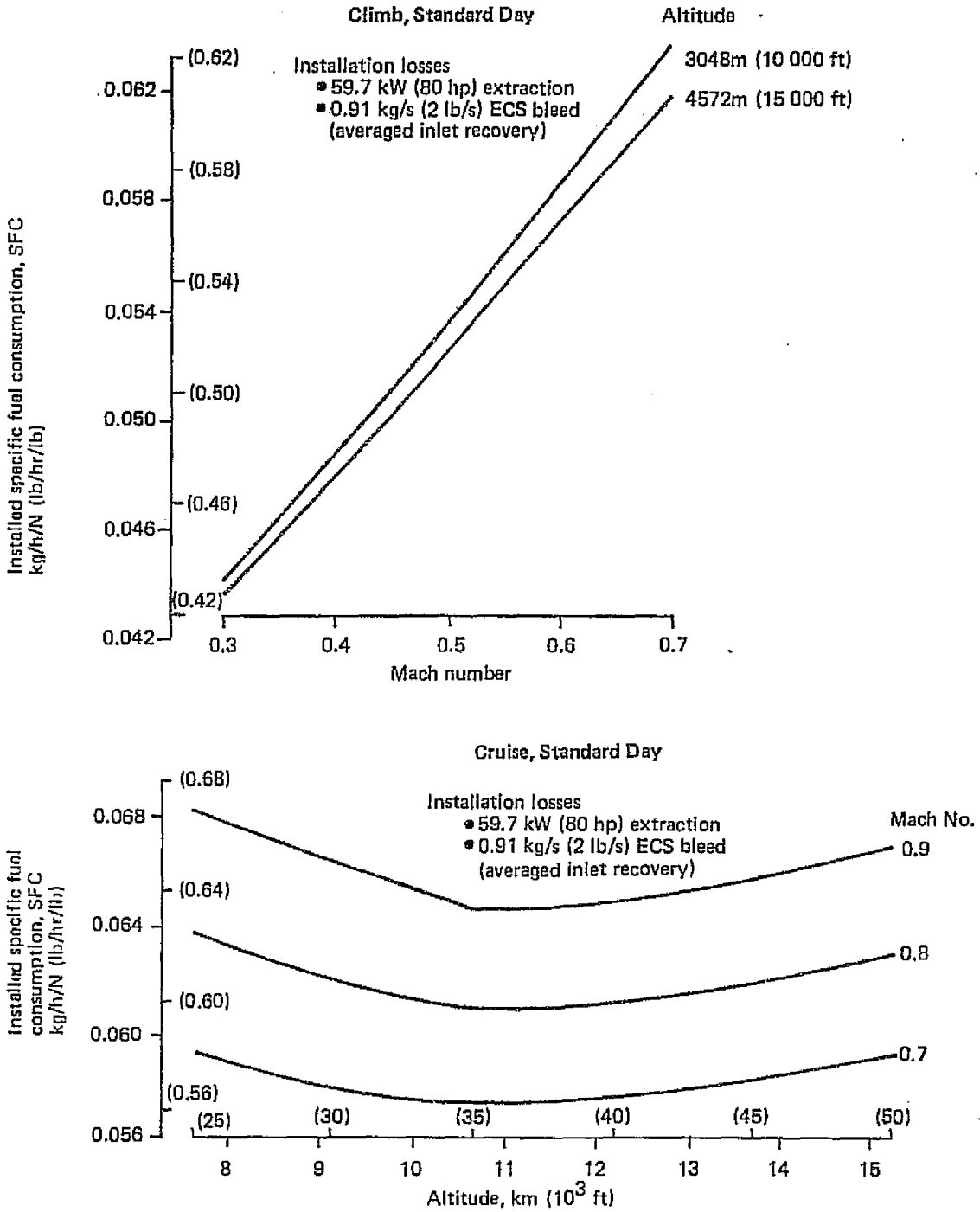

Figure 6.6-2. Engine SFC Characteristics P&WA STF-482 (7.3 Bypass Ratio)

A list of the more important airplane size and performance characteristics are shown in Table 6.6-1. The engine size was determined by the initial cruise altitude requirement of 12 190 m (40 000 ft). The wing loading was kept low to meet the approach speed objective and to keep the cruise C_L within acceptable limits without significant compromise in either DOC or fuel efficiency.

Table 6.6-1. Airplane Performance and Characteristics—Model 767-811

- Cruise Mach No. 0.80
- Payload 201 passengers
- Still air range 10 190 km (5500 nmi)
- Reserves 1967 ATA International
- Altitude, ICAC 12 190m (40 000 ft)
- Wing loading 490 kg/m^2 (100 lb/ft^2)

Item	Value	
TOGW	152 100 kg	(335 030 lb)
OEW	85 060 kg	(187 360 lb)
Block fuel	41 890 kg	(92 260 lb)
Block time	12.36 hr	
Reserves	6 030 kg	(13 290 lb)
Mission landing weight	110 440 kg	(243 260 lb)
Wing area	310 m^2	(3350 ft^2)
Wing aspect ratio	10	
Wing sweep	25 deg	
Horizontal tail area	58.5 m^2	(629 ft^2)
Vertical tail area	48.5 m^2	(521 ft^2)
Body length	50.3m	(1650 ft)
Body diameter	5.39m	(212 in)
Engine BPR	7.3	
$SLST_{UNINST}$	124.6 kN	(28 000 lb)
Range factor	34 300 km	(18 520 nmi)
$(L/D)_{max}$	25.5	
SFC	0.0635* kg/h/N	(0.6221* lb/h/lb)
FAR TOFL, SL 29°C (84°F)	2 440m	(8000 ft)
FAR landing field length (mission weight)	1 430m	(4700 ft)
Approach speed	246 km/h	(133.3 kn)

*Includes a 2.7% fuel flow for suction engines

6.6.1 BASIC PERFORMANCE

Figure 6.6-3 illustrates the payload-range performance of the final configuration. In the event of LFC failure at mid-cruise weight, the design mission can be completed. Total fuel volume including center section tank is approximately 73 050 kg (160 900 lb) which is sufficient volume to off-load the entire payload.

Figure 6.6-4 shows the fuel efficiency as a function of range. A comparison with the 747 airplane shows a 70% improvement in fuel efficiency due to LFC and the other technology advances incorporated in the Model 767-811. The effect of LFC alone for a cycled design of this type, is estimated to approach 45% increase in fuel efficiency.

Takeoff and landing performance for the Model 767-811 is shown on Figures 6.6-5 and 6.6-6. The FAR takeoff field length at sea level, 84°F, is only 2470 m (8000 ft) and well below the objective of 11 700 ft. The FAR landing field length is 1570 m (5150 ft) at maximum landing weight. The mission approach speed of 246 km/hr (133.3 kn) is slightly better than the original objective of 250 km/hr (135 kn) or less.

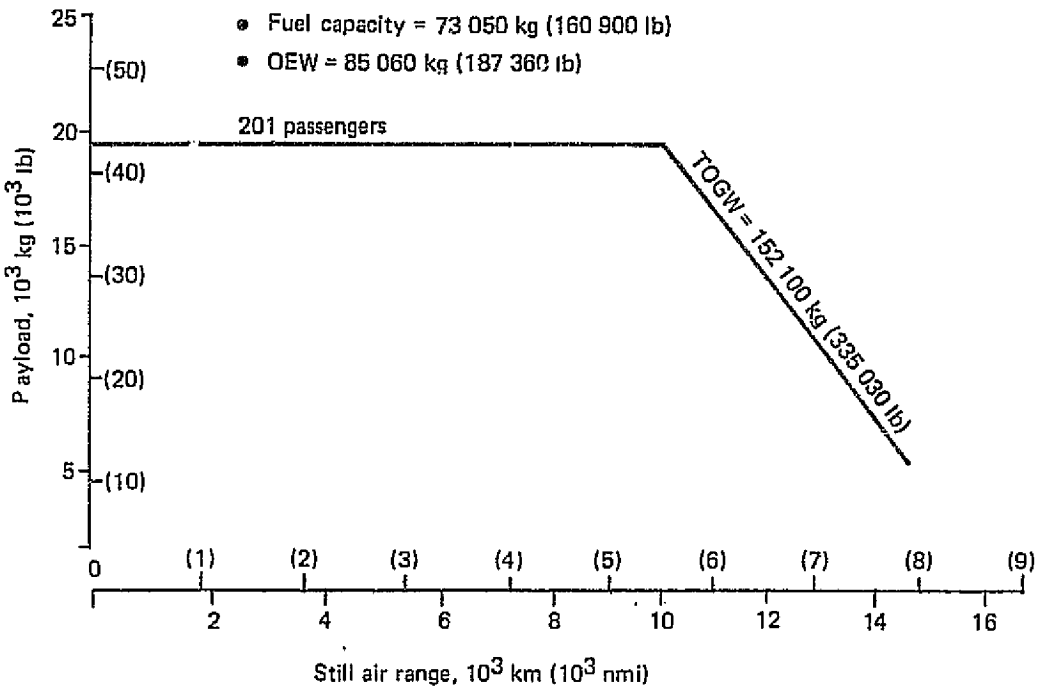

Figure 6.6-3. Payload-Range—Model 767-811

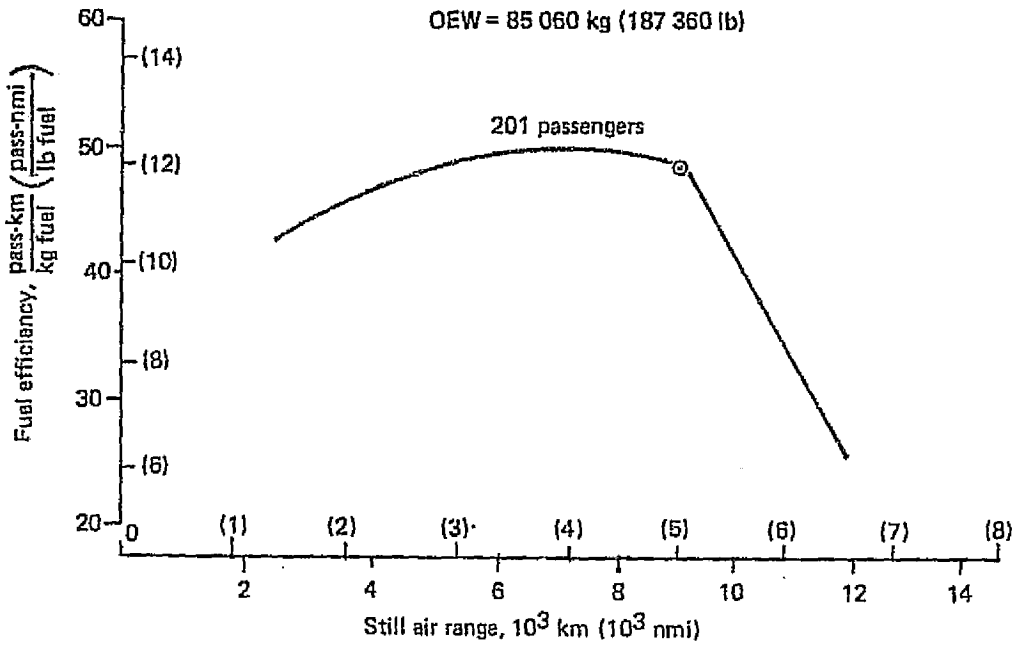

Figure 6.6-4. Fuel Efficiency—Model 767-811

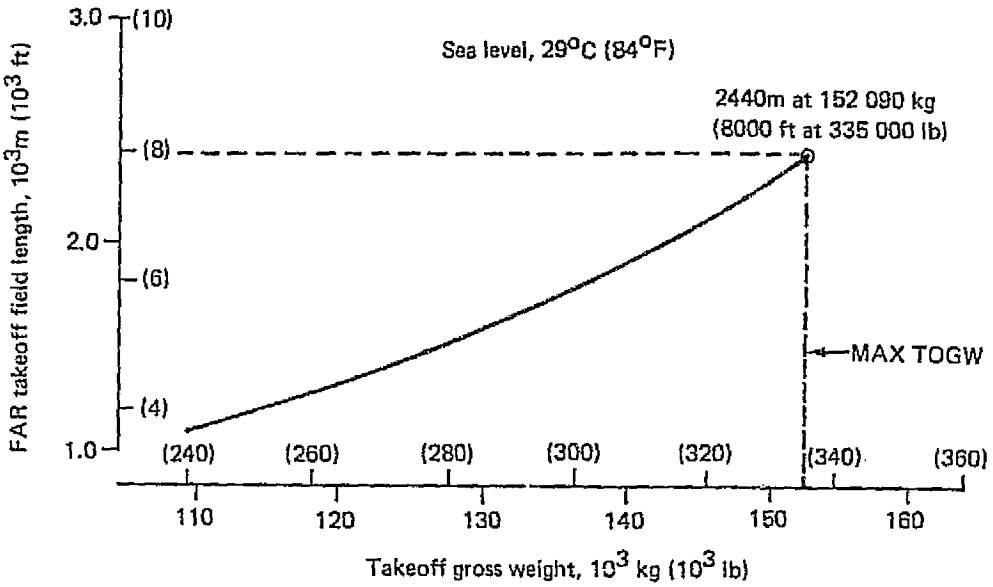

Figure 6.6-5. Takeoff Performance—Model 767-811

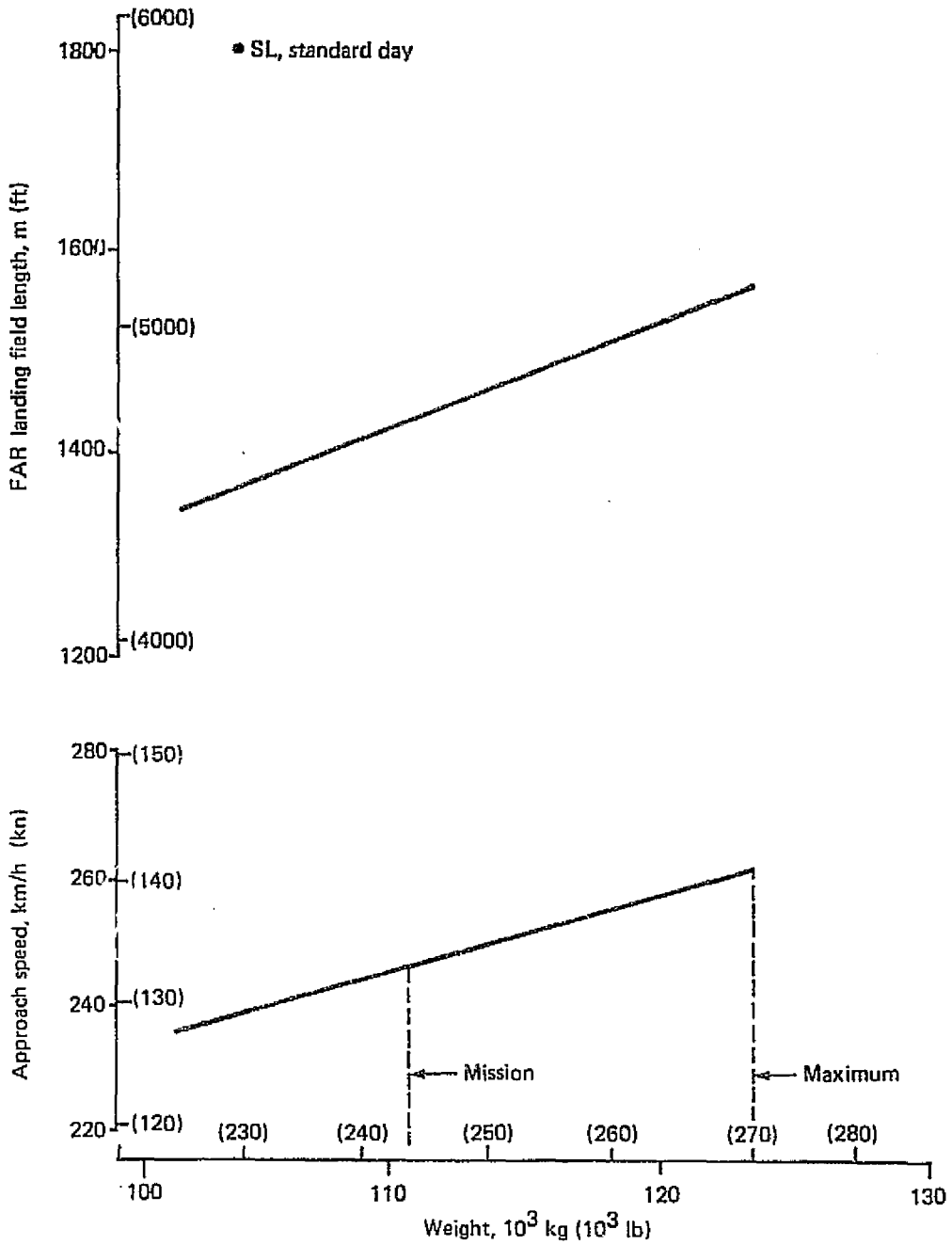

Figure 6.6-6. Landing Performance—Model 768-811

6.6.2 COMMUNITY NOISE

The noise characteristics of the LFC study aircraft Model 767-811 have been estimated for an entry into service date in the 1990 time frame. Engine noise and nacelle acoustical treatment were estimated assuming technology levels forecast for conventional commercial jet transports in service in the same period. Three STF-482 (7.3 BPR) engines were assumed with maximum takeoff thrust of 124 684 N (28 030 lb) SLST each and 270 km/hr (146 Kn) takeoff speed, and an approach thrust of 27 041 N (6160 lb) SLST at an approach speed of 250 km/hr (135 kn). The maximum takeoff gross weight was 152 400 kg (335 000 lb).

The estimated noise levels at the three FAR 36-9 certification points are shown in Table 6.6-2 together with the latest (1978) FAR 36-8 noise rule levels for new aircraft with three engines and 152 400 kg (335 000 lb) maximum gross weight. Although noise level trades are allowed between the certification points (FAR 36-9) if required in order to meet the rule, these have not been used for the estimates. It will be seen that the estimated levels are below the required noise levels by 2 to 5 EPNdB depending upon the certification point. It should be noted, however, that the estimates shown are nominal values, and appropriate design or demonstration tolerances are required for certification or guarantee levels.

6.6.3 WEIGHT AND BALANCE

The mission sized LFC airplane, Model 767-611, has an operating empty weight (OEW) of 84 970 kg (187 320 lb) as shown in Table 6.6-3. A preliminary balance evaluation of this configuration shows an acceptable loadability between the center of gravity limits of 5% to 39% MAC as defined in Figure 6.6-7. A maximum of twelve LD-3 containers in the forward lower level cargo hold may be used with a full passenger load. Cargo density of

Table 6.6-2. Community Noise for Model 767-811

	Takeoff[1] EPNdB	Sideline[2] EPNdB	Approach[3] EPNdB
Model 767-811*	94.0	94.5	101.0
FAR 36-8 rule† for new aircraft	98.7	99.4	102.9

[1]6500m (3.5 nmi) from brake release

[2]450m (0.25 nmi) to sideline

[3]2000m (1.08 nmi) from approach

*Nominal estimates shown; approproiate design/demonstration tolerances required for certifiable/guarantee levels

†No trades used

Table 6.6-3. Weight Statement for Model 767-811

Item	Weight, kg (lb)	
Total structure:	49 850	(109 900)
Wing	17 700	(39 010)
Empennage	3 990	(8 800)
Body	17 130	(37 770)
Nacelle	4 040	(8 910)
Gear	6 990	(15 410)
Propulsion system	7 510	(16 550)
Fixed equipment and options*	20 570	(45 350)
Standard and operating items	7 040	(15 520)
Operating empty weight (OEW)	84 970	(187 320)

*Includes suction unit weights for wing and empennage laminarization

160 kg/m^3 (10 lb/ft^3) is assumed. Full forward lower level cargo may be utilized if aft bulk cargo provisions are incorporated in the airplane design.

For the LFC configuration, prior to component sizing, the wing analysis was conducted using a computerized multistation beam analysis program to determine the load-sensitive wing box weight. This evaluation was combined with the application of statistical/parametric techniques to account for non-optimum wing box and secondary structure weight. Statistical/parametric techniques were also used to determine the remaining airplane structure, propulsion system, fixed equipment, and standard and operational equipment weights. These techniques are derived from Boeing production airplane experience modified by adjustments for configuration differences and advanced technology benefits.

Weight scaling philosophy involving interrelationships between component weights and design parameters (e.g., gross weight, wing area and engine thrust) can be expressed in terms of partial derivatives. These weight sensitivities were developed individually for various airplanes in recognition of their configuration characteristics as part of the series of parametric studies reported in Section 6.3. This enabled development of a consistent set of airplane operating empty weights as inputs to support the final airplane component sizing process.

Since a constant payload was maintained throughout the study, the primary weight effects due to variations in gross weight, wing area and engine thrust were limited to the airplane structure, surface controls and propulsion-related items. Payload related weight such as fixed equipment, customer options and standard and operational items remained unchanged.

The listing of Table 6.6-3 provides a weight breakdown for the principal components and systems of the airplane. Figure 6.6-7 shows the C.G. position variations for several airplane loading options. A restriction in forward cargo loading is apparent unless some aft cargo is also loaded. This is not considered to be a significant operational restriction.

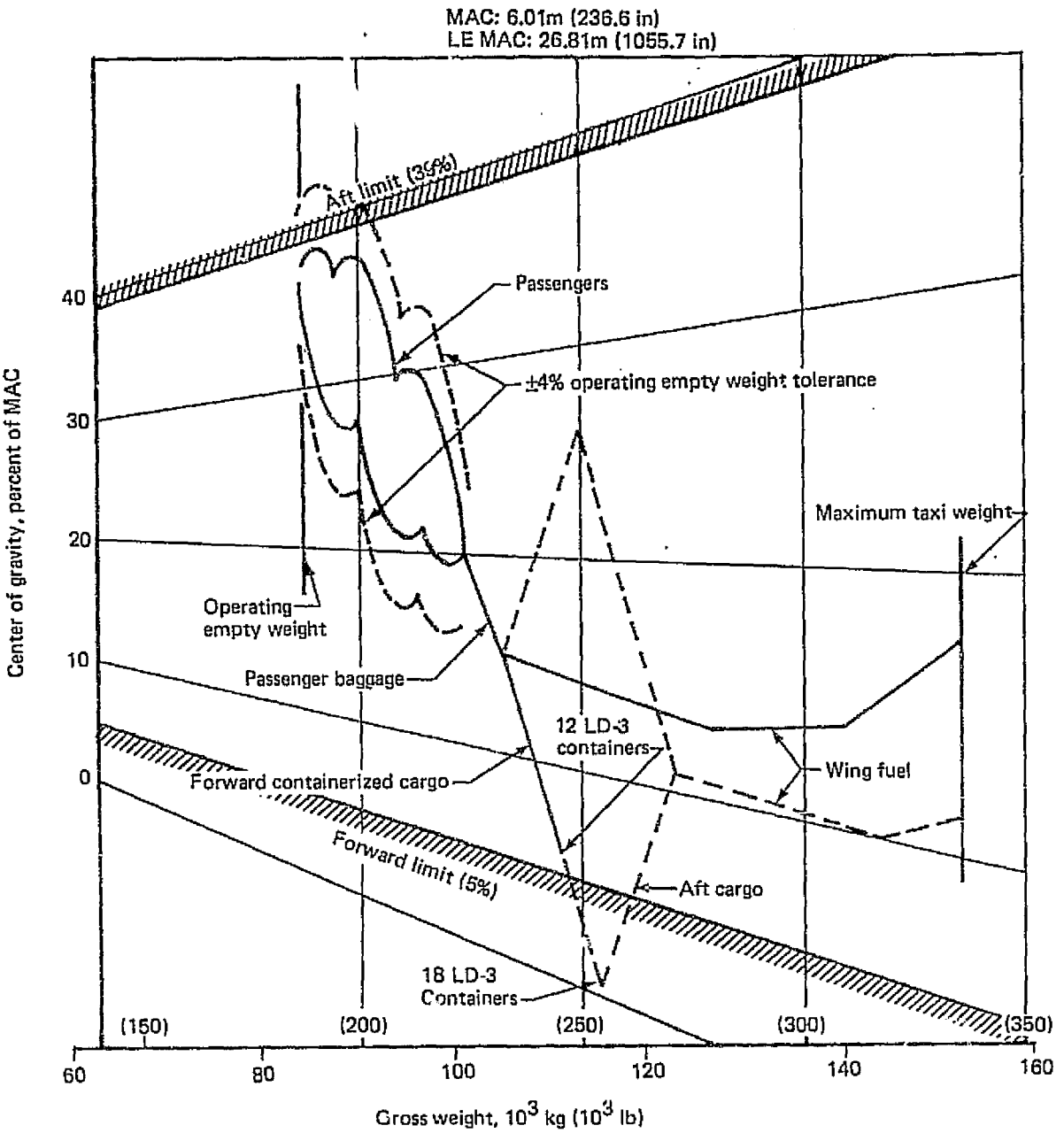

Figure 6.6-7. Loadability Diagram —Model 767-811

7.0 CONCLUSIONS AND RECOMMENDATIONS

Results of the NASA-sponsored LFC technology development effort in Phase I has shown significant progress and indicated the potential for airplane operating cost reductions and substantial fuel savings. Airplane design work conducted during the contract and augmented by Boeing-sponsored independent research and development has actively supported this development by closely following or anticipating technology advances and solutions to critical problems.

Aerodynamic Design

The aerodynamic design of an LFC wing has been developed to the point where it could serve as a basis for further refinement in the wind tunnel. Advanced high-speed airfoils have been shown to be compatible with LFC requirements and to provide a reasonable envelope to incorporate LFC systems and ducting. Nevertheless, continuing development of advanced high-speed airfoils for modern wing design is important to provide increased wing thickness and reduced weight with no reduction in speed. The impact of such development is even more favorable for LFC airplanes since their requirements for wing volume and controlled pressure distributions are more demanding than for turbulent airplanes. While the current aerodynamic design appears viable, further optimization is necessary to minimize drag and reduce internal flow losses. Further objectives should include reducing sensitivity to off-design operation and various disturbances, minimizing the number of slots and reducing the criticality of the leading edge. Ultimately, validation of the aerodynamic design is required throughout the operating envelope.

Recent advances in laminar boundary layer development and stability theory provide important new aids for the aerodynamic design of LFC wings. There is, however, a need for further validation and automation of methods to facilitate design decisions. New methods are needed to analyze the local effects of flow through suction surfaces including disturbances generated in this process. Ultimately, a complete three-dimensional analysis involving all possible modes including sound, may be necessary to provide a valid theoretical basis for predicting suction requirements in the presence of disturbances associated with the flight environment.

Wind Tunnel Testing

Wind tunnel testing is an essential supporting activity which is needed to provide basic data leading to design decisions which result in airplane performance improvements. The implementation of a wind tunnel test program by Boeing and the achievement of all major test objectives represents a first step toward filling these needs which will hopefully contribute to the advancement of LFC technology. Particularly significant results achieved during these tests include:

- Validation of the Boeing Research Wind Tunnel and the current test arrangement as a suitable facility for conducting laminar flow research on swept wings.

- Successful evaluation of a leading edge design for LFC on a swept wing at near-full-scale Reynolds numbers and accumulation of valuable experience in coping with the realities of achieving laminar flow in a less than ideal operating environment.
- Determination of the sensitivity of LFC to suction inflow distribution and to off-design operation.
- Extension of transition criteria for both two-dimensional and three-dimensional surface protuberances to include the effects of crossflow and suction quantity.
- Achievement of a better understanding of interactions between sound fields and the controlled laminar boundary layer and development of preliminary criteria for tolerable sound levels on a swept wing.

Wind tunnel testing should be continued in fundamental areas and extended to support design development and evaluation prior to committing to major flight programs.

Structural Approaches

The search for satisfactory solutions to the structural and systems problems imposed by the requirements for maintaining laminar flow has involved the consideration of a large number of alternate concepts and arrangements. This has resulted in the development of at least twelve different structural approaches involving the use of advanced structural arrangements and materials. These have been subjected to critical evaluation and review resulting in the selection of the conventional structure/fiberglass cover arrangement which is well-suited to application in the near-term. It can also be readily applied to almost any structural arrangement including those using graphite/epoxy composites. The use of graphite/epoxy composites in wing structure has been shown to be compatible with LFC requirements and to provide outstanding weight reduction potential. However, on the basis of current and foreseeable development activity, it is considered to be applicable only in the longer term. For the near term, a feasible structural concept has been defined which shows promise of providing a practical design that can be built and operated for reasonable cost. However, extensive design development is still required to reduce weight and cost and to resolve operational and manufacturing concerns. Validation of the concept by analysis and tests is an essential step in advancing the design to a state of readiness for production.

LFC Systems

The major additional systems requirements due to LFC are associated with the wing suction distribution and ducting systems and the suction compressor and drive. The important options for the various elements of these systems including their location on the airplane have been evaluated and the overall arrangement selected. The wing suction units, each consisting of a two-pressure level compressor with turboshaft engine drive, are located at the trailing edge of each wing/body intersection. Suction for the horizontal tail is provided by an APU which retains its normal function for ground operation.

In the category of special systems, protection against the accumulation of insects at the wing leading edge is of critical importance. Several promising candidates for such a system have been identified and assessed for technical feasibility. These involve the use of

1) A liquid film (water + anti-freeze), 2) A cryogen (liquid nitrogen) expanded into the leading edge cavity to produce frost on the leading edge, and 3) An air shield using high velocity jets. These must be subjected to further analysis and testing under simulated operational conditions and eventually integrated into a total leading edge design for evaluation in flight.

Operational Problems

Key operational problems have been identified and explored, the most important of which are: a) Protection against wing leading edge damage, b) Avoiding insect contamination, c) Establishing operational reliability, particularly in the presence of ice clouds and d) Evolving procedures and techniques that will provide low-cost maintenance and repair characteristics. Solutions to these problems must be developed and validated either in the laboratory or in flight before serious consideration of LFC application can be expected.

LFC Transport Design Trends

An LFC transport configuration has been developed incorporating the most promising structural arrangement and systems concepts developed during this study. Combining other elements of advanced technology with LFC provides attractive fuel utilization benefits which will have a very favorable impact on airplane economics. Nevertheless, further trade studies are needed to define the combination of features that will lead to a design most competitive with a turbulent airplane. In particular, more work is necessary to establish better design criteria and operational requirements. In this connection, cruise altitude and turbulent climb capability have been shown to have a major influence on the geometric definition of the long-range LFC transport to provide near-optimum performance and economics. For example, configurations tend toward lower wing loadings and thrust loadings and somewhat higher aspect ratios than for turbulent aircraft. The wing sweep will tend toward a near-optimum value based on wing weight (25° sweep at M = 0.8). However, the final sweep selection should be based on the careful consideration of the sensitivity of laminar flow to sweep and leading edge design details. The compromise must be strongly biased by the need to maintain LFC with high reliability in the airline operational environment.

It is recognized that the work under existing Phase I contracts represents only a start toward full-scale system design and that further work is required in technology development and testing of advanced structural and systems concepts. The LFC program should continue to focus on hardware design and development leading to construction of a validator airplane. This is essential to provide the practical experience needed to determine the operational and economic feasibility of introducing LFC transport aircraft onto commercial airline routes in the foreseeable future.

REFERENCES

1. Northrop Report NOR 67-136, Final Report on LFC Aircraft Design Data, Laminar Flow Control Demonstration Program, X-21A Engineering Section, June 1967.

2. Pfenninger, W.: *Flow Problems of Swept Low-Drag Suction Wings of Practical Construction at High Reynolds Numbers.* Annals New York Academy of Sciences, Vol. 154, Art. 2, November 1968.

3. Barnes, Jr., A.A. and Metcalf, J.I.: *ALCOR High Altitude Weather Scans.* AFCRL/ A.N.T. Report No. 1. AFCRL-TR-75-0645, Air Force Cambridge Research Laboratories, December 31, 1975.

4. Bohn, A.J. and Mangiarotty, R.A.: *Study of Noise Effects on Laminar Flow Control Due to Engine Placement on Wings of LFC Aircraft.* Boeing Document D6-44651, January 1978.

5. *"Limit of Surface Waviness for Laminar Flow over Wings,"* Royal Aeronautical Society Data Sheets, Wings 02.04.11, August 1957.

6. Carmichael, R.H. and Pfenninger, W.: *Surface Waviness Criteria for Swept and Unswept Laminar Suction Wings,* Report NOR-59-438 (BLC 123), August 1959.

7. *"Limit of Grain Size for Laminar Flow Over Wings or Bodies,"* Royal Aeronautical Society Data Sheets, Wings 02.04.09, July 1955.

8. Doenhoff, A.E. von and Braslow, A.L.: *The Effect of Distributed Surface Roughness on Laminar Flow.* Lachman, G.V., Boundary Layer Control, Vol. 2, Pergamon Press. 1961.

9. Nenni, J.P. and Gluyas, G.L.: *Aerodynamic Design of an LFC Surface,* Astronautics and Aeronautics, July 1966.

10. Hahn, M. and Pfenninger, W.: *Prevention of Transition over a Backward Step by Suction.* Journal of Aircraft, Vol. 10, No. 10, October 1973.

11. Srokowski, Andrew J., and Orszag, Steven A.: *Mass Flow Requirements for LFC Wing Design.* AIAA Paper 77-1222, Presented at AIAA Aircraft Systems and Technology Meeting, Seattle, Washington, August 22-24, 1977.

12. Mack, L.M.: *Computation of the Stability of the Laminar Compressible Boundary Layer.* Methods in Computational Physics, Vol. 4, B. Alder, ed., Academic Press, Inc., 1965, pp. 247-299.

13. Jaffe, N.A.; Okamura, T.T.; and Smith, A.M.O.: *Determination of Spatial Amplification Factors and Their Application to Predicting Transition.* AIAA Journal, Vol. 8, No. 2, February 1970. pp. 301-308.

14. Raspet, August and George-Falvy, Dezso: *Boundary Layer Studies on the Phoenix Sailplane.* Paper Presented at the VIII Congress of O.S.T.I.V., Koln Germany, June 1960.

15. Boltz, Frederick W.; Kenyon, George C.; and Allen, Clyde Q.: *Effects of Sweep Angle on the Boundary Layer Stability Characteristics of an Untapered Wing at Low Speeds.* NASA Technical Note D-338, 1960.

16. Bacon, J.W. and Pfenninger, W.: *Hot Wire Investigation of Suction Slot Flow Disturbances.* Northrop Report BLC-174, July 1976.

17. George-Falvy, D.: *Initial Tests on a 20-ft Chord, 30° Swept Wing Section with Laminar Flow Control over 30% of the Chord.* Boeing Document D6-46302, February 1978.

18. Bohn, A.J. and Mangiarotty, R.A.: *Test Report on Wind Tunnel Evaluation of Induced Acoustical Effects on Laminar Flow Control.* Boeing Document D6-47017. January 1979

19. Traeger, F.J.: *Test Report on Laminar Flow Control (LFC) Suction Slot Geometry Development.* Boeing Test Report T6-6279, October 1978.

20. Weiss, D.D. and Lindh, D.V.: *Development of the Technology for the Fabrication of Reliable Laminar Flow Control Panels.* NASA CR-145124, February 1976.

21. Bess, V.B.: *LFC Structural Development Test Report.* Boeing Document D6-46303, January 1978.

22. Sudderth, R.W.: *Environmental Test Report Covering Freeze Tests, Lighting Strike Tests, and Clogging Tests of LFC Concepts.* Boeing Document D6-47076, September 1978.

23. Hunt, J.: *Design Data for Selected LFC Structural Concept.* Boeing Document D6-47086. To be released.

24. Coleman, W.S.: *Roughness Due to Insects.* Boundary Layer and Flow Control, Vol. 2, edited by G.V. Lachman, 1961.

25. Fisher, David F. and Peterson, John B.: *Flight Investigation of Insect Contamination and Its Alleviation.* NASA Conference Publication 2036, Part I (Paper 21), February 28, 1978.

26. Gratzer, L.B. and George-Falvy, D.: *Application of Laminar Flow Control Technology to Long Range Transport Design.* The Boeing Company, CTOL Transport Technology Conference, NASA-Langley, February 28 to March 3, 1978.